# INVESTIGATIONS ON VIBRATIONAL OVERTONES IN THE NIR REGION AND LASER INDUCED FLUORESCENCE IN SOME SELECTED COMPOUNDS

*Thesis submitted to*

*Cochin University of Science and Technology*

*in partial fulfilment of the requirements*

*for the award of the degree of*

Doctor of Philosophy

by

K.K. VIJAYAN

DEPARTMENT OF PHYSICS

COCHIN UNIVERSITY OF SCIENCE AND TECHNOLOGY

KOCHI - 682 022

INDIA

NOVEMBER 2003

....................to my wife

Department of Physics
Cochin University of Science and Technology
Cochin 682 022

## CERTIFICATE

Certified that the work presented in this thesis entitled **"Investigations on Vibrational Overtones in the NIR region and Laser Induced Fluorescence in some selected compounds"** is based on the bonafide research work done by Mr. Vijayan K.K. under my guidance in the Department of Physics Cochin University of Science and Technology, Cochin 682 022, and has not been included in any other thesis submitted previously for the award of any degree.

Cochin- 22
08-10-2003

Dr. T.M Abdul Rasheed
(Supervising guide)
Reader, Dept. of Physics
CUSAT, Kochi-22
Present Affiliation:
Assistant professor
Department of Physics
King Faisal University
Damam, Saudi Arabia

Department of Physics
Cochin University of Science and Technology
Cochin 682 022

## CERTIFICATE

Certified that the work presented in this thesis entitled "**Investigations on Vibrational Overtones in the NIR region and Laser Induced Fluorescence in some selected compounds**" is based on the bonafide research work done by Mr..Vijayan K.K. under my guidance in the Department of Physics, Cochin University of Science and Technology, Cochin 682 022 and has not been included in any other thesis submitted previously for the award of any degree.
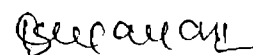
Cochin- 22

10-10-2003

Prof. K.P Rajappan Nair

(Co-guide)

Dean, Faculty of Science,

CUSAT, Cochin-22

# DECLARATION

I hereby declare that the present work entitled "INVESTIGATIONS ON VIBRATIONAL OVERTONES IN THE NIR REGION AND LASER INDUCED FLUORESCENCE IN SOME SELECTED COMPOUNDS" is based on the original work done by me under the guidance of **Dr.T.M.Abdul Rasheed**, Reader, Department of Physics and under the co-guidance of **Prof.K.P.Rajappan Nair**, Dean, Faculty of Science, Cochin University of Science and Technology, Kochi-22 has not been included in any other thesis submitted previously for the award of any degree.

Kochi-22

Date: 24 -11-2003

**K.K.Vijayan**

# Acknowledgement

It is a great pleasure to thank my supervising guide Dr.T.M.Abdul Rasheed, Reader, Department of Physics, Cochin University of Science and Technology for his excellent guidance, constant encouragement and supervision, which has been a tremendous help for me over the years. The many informative discussions we had, in which he showed his enthusiasm and positive attitude towards the topic that kept me on the right track.

With great pleasure I express my deepest gratitude to my guide-in-charge Prof.K.P.Rajappan Nair, Dean, Faculty of Science, Cochin University of Science and Technology for the encouragement and help given by him throughout the course of this work.

My sincere thanks are also due to Prof K.P Vijayakumar, Head, Prof. M. Sabir, and Prof. Elizabeth Mathai, former Heads, Department of Physics, Cochin University of Science and Technology for providing me the facilities required for this work.

Most of my experiments wouldn't have been possible without the excellent help from Dr.S.Shaji, Dr.Shibu M Eappen and Ms. Jyotsana of the laser and spectroscopy lab. I record my deep appreciation of their co-operation with me.

I also wish to thank my colleagues Mr.Sunny Kuriakose, Mrs.Syamala Kumari, and Mrs. Nandini. Their support and co-operation have been great.

Thanks are also due to Mrs.Usha John, Mr. Raveendran and Mr. Thomas Zacharia, the other teacher fellows in the laser and spectroscopy lab, for their help and support. I would like to express my thanks to Dr. Bindu for her help and encouragement.

I am also very grateful to my parents for their support. My deepest gratitude I must reserve for my wife Mrs. Syamala, children Vishnu and Nandu, whose patience and understanding I am very thankful for.

The financial support from UGC under FIP (IX) plan is gratefully acknowledged.

I would like to thank the Principal and my colleagues in Maharajas College, Ernakulam for their help and co-operation.

Thanks are also due to the Director of Collegiate Education, Thiruvananthapuram for granting me permission to do this work.

# CONTENTS

# Preface

Spectroscopy plays a key role in our understanding the basics of physical and life sciences. This thesis covers the spectroscopy of several polyatomic organic molecules, unravelling their structures, and electronic configurations.

Vibrational overtone spectroscopy of polyatomic molecules containing X-H oscillators (X=C, N, O, etc) provides valuable information regarding molecular structure, conformation, intra- and inter-molecular interactions, radiationless transitions, intramolecular vibrational relaxations, multiphoton excitations, chemical reactivities, anisotropic environment created by lone pair and / or $\pi$ electron interaction and the effect of substitution on the strength of individual X-H bonds on the parent molecule. Local mode model, in which X-H bonds are considered to be loosely coupled anharmonic oscillators, has been widely used to interpret the observed vibrational overtone spectra of these molecules.

The central theme of this research concerns the study of vibrationally excited molecules. We have used the local mode description of such vibrational states, and this model has now gained general acceptance. A central feature of the model is the localization of vibrational energy. A study of these high-energy localized states provides exciting new information about the structural and dynamical properties of molecules. For example, because of this localization, overtone spectra, which measure the absorption of vibrational energy, are extremely sensitive to the properties of X-H bonds. We also use overtone spectra to study the conformation of molecules, *i.e.*, the relative internal orientation of their bonds. The thesis comprises six chapters.

The first chapter presents a review of the earlier works on vibrational overtone spectroscopy of X-H containing molecules. This chapter also discusses an outline of the local mode theory and its refinements including the theory of coupled local mode oscillators. A description of the spectrophotometric measurements of the overtones is given at the end of this chapter. The next two chapters (2 and 3) deal in detail the results of experimental investigations on the vibrational overtone spectra of some organic molecules in the liquid phase.

In the second chapter, the analysis of the NIR vibrational overtone spectra of liquid phase six and five membered aromatic molecules- benzyl amine, furfuyl amine, furfural and cinnamaldehyde and some methoxy substituted benzenes- anisole, o-anisidine, p-anisidine and p-anisaldehyde are presented. A comparison of the local mode parameters of the ring C-H and N-H oscillators in benzyl amine and furfuryl amine indicates that the electron donation from the-$CH_2NH_2$ group to the aromatic ring is similar in both molecules. The hetero oxygen atom in furfuryl amine is thus not involved in any interaction to the -$CH_2NH_2$ group attached to the ring. A direct inductive interaction between the substituent aldehydic oxygen and the ring oxygen atom is observed in furfural. In cinnamaldehyde molecule the effect of lone pair effect is analyzed. The presence of non-equivalent methyl C-H bonds in methoxy benzenes is established and the possible factors influencing the local mode parameters of the ring C-H and methyl C-H bonds are discussed. The substituent effects are also analyzed in detail for each molecule.

The third chapter discusses the overtone spectra of the aliphatic compounds- t-butyl amine and n-butyl amine. The effect of the amine group in these molecules is discussed in detail. The analysis of overtone spectra of t-butyl amine reveals that the methyl group in this molecule maintains $C_{3v}$ local symmetry. The vibrational Hamiltonian of three-coupled oscillator system is used to predict the pure local mode overtones and local- local combination peaks. Calculated frequencies obtained by diagonalizing the coupling matrices of the $C_{3v}$ Hamiltonian are consistent with experimentally observed frequencies.

A number of applications of laser spectroscopy have been outlined in Chapter 4 and 5. The fourth chapter describes the experimental work done using a pulsed Nd: YAG laser. Pulsed lasers are ideal for the study of the different physico-chemical events as the delivery of photons to the system can be achieved in a well-defined time interval, and then the evolution of the subsequent physical and chemical events can be followed by appropriate optical techniques. In our set up, the emitted photons are collected using a monochromator –CCD detector assembly. Raman spectroscopy is a useful technique for the identification of substances in any phase. The pulsed Raman spectra of 3-fluorotoluene, anisole, t-butyl amine and p-anisidine are recorded and the assignments of

observed Raman shifts are done. The observed Raman spectra contain some new lines corresponding to low lying states. The pulsed LIF spectrum of polymerized samples of benzyl amine and n-butyl amine, and monomer sample of n-butyl amine are recorded and analyzed.

The fifth chapter deals with Tunable Diode Laser Absorption Spectroscopy (TDLAS). It gives a brief review of TDLAS, its application and high-resolution spectroscopic studies. The tunability of the laser wavelength is utilized to excite different conformers of isobutanol molecule. The high-resolution overtone spectrum of O-H in the second overtone region in isobutanol is recorded using a linear and a long path length high resolution set up and the conformations are studied.

The summary and conclusion of the present studies is given after the last chapter.

CHAPTER 1

# SPECTROSCOPIC STUDIES OF VIBRATIONAL OVERTONES IN THE GROUND ELECTRONIC STATE OF POLYATOMIC MOLECULES

CHAPTER 1

# SPECTROSCOPIC STUDIES OF VIBRATIONAL OVERTONES IN THE GROUND ELECTRONIC STATE OF POLYATOMIC MOLECULES

## 1.1 Introduction

Until recent times the near infrared (NIR) region of electromagnetic spectrum between 2000-700nm did not get much attention for diagnosing the absorption spectra of polyatomic molecular species. This was mainly because of the non-availability of powerful spectral sources in this region as well as the fact that many molecules have only very few absorption features due to overtones and combinations of high frequency vibrational modes. With the availability of high sensitive spectrophotometers and tunable coherent sources like lasers, the NIR vibrational overtone absorption spectra of a large number of polyatomic molecules could be recorded. In organic molecules the absorption bands in this region generally correspond to overtones and combinations of fundamental vibrations involving C-H, N-H, and O-H bonds.

In recent years considerable interest has been focused to the study of the different aspects of higher excited vibrational levels of the ground electronic state of polyatomic molecules containing X-H bonds [1-4]. The following are the major reasons for this interest. First, it is recognized in the study of nonradiative electronic relaxation process that higher excited vibrational levels of the ground electronic state play a key role in accepting the excited electronic energy [5-9]. Second, the normal mode model, which is found successful in describing the fundamental vibrations of molecules, fails to provide a satisfactory explanation of the observed higher overtones. Normal mode anharmonic coupling terms introduced into the normal mode model actually predicts a complicated absorption spectrum [10-12]. Third, an understanding about the nature of higher excited vibrational levels is essential in the development of the theory of multiphoton photochemistry and bond selective chemistry [13]. Finally overtone spectroscopic studies

provide an important link between spectral properties and chemical reactivity by measuring the behavior of the molecule as it moves along a coordinate associated with bond breaking.

The different spectroscopic methods provide different information of chemical interest by small-scale non-destructive experiments. NIR spectroscopy has now become a well-established technique for obtaining important structural information about polyatomic molecules. With the help of recent advances in technology NIR spectroscopy has applications in almost all fields such as remote data collection, agriculture applications etc. NIR spectroscopy analysis has greatly increased sensor abilities with the help of recent advances in chemometrics. It has been used for chemical process monitoring. In polymer production plant it is used for in-line measurement of polymer composition [14] and polymer viscosity [15]. Baker et al [16] used NIR spectroscopy to separate infected kernels of wheat from uninfected kernels. The unique characteristics of NIR is used for quality control by determining percentage parasitisation within mass cultures and to stage classify cultures to ensure synchronous or asynchronous release patterns.

## 1.2 Vibrational Spectroscopy

This term covers the two common techniques, Infrared and Raman spectroscopy, which deal with interaction of vibrational energy levels in molecules with incident photons. IR spectroscopy is based on changing dipole moment, while Raman is based on changing polarizability during molecular vibration. It is found that the energy of most molecular vibrations corresponds to that of their IR region of the electromagnetic spectrum. Thus IR region of the electromagnetic spectrum has been of great interest to researchers for many years, especially in the frequency region from 100 to 4000 cm$^{-1}$. The reason for the interest is that vast majority of chemical substances have vibrational fundamentals in this region; the corresponding absorption bands provide a nearly universal means for their detection. These interactions are very useful to chemists because they can be used to diagonize chemical structure.

3

At room temperature, most of the molecules are in their lowest vibrational state (V=0) and the most probable vibrational transition is to the state V=1. Both the IR and Raman spectrum at room temperature also contains the transitions V=0 to V=2,3,etc. The vibrational band corresponding to the transition $0 \rightarrow 1$ is called the *fundamental* band. The transition $0 \rightarrow 2, 0 \rightarrow 3$ etc give rise to *overtone* bands. The spectra may also contain combination bands. In general, the overtone and combination bands are of weaker intensity than the fundamental bands and in the Raman spectrum they are usually few in number.

## 1.3 Vibrational Excitations in Polyatomic Molecules-Normal Mode Model

A non-linear polyatomic molecule containing N atoms has 3N-6 internal degrees of freedom (corresponding to relative motion between atoms, namely molecular vibrations) whereas a linear polyatomic molecule has 3N-5 internal degrees of freedom. The (3N-6)/(3N-5) internal motions are called fundamental vibrations or normal vibrations.

The study of the vibrational transition without rotation of a polyatomic molecule begins with the assumption that the vibrational amplitudes are infinitesimal. This implies that the potential energy is a purely quadratic function of the vibrational co-ordinates. Then the vibrational problem reduced to that of a set of (3N-6)/(3N-5) uncoupled harmonic oscillators. The total vibrational energy equals the sum of the energies of the simple harmonic oscillations or normal modes.

$$E = \sum_K (V_K + \frac{1}{2}) \, \hbar \, \omega_K = E_0 + \sum_K V_k \hbar \, \omega_K \qquad (1.1)$$

where $V_K$ is the vibrational quantum number and $\omega_K$ the harmonic frequency associated with the normal mode K

Although this model, where the vibrational amplitudes are small, provides a reliable description for fundamental vibrations that occurs from a non-vibrating state (V=0) to a state with one quantum of excitation (V=1). But this simple model is found to be inaccurate when the quantum numbers are not small, and to fail completely when they

4

are large. A more accurate description requires inclusion of anharmonic terms in the vibrational potential. In polyatomic molecules there are two types of anharmonic terms: (1) diagonal terms which depends on the co-ordinates of a single oscillator (2) off-diagonal terms that depends on the co ordinates two or more oscillators. Due to latter terms, which couples the motions of different oscillators, the total vibrational energy becomes

$$E = \sum_K (V_k + \frac{1}{2}) \, \hbar \omega_K + \sum_K \sum_L (V_k + \frac{1}{2})(V_L + \frac{1}{2}) \hbar X_{KL} + \cdots$$

$$= E_0 + \sum_K V_k \hbar \omega_K{}^0 + \sum_K \sum_L V_k V_L \hbar X_{KL}{}^0 \qquad (1.2)$$

where $X_{KL}$ are the normal mode anharmonicity constants.

### 1.3.1 Limitations of Normal Mode Model

Very large vibrational amplitudes correspond to dissociation. In diatomic molecules if the Morse potential is considered as the vibrational potential the relation connecting the anharmonicity constant X and dissociation energy D is of the form:

$$X = - \omega^2 / 4D \qquad (1.3)$$

But in polyatomic molecules the relation connecting normal mode anharmonicity constants $X_{KL}$, bond dissociation energies $D_i$ and normal mode dissociation energies $D_K$ are not obvious. In normal mode model the vibrational energy is uniformly distributed among a number of equivalent chemical bonds then the dissociation energy $D_K$ is the sum of all bond energies $D_i$

$$D_K = \sum_i D_i \qquad (1.4)$$

This implies a large value of $D_K$ and thus a small value of $X_{KK}$. In a polyatomic molecule the physically important dissociation process is the rupture of a single bond. This dissociation energy $D_i < D_k$, so that the corresponding anharmonicity constant $X_{ii}$ will be much larger than $X_{KK}$. Thus for large values of vibrational energy the oscillations do not occur in a normal mode pattern.

As an example, the fundamental vibrations of benzene molecule are given by the normal mode. But when we calculate the dissociation energy using this model the value

5

obtained is very large. The reason is that if one continuously pumps energy into the totally symmetric vibrational mode of benzene, the dissociation along this co-ordinate requires the simultaneous rupture of all the six C-H bonds:

$$C_6H_6 \rightarrow C_6 + 6H$$
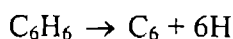
This is prohibitively high-energy process. The dissociation in the above equation requires almost six times the C-H bond dissociation energy. The breaking of only one C-H bond is actually take place:

$$C_6H_6 \rightarrow C_6H_5 + H$$

The difficulty in formulating vibrational problem under this condition is that the co-ordinates corresponding to rupture of a C-H bond involve the coupling of several normal modes. Thus, as the vibrational energies approach the dissociation limit, the normal mode description cannot be valid.

In molecules having no electronic absorption in the NIR region, at these level the observed spectra show only weak and simple features. For example, the $V=0 \rightarrow 6$ transition of a $-CH_2$ group in cyclohexane contain only one peak. In this example, there are two modes and six quanta and hence there are $6!/(4!\ 2!) = 15$ ways to put in the energy. In the normal mode picture all these should have different energies and should be spectroscopically resolved.

All these findings lead to the conclusion that higher vibrational states exhibit a new type of behavior and hence cannot be described by a set of normal mode quantum numbers.

## 1.4 Local Mode Model

The limitations of the normal mode model described above gave two important results: (1) the vibrational progressions are very anharmonic (2) at higher vibrational state the energy is localized on one of the equivalent oscillators.

Henry and Siebrand [7] introduced the Local Mode (LM) model in their attempt to model radiationless electronic transition in aromatic polyatomic molecules. In these transitions most of the electronic energy is transferred to CH stretching modes and that anharmonicity of these modes plays a major part in the transfer. Since then considerable

6

interest has been focused on the success of this theory for describing higher excited vibrational states of polyatomic molecules containing X-H bonds [17-31].

The Local Mode (LM) model treats a molecule as a set of loosely coupled anharmonic oscillators in which the vibrational energy is localized within one of the equivalent X-H oscillators. This localization of energy in a single bond makes the overtone spectra of large molecules appear very simple. In the absence of coupling one transition peak is observed for each nonequivalent X-H bond. The localization of energy in X-H oscillators makes the overtone spectroscopy an extremely sensitive tool for detecting changes in molecular environment, which can manifest themselves as small changes in bond length, conformation etc.

In the local mode model the vibrational energy of a polyatomic molecule assumes much the same form as in normal mode model:

$$E = \sum_i (V_i + \frac{1}{2}) \hbar \omega_i + \sum_i \sum_j (V_i + \frac{1}{2})(V_j + \frac{1}{2}) \hbar X_{ij} + \sum_i \sum_j c_{ij} \hbar \omega_{ij}$$

$$= E_0 + \sum_i V_i \hbar \omega_i^0 + \sum_i \sum_j V_i V_j \hbar X_{ij} + \sum_i \sum_j c_{ij}^0 \hbar \omega_{ij}^0 \qquad (1.5)$$

Compared to Eq. (1.2) the extra terms in Eq. (1.5) are the harmonic coupling term $c_{ij}^0 \hbar \omega_{ij}^0$ where $c_{ij}^0$ is the order of $(v_i v_j)^{1/2}$ and $\omega_{ij}^0$ of the order of $(\omega_K^0 - \omega_L^0)$. Thus local modes are also coupled but their coupling is smaller than the coupling between normal modes for large value of vibrational energy. Hence for high values of V local mode representation has advantages over the normal mode description. In LM model the interaction of the local modes with other local modes is weak then the diagonal anharmonicity constants $X_{ii}$ are expected to outweigh the off-diagonal ones. In other words in LM model $| X_{ii} | > | X_{ij} |$. The anharmonicity matrix $X_{ij}$ is closer to diagonal form, especially for large V. The harmonic coupling constants $c_{ij}$ between the local modes are extremely small compared to $\omega_i^0$. This suggests that the anharmonic coupling constant $X_{ij}$ are also small compared to $X_{ii}$. If we neglect to $\omega_{ij}^0$ and $X_{ij}$ for $i \neq j$ the molecule corresponds to a system of uncoupled local modes and the energy is sum of the contributions of these local modes. This suggests that Eq. (1.5) represents a system of weakly coupled anharmonic oscillators and results in a single frequency for high overtone excitations in a system of equivalent oscillators. While studying the C-H vibrations in

7

benzene molecule Hayward et al [10] noticed that in a normal mode representation contribution involving coupling of normal modes (off-diagonal contributions) were more important than diagonal anharmonic contributions. But in a local mode representation the situation is reversed and the diagonal anharmonic terms become dominant. Thus as more and more energy is placed into a group of oscillators, the vibrational energy become more diagonal in a local mode representation than in a normal mode representation.

In the LM model the transition peak energies of a vibrational overtone are found to fit the one dimensional Birge –Sponer equation [32] for an anharmonic oscillator,

$$\Delta E_{v,0} = V(A + BV) \tag{1.6}$$

$\Delta E_{v,0}$ is the observed energy difference between the $V^{th}$ vibrational quantum level and the ground level. A plot of $(\Delta E/V)$ verses $V$ for the observed bands yield A and B values.
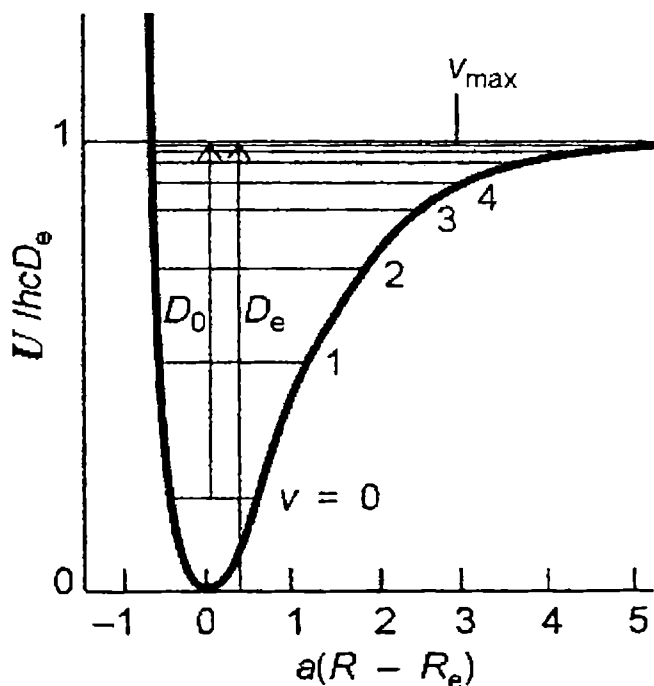


**Figure1.1** The Morse curve and the energy levels

e Morse potential

$$U\ (R\text{-}R_e) = D_e\left[1 - e^{-a(R-R_e)}\right]^2 \tag{1.7}$$

re $D_e$ is the dissociation energy, $R_e$ is the internuclear distance and $a$ is a constant for given molecule, is applied for the analysis of the high vibrational CH overtone the ational energy [33 ] is

$$E\ (V) = a\ \sqrt{\frac{D_e h}{2\pi^2 c\mu}}\left(V + \frac{1}{2}\right) - \frac{ha^2}{8\pi^2 c\mu}\left(V + \frac{1}{2}\right)^2$$

$$= \omega_e(V+1/2) - \omega_e X_e(V+1/2)^2 \tag{1.8}$$

$\mu$ is the reduced mass of the C-H oscillator system.

ce, $\Delta E_{V,0} = (\omega_e - \omega_e X_e)\ V - \omega_e X_e V^2$ \hfill (1.9)

LM parameters A and B are then,

$$A = \omega_e - \omega_e Xe \qquad\qquad B = -\omega_e Xe \tag{1.10}$$

se empirical parameters are related to the mechanical frequency $X_1$=A-B and the rmonicity $X_2$=B of the X-H oscillator. $X_1$ and $X_2$ are related to conventional troscopic parameters through $X_1$=$\omega_e$ and $X_2$= $-\omega_e X_e$. From the values of A and B the ociation energy of the anharmonic XH oscillator is

$$\Delta E_{max} = -A^2/\ 4B \tag{1.11}$$

## Quantum Mechanical Description of LM Model

Swofford et al [12] gave a quantum mechanical description of the one-dimensional aarance of CH overtone spectra with particular application to benzene. They assumed the vibrational Hamiltonian H for the (3N-6) molecular space could be separated into independent subspaces. (1) A subspace of dimension S having coordinates $R_1$..... $R_S$ in which H is partitionable to one-dimensional Hamiltonians and (2) the remaining ce S' =(3N-6-S) is unpartitionable. Hence,

$$H = \sum_{j=1}^{S} H_j + H_{S'} \tag{1.12}$$

9

,

with $H_j = \frac{1}{2} g_{jj} P_j^2 + V_j(R_j)$                                     (1.13)

$H_{S'}$ is the Hamiltonian for the unpartitionable space. $P_j$ are conjugate to $R_j$. The $g_{jj}$ are the diagonal elements of the g matrix for the S coordinate system. For separability no only the S dimensional block in g be diagonal but the variation of $|g|$ with respect to $R_1 ..... R_S$ also be negligible.

Once the Hamiltonian is partitioned the $k^{th}$ molecular eigen state $|\psi_k\rangle$ is characterized by a set of quantum numbers vj(k) each belongs to a subspace.

$$H|\psi_k\rangle = E_k |\psi_k\rangle$$                                     (1.14)

with     $|\psi_k\rangle = \prod_j |\phi_{v_j}(k)\rangle$           (j=1....S, S')                 (1.15)

and     $H_j|\phi_{v_j}(k)\rangle = E_{v_j}(k)|\phi_{v_j}(k)\rangle$                         (1.16)

The energy of the $k^{th}$ state is given by

$$E_k = \sum_j E_{v_j}(k)$$                                     (1.17)

Any operator $\hat{O}$ which can be partitioned in the same subspace such that

$$\hat{O} \quad = \sum_j \hat{O}_j(R_j), \quad \text{then}$$                         (1.18)

$\langle\psi_k|\hat{O}|\psi_l\rangle \neq 0$ is possible only when $v_j(k)=v_j(l)$ for all j but one. Thus if the electric dipole moment operator (belongs to the class of operators like $\hat{O}$) is separable in the same subspace as the Hamiltonian then electric dipole transitions which couple the ground state (all $v_j=0$) and excited states containing excitations ($v_j \neq 0$) in more than one coordinate of the partitioned space are forbidden. That is electric dipole moment operator couples ground state with only one of the coordinate in the excited state. Thus light incident on an unexcited state leads to excited states in only one local mode at a time Thus the LM predicts a unique single state excitation at all V. The workers verified that in the case of benzene, the spectroscopic energies of these single state excitations are given by Eq. (6). In a later study, these authors further demonstrated the validity of the local mode model by comparing the fifth overtone band of benzene and benzene-$d_5$. No significant difference in band shape or peak energy are observed for the two molecules in

:rast to the predictions of the strongly coupled normal mode model. On the other
i, LM model predicts a similarity in the two spectra as observed experimentally.

## Refinements in LM Model

The local mode model outlined in the previous section was successfully used in
gning the overtone peak positions for molecules with structurally non-equivalent and
formationally dissimilar X-H bonds and molecules with different X- atom constitutes
. The zeroth order local mode model includes anharmonicity but neglects inter-bond
plings. The appearance of combination bands in the overtone spectra of many
ecules indicates the presence of small terms in the molecular Hamiltonian that couple
erent molecular motions. It is observed that both kinetic energy and potential energy
pling terms lead to combination bands in the spectrum [35]. The dominant
ibinations built on each pure LM overtone level involve one quantum of some other
er frequency vibration of the molecule. These lower frequency vibrations are often
ʹ nearly normal modes of the molecules and hence the combinations are often referred
s local–normal bands [11].

An insight into intramolecular coupling of LM vibrations may be available from
study of the spectral energies of the absorption bands assigned as combinations
al-local and the local-normal) in the overtone region. Following Herzberg [36], the
sition energy for a system of two coupled anharmonic oscillators is given by

$$\Delta E\ (V_1,\ V_2) = V_1\ (A_1 + B_1 V_1) + V_2\ (A_2 + B_2\ V_2) + B_{12} V_1 V_2 \qquad (1.19)$$

re $V_1$ and $V_2$ are the quantum numbers and $B_{12}$ is the coefficient of anharmonic
pling between the two oscillators. This expression is found to provide a satisfactory fit
energies of both local-local and local-normal combinations. The anharmonic coupling
fficient $B_{12}$ is related to the presence of interaction terms (cross terms) in the
lecular Hamiltonian [37].

Many workers suggested refinements in the calculation of overtone energies by
luding the terms neglected in the zeroth order LM vibrational Hamiltonian. Sage [38-
and Wallace [41-42]] used Morse oscillator function to model CH bond potential. In
lition, Wallace used potential energy cross terms of the types $F_{ij} Q_i Q_j$ in the

11

hamiltonian, where $Q_i$ and $Q_j$ are the internal bond co-ordinates and $F_{ij}$ are the interaction force constant. Sage and Williams III [43] investigated the effects of anharmonicity and kinetic and potential interactions on the properties of coupled identical Morse oscillators using a Hamiltonian with a coupling potential which is well behaved at all vibrational amplitudes. They found that the main factor that determines the nature of the energy level structure and wave functions is the sum of kinetic and potential coupling constants. Intensities of spectral lines change dramatically with small changes in coupling parameters but make relatively small changes in properties of the coupled oscillators.

In the ground electronic state the general form of the coupled local mode vibrational Hamiltonian for an $XH_n$ system is [44-48]

$$(H-E_0) = \omega \sum_{i=1}^{n} V_i + \omega x \sum_{i=1}^{n} (V_i + V_i^2) + (\omega/2) \sum_{i=1}^{n} \sum_{j=1}^{n} \gamma (a_i^\dagger - a_i)(a_j^\dagger - a_j)$$

$$+ (\omega/2) \sum_{i=1}^{n} \sum_{j=1}^{n} \varphi (a_i^\dagger + a_i)(a_j^\dagger + a_j) \tag{1.20}$$

In this equation the first two terms represent the unperturbed local mode energy and the next terms represents harmonic coupling between local modes. This harmonically coupled anharmonic oscillator (HCAO) model includes coupling between the bond modes has been immensely useful and has enabled to understand the spectra of excited vibrational states [49-51].

In Eq. (20), $\omega$, $\omega x$ and $E_0$ are respectively the harmonic (or mechanical) frequency $(X_1)$, anharmonicity $(-X_2)$ and ground state energy of the local XH oscillator $V_i$ and $V_j$ are the quantum numbers for the $i^{th}$ and $j^{th}$ XH bonds. The parameter $\gamma$ characterizes the kinetic energy coupling and $\varphi$ characterizes the potential energy coupling between different XH oscillators. These coupling parameters are related to the Wilson G and F matrix elements through

$$\gamma = -\frac{1}{2} \frac{G_{ij}}{G_{ii}} \tag{1.21a}$$

$$\varphi = \frac{1}{2} \frac{F_{ij}}{F_{ii}} \tag{1.21b}$$

12

nd a are creation and annihilation operators related to normalized momentum( $p_i$ )and rdinate ($q_i$) variables by

$$p= a^\dagger - a \qquad\qquad (1.22)$$

$$q= a^\dagger + a \qquad\qquad (1.23)$$

have the usual raising and lowering properties in the harmonic oscillator limit

$$\langle V+1|a^+|V\rangle = (V+1)^{1/2} \qquad\qquad (1.24\ a)$$

$$\langle V-1|a|V\rangle = V^{1/2} \qquad\qquad (1.24\ b)$$

se properties are shown to be valid to a good approximation even for Morse llators [52]. Since manifolds corresponding to different values of the total quantum ber ($\sum_i V_i$) are well separated in energy inter-manifold coupling are neglected. With e approximations the Hamiltonian matrix elements are calculated for the symmetrized s sets relevant to the problem. Table1.1 shows Hamiltonian matrices for $XH_3$ groups. liffers from $\omega$ by small second order corrections [45] and $\lambda$ measures the net coupling in a given overtone manifold and is given by, $\lambda= -\omega(\gamma-\phi)$.

The experimentally observed vibrational overtones in $XH_n$ type molecules are of :h interest not only because their spectral appearance is in the sharp contrast with the litional normal mode picture in which excitation of one bond leads to periodic rchange of the excitation from one equivalent bond to another, but also due to the iortant mechanism leading to vibrational localization. If the central atom X is heavy the side atoms A and B are light then inter band-coupling parameter for an AXB type lecule becomes very small. When vibrational quantum number V increases the :ctive inter-bond coupling between local mode states and non-local mode states iinishes [53]. Both theoretical and experimental study have shown the interesting nomena of symmetry reduction in high overtones due to the vibrational iarmonicity, indicating the life time of single-bond vibration can be as long as the itional period.

$$V=1 \quad \langle 100;A_1| \quad \omega' - 2\omega x + 2\lambda$$
$$\langle 100;E| \quad \omega' - 2\omega x - \lambda$$

$$V=2 \quad \begin{matrix}\langle 200;A_1| \\ \langle 110;A_1|\end{matrix} \quad \begin{bmatrix} 2\omega' - 6\omega x & 2\sqrt{2}\lambda \\ 2\sqrt{2}\lambda & 2\omega' - 4\omega x + 2\lambda \end{bmatrix}$$

$$\begin{matrix}\langle 200;E| \\ \langle 110;E|\end{matrix} \quad \begin{bmatrix} 2\omega' - 6\omega x & -\sqrt{2}\lambda \\ -\sqrt{2}\lambda & 2\omega' - 4\omega x - \lambda \end{bmatrix}$$

$$V=3 \quad \begin{matrix}\langle 300;A_1| \\ \langle 210;A_1| \\ \langle 111;A_1|\end{matrix} \quad \begin{bmatrix} 3\omega' - 12\omega x & \sqrt{6}\lambda & 0 \\ \sqrt{6}\lambda & 3\omega' - 8\omega x + 3\lambda & 2\sqrt{3}\lambda \\ 0 & 2\sqrt{3}\lambda & 3\omega' - 6\omega x \end{bmatrix}$$

$$\langle 210;A_2| \quad 3\omega' - 8\omega x - 3\lambda$$

$$\begin{matrix}\langle 300;E| \\ \langle 210;1E| \\ \langle 210;2E|\end{matrix} \quad \begin{bmatrix} 3\omega' - 12\omega x & \sqrt{6}\lambda & 0 \\ \sqrt{6}\lambda & 3\omega' - 8\omega x & -\sqrt{3}\lambda \\ 0 & -\sqrt{3}\lambda & 3\omega' - 8\omega x \end{bmatrix}$$

$$V=4 \quad \begin{matrix}\langle 400;A_1| \\ \langle 310;A_1| \\ \langle 220;A_1| \\ \langle 211;A_1|\end{matrix} \quad \begin{bmatrix} 4\omega' - 20\omega x & 2\sqrt{2}\lambda & 0 & 0 \\ 2\sqrt{2}\lambda & 4\omega' - 14\omega x + \lambda & 2\sqrt{3}\lambda & \sqrt{6}\lambda \\ 0 & 2\sqrt{3}\lambda & 4\omega' - 12\omega x & 2\sqrt{2}\lambda \\ 0 & \sqrt{6}\lambda & 2\sqrt{2}\lambda & 4\omega' - 10\omega x + 4\lambda \end{bmatrix}$$

$$\langle 310;A_2| \quad 4\omega' - 14\omega x - \lambda$$

$$\begin{matrix}\langle 400;E| \\ \langle 310;1E| \\ \langle 310;2E| \\ \langle 220;E| \\ \langle 211;E|\end{matrix} \quad \begin{bmatrix} 4\omega' - 20\omega x & 2\sqrt{2}\lambda & 0 & 0 & 0 \\ 2\sqrt{2}\lambda & 4\omega' - 14\omega x + \lambda & 0 & -\sqrt{3}\lambda & \sqrt{6}\lambda \\ 0 & 0 & 4\omega' - 14\omega x - \lambda & 3\lambda & 0 \\ 0 & -\sqrt{3}\lambda & 3\lambda & 4\omega' - 12\omega x & -\sqrt{2}\lambda \\ 0 & \sqrt{6}\lambda & 0 & -\sqrt{2}\lambda & 4\omega' - 10\omega x - 2\lambda \end{bmatrix}$$

ible 1.1 Symmetrized effective Hamiltonian matrices for the overtone manifolds V=1

4 for the $CH_3$ group. The symmetrized bra labels $\langle abc;\Gamma|$ are indicated by rows, these

)els also applying to the corresponding column.

14

When more than one hydrogen atom share a common atom, the coupling between the oscillators produce symmetry effects in the spectra [12,44-46]. We have studied the overtone spectra of liquid state t-butyl amine [54] in the wavelength region 2000-700 nm where symmetry effects are observed. It is found that the observed CH local mode overtone and local-local combination frequencies are well predicted by the eigen states of a $C_{3v}$ coupled oscillator Hamiltonian. The analysis enabled the determination of the dependence of the coupling between CH oscillators in a methyl manifold on factors such as overtone energy. The details of this calculation are included in Chapter 3.

## 1.7 Factors Influencing Overtone Spectra

### 1.7.1 Fermi resonance

The analysis of the overtone spectra of monohalogenated acetylenes [55] shows that in addition to main CH stretching overtone bands several other bands appear in the spectrum with a comparable intensity. The reason for the large number of observed bands is the occurrence of Fermi resonance or accidental degeneracy. Fermi first elucidated this phenomenon by analysis of the vibrational spectrum of $CO_2$ molecule. A two level Fermi resonance is an anharmonic coupling between two vibrational levels of the same symmetry, when their frequency ratio is 2:1 or approximately so. The Fermi resonance interaction becomes more significant in polyatomic molecules due to the increased chance for the interacting higher vibrational states to become closer in energy. The resulting combination bands can gain substantial intensity from the main overtone band through the resonance. If two zero order degenerate states are close enough in energy with the appropriate symmetry, the Fermi resonance causes them to strongly repel each other. Ahmed and Henry reported the Fermi resonance shifts in the overtone spectra of dichloromethane and dichloromethane-d [25]. Their analysis revealed the existence of a near resonance interaction between the pure local mode CH stretching states and combination states with V-1 quanta of CH stretching and two quanta of HCH bending, in the region $\Delta V_{CH}$ =2-6. Fermi resonance becomes more complex in higher vibrational

15

vertone levels and is now recognized as a major pathway of intramolecular energy flow
ι organic molecules [56]. This aspect is discussed in a later section.

## l.8 Molecular Structural Studies Using Overtone Spectroscopy

The success of the LM model in explaining the overtone spectra of different kinds f molecules is now well established [57-65]. Vibrational overtone spectroscopy is not nly capable of distinguishing between aromatic and aliphatic CH bonds, but also rimary, secondary and tertiary CH bonds. Overtone vibrations are very sensitive to the ιcal environment of the relevant X-H oscillator - structural or conformational ɔnequivalence of the X-H bonds result in distinct absorption bands. Several techniques ke photoacoustic spectroscopy, long-path absorption spectroscopy, thermal lens ɔectroscopy, cavity ring-down spectroscopy etc have become popular for the detection f even very weak overtone progressions. These aspects urged spectroscopists to use vertone spectroscopy along with the LM model as sensitive probe to elucidate structural ɜtails of polyatomic molecules such as bent triatomic molecules [57,58] $XH_3$ type yramidal molecules [59-61], $XH_4$ type tetrahedral molecules [62], Methanol [63-65]. ang et al [35] successfully applied LM model to assign the CH stretching overtones in ιethanol for the fourth overtone region.

The IR spectral studies of fundamental vibrations provide important structural ιformation about molecules. But the spectra of the strongly coupled fundamentals of the 'H stretching vibrations are difficult to understand in terms of the influence of nvironment of a particular CH oscillator. The use of overtone spectroscopy has several dvantages over IR spectroscopy in characterizing individual CH bonds. First is the ractical reason that one can avoid the use of deuterated samples that are not often vailable and also difficult to prepare. Second, the overtone bands are quite well resolved. hird, the stretching frequency parameters obtained from fitting a number of sequential vertones for each LM oscillator promise higher precision than single measurement in the R. Lastly, the LM theory also gives the anharmonicity of the CH oscillators that etermines the shape of the oscillator potential, whereas IR studies give only the requencies of isolated CH oscillators.

16

## 1.8.1 Investigations on CH bond lengths

The overtone absorption peak positions are found to be sensitive to small changes in bond length of the local oscillator, implying that information about bond length changes can be obtained from vibrational overtone transitions. Changes occurring in CH bond length upon chemical substitution may be determined with an accuracy of $0.001A^0$, which is the same level as that of *ab initio* approaches [4]. Gough and Henry [22] used overtone spectra to estimate the relative bond length changes. The success of LM model helps us to better understand the cause of the variation in bond strength with local environment. The conventional way of correlating stretching frequency with bond length is through isotopic isolation. One uses selective deuteration of all CH bonds except one to decouple the CH bond of interest from the rest of CD stretching frequencies. Using this method, Mckean [66] had successfully demonstrated a correlation between CH bond lengths and isolated CH stretching frequencies. The sensitivity of the overtone transition energies to the local environment of the oscillator allows us to study the correlation between vibrational transition frequencies and chemical bond strengths by deuteration of selected positions in the molecule, with the same precision as given by IR studies with isotopic isolation. Jasinski [67] demonstrates that deuteration of neighboring CH bonds in methanol reduces spectral overlap with the OH overtone. A subsequent paper by Fang and Compton [68] reported the overtone absorption in ethanol and deuterated ethanol confirming the reduction of spectral congestion, up on deuteration, near $\Delta V_{OH}=5$ region. Rospenk et al [69] investigated the room temperature NIR spectra of several phenol derivatives and 3,5-dichlorophenol-pyrazine complex, dissolved in carbon tetrachloride. They also studied the mid-infrared spectra of some phenol-OD compounds, where in addition to the first OH overtone peak, six other absorption peaks also disappear upon deuteration.

Wong and Moore [70] found that a change of $0.001A^0$ in CH bond length causes a frequency shift of about 70 $cm^{-1}$ in the $\Delta V = 6$ overtone region as compared to a frequency shift of only 10 $cm^{-1}$ in the fundamental region. Previous experimental data on substituted benzenes led Henry and co-workers [61] to propose the following equation for a qualitative estimation of the aryl CH bond length in angstroms.

$$r_{CH} = 1.084 - (\Delta v / 11V)\, 0.001$$

Here the value 1.084 $A^0$ is the CH bond length in benzene and $\Delta v$ is the wave number shift (cm$^{-1}$) of the observed overtone peak position relative to the corresponding overtone peak position in benzene [71]. At higher overtone regions the peaks between non-equivalent oscillators become well distinct. A small difference in the fundamental frequencies of a molecule is well resolved in its high vibrational overtone levels because the difference is amplified about n times in the V=n overtone level [72]. Fedorov and Snavely [73] recorded the vibrational overtone spectra of gaseous biphenyl, anthracene, isobutanol, 2-chloethanol and ethylene diamine at the $\Delta V=4$ region using an intracavity laser photoacoustic spectrometer. Linear correlations were determined between the *ab initio* bond length and the overtone transition energies of these compounds. The bond lengths were obtained from ab initio geometry optimizations using both the 3-21G and the 6-31G basis sets. These bond lengths were used to predict the transition wavenumbers for $\Delta V=4$ transitions which could then be compared to the experimental values.

Spectra of CH overtones in alkane derivatives show that the higher energy band corresponds to primary and the lower energy band to the secondary CH bonds [74] .The OH stretching overtone transition frequencies also follow the general trend for frequency as primary > secondary > tertiary, which is consistent with that observed in fundamental OH stretching frequencies [68]. Rai and Srivastava [75] studied the overtone spectra of CH up to sixth overtone level and OH up to fifth overtone level in normal, secondary, and tertiary butanol using thermal lens technique. The observations were analyzed in the local mode picture.

## 1.8.2 Conformational analysis

LM model, which bridges the gap between experiment and theory, is widely used in conformational analysis. Fang et al [76] studied CH stretching overtone vibrations in a number of molecules containing methyl groups in a conformationally anisotropic environment created by an adjacent heteroatom (N, O, S). Two distinct bands at each

overtone are seen in these molecules, which are assigned as the overtones of non-equivalent methyl CH bonds. The effect is explained as the interaction of an electron pair with the CH bond situated trans to the lone pair. The influence of lone-pair electrons in IR spectra was well studied by Bellamy and Mayo [77]. The $2s^2$ $2p^4$ electron configuration leads to oxygen's divalency and to the presence of lone pairs of electrons occupying hybridized orbitals in oxygen containing compounds. These orbitals' spatial orientation allows interaction between the electron pairs and suitably oriented bonds on neighboring atoms. Bellamy and Mayo suggested the lone pair trans effect originate from the donation of electron density from the lone pair into the antibonding orbital of a CH bond situated trans with respect to the lone pair. This idea is now a generally accepted one, even though the mechanism of its operation is not fully understood. For heteroatoms the strength of lone pair effect follows the trend N>O >S.

Weibel et al [78] reported the intracavity dye laser photoacoustic absorption spectra of ethanol, ethanol (1,1-$d_2$) and ethanol (2,2,2-$d_3$) in the fourth OH overtone region. The distinct absorption bands were assigned as due to the *trans* and *gauche* conformational isomers. Comparison of the spectra revealed that a coupling between the OH and methylene CH vibrations occur only in the *gauche* conformer of ethanol, an effect that had not been revealed by the fundamental IR spectrum. *Ab initio* electronic structure and vibrational frequency calculations were used to verify the analysis of the ethanol OH vibrational spectrum and to evaluate the relative energies of the conformers

Fang and Swofford [74] successfully studied the molecular conformers of gas phase ethanol by its vibrational overtones. The overtone spectrum clearly indicates the existence of two conformers of the OH bond, either trans or gauche to the methyl group, with the more stable trans conformer having the higher mechanical frequency. Wong et al [70] studied the molecular conformation of alkanes and alkenes in the gas phase by overtone spectroscopy. Xu et al [79] measured the O-H stretching vibrational overtone spectra in the $\Delta V$= 3,4 and 5 regions of gaseous 2-butanol by using cavity ring-down spectroscopy (CRDS). Two bands are observed for each overtone level corresponding to two kinds of conformers. These authors also measured the O-H stretching vibrational overtone spectra in the $\Delta V$= 3,4 and 5 regions of gaseous isobutanol by using CRDS [72]. The overtone spectra of this molecule show three bands in each overtone level

corresponding to three kinds of conformers. The C-H local mode overtone spectrum of benzyl chloride in the visible and NIR regions recorded using laser induced thermal lens and conventional NIR absorption was reported by Rasheed and Nampoori [80]. Their analysis proved that, between the two possible conformational models predicted by the electron diffraction studies, the one with the -CH$_2$Cl group symmetrically oriented with respect to the benzene ring plane is the acceptable one.

### 1.8.3 Substituent effects

Overtone frequencies are quite sensitive to inductive effects of adjacent substituents [81,71]. Overtone spectroscopy can also be used for probing the effect of resonance structures in molecules. Mizugai and Katayama [33] using thermal lens technique have observed the fifth overtones of aryl CH stretching vibrations of more than 30 kinds of mono substituted benzenes in the liquid state. The frequency shifts of the substituted benzene from that of benzene were fond to be proportional to the $\sigma_I$ value, the inductive contribution of the Hammet $\sigma$, of the substituents. The parameter $\sigma_I$ may be regarded as a measure of the free-energy effect of the substituent relative to the H atom resulting from its power to attract or repel electrons through space and $\sigma$ bonds of the benzene system. This reveals that the strength of aryl CH bond increases if the substituent is an electron withdrawing one ($\sigma_I$ positive). When the substituent is halogen, NH$_2$, O-X or S-X not only $\sigma_I$ value but also the lone pairs of halogen, O, N, and S atoms in these substituents affect the bond strength of the aryl CH bond. In a subsequent paper Mizugai et al [82] reported fifth overtone spectra of aryl CH stretching vibrations of a number of di substituted benzenes in the liquid state. The frequency shifts of the overtones from that of benzene were found to be proportional to the sum of $\sigma_I$ values of the substituents. If the two substituents have opposite polarities a doublet structure of the spectrum is observed whereas an unresolved single absorption is obtained when the substituent have the same nature of polar effect.

Rasheed [83] reported the CH overtone spectrum of biphenyl in the $\Delta V_{CH}$ = 2-6 regions. The increase in CH mechanical frequency of this molecule with respect to

benzene is attributed to the cumulative effect of polar resonance structures involving both phenyl rings.

Fang and Compton [68] reported overtone absorption spectra of gas phase 1-propanol, 2-propanol and tert-butyl alcohol measured with intracavity photoacoustic and FT-IR spectroscop. Prominent features in the spectra are assigned as OH and CH stretching overtones within the LM model. Remaining features are assigned as combinations involving an LM overtone and lower frequency motions of molecules.

The room temperature vibrational overtone spectra of aryl and alkyl CH stretch vibrations in benzaldehyde were studied by Srivastava et al [84] using conventional and thermal lens techniques. In a subsequent paper, Srivastava et al [85] analyzed the local mode overtone spectra of o-, m-and p-nitrobenzaldehyde and p-chlorobenzaldehyde in the 2000-12000cm$^{-1}$ regions. The substitution effects in these molecules were studied by determining the change in aryl CH bond.

We have analyzed the near infrared vibrational overtone absorption spectrum of aryl and aldehydic CH oscillators in liquid phase 2-furaldehyde [86]. A local mode analysis has shown that the nature of interaction between the substituent -CHO group and the ring is influenced by the heteroatom present in the ring part of the molecule. Consequently the electron withdrawing ability of aldehydic group is considerably reduced in furfural compared to its six membered counterpart- benzaldehyde.

## 1.8.4 Inter and intra molecular bonding

Vibrational overtone spectroscopy is used as an effective tool for studying inter- and/ intra molecular interactions also. The presence of intra/ inter molecular hydrogen bond is reflected in the overtone transition energy values due to its effect on the mechanical frequency. Shaji and Rasheed [87] reconfirmed the presence of intramolecular hydrogen bond in o-chloroaniline by analyzing C-H and N-H overtones in o-, m-and p-chloroanilines. Eapen et al [88] analyzed C-H and O-H overtone spectrum of α-naphthol and found that intramolecular hydrogen bonding exists in this molecule.

Howard and Henry [89] measured the overtone spectra of adamantane, 1-chloroadamantane, and hexamethylenetetramine in different phases at different

temperatures using conventional NIR and intracavity laser photoacoustic spectroscopy. The overtone spectra provided evidence for an increased harmonicity of the CH stretching potential in the condensed phase.

Proose and Henry [90] measured the conventional NIR and intracavity laser photo acoustic overtone spectra in vapour phase 4-methylpyridine-$d_o$, 3- methyl pyridine-$d_o$ and 2-methylpyridine- $d_o$ in the $\Delta V_{CH}$ = 2-6 regions. These methods were also used to record the hydrogen impurity spectra of 4-methylpyridine-$d_7$ and 3- methylpyridine-$d_7$ in the $\Delta V_{CH}$ = 2-5 region. Oscillator strengths are calculated using an anharmonic oscillator LM model and ab initio dipole moment functions.

Gough et al [91] measured the gas phase C-H vibrational overtone spectrum of 1-cis-3-cis-5-trimethylcyclohexane in the 5-7 regions with intracavity dye laser photoacoustic spectroscopy. The spectrum is interpreted within the local mode description. Luckhaus et al [92] presented photoacoustic absorption spectra of C-H stretching overtones in formaldehyde in the $\Delta V$=3-6 regions. The analysis of the coarse rotational structure on the basis of asymmetric rotor simulations provides band centers. The observed intensity distribution reflects the increasing LM character of higher overtone wave functions within the normal co-ordinate subspace.

The vibrational overtone spectra of gaseous pyridine, 3-fluoropyridine and 2,6-difluoropyridine were reported by Snavely and Overly [93]. These spectra exhibit two LM progressions. In pyridine the assignment of the progression to the C-H bonds at the (2,6) and (3,4,5) positions is consistent with the known C-H bond lengths. Fluorination at the 2 and 6 positions eliminate these oscillators but splits the frequencies corresponding to the (3,5) and 4 positions, resulting in two distinct overtone bands again. In 3-fluoropyridine the two peaks are assigned to pairs of nonequivalent C-H bonds.

We have reported the NIR vibrational overtone absorption spectrum of liquid phase cinnamaldehyde in the region 2000-700nm[94]. A local mode analysis of the observed aryl and aldehydic CH bands has shown that the extended conjugation among the groups' aryl, olefinic and aldehyde causes increase in the aryl CH mechanical frequency. The increase in aldehydic CH mechanical frequency suggests the presence of indirect lone pair trans effect in this molecule.

Chen and Hsu [95] investigated eight typical sample molecules with five membered ring structures where intramolecular hydrogen bond is present, and found that intramolecular hydrogen bond strength for this set of structures is comparably weaker than the strength for the corresponding six membered ring structures. The authors also discussed the relative influence of various functional groups -COOH, -CHO, -OH and – $CH_3$ on the strength of intramolecular hydrogen bonding.

## 1.8.5 Polymer studies

The overtone spectroscopy can be used as an effective tool in probing polymerization and understanding bond linkage in polymers. Rasheed et al [96] studied overtone spectra of liquid phase acrylonitrile and thin film of polyacrylonitrle prepared by RF plasma polymerization using LM model. The analysis shows that the polymerization occurs through saturation of the C=C bond.

Vibrational overtone excitation of highly excited vibrational states is also used to initiate chemical reactions. Grinevich and Snavely [97] demonstrated a new technique of vibrational overtone polymerization of ethyl acrylate and methyl methacrylate monomers. Vibrational overtone polymerization involves intracavity photolysis of a monomer/initiator mixture that initiates a polymerization reaction. In these experiments the fifth CH overtone transition of benzyl peroxide activate benzoyl peroxide to form radicals. These radicals subsequently begin polymerization of the ethyl acrylate monomer. The polymerization yield was monitored by the decrease in intensity of the first overtone absorption band of olefinic CH stretch in the monomer. The molecular weights for the vibrational overtone polymers were compared to those resulting from low temperature thermal polymerizations. The average molecular weights for vibrational overtone-initiated polymers were found to be an order of magnitude larger than those for the thermal polymers. A thermal (60°C) polymerization of ethyl acrylate yielded a polymer with an average molecular weight of $4 \times 10^5$ whereas the vibrational overtone polymerization yielded a polymer with molecular weight of $3 \times 10^6$. Similar results were obtained for methyl metharylate.

# 1.9 Absorption Intensities in Overtone Spectra

Overtone intensity of a local mode transition is generally reported in terms of the dimensionless quantity of oscillator strength $f$. The oscillator strength of a vibrational transition from the ground state $g$ to an excited state $e$ is given by [89, 90]

$$f = 4.702 \times 10^{-7} (\text{cm}^{-1}\text{D}^{-2})\, v_{eg}\, |\mu_{eg}|^2 \qquad (1.25)$$

where $v_{eg}$ is the transition frequency in cm$^{-1}$ and $\mu_{eg} = \langle e|\mu|g \rangle$ is the transition dipole moment in Debyes.

The intensity of a vibrational transition can be calculated by knowing the transition frequency, the vibrational wave functions of the two states and the transition dipole moment. Transition frequencies and the vibrational wave functions are obtained using the HCAO model. In this model X-H oscillators are approximated as Morse oscillators and the coupling between X-H oscillators that are not attached to the same X atom is negligible. Transition dipole moment can be found ab initio by expanding the dipole moment in Taylor series as a function of displacement of the X-H bond about equilibrium. For an isolated system with the displacement coordinate q

$$\mu(q) = \sum_{i=0}^{n} \mu_i q^i \qquad (1.26)$$

with the coefficients $\mu_i$ given by

$$\mu_i = \frac{1}{i!}\frac{\partial^i \mu}{\partial q^i} \qquad (1.27)$$

In solution, the oscillator strength is given by the expression [89]

$$f = 4.3192 \times 10^{-12}\ (\text{mol cm}^{-1})\frac{9n}{\left(n^2+2\right)^2}\frac{1}{cl}\int A_{liq}(v)dv \qquad (1.28)$$

where $n$ is the refractive index of the liquid, $c$ is the molar concentration, $l$ is the path length, and $A_{liq}$ is the absorbance of the solution.

Xu et al [72.79] measured the band intensities of the OH stretching vibrations of different conformers of isobutanol and 2-butanol from the CRD spectra. The band intensities of the whole absorption of isobutanol are nearly equal to that of 2-butanol and larger by 20-30% than those of 2-propanol.

Intensities for several O-H vibrational overtone bands have been measured for vapor phase methanol, ethanol and isopropanol [98]. The trends in the intensities as a function of excitation level have been modeled by two empirical approaches yielding intensity predictions for the higher overtone transitions up to sixth OH overtone level. These methods are applied to recent $HNO_3$ overtone measurements resulting in new intensity predictions for higher photochemically active overtone bands. Their study reveals that the OH overtone intensities are more consistent than those of CH

Turnbull et al [99] measured the gas phase spectra of cis- and trans-2butene in the$\Delta V_{CH}$ =1-9 regions and have determined oscillator strengths from HCAO model and a Taylor expanded ab initio dipole moment function.

### 1.9.1 Mechanical anharmonicity

Infrared absorption spectra occurs due to dipole transition and their intensities are proportional to

$$\sum_{ij} \left| \int \varphi_i M_q \varphi_j dv \right|^2 \qquad (1.29)$$

where $\varphi_i$ and $\varphi_j$ are the two vibrational wavefunctions of the molecule. For vibrational transitions a change in the dipole moment must be considered. The dipole moment of the molecule p be expanded by a Taylor series in the small displacements $q_i$

$$p = p^0 + \sum_i \left( \frac{\partial p}{\partial q_i} \right)^0 q_i + \frac{1}{2} \sum_{i,j} \left( \frac{\partial^2 p}{\partial q_i \partial q_j} \right)^0 q_i q_j + \ldots \ldots$$

$$p = p^0 + \sum_i p_i q_i + \frac{1}{2} \sum_{i,j} p_{ij} q_i q_j + \ldots \ldots \ldots \qquad (1.30)$$

If this equation is introduced in the Equ. (1.29 ) the first term is zero in the harmonic oscillator approximation because the vibrational functions are orthogonal. The second term determines the intensity in the harmonic approximation and follows that dipole

moment must change during vibration. The presence of the third and higher terms results in mechanical anharmonicity and permits the appearance of overtones and combinations.

Mechanical anharmonicity influences the overtone spectra in different ways. The first and the direct manifestation is the displacement of the observed overtone frequencies from the positions expected for harmonic oscillators. The effect of mechanical anharmonicity is to relax the selection rules and to give more or less intense overtone and combination bands. The third consequence of mechanical anharmonicity is the strong and abnormal vibration rotation interaction in gas samples. The frequency of vibration depend not only on the vibration's own anharmonicity constants $X_{ii}$ but also on the coupling constants $X_{ij}$.

### 1.9.2 Electrical anharmonicity

Both the electric dipole moment $\mu$ and the electric polarizability tensor $\alpha$ is in the electronic ground state are functions of internal co-ordinates $q_i$ and hence may be expanded in a power series:

$$\rho = \rho^0 + \sum_i \left( \frac{\partial \rho}{\partial q_i} \right)^0 q_i + \frac{1}{2} \sum_{i,j} \left( \frac{\partial^2 \rho}{\partial q_i \partial q_j} \right)^0 q_i q_j + \ldots\ldots$$

$$\rho = \rho^0 + \sum_i \rho_i\, q_i + \frac{1}{2} \sum_{i,j} \rho_{ij}\, q_i q_j + \ldots\ldots\ldots \tag{1.31}$$

Where $\rho$ now stands for any component of $\mu$ or $\alpha$. The presence of the third and higher terms results in electrical l anharmonicity and permits the appearance of overtones and combination frequencies with measurable intensity. Thus it is possible, at least in theory, even when mechanical anharmonicity is absent overtone and combination transitions are possible if electrical anharmonicity is present.

Several authors [35,44] discussed the importance of electrical anharmonicity on the intensity pattern at each overtone level. However, it is difficult to separate the two anharmonicity effects in an actual case and it is vary difficult to assess the relative contributions of mechanical and electrical anharmonicity [100].

26

In absorption spectra, the intensity of a transition to the state $|v_1 v_2 v_3\rangle$ is proportional to the square of the transition matrix element Theoretical study of the effects of electrical anhrmonicity on the relative intensity of the Franck-Condon components of the XH profile predicts low frequency components are intensified at the expense of the high-frequency ones [101].

## 1.10 Intramolecular Vibrational Redistribution (IVR)

It is demonstrated that selected vibrational excitations can be used to control chemical reactions [102]. Hence an understanding the redistribution of energy among the internal degrees of freedom in a molecule is a prerequisite to controlling chemistry with vibrational excitation. Atomic displacements from the equilibrium geometry of a molecule are small at low vibrational energies. In this region the vibrations of molecules behave as uncoupled harmonic oscillators. The potential energy is purely quadratic. In this energy state if vibrational energy is placed in one state and there is no flow of energy into the other states. However as the vibrational energy increases the vibration becomes anharmonic and higher terms in the potential has to be taken into consideration. As a result of the coupling, more than one co ordinate mix with ach other. The magnitude of the mixing is determined by the energy separation between any two sates and the strength of the coupling matrix element.

When an overtone state is prepared by optical excitation one often considers that only one zeroth order local mode state called a 'bright' state. At sufficiently high vibrational energy the bright state will be coupled to a bath of zeroth order states called the 'dark' states, which do not have any transition probability. That is if the zeroth order states are not coupled, the overtone spectrum would show a single line corresponding to the single bright state otherwise the spectrum appears as clumps of lines. This sets very clearly the correspondence between the spectrum of vibrationally excited molecules and IVR.

Vibrational relaxation is very fast in liquids and solids. The time for intramolecular vibrational energy redistribution is shorter than that for bond breaking.

27

Jacob and Persson [103] observed that the energy relaxation rate for the overtone is twice as large as for the fundamental. Studies of vibrational relaxation show that overtone vibrations often relax in two consecutive steps. First the high frequency energy flows from the initial state into strongly coupled states nearby in energy that are combinations of other modes in the molecule. Such relaxation is referred as intramolecular vibrational energy redistribution (IVR). Once the energy spreads out among the internal degrees of freedom of the molecule then the energy flows out the molecule by intermolecular energy transfer [104]. Cheatum et al studied IVR in $CH_2I_2$ by transient electronic absorption spectroscopy and reveals that density of states determines the speed of the relaxation process. Resonances among the rovibrational states are recognized to have a central part in the IVR. These authors also suggested that IVR might be more probable in molecules possess more number of vibrational states in a particular overtone region due to strong Fermi resonance interaction [55]. Fang and Compton [68] studied the vibrational overtones for a number of alcohols. Their study shows a more isolated nature of the OH stretching vibration compared to C-H or N-H stretching vibrations, which lead to a possible slower IVR in OH oscillators.

Petryk and Henry [105] compared the C-H vibrational overtone spectra of gas phase neopentane-$d_0$,-$d_6$,-$d_9$ and tetramethylsilane(TMS) in the $\Delta V_{CH} = $ 4-8 region and observed a pronounced difference between the spectra of neopentanes and subtle differences among the spectra of neopentanes. These spectral differences are interpreted as a manifestation of geometry and vibrational frequency dependences in coupling efficiencies that facilitates the de-excitation of local modes of vibration via IVR. Fermi resonance plays a key role in this coupling. Some of the states are perturbed by through space coupling that can facilitate IVR.

## 1.11 Bond Selective Chemical Reactions and Long-lived LM States

The local mode model provides us a clear and natural physical picture of the molecular vibrations in high manifolds. It also seems to provide us a good candidate for intermediate state in bond selective reaction. With the development of high power lasers chemists began to concentrate on bond selective chemical reactions and performed numerous experimental studies. The earlier works were based on the idea of assigning local mode vibrational states associated with the selected bond and then induce bond selective chemical reactions by pumping intense laser beam. But this technique was not successful as the localized vibrational energy redistribute throughout the molecule very rapidly thus destroying the bond selectivity. Therefore it is essential to prepare molecules in a 'long-lived local mode states' to induce bond selective chemical reactions. The problem is then the extent to which the vibrational overtone states can be considered as local mode states and the time in which the molecule left in their vibrational excited state. Zhu and coworkers [53] suggested high-resolution spectroscopic studies answer these problems. Their argument is based on two reasons. (1) A long-lived local mode state may reduce the molecular symmetry and produces an observable change in the vibrational rotational energy levels. (2) Intra molecular vibrational relaxation (IVR) causes mixing of ' bright' local mode states with 'dark' states. If this mixing distributes the local mode behavior in among more than one eigen states then each rotational transition will be split into a cluster of fine lines. This study allows us to determine the extent to which one can consider an overtone state to be a local mode state and how fast the excited state transfers the localized energy. Many proposals based on theoretical studies put forward during the last several years show that long lived local mode states can be prepared by interaction of laser beams with molecules. But technical problems limit their actual laboratory application. Recently a new approach based on quantum interference effect is proposed to be feasible [53].

## 1.12 The present work

In the present study, the NIR absorption features of a number of organic molecules are investigated. The spectra are recorded using NIR spectrophotometer / tunable NIR diode laser. The NIR absorption spectra of liquid phase samples in the region 2000-700mm are recorded using a Hitachi Model 3410 UV-VIS-NIR spectrophotometer with air as reference. This dual beam instrument uses a tungsten lamp as the NIR source and a lead sulphide (PbS) cell as the detector. A grating monochromator is used for wavelength dispersion. The sample cell is a quartz cuvette of path length of 1 cm. All spectra are recorded at room temperature ($26 \pm 2^{\circ}C$). The spectral features are analyzed using the LM model. When more than one hydrogen atom is attached to a common heavy atom, the coupled LM model is used. The LM parameters such as mechanical frequency, anharmonicity, and kinetic and potential energy coupling coefficients are determined. The variations of these parameters in different series of molecules are studied. The analysis yielded important information regarding molecular structure, conformation, intra- and inter-molecular interactions, anisotropic environment created by lone pair and / or $\pi$ electrons and the effect of substitution on the strength of individual XH bonds. The present work will also be relevant in the analysis of radiationless transitions, intramolecular vibrational relaxations, multiphoton excitations and chemical reactivity.

Tunable Diode Laser Absorption Spectroscopy (TDLAS) is a technique that finds widespread use in obtaining high-resolution spectra of gas species. This method utilizes a Tunable Diode Laser (TDL) source to access specific regions of the molecules. In the present work we use a TDL in conjunction with a long path length cell that provides high sensitivity local measurements. The high-resolution overtone spectra of the O-H stretching vibrations in the $\Delta V=3$ region of isobutyl alcohol in the gas phase are measured using the highly sensitive TDLAS, which shows the presence of the different conformations of the hydroxyl group in this molecule. The details of this work are included in Chapter 5.

# References

[1]     B.R.Henry, *Vibrational spectra and structure*, Ed. J. R. Durig (Elsevier, Amsterdam,1981)Vol.10, p.269.

[2]     H.L.Fang and R.L.Swofford, *Advances in Laser Spectroscopy*, Ed. B.A.Garetz and J.R.Lombardi (Heyden, London, 1982) Vol.1, p.1.

[3]     M.S.Child and L.Halonen,*Adv.Chem.Phys.*,57(1984)1.

[4]     B.R.Henry *Acc.Chem.Res*,20( 1987)429.

[5]     W.Siebrand, *J.Chem.Phys.*,46(1967)440.

[6]     W.Siebrand and D.F.Williams, *J.Chem.Phys.*,49(1968)1860.

[7]     B.R.Henry andW.Siebrand, *J.Chem.Phys.*,49(1968)5369.

[8]     E.W.Schlag,S.Schneider and S.F.Fischer, *Ann.Rev.Phys.Chem.*,22(1971)465.

[9]     B.R.Henry,*J.Phys.Chem.*,80(1976)2160.

[10]    R.J.Heyward and B.R.Henry, *J.Mol.Spectrosc.*,50(1974)58.

[11]    B.R.Henry *Acc.Chem.Res*,10( 1977)207.

[12]    R.L.Swofford,M.E.Long and A.C.Albrecht, *J.Chem.Phys.*,65(1976)179.

[13]    M.Quack,*Adv. Chem.Phys.*,50(1982)395.

[14]    A.Khettry and  M.G.Hansen, *Polym. Eng.Sci.*,36 ( 1996)1232.

[15]    M.G.Hansen and S.Vedula,*J.Appl.Polym.Sci.*,68(1998)859.

[16]    J.E.Baker, F.E.Dowell and J.E.Throne, *Biological control*,16(1999)88.

[17]    R.T.Lawton and M.S.Child,*Mol.Phys.*,37 (1979)1799.

[18]    W.R.A.Greenlay and B.R.Henry,*Chem.Phys,Lett.*,53(1978)325.

[19]    B.R.Henry and J.A.Thomson, ,*Chem.Phys,Lett.*,69(1980)275.

[20]    H.L.Fang and R.L.Swofford,*Appl.Opt.*,21(1982)55.

[21]    K.M.Gough and B.R.Henry *J.Phys.Chem*,87(1983)3433.

[22]    K.M.Gough and B.R.Henry, *J.Phys.Chem*,88(1984)1298.

[23]    A.W .Tarr and B.R.Henry, *Chem.Phys,Lett*,112(1984)295.

[24]    H.L.Fang, R.L.Swofford, M.McDevitt and A.R.Anderson, *J.Phys.Chem.* 89(1985)225.

[25]    M.K.Ahmed and B.R.Henry, *J.Phys.Chem.*,90(1986)1993.

[26]    M.K.Ahmed,D.J.Swanton and B.R.Henry, *J.Phys.Chem.*,91(1987)293.

[27]    M.K.Ahmed and B.R.Henry, *J.Phys.Chem.*,91(1987)3741.

[28]    M.G.Sowa, B.R.Henry, and Y.Mizugai, *J.Phys.Chem.*,97(1993)809.

[29]    H.G.Kjaergaard and B.R.Henry, *J.Phys.Chem.*,99(1995)899.

[30]    D..M.Turnbull,M.G.Sowa, and B.R.Henry, *J.Phys.Chem.*,100(1996)13433.

[31]    H.G.Kjaergaard, D.M.Turnbull and B.R.Henry, *J.Phys.Chem.*,101(1997)2589.

[32]    R.T.Birge and H.Sponer, *Phys.Rev.*,28(1926)259.

[33]    Y.Mizugai, and M.Katayama, *J.Am.Chem.Soc.*, 102(1980)6424.

[34]    R.L.Swofford, M.S.Burberry, J.A.morrell and A.C.Albrecht
         *J.ChemPhys.*,66(1977)5245.

[35]    H.L.Fang, D.M.Meister and R.L.Swofford, *J.Phys.Chem.*, 88(1984)405.

[36]    G.Herzberg, *Spectra of Diatomic Molecules,* (Von Nostrand,New York,1950).

[37]    H.L.Fang and R.L.Swofford, *J.Chem.Phys.*,72(1980)6382.

[38]    M.L.Sage, *Chem.Phys.*,35(1978)375.

[39]    M.L.Sage, J.Jortner, *Chem.Phys.*Lett,62(1979)451.

[40]    M.L.Sage, *J.Phys.Chem*,83(1979)1455.

[41]    R.Wallace, *Chem.Phys.*,11(1975)189.

[42]    R.Wallace and A.A.Wu, *Chem.Phys.*,39(1979)221.

[43]    M.L.Sage and J.A.Williams III, *J.Chem.Phys.*, 78(1983) 1348.

[44]    B.R.Henry, A.W.Tarr, O.S.Mortensen, W.F.Murphy and D.A.C.Compton,
         *J.Chem.Phys.*, 79(1983)2583.

[45]    L.Halonen and M.S.Child, *J.Chem.Phys.*, 79(1983)4355.

[46]    T.M.A.Rasheed,V.P.N.Nampoori and K.Sathianandan,*Chem.Phys.*108(1986)349.

[47]    M..K.Ahmed and B.R.Henry, *Can. J.Chem*, 66(1988) 628.

[48]    M.W.P.Petryk and B.R. Henry, *Can J.Chem.*, 79(2001)279.

[49]    H.G.Kjaergaard and B.R.Henry, *J..ChemPhys.*,96(1992)4841.

[50]    H.G.Kjaergaard, D.M.Turnbull and B.R.Henry, *J..Chem.Phy.,*,99(1993)9438.

[51]    D.M.Turnbull , H.G.Kjaergaard and B.R.Henry, *ChemPhys.,*195(1995)129.

[52]    O.S.Mortenson,B.R.Henry and M.A.Mohammadi, *J..Chem.Phy.*,75(1981)4800.

[53]    *Spectroscopy-Perspective and Frontiers*, Ed. A.P.Roy, Narosa Publishing House,
         New Delhi,1997, p.194.

[54]    K.K.Vijayan, Sunny Kuriakose, K.P.R.Nair and T. M. A. Rasheed, *Asian*

*J.Spectrosc.*,6(2002)125.

[55] J.Lummila, O.Vaittinen, P.Jungner ,L.Hlonen and A.Tolonen, *J.Mol.Spectrosco.*, 185(1997)296.

[56] M.Quack, *Annu.Rev.Phys.,Chem.*,41(1990)839.

[57] H.G.Kjaergaard, B.R.Henry, H.Wei ,S.Lefebure, T.Carrington, O.S.Mortensen and M.L.Sage, *J.Chem.Phys.*, 100(1994) 6228.

[58] E.Kauppi and L.Halonen,*J.Chem.Phys.*, 96 (1992)2933.

[59] T.Lukka, E.Kauppi ,and L.Halonen, *J.Chem. Phys.*,102 (1995)5200.

[60] E.Kauppi and L.Halonen,*J.Chem.Phys.*, 103(1995)6861.

[61] J.Lummila, T.Lukka ,L.Halonen, H.Burger andO.Polanz, *J.Chem.Phys.*, 104 (1996)488.

[62] L.Halonen,*J.Chem.Phys.*,106 (1997)831.

[63] L.Halonen, *J.Chem.Phys.*,106 (1997)7931.

[64] V.Hanninen, M.Horn and L.Halonen, *J.Chem.Phys.*, 111(1996)3018.

[65] X.Wang and D.S.Perry,*J.Chem.Phys.*,109(1998)10795.

[66] D.C.McKean,*Chem.Soc.Rev.*,7(1978)399.

[67] J.M.Jasinski, *Chem.Phys.Lett.*,109(1984)462.

[68] H.L.Fang and D.A.C.Compton, *J.Phys.Chem.*,92(1988)6518.

[69] M.Rospenk, N.Leroux, and T-Huyskens, *J.Mol Spectros.* 183(245)1997.

[70] J.S.Wong and C.B.Moore, *J.Chem.Phys.*,77(1982)603.

[71] K.M.Gough and B.R.Henry, *J.Am.Chem.Soc.*,106(1984)2781.

[72] S.Xu, Y.Liu, J.Xie G.Sha, C.Zhang,*J.Phys.Chem.* 105(A) (2001) 6048.

[73] V.Fedorov and D.L.Snavely, *Chem.Phys.*,254(2000)169.

[74] H.L. Fang and R.L Swofford, *Chem.Phys Lett.*,105 (1984)5.

[75] S.B.Rai and P.K.Srivastava, *Spectrochimica Acta Part A* ,55 (1999) 2793.

[76] H.L.Fang, D.M. Meister and R.L Swofford, *J.Phys.Chem.*, 88(1984) 410.

[77] L.J.Bellamy and D.W.Mayo, *J.Phys.Chem,* 80,(1976)1217.

[78] J.D.Weibel, C.F.Jackels, and R.L.Swofford, *J.Chem.Phys.*,117(2002)4245.

[79] S.Xu, Y.Liu, G.Sha, C.Zhang and J.Xie, *J.Phys.Chem.A* 104 (2000)8671.

[80] T.M.A.Rasheed and V.P.N.Nampoori, *Pramana –J.Phys.*,42,(1994)245.

[81] Y.Mizugai, M.Katayama,and N.Nakagawa, *J.Am.Chem.Soc.*, 102(1980)6424.

[82]    Y.Mizugai, M.Katayama,and N.Nakagawa, *J.Am.Chem.Soc.*, 103(1981)5061

[83]    T.M.A.Rasheed, *Spectrochimica Acta A* 52,( 1996) 1493.

[84]    P.K.Srivastava, G.Ullas, and S.B.Rai, *Pramana –J.Phys.*, 43(1994) 231.

[85]    P.K.Srivastava, D.K.Rai and S.B.Rai, *Pramana –J.Phys.*, 56 (2001) 823.

[86]    K. K. Vijayan Sunny Kuriakose, S.Shaji, and T. M. A. Rasheed,
        *Asian J.Phys.*,11(2002)66.

[87]    S.Shaji and T.M.A.Rasheed, *Spectrochim.Acta A*,57(2001)337.

[88]    S.M.Eappen, S.Shaji, and K.P.R.Nair, *Asian J.Spectros.*,2(2001)89.

[89]    D.L.Howard and B.R.Henry, *J.Phys.Chem.A.*, 102(1998)561.

[90]    R.J.Proos and B.R.Henry, J.*Phys.Chem.A*, ,103(1999)8762.

[91]    K.M.Gough, B.R.Henry, B.J.Schattka and T.A.Wildman,
        *J.Phys.Chem,*.95 (1991)1579.

[92]    D. Luckhaus, M.J.coffey, M.D.Fritz and F.F.Crim,  *J.Chem.Phys.*,104(1996)3472.

[93]    D.L.Snavely, J.A.Overly and  V. A. Walters,*Chem.Phys.*201(1995)567.

[94]    K. K. Vijayan Sunny Kuriakose, S.Shaji, Shibu M Eapen, K.P.R. Nair and
        T. M. A. Rasheed,  *Asian J.Spectros.*,5(2001)185.

[95]    C.Chen and F. –S.Hsu, *J.Mol.Structure(Theochem)*, 506(2000)147.

[96]    T.M.A.Rasheed, S.P.Shamsudeen and M.K.Jayaraj,
        *Indian J.Pure.Appl.Phys.*, 34(1996)534.

[97]    O.Grinevich, and D.L Snavely, *Chem. Phys. Lett.*, 267(1997)313.

[98]    J.A.Phillips, J.J.Orlando, G.S.Tyndall and V.Vaida,
        *Chem.PhysLett.*.,296(377)1998.

[99]    D.M.Turnbull, H.G.Kjaergaard and B.R.Henry, *Chem.Phys*, 195(1995)129.

[100]   Techniques of Organic Chemistry, Vol.IX, Ed. A.Weissberger,
        Interscience Publishers Inc, 1963, New York.

[101]   Y.Bouteiller and Y.Guissani, *Mol.Phys.*,38(1979) 617.

[102]   F.F. Crim,*J. Phys.Chem*,100(1996)12725.

[103]   P.Jakob and B.N.J.Persson, *J.Chem.Phys.*, 109(1998)8641.

[104]   C.M.Cheatum, M.M.Heckscher, D.Bingeman, and F. F. Crim,
        *J.Chem.Phys,* 115(2001) 7086.

[105]   M.W.P.Petryk and B.R.Henry, *J.Phys.Chem. A*,106(2002)8599.

CHAPTER 2

# OVERTONE SPECTROSCOPIC STUDY OF SIX AND FIVE MEMBERED AROMATIC MOLECULES

# OVERTONE SPECTROSCOPIC STUDY OF SIX AND FIVE MEMBERED AROMATIC MOLECULES

## 2.1 Introduction

Extensive investigations of the vibrational overtone spectra of the X-H stretch in hydrocarbons have been performed for the last several years. The analysis of the stretching overtone spectra can be done successfully by using the local mode model [1-3]. This model provides a new way of looking at excited stretching vibrational states of molecules containing hydrogen atoms. As described in detail in the first chapter, this model treats the X-H bonds of a polyatomic molecule as an assembly of loosely coupled anharmonic Morse oscillators. In this model the overtone transition energies of the peaks observed due to a particular type of X-H bond fit very well to the one dimensional Birge-Sponer equation

$\Delta E_{v,0} = V (A+BV)$, which gives the bond dissociation energy the local oscillator as

$$D = - A^2/4B$$

Here V is the quantum level of excitation, $A-B = X_1$ is the mechanical frequency and $B = X_2$ is the anharmonicity of X-H bond. It is noted that the mechanical frequency is related to the equilibrium bond force constant, while both mechanical frequency and anharmonicity are related to the bond dissociation. The parameters $X_1$ and $X_2$ are sensitive not only to the bond type (primary, secondary, tertiary, aliphatic, aromatic etc) but to the conformational state of the molecule and the intra and/or inter molecular environment of the X-H bond. In a molecule containing non-equivalent X-H bonds, different overtone progressions are formed due to their differing $X_1$ and/or $X_2$ values. Overtone spectroscopy has thus become an effective tool for the molecular structural analysis through characterization of X-H bonds [4 – 14]. Overtone spectroscopy has also been used to study the influence of various substituents on the parent molecule [15-20].

This chapter describes the local mode analysis of the near infrared vibrational overtone spectra of a number of organic molecules viz benzyl amine, furfuryl amine, furfural, cinnamaldehyde, anisole, p-anisaldehyde, o-anisidine and p-anisidine. The analyses of the spectral data have led us to draw a number of conclusions about the structural aspects of these molecules.

## 2.2 Experimental

High purity (>99%) samples benzyl amine, furfuryl amine, furfural, cinnamaldehyde, anisole, anisaldehyde, p-anisidine and o-anisidine supplied by M/s Sisco Research Laboratories, Mumbai (India) and Central Drug House Pvt. Ltd., Mumbai (India) are used for the present investigations. The near infrared absorption spectra in the region 2000-700mm are recorded on a Hitachi Model 3410 UV-Vis-NIR spectrophotometer, which uses a tungsten lamp as the near infrared source. The spectra are recorded using a path length of 1 cm with air as reference at room temperature ($26 \pm 2$) $^0$C. The spectra of all the samples except p-anisidine are recorded from pure liquids. The compound p-anisidine is a solid at room temperature and hence the absorption spectrum is recorded from a near saturated solution in spectrograde carbon tetrachloride. For this sample, the spectra could be recorded only in the 2000-800nm range, due to the poor signal to noise ratio in this region. We could thus record only two N-H overtone bands of this molecule. The signal to noise ratio was poor even in the third C-H overtone region (above 800 nm) where multiple peaks are found to appear. We could however, assign the CH overtone peak in the spectrum.

## 2.3 Overtone spectra of benzyl amine and furfuryl amine.
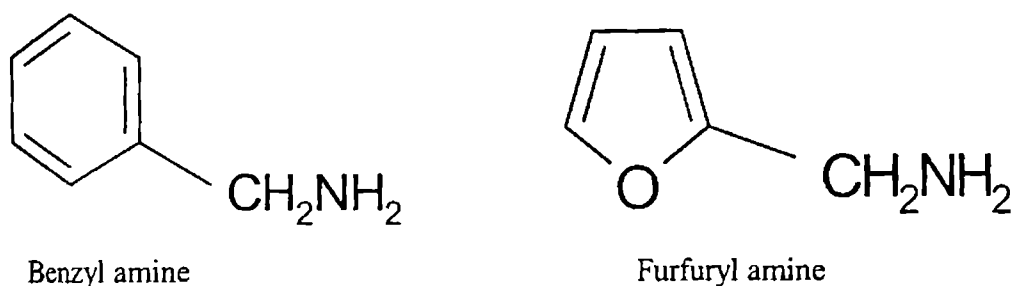


Benzyl amine                                    Furfuryl amine

**Figure 2.1** The molecular structures of benzyl amine and furfuryl amine

**Table 2.1** Observed overtone transition energies ($cm^{-1}$), mechanical frequency $X_1$ ($cm^{-1}$) and anharmonicity $X_2$ ($cm^{-1}$) of ring CH and side group NH of benzyl amine and furfuryl amine. The least square correlation coefficients ($\gamma$) are also given. The mechanical frequencies and anharmonicity of furan and benzene are also given for a comparison.

| Molecule | $\Delta V=2$ | $\Delta V=3$ | $\Delta V=4$ | $\Delta V=5$ | $X_1$ | $X_2$ | $\gamma$ |
|---|---|---|---|---|---|---|---|
| Benzene | 5983 | 8760 | 11442 | 14015 | 3148.1 | -57.6 | |
| Furan | | | | | 3259 | -59.0 | |
| **Benzyl amine** | | | | | | | |
| Ring CH | 5934 | 8752.7 | 11418.1 | 13997.8 | 3139.1 | -56.5 | -0.999 |
| $NH_2$ | 6533 | 9559.3 | 12428.5 | | 3505.4 | -79.7 | -1 |
| **Furfuryl amine** | | | | | | | |
| Ring CH | 6129.7 | 9028.5 | 11807.8 | | 3234.6 | -56.5 | -0.99994 |
| $NH_2$ | 6539.4 | 9573 | 12437.8 | | 3510.5 | -80.1 | -0.99995 |

The overtone spectra of benzyl and furfuryl amines in the spectral regions of quantum levels V = 2 to V = 4 are shown in Figures 2.2-2.7. The $\Delta V$ = 5 spectrum could be recorded only for the aryl C-H local mode of benzyl amine (Figure 2.3). The various overtone absorption bands corresponding to different local oscillators show single peaks. The peak positions, corresponding transition energies, their assignments and the calculated local mode parameters of the aromatic C-H, and N-H oscillators are given in Table 2.1. The ring C-H local mode parameters of benzene [21] and furan [22] are also given in the table for a comparison.

Mizugai and Katayama [22] reported the C-H stretch vibrational overtone spectra of liquid phase five membered heterocyclic molecules thiophene, furan and pyrrole in the $\Delta V$=2-6 regions. These workers observed that the overtone frequency shift with respect to benzene is proportional to the decrease in the relevant C-H bond length. The band splitting in observed in the $\Delta V$=2 and 3 regions of the furan spectrum indicated evidence for the existence of two types of nonequivalent oscillators, one pair residing near the heteroatom and the other away from it [22,23]. The corresponding CH bond lengths were reported as 1.075 and 1.077 $A^0$ [22]. The bond length difference of 0.002 $A^0$ resulting in two overtone peaks in furan separated by 84cm$^{-1}$ at the fourth overtone level [23]. Mizugai and Katayama proposed the following relation for the mean positions of ring C-H overtone transitions

$$\Delta E_{v,0} = 3200V - 59V^2$$

The blue shift in the overtone transition energy of the compounds with respect to benzene was shown to occur due to an increased value of C-H mechanical frequency. They obtained a good correlation between overtone frequency shift and decrease in the (average value of) C-H bond length with respect to benzene. However these authors did not give any explanation for the increase in C-H mechanical frequency in the heterocyclic compound with respect to benzene. Keeping in mind the well established result from overtone studies of substituted benzenes that an electron withdrawing substituent causes an increase in ring C-H mechanical frequency [15-19], one can conclude that the increase in the value of C-H mechanical frequency in furan compared to benzene occurs due to the electron withdrawing power of the oxygen atom. The oxygen atom withdraws the $\pi$ electron cloud inductively from the aromatic ring thus acquiring a net negative charge. This is evident from the smaller value of the molecular dipole moment in furan (0.70D) compared to that in tetrahydrofuran (1.73D)[24].

Snavely et al [25] analyzed the C-H overtone spectra of pyrrole and pyrrolidine and observed evidence for intramolecular vibrational coupling in the N-H oscillators. Katayama et al [26] reported the fifth CH overtone spectra of liquid phase pyridine, pyrazine, pyrimidine, pyridazine and triazine. They derived simple rules for determining frequency shifts of the overtones due to nitrogen atom present in the heterocyclic ring. Snavely et al [27] studied the C-H overtone spectra of the six membered heterocyclic

compounds pyridine, 3-fluoropyridine and 2,6-difluoropyridine. It was shown that the presence of the heteroatom in these molecules removes the equivalency of the C-H bonds and consequently the overtone spectra exhibit two vibrational progressions. Sowa et al [23] carried out an overtone spectroscopic study of vibrational state interactions in furan and some thiophenes. These workers found spectral evidence for Fermi resonance, which behaves differently in furan and thiophenes. In furan, at the $V_{CH} = 4$ level, the dynamics of the aryl C-H stretching overtones is found to be affected by the zero order energy match between the local mode overtone states and the stretch bend combination states. It is concluded from gas phase electron diffraction studies that, at room temperature, the conformers of furfuryl amine are stabilized by forming hydrogen bonds between the amino hydrogen atoms and the oxygen of the furan ring and / or the πelectrons of the carbon-carbon double bond [28]. It is generally established from the above studies that the ring C-H mechanical frequency value depends on the nature of the heteroatom in the ring and also on the nature of substituent group attached to the ring. Hence, the study of monosubstituted heterocyclic ring compounds is a good testing ground for the evaluation of the substituent effect.

The compounds studied in the present work – benzyl amine and furfuryl amine (Figure 2.1) are substituted compounds of benzene and furan respectively. Both furfuryl amine and benzyl amine molecules are expected to contain nonequivalent ring C-H oscillators. However the ring C-H mechanical frequency values cited in Table 2.1 represent the average values over the ring sites, since the corresponding absorption bands in the present liquid phase spectrum do not show a resolved structure. A comparative analysis of the observed local mode parameters in furfuryl amine and benzyl amine with respect to the parameters of the parent molecules furan and benzene reveals that the substituent group (-CH$_2$NH$_2$) has the same effect on the ring part of both the molecules.
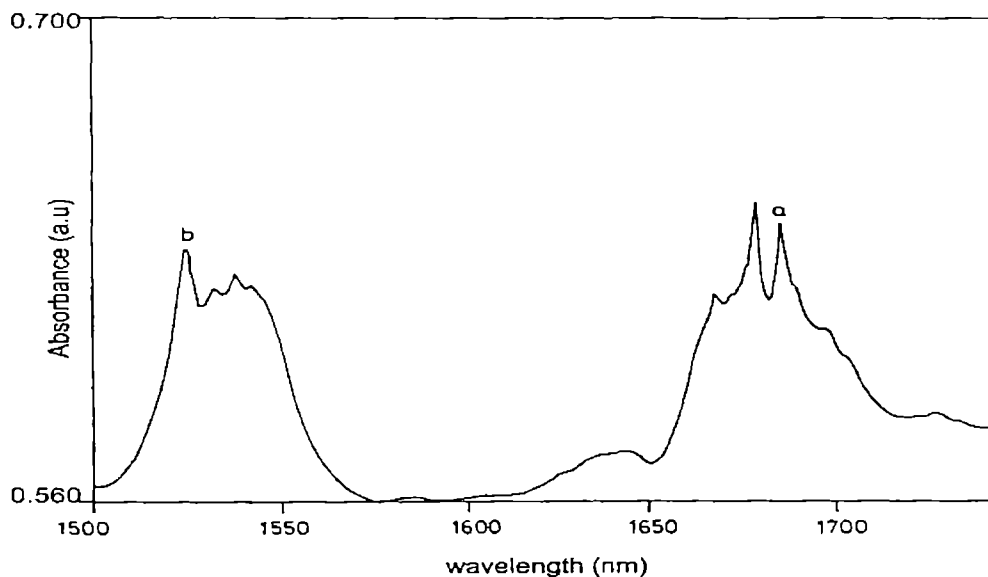
**Figure 2.2** Ring C-H and side group N-H band structures of benzyl amine in the $\Delta V=2$ region. The pure overtone peak of C-H is marked as 'a' and that of N-H is marked as 'b'.
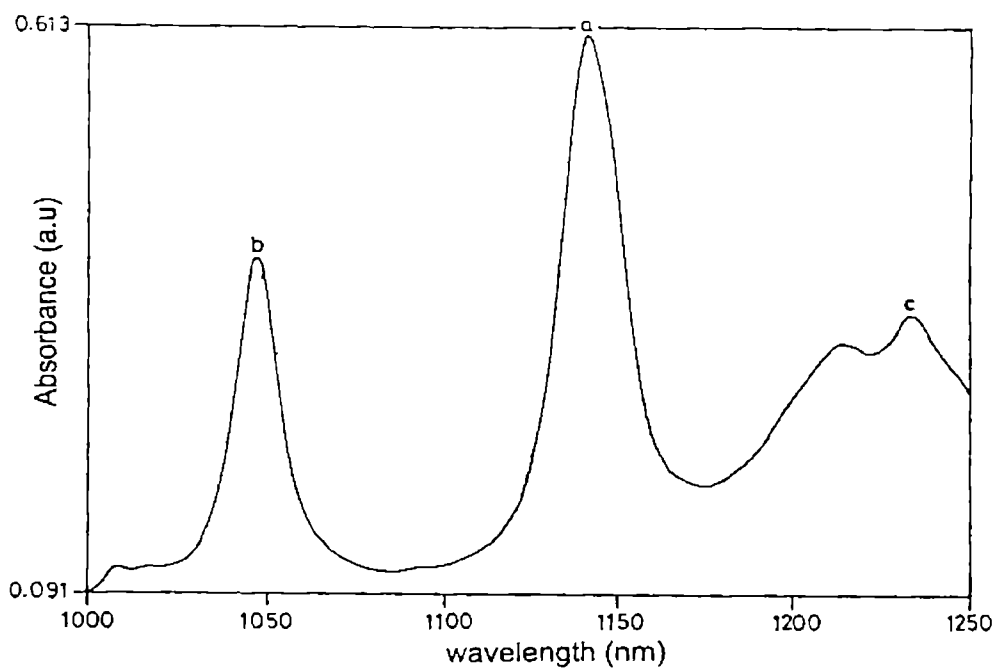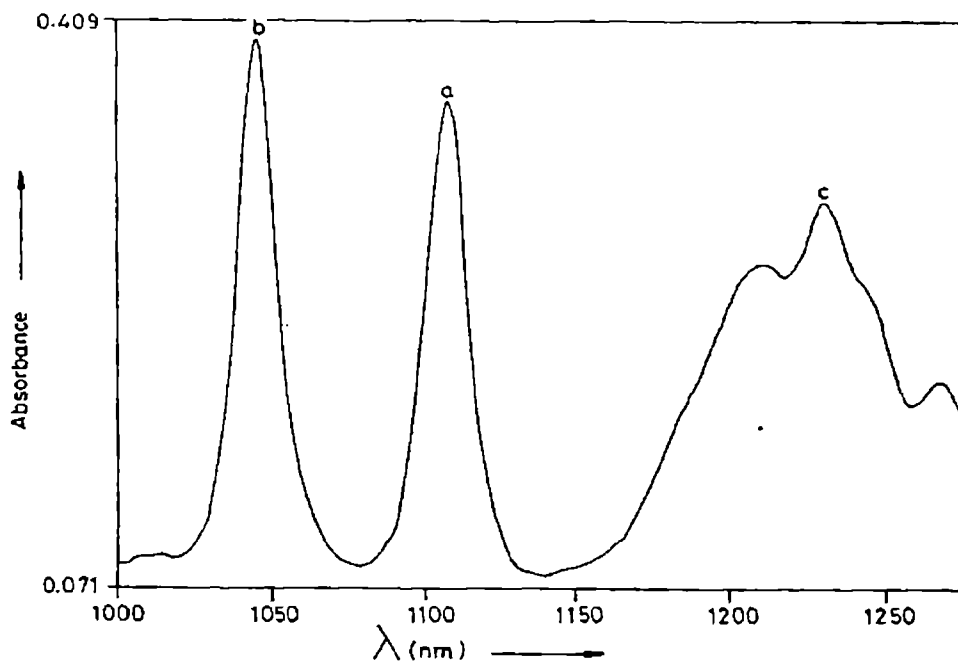


**Figure 2.3** Ring C-H and N-H overtone peaks of benzyl amine in the $\Delta V= 3$ region; 'c' represent methylene C-H overtone peak of benzyl amine in the $\Delta V = 3$ region.
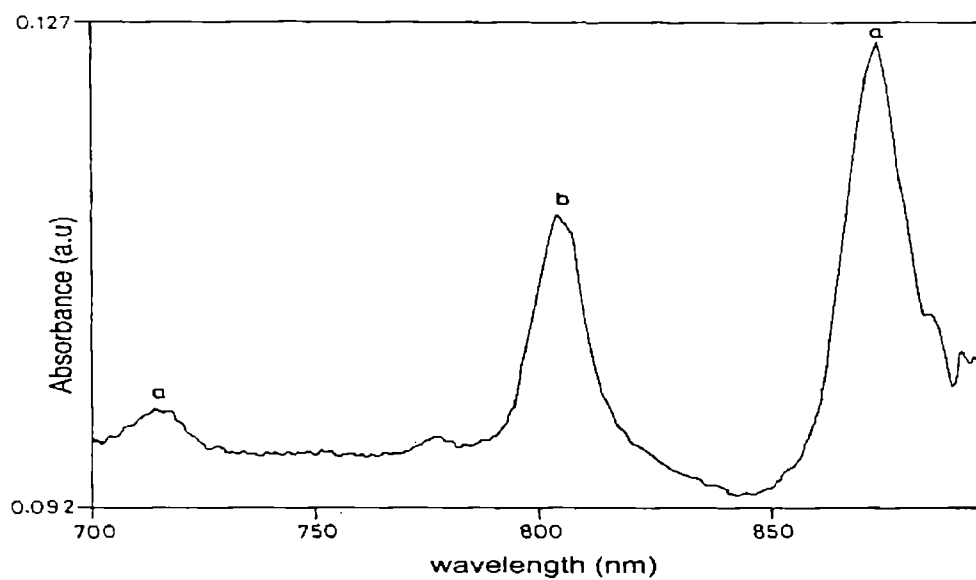
**Figure2.4** Ring C-H overtone peak in the ΔV= 4 and 5regions and N-H overtone peak in the ΔV=4 region of benzyl amine.
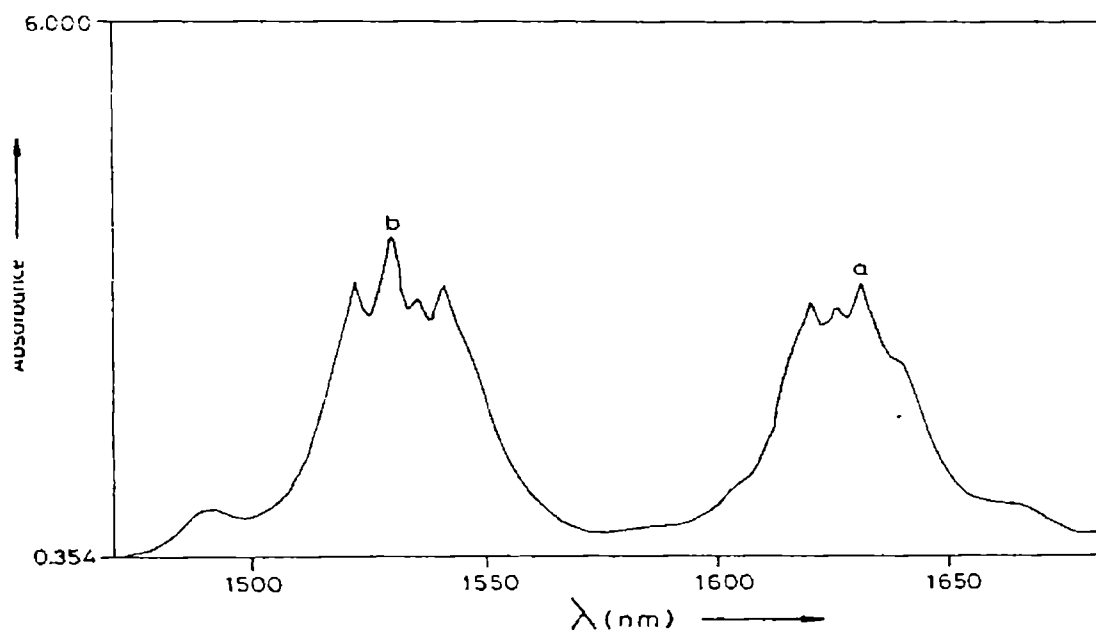


**Figure2.5** Ring C-H and side group N-H band structures of furfuryl amine in the ΔV=2 region. The pure overtone peak of C-H is marked as 'a' and that of N-H is marked as 'b'.

42

**Figure 2.6** Ring C-H and N-H overtone peaks of furfuryl amine in the $\Delta V = 3$ region; 'c' represent methylene C-H overtone peak of furfuryl amine in the $\Delta v = 3$ region.
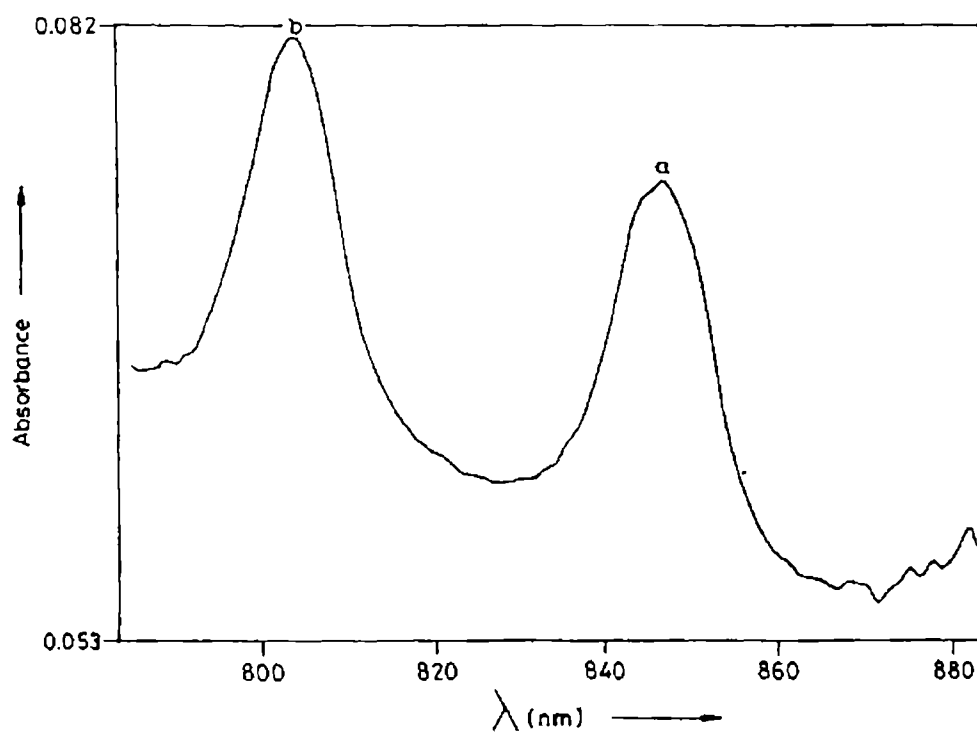


**Figure 2.7** Ring C-H and N-H overtone peaks of furfuryl amine in the $\Delta V = 4$ region.

As can be read from Table2.1, the ring C-H mechanical frequency in furfuryl amine is much larger than that in benzyl amine (Table 2.1). Specifically the ring C-H mechanical frequency in benzyl amine is smaller than in benzene by ~ 9cm$^{-1}$ whereas the corresponding reduction in furfuryl amine with respect to furan is ~ 24cm$^{-1}$. The reduction in ring C-H mechanical frequency is expected in both the compounds due to the electron donating nature of the $-CH_2NH_2$ group ($\sigma$ = -0.15). The reduction in furfuryl amine with respect to furan is much larger (by ~15cm$^{-1}$) than the corresponding reduction in benzyl amine with respect to benzene. If the difference in reduction of ring C-H mechanical frequency occurs due to the difference in the amount of electron donation by the $-CH_2NH_2$ group to the two rings, it must follow that the heterocyclic ring and phenyl ring affect the $-CH_2NH_2$ group differently. Consequently one can expect a difference in the density of nitrogen lone pair electrons between the two molecules, which in turn can be expected to cause a difference between the values of the local mode parameters of the $NH_2$ groups of the two compounds. An inspection of the Table1 however shows that the N-H local mode parameters of the $-CH_2NH_2$ side chain do not show much difference between the two compounds. The C-H local mode parameters of the side chain are also similar in the two compounds. This observation clearly indicates that the hetrocyclic and the phenyl rings have almost similar effect on the $-CH_2NH_2$ side chain group. Thus we conclude that the amount of electron density donated by the $-CH_2NH_2$ group in either case is almost equal.

The observed difference in the reduction of ring C-H mechanical frequency in the two compounds with respect to their parent compounds can be explained as follows. Assuming that the electron density donated by the $-CH_2NH_2$ group is equal in both the molecules and is shared by six carbon sites in benzyl amine and by four carbon sites by in furfuryl amine, thus increasing the effective electron density per carbon site in the latter compound, which causes an increased reduction of ring C mechanical frequency in furfuryl amine with respect to furan compared to that in benzyl amine with respect to benzene.

The N-H local mode mechanical frequency in aniline [29] is 3550cm$^{-1}$, which is much larger than that in benzyl amine (~ 45cm$^{-1}$) and furfuryl amine (~ 40cm$^{-1}$). It is well

known that in the unperturbed molecule aniline the ring part acts as an electron sink and so the unshared electron lone pair of the nitrogen atom gets conjugated with the electron cloud of the benzene ring. The electronic valence structure of N-atom of aniline molecule assumes the configuration of quatrivalent positive [$=N^+<$] atom doubly bonded to the carbon atom of the ring. This increases the contributions of the $\sigma$ electrons of the N-atom to the N-H bond and thus strengthens the N-H bond. So the high value of N-H frequency in the unperturbed aniline molecule is brought about by the strong electronic displacement from the $NH_2$ part to the ring part mentioned as above. But in benzyl amine and in furfuryl amine the conjugation between the ring and amino part is interrupted due to the presence of $CH_2$ group in between them and hence no displacement of electron density can take place. Therefore the N-H frequency in these compounds is considerably less than that in aniline.

In conclusion, the values the local mode parameters of the ring C-H and N-H oscillators indicate that the electron donation from the-$CH_2NH_2$ group to the aromatic ring is similar in either molecule. The hetero oxygen atom in furfuryl amine is thus not involved in any interaction to the -$CH_2NH_2$ group attached to the ring. The hetero oxygen atom in furfuryl amine plays the same role as in furan, namely electron withdrawal from the ring carbon sites causing increase in ring C-H mechanical frequency with respect to that in benzyl amine.

## 2.4 Overtone spectrum of 2-furaldehyde
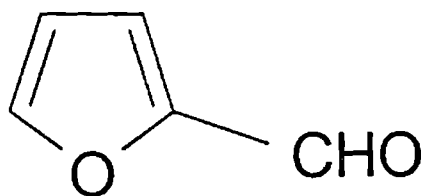


Figure 2.8 The molecular Structure of furfural

The observed overtone absorption spectra of 2-furaldehyde (furfural) in the spectral regions of quantum levels V = 2 to V= 4 are shown in Figures 2.9-2.12. The regions that show multiple peaks arise from combination bands, and we could assign the

pure overtone peaks from the structures as those giving good least square fit for the Birge-Sponer plot with the pure overtone peaks in the other regions. The peak positions, corresponding transition energies, their assignments, and the calculated local mode parameters of the ring and aldehydic C-H oscillators are given in Table1. The C-H local mode parameters of benzaldehyde [30], furan [22] and benzene [21] are also given in Table 2. 2.

Table 2.2 Observed overtone transition energy values ($cm^{-1}$), mechanical frequency $X_1$ ($cm^{-1}$), and anharmonicity $X_2$ ($cm^{-1}$) of ring and aldehydic C-H in furfural. The least square correlation coefficients ($\gamma$) are also given. The mechanical frequency and anharmonicity values of benzaldehyde, furan and benzene are also given for a comparison.

| Molecule | $\Delta v{=}2$ | $\Delta v{=}3$ | $\Delta v{=}4$ | $X_1$ | $X_2$ | $\gamma$ |
|---|---|---|---|---|---|---|
| **Furfural** | | | | | | |
| Ring CH | 6165.2 | 9053.9 | 11846.9 | 3262.5 | -60.4 | -0.9992 |
| Aldehyde CH | 5482.2 | 8047 | 10516.4 | 2908.1 | -60.0 | -0.9996 |
| **Furan** | | | | 3259 | -59 | |
| **Benzaldehyde** | | | | | | |
| Ring CH | | | | 3172 | -60 | |
| Aldehyde CH | | | | 2857.4 | -54.6 | |
| **Benzene** | | | | 3148.1 | -57.6 | |

As already stated in the earlier section, it is established that the ring C-H mechanical frequency in heterocyclic compounds is affected by the presence of hetero atom in the ring and also the substituent group attached to the ring. In general it appears that the effect of electron donating group substituted in a heterocyclic molecule is in

accordance with the expectations based on similar results in substituted benzenes. However, the results in some heterocyclic compounds show evidence for direct interaction between the substituent and the ring hetero atom [31]. As explained below, a comparison of the present results for furfural with those reported for its six membered analogue benzaldehyde reveals that the electron withdrawing effect of the aldehyde substituent group on the ring C-H oscillators is strongly influenced by the oxygen hetero atom present in furfural.

Since furfural is a substituted furan molecule (Figure 2.8), the frequency shifts of the ring C-H overtone from that of furan manifest the effect of aldehyde group on the ring. It is observed that the ring C-H mechanical frequency and anharmonicity constant for furfural are not much different from that of furan. But the title molecule's six membered counterpart benzaldehyde shows an increased value of ring C-H mechanical frequency ($\sim$24cm$^{-1}$) and anharmonicity ($\sim$2.4cm$^{-1}$) with respect to benzene and is attributed to the electron withdrawing property of the aldehyde group. We propose the following explanation for the observed ring C-H mechanical frequency in furfural. For a moderately strong electron-withdrawing group like aldehyde the interaction occurs mainly due to its inductive effect. The strongly electronegative oxygen atom present in the furfural ring withdraw electron by induction from the ring. The inductive effect of ring oxygen is different at 2 and 3 positions of the ring. At the 2- position the short-range induction has a strong electron withdrawal property. So the deviation observed for the electron withdrawing substituent is presumably due to a direct inductive interaction between the substituent and the ring oxygen atom. The inductive value of the Hammet $\sigma$ supports our assumption. At the 2-position the $\sigma$ value for the heteroatom oxygen is +0.32 [32] and that of substituent aldehyde is +0.35 [15].
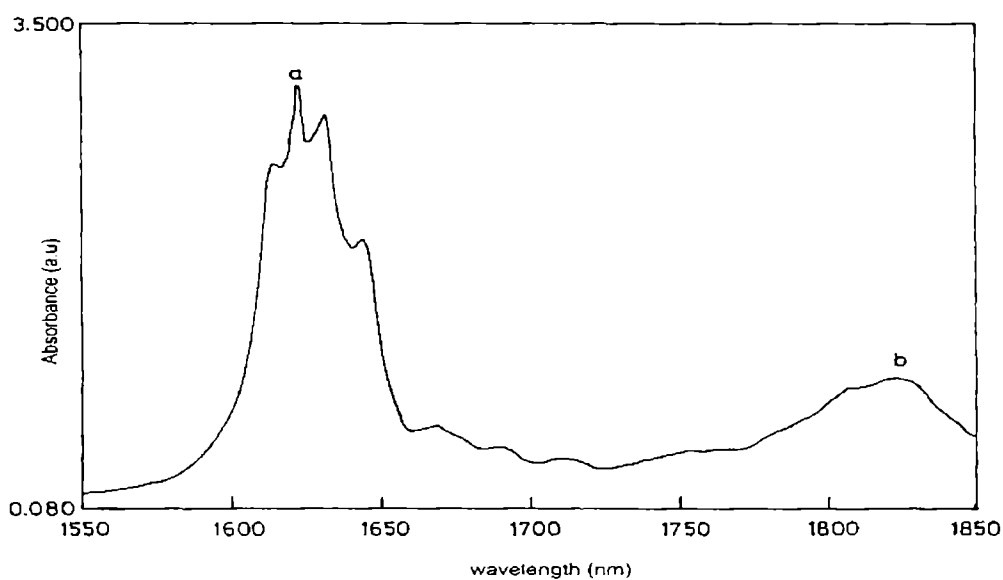
**Figure 2.9** Ring and aldehydic C-H band structures of furfural in the ΔV=2 region. The pure overtone peak of ring C-H is marked as 'a' and that of aldehydic C-H is marked as 'b'.
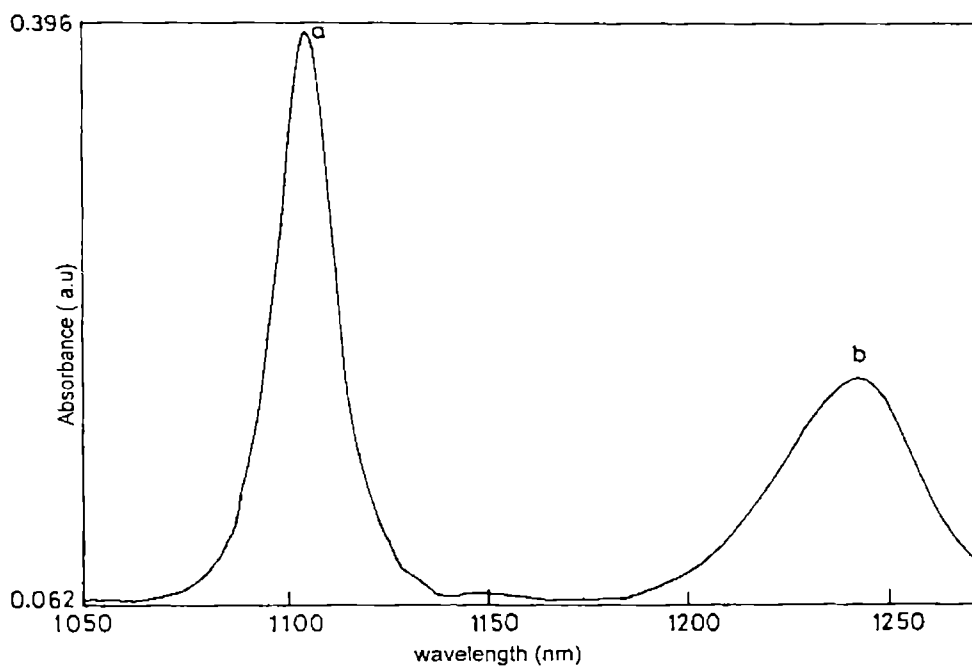


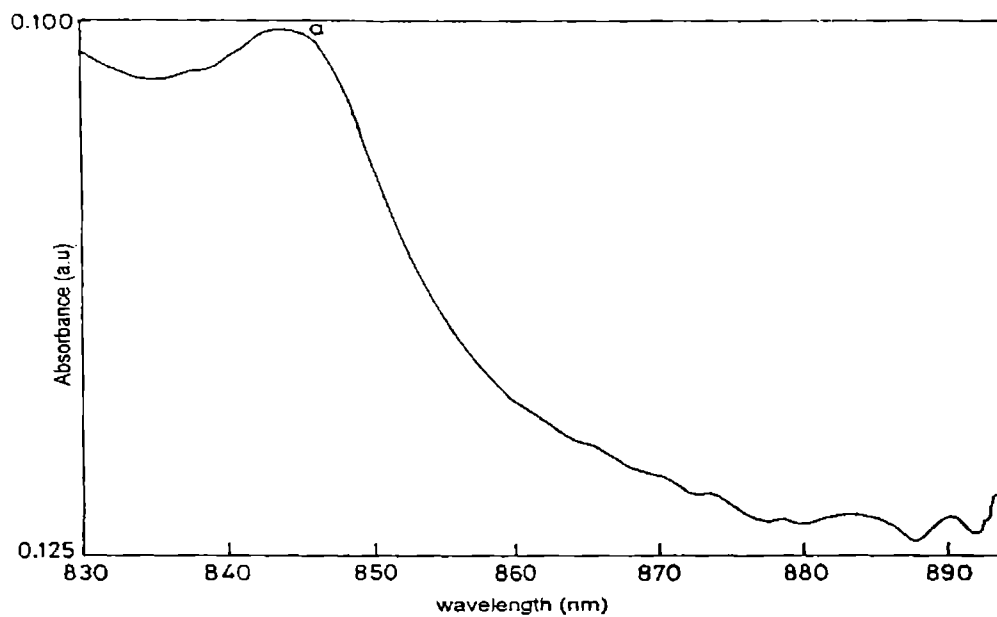**Figure 2.10** Ring ('a') and aldehydic ('b') C-H overtone peaks of furfural in the ΔV=3 region.

48

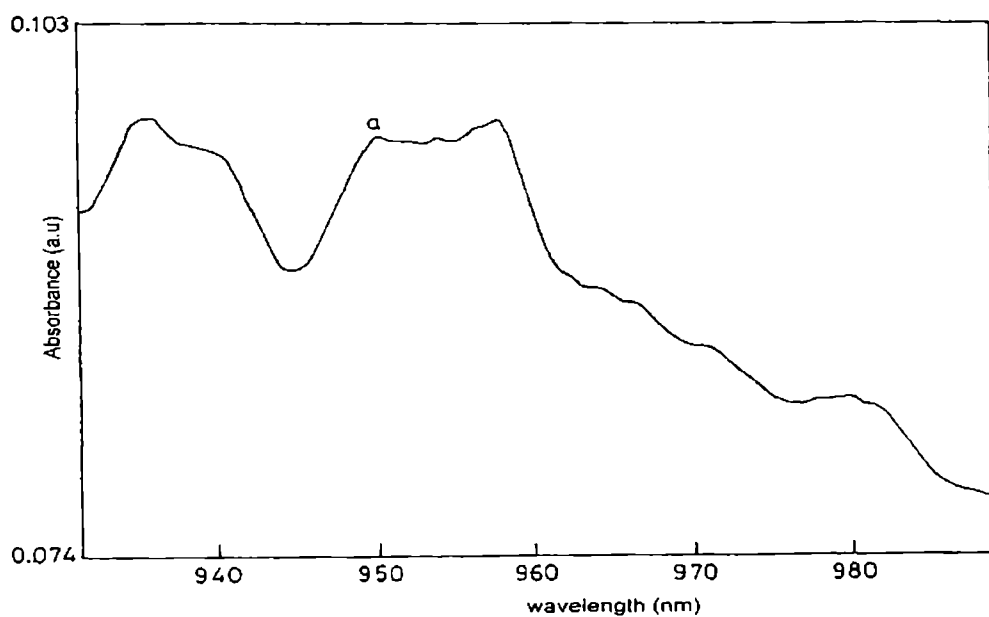**Figure 2.11** Ring C-H overtone peak of furfural in the $\Delta V = 4$ region.



**Figure 2.12** Aldehydic C-H overtone peak of furfural in the $\Delta V = 4$ region.

The observed values of aldehydic mechanical frequency and anharmonicity in furfural are 2908 cm$^{-1}$ and -60 cm$^{-1}$ whereas the corresponding values in benzaldehyde are 2857 cm$^{-1}$ and -54.6 cm$^{-1}$ respectively. The large value of mechanical frequency (~51 cm$^{-1}$ more than in benzaldehyde) in furfural is explained as follows. As mentioned earlier, the inductive effect of the ring oxygen at the 2 position in furfural reduces the electron withdrawing ability of aldehydic group considerably. Hence the charge conjugation between the ring and the aldehydic group becomes less. This reduces the electron density of the aldehyde group in furfural causing an increase in mechanical frequency. However, the aldehydic C-H mechanical frequency value in furfural is less than that in formaldehyde (2965cm$^{-1}$) [33]. The decreased value of C-H mechanical frequency in furfural with respect to formaldehyde is in accordance with the small conjugation present between the ring and aldehyde group and the increased lone pair trans effect when an aldehydic group attached to an aromatic ring.

In conclusion, the near infrared vibrational overtone spectra of liquid phase 2-furaldehyde is measured spectrophotometrically and analyzed using local mode model. It is observed that the effect of substitution of the electron-withdrawing group at 2- position of furan is appreciably affected due to the presence of the hetero oxygen atom. The substituent exerts their effect predominantly through inductive effect revealing the strong influence of short-range induction by the heteroatom. Though the substituent effect on the ring part is understandable, a deeper understanding of the nature of the interaction requires further detailed comparative study with the results for other heterocyclic compounds.

## 2.5 Overtone spectrum of cinnamaldehyde

The cinnamaldehyde molecule contains three different types of CH bonds - aryl, olefinic and aldehydic (Figure 2.13). However, it is known that the overtones of the aryl and olefinic CH bonds appear in the same spectral region [34]. A greater s electron contribution to the olefinic C-H bonds causes them to have higher overtone energies than alkanes. Hence in a molecule like cinnamaldehyde, which contains both aryl and olefinic part, the olefinic

C-H overtones are masked by the more intense ring C-H overtones. Hence the observed spectrum resembles that of benzaldehyde – it shows only two overtone progressions corresponding to aryl and aldehydic C-H local modes. A comparison between the spectral data of cinnamaldehyde and benzaldehyde reveals that the mechanical frequency and the inharmonicity constants of both aryl and aldehydic C-H oscillators are higher in cinnamaldehyde.
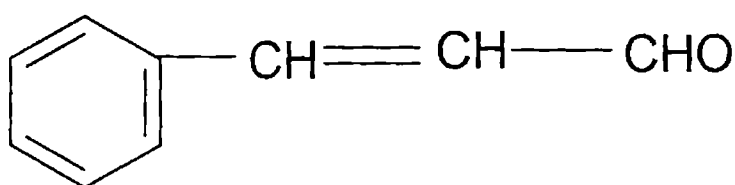


**Figure 2.13** The molecular structure of cinnamaldehyde.

The observed overtone absorption spectra of the aryl and aldehydic C-H local modes of cinnamaldehyde in the spectral regions of quantum levels V=2 to V=4 are shown in Figures 2.14 -2.18. The regions that show multiple peaks arise from combination bands; we could assign the pure overtone peaks from the structures as those giving good least square fit for the Birge-Sponer plot with the pure overtone peaks in the other regions. The peak positions, their assignments, corresponding transition energies and the calculated values of the local mode parameters and the dissociation energies of the ring and aldehydic CH oscillators, are given in Table2.3. The C-H local mode parameters of benzaldehyde [30] and benzene [21] are also given for a comparison.
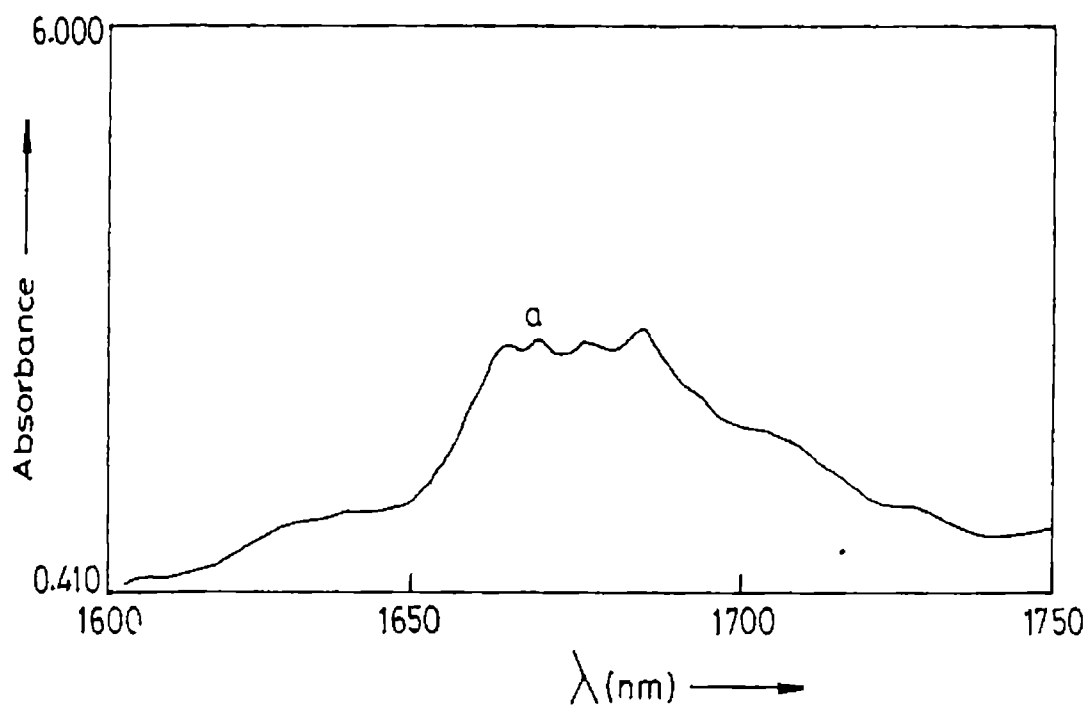
**Figure 2.14** Aryl C-H band structures of cinnamaldehyde in the $\Delta V=2$ region.
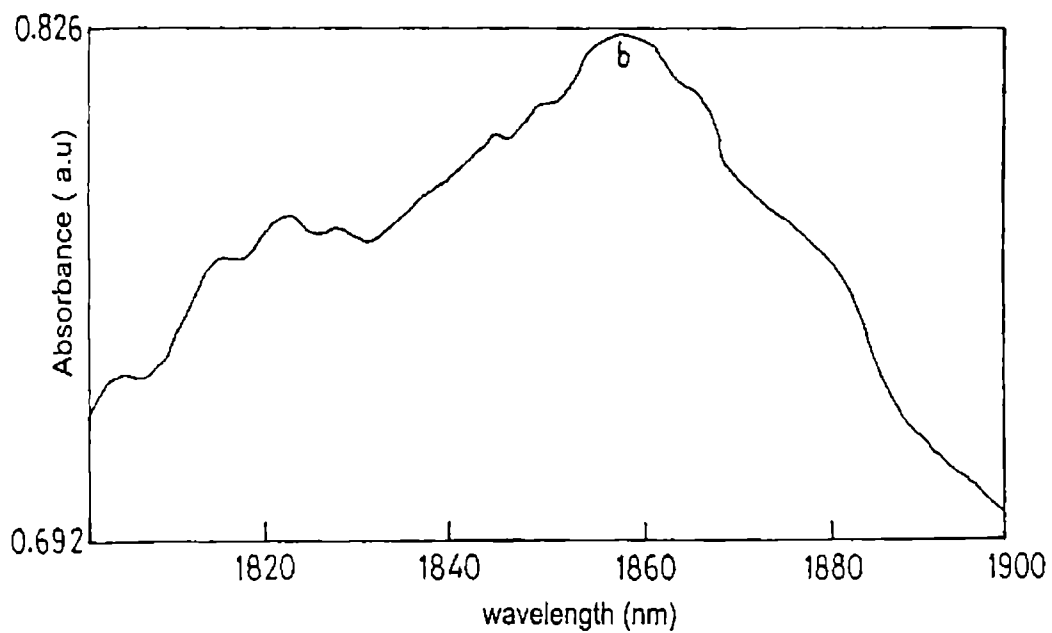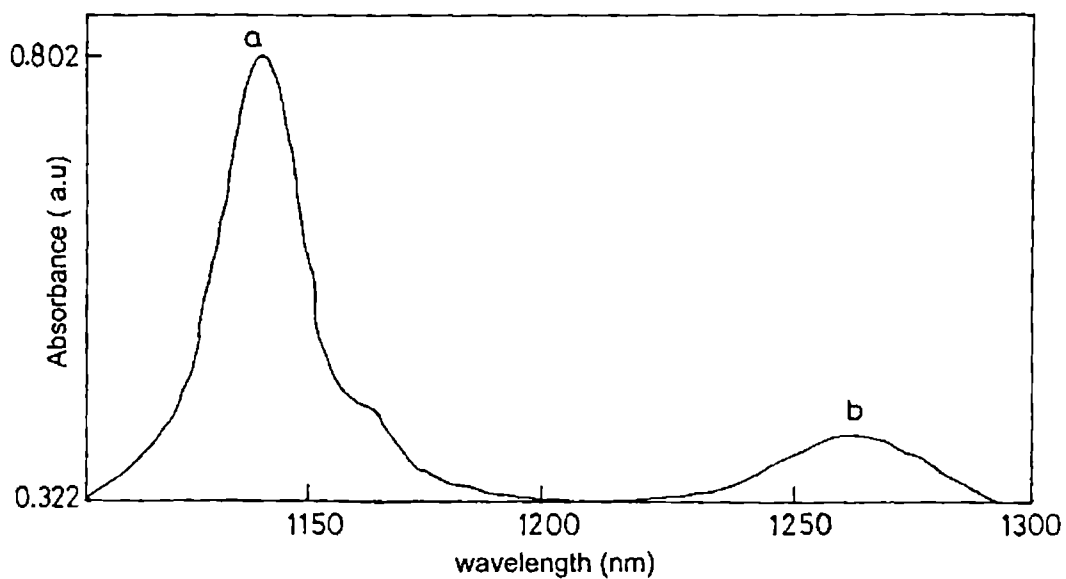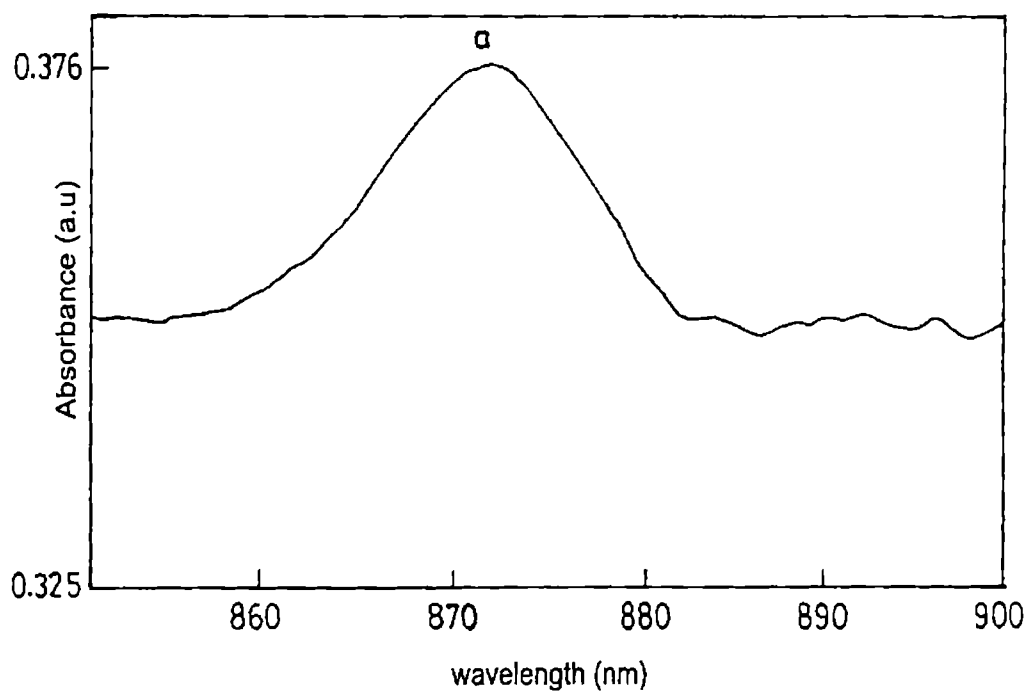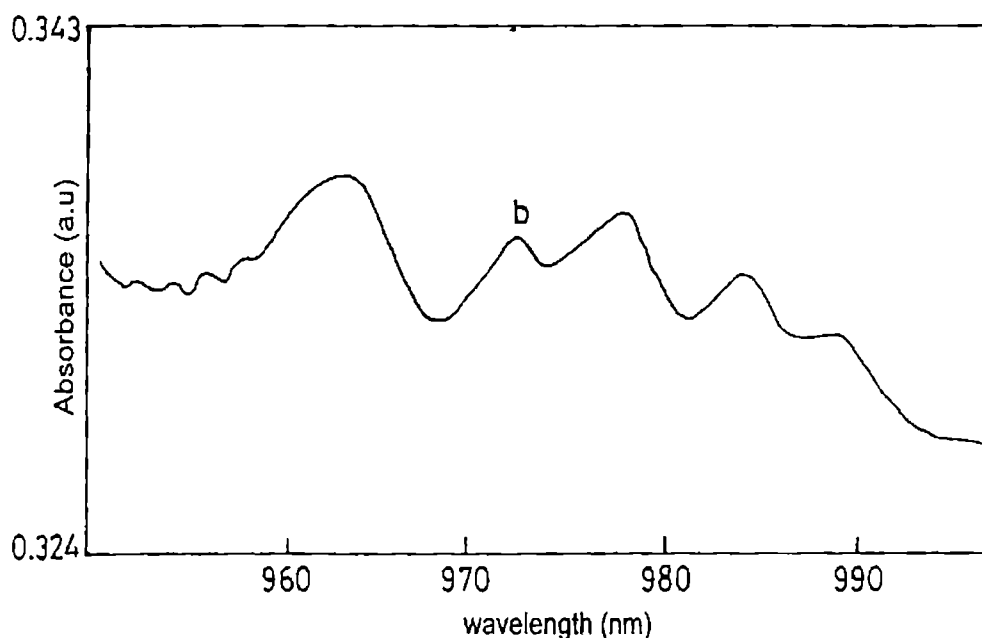


**Figure 2.15** Aldehydic C-H overtone peak of cinnamaldehyde in the $\Delta V=2$ region.

**Figure 2.16** Aryl and aldehydic C-H overtone peaks of cinnamaldehyde in the $\Delta V = 3$ region. The pure overtone peak of aryl C-H is marked as 'a' and that of aldehydic C-H is marked as 'b'



**Figure 2.17** Aryl C-H overtone peak of cinnamaldehyde in the $\Delta V = 4$ region

**Figure 2.18** Aldehydic C-H overtone peak (b) of cinnamaldehyde in the $\Delta V = 4$ region.

An understanding of the nature of interactions between the olefinic CH bonds will be useful in the interpretation of the overtone spectra of cinnamaldehyde molecule. Jasinski [35] analyzed the coupling between local mode oscillators attached to the same carbon atom, while analyzing the fifth overtone spectra of ethylene and deuterated ethylenes. Cinnamaldehyde molecule is obtained when a -CHO group replaces one of the terminal olefinic hydrogen atoms in styrene. Mizugai and Katayama [15] observed that no frequency shift occurs when an ethylenic group (-CH=CH₂) is substituted in benzene, which means that aryl CH oscillators in benzene and styrene are similar. But, further substitution either in the ring or olefinic part of styrene changes the mechanical frequency and anharmonicity of the aryl C-H oscillators [36]. Our main interest in this study is to understand the way in which the ring and aldehydic C-H local modes are affected when an olefinic part appear in between the ring and aldehyde group. As explained below, a comparison of the local mode parameters of cinnamaldehyde with those of benzaldehyde leads to specific conclusions in this direction.

**Table 2.3** Observed values of overtone transition energies (cm$^{-1}$), mechanical frequencies $X_1$ (cm$^{-1}$), anharmonicities $X_2$ (cm$^{-1}$) and dissociation energies of ring and aldehydic C-H local modes in cinnamaldehyde. The parameter ($\gamma$) is the least square correlation coefficient for the Birge-Sponer plot. The mechanical frequencies and anharmonicities of benzaldehyde and benzene are also given for a comparison.

| Molecule | $\Delta v=2$ | $\Delta v=3$ | $\Delta v=4$ | $X_1$ | $X_2$ | $\gamma$ | D |
|---|---|---|---|---|---|---|---|
| **Cinnamaldehyde** | | | | | | | |
| Ring CH | 5986.2 | 8778.9 | 11449.5 | 3188.7 | -65.4 | -0.99992 | 37309 |
| Aldehyde CH | 5393.7 | 7914.5 | 10293.36 | 2883.2 | -61.8 | -0.99959 | 32218 |
| **Benzaldehyde** | | | | | | | |
| Ring CH | | | | 3172 | -60 | | 40218 |
| Aldehyde CH | | | | 2857.4 | -54.6 | | 35969 |
| **Benzene** | | | | 3148.1 | -57.6 | | 41455 |

In cinnamaldehyde the aryl C-H mechanical frequency is increased by ~ 41 cm$^{-1}$ and anharmonicity constant by ~ 8 cm$^{-1}$ with respect to their values in benzene. The corresponding increase in benzaldehyde are ~ 24 cm$^{-1}$ and ~ 2.4 cm$^{-1}$ respectively. It is established from the overtone spectroscopic studies of substituted benzenes that the aryl CH mechanical frequency is increased due to electron withdrawing substituent [15-19]. This is because an electron-withdrawing substituent group reduces the electron density at the ring carbon sites. This results in a net positive charge on them thus increasing the force constant of the ring CH bands. The increase in mechanical frequency is expected for aryl aldehydes since the aldehyde group is an electron withdrawing substituent. But

the appreciably larger value of aryl CH mechanical frequency observed in cinnamaldehyde over benzaldehyde (by about 17cm$^{-1}$) cannot be attributed to the inductive effect of the aldehyde group alone. In the following, we explain this effect as a consequence of the extended conjugation present in cinnamaldehyde molecule. It is known that the resonance-stabilized conjugation between the benzene ring and the ethylenic double bond give the unusual stability of the styrene molecule [37]. The most preferred conformation of aldehydic group is also a conjugation-stabilized form [38]. Thus in cinnamaldehyde the $\pi$ electron system is spread over three groups, giving an extended conjugation. The lengthened $\pi$ electron system results in greater delocalization of the mobile electrons. Since both the ring and C=C are good sources of electrons, the greater delocalization increases the conjugation. Hence the extended conjugation decreases the electron density on aryl/olefinic carbon atoms and this causes an increase in the mechanical frequency of the aryl C-H oscillators. Thus the increased mechanical frequency of aryl C-H oscillators in cinnamaldehyde is not simply due to the electron withdrawing ability of the aldehydic group, but to the existence of the extended conjugated system that permits formation of the resonance stabilized structure. The present observation also shows that the aryl C-H oscillators in cinnamaldehyde are more anharmonic compared to benzaldehyde, which results in a reduced value of aryl C-H bond dissociation energy (Table 2.3).

The observed values of aldehydic C-H mechanical frequency and anharmonicity in cinnamaldehyde are $\sim$ 2883 cm$^{-1}$ and $\sim$ 62 cm$^{-1}$ respectively, whereas the corresponding values in benzaldehyde are $\sim$ 2857 cm$^{-1}$ and $\sim$ 55 cm$^{-1}$. The low C-H stretching frequencies characteristic of aldehydic group was explained as due to the donation of electron density from one of the lone pairs of carbonyl oxygen situated trans to the aldehydic C-H bond into its anti-bonding ($\sigma^*$) orbital [6,39,40]. The extent of donation of the non-bonding electron pair density of the oxygen to the aldehydic CH anti-bonding orbital can be assumed to depend on C=O bond length [41]. In cinnamaldehyde, the extended $\pi$ electron conjugation of the carbonyl group to the ethylenic double bond /benzene ring causes an increase in C =O length due to increased $\pi$ electron flow from the olefinic/aryl part to aldehyde compared to benzaldehyde. Hence one can expect a decrease in lone pair trans effect and a corresponding small increase of aldehydic CH

mechanical frequency in cinnamaldehyde over benzaldehyde. But the large difference (~ 26cm$^{-1}$) observed cannot be explained by this effect alone; we propose the following explanation for the observation. In a molecule like acetaldehyde the aldehydic C-H bond interacts with an in plane methyl C-H bond through an indirect lone pair effect; the aldehydic C-H bond, which is originally influenced by the lone pair trans effect of the carbonyl oxygen, donate electron density from its σ*orbital to the σ*orbital of the adjacent in plane C-H bond. This effect is absent in benzaldehyde as the aldehydic group is directly attached to the phenyl ring. But in cinnamaldehyde, the aldehydic group is attached to phenyl ring through ethylenic part and hence one can expect that the indirect lone pair effect is active in this molecule, i.e., the aldehydic C-H bond can be expected to involve in an interaction with an in plane ethylenic CH bond. Thus it is clear that the aldehydic C-H bond is now subjected to a reduced lone pair trans effect, which results in an increase in its mechanical frequency value. As can be read from table 2.3, the aldehydic C-H oscillator in cinnamaldehyde becomes more anharmonic compared to that of benzaldehyde. Hence, even though the mechanical frequency of aldehydic C-H is higher in cinnamaldehyde the bond dissociation energy is found to be smaller than that in benzaldehyde.

To conclude, the near infrared vibrational overtone spectra of liquid phase cinnamaldehyde is measured spectrophotometrically and analyzed using local mode model. The analysis of the aryl C-H bonds in cinnamaldehyde reveals that substitution of an electron-withdrawing group on the olefinic part of the molecule appreciably influences the ring C-H mechanical frequency and anharmonicity values. This observation is explained as due to the presence of extended conjugation in the side chain. The large value observed for aldehydic C-H mechanical frequency is attributed as mainly due to the presence of indirect lone pair trans effect.

## 2.6 Overtone spectrum of benzoyl chloride

The liquid phase overtone spectra of the aromatic acid chloride- benzoyl chloride ($C_6H_5$-COCl) in the region $\Delta V_{CH}$= 2-5 are shown in figures 2.20- 2.21. The major peaks observed in the overtone spectra are due to the ring C-H bonds. The peak positions, assignments and the local mode parameters obtained from Birge-Sponer plot are given in

Table 2.4. The CH local mode parameters reported for liquid benzene [21] are also given in the table.
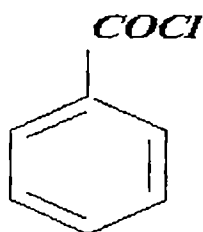
$$COCl$$



**Figure 2.19** Molecular structure of benzoyl chloride

The aryl peak positions of benzoyl chloride are blue shifted with respect to those of benzene. It can be seen from the Table 2.4 that this blue shift in overtone energy is due to an increased mechanical frequency of the ring CH bonds compared to that in benzene, consequent to the electron withdrawing effect of the COCl group.

**Table 2.4** Observed overtone energies ($cm^{-1}$), their assignments, mechanical frequency $X_1$ ($cm^{-1}$) and anharmonicity $X_2$ ($cm^{-1}$) of aryl CH local modes in benzoyl chloride. The corresponding data for benzene [21] and benzaldehyde [30] are also given for a comparison.

| Molecule | $\Delta V=2$ | $\Delta V=3$ | $\Delta V=4$ | $\Delta V=5$ | $X_1$ | $X_2$ | $\gamma$ |
|---|---|---|---|---|---|---|---|
| Benzene | 5983 | 8760 | 11442 | 14015 | 3148.1 | -57.6 | |
| Benzoyl chloride | 6003 | 8827 | 11534 | 14130 | 3176.5 | -58.5 | -0.99998 |
| Benzaldehyde | 5986 | 8791 | 11486 | 14060 | 3172.2 | -60.2 | -0.9999 |

Benzoyl chloride molecule is obtained from benzaldehyde molecule when a chlorine atom replaces the aldehydic hydrogen atom. It is known that the aldehydic oxygen atom draws electron from both the ring and the aldehydic hydrogen atom.

58

However the electron withdrawal from the aldehydic hydrogen atom is counter acted by the back-donation process due to the lone pair trans effect described in earlier sections. The net effect is an effective donation of electron density to the $\sigma^*$ orbital of the aldehydic C-H bond [39,40]. It is clear that the high electronegativity of the chlorine atom makes it hard for the oxygen to draw electrons from the chlorine and hence draw more electrons from the ring part. Moreover, the lone pair trans effect operative in benzaldehyde will also be absent in benzoyl chloride. We can thus conclude that the electron withdrawal from the aromatic ring is similar in the two compounds. From Table 2.4 it is observed that the aryl C-H mechanical frequency in benzoyl chloride is close to that in benzaldehyde. This result agree with those of previous studies, which indicate that the action of the functional groups (-COCl and -CHO) remain essentially the same, being governed by the electron withdrawal power of the carbonyl group [41].
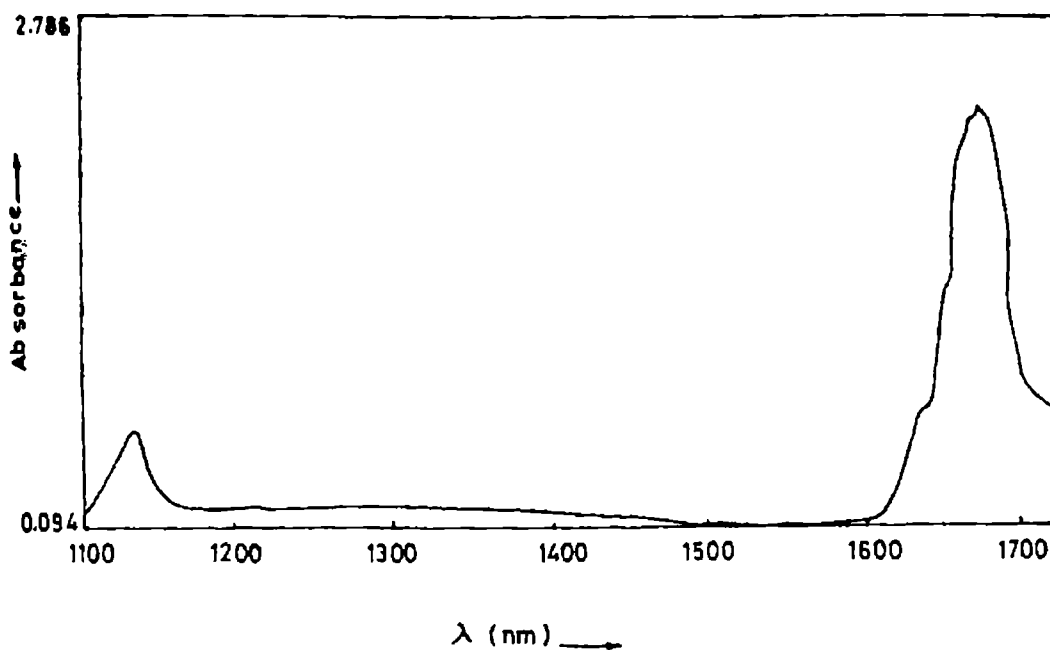


Figure 2.20 Ring C-H overtone spectrum of benzoyl chloride in the $\Delta V=$ 2 and 3 regions
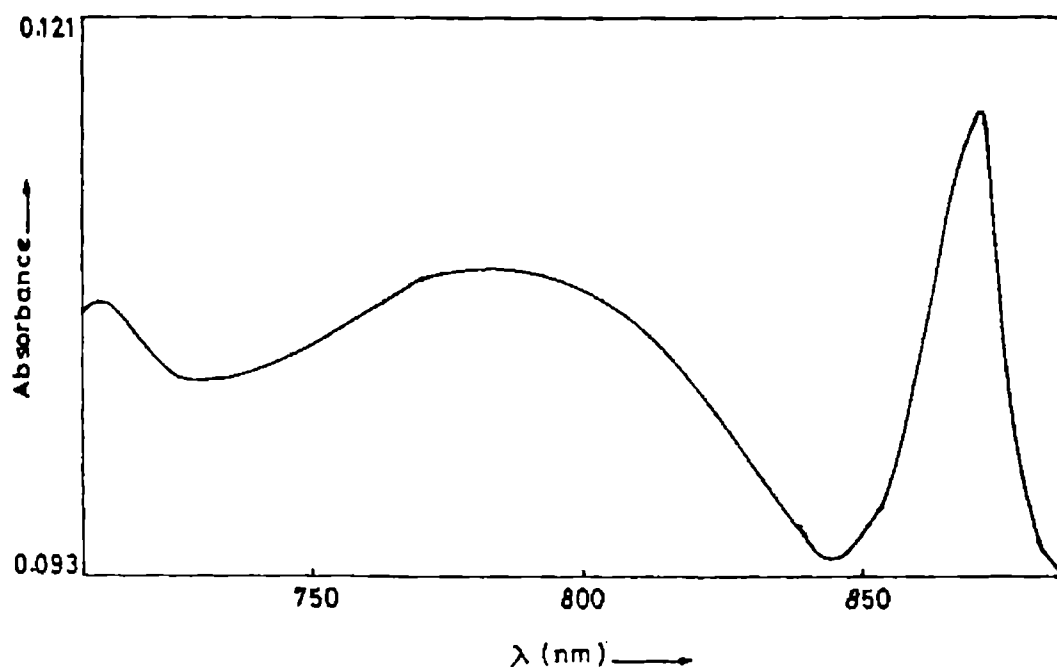
**Figure 2.21** Ring C-H overtone spectrum of benzoyl chloride in the $\Delta V = 4$ and 5 regions

## 2.7 Overtone spectra of methoxy molecules

As outlined in the earlier chapters, the local mode parameters and hence the overtone spectra are sensitive to the intramolecular environment of the X-H oscillator as well as the conformational state of the molecule. Methoxy group exhibits some internal rotational freedom, which can produce changes in properties of the molecule. In addition, methoxy group may give rise to $\pi$-electron conjugation with the aromatic system. Due to the non-bonding electron density at the oxygen atom the methoxy group is also able to form hydrogen-bonded networks. A number of methoxy molecules and their conformational orientations are important in governing the pharmacological properties of many drugs [41].

This section presents the overtone spectral investigations of some methoxy compounds namely, anisole, o-anisidine, p-anisidine and p-anisaldehyde (Figure 2.24). The study is aimed at examining the effect of the heteroatom oxygen on the methyl and aryl C-H bonds in relation to the conformational sensitivity of the molecules.
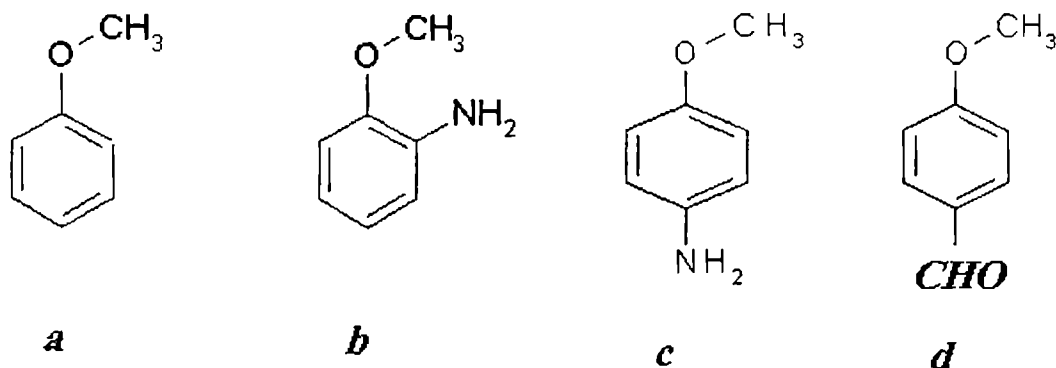


**Figure 2.22** Molecular structure of (a) anisole, (b) o-anisidine, (c) p-anisidine and (d) p-anisaldehyde

The near infrared spectra of the above compounds in the region 2000-700 nm show bands due to pure overtone transitions and also due to combination transitions involving several vibrational degrees of freedom. In the present analysis we consider pure overtone bands only. The overtone absorption spectra of anisole, o-anisidine, p-anisidine and p-anisaldehyde in the regions $\Delta V=2-5$ are shown in figures 2.25-2.40. Multiple peaks are observed in some overtone regions due to the presence of combination bands. We could assign the pure overtone peaks from these structures as the ones giving good least square fit for the Birge-Sponer plot with the pure overtone peaks in the other overtone regions. The peak positions, their assignments, corresponding transition energies, the calculated local mode parameters and dissociation energies of the ring C-H, methyl C-H, aldehydic C-H and N-H oscillators, are given in Tables 2.5-2.8. The ring C-H local mode parameters in all the compounds represent the

61

average value over the various non-equivalent ring C-H oscillators, as the observed liquid phase spectra do not show a corresponding resolved structure.

A substituent group can donate or withdraw electron density by induction or resonance. Mizugai and Katayama [15] observed the fifth overtones of aryl C-H stretching vibrations of more than 30 kinds of monosubstituted benzenes in the liquid phase using thermal lens technique. The studies revealed that the inductive effect of the substituent groups play the important role in causing the frequency shift. The inductive effect can be represented as the sum of contributions from 'through-bond' (withdrawal or donation of electrons depending on the electronegativity of the substituent) and 'through-space' field effect [17]. The shift in the frequency of the ring C-H overtone from that of benzene is found to be proportional to the inductive value ($\sigma_I$) of the substituent. This result indicated that the resonance effect has little influence on deciding the substituent effect in monosubstituted benzenes. In a subsequent paper Mizugai et al [16] reported the fifth overtone spectra of the aryl C-H stretching vibrations in several disubstituted and tri-substituted benzenes measured by thermal lens technique in the liquid state. For disubstituted benzenes the frequency shifts of the aryl C-H vibrations from that of benzene are found to be proportional to the sum of the inductive contributions of the Hammet $\sigma$ values of the substituents. However, the studies also exposed that this additivity rule of the frequency shifts is violated in molecules like p-methyl anisole, p-xylene etc. This indicates that the effect of di-substitution of $OCH_3$, $CH_3$ and $COOCH_3$ is quite different from those of monosubstituted benzenes because of their different nature of the conjugation among the substituent and the benzene ring. The resonance effects also seem to play a major role in this case. In aromatic amines such as aniline the lone pair electrons on the nitrogen are delocalized into the aromatic $\pi$ system [29]. This stabilizes the free amine and the molecule become energetically favorable. The methoxy group exhibits some interesting phenomena [38]. In 2, 6-dimethyl anisole, the - $OCH_3$ group becomes perpendicular the plane of the benzene ring and thus the conjugation between the ring and the methoxy group is disturbed. If

62

the methoxy group is adjacent to a nitro group the methoxy group remains in the plane of the benzene ring and the latter turns perpendicular to the plane.

The aryl C-H overtones of all the methoxy compounds are blue shifted with respect to benzene, primarily due to an increased mechanical frequency value. A comparative analysis of the relative values of the aryl C-H local mode parameters of the methoxy compounds leads to the evaluation of the roles played by inductive and resonance effects.

The methyl C-H overtone bands of all the molecules studied show two distinctive absorption peaks at each overtone levels caused by the presence of two types of nonequivalent methyl C-H bonds. This observation is exactly similar to that made by Fang et al [43] in the overtone spectra of dimethyl ether and methanol where two methyl peaks are found to appear at each overtone level. As already outlined in chapter 1, the conformational nonequivalence of the methyl C-H bonds occurs due to the donation of electrons from the oxygen lone pairs into the σ antibonding orbital of the C-H bond oriented trans to the lone pair. The donation of electrons from the lone pair into an antibonding orbital of a trans C-H group causes decrease in the mechanical frequency of that C-H bond compared to the C-H bond which do not get the lone-pair contribution. Consequently the two out-of-plane C-H bonds of methyl groups in molecules like dimethyl ether and methanol have lower energy than those of the in-plane C-H [43]. As shown below, a comparative study of the values of the methyl C-H local mode parameters in the methoxy compounds helps us in evaluating the relative strength of the lone pair trans effect in them.

Table 2.5 Observed overtone transition energies (cm$^{-1}$), mechanical frequencies $X_1$ (cm$^{-1}$) and anharmonicities $X_2$ (cm$^{-1}$) of ring CH of anisole, o-anisidine, p-anisidine and p-anisaldehyde. The least square correlation coefficients ($\gamma$) are also given. The corresponding quantities for liquid phase benzene [26] are also shown for comparison.

| Molecule | $\Delta V=2$ | $\Delta V=3$ | $\Delta V=4$ | $\Delta V=5$ | $X_1$ | $X_2$ | $\gamma$ |
|---|---|---|---|---|---|---|---|
| Anisole | 5981 | 8794 | 11474 | 14049 | 3172.1 | -60.5 | -0.9993 |
| o-anisidine | 5967 | 8773 | 11452 | | 3166.9 | -60.9 | -0.9999 |
| p-anisidine | 5972 | 8797 | 11507 | | 3150.4 | -54.6 | -0.9999 |
| p-anisalde-hyde | 5988 | 8814 | 11532 | 14150 | 3157.1 | -54.6 | -0.9999 |
| Benzene | 5983 | 8760 | 11442 | 14015 | | 3148.1 | -57.6 |

Table 2.6 Observed overtone transition energies (cm$^{-1}$), mechanical frequencies $X_1$(cm$^{-1}$) and anharmonicities $X_2$ (cm$^{-1}$) of in-plane methyl CH of anisole, o-anisidine, p-anisidine and p-anisaldehyde. The least square correlation coefficients ($\gamma$) are also given.

| Molecule | $\Delta V=2$ | $\Delta V=3$ | $\Delta V=4$ | $\Delta V=5$ | $X_1$ | $X_2$ | $\gamma$ |
|---|---|---|---|---|---|---|---|
| Anisole | 5802 | 8548 | 11172 | 13691 | 3065.7 | -54.5 | -0.9998 |
| o-anisidine | 5805 | 8538 | 11146 | 13635 | 3079 | -58.6 | -0.9999 |
| p-anisidine | 5792 | 8519 | 11127 | | 3067.2 | -54.4 | -0.9999 |
| p-anisaldehyde | 5792 | 8527 | 11148 | | 3097.1 | -59.9 | -0.9999 |

**Table 2.7** Observed overtone transition energies ($\text{cm}^{-1}$), mechanical frequencies $X_1$ ($\text{cm}^{-1}$) and anharmonicities $X_2$ ($\text{cm}^{-1}$) of out-of-plane methyl CH of anisole, o-anisidine, p-anisidine and p-anisaldehyde. The least square correlation coefficients ($\gamma$) are also given.

| Molecule | $\Delta V=2$ | $\Delta V=3$ | $\Delta V=4$ | $\Delta V=5$ | $X_1$ | $X_2$ | $\gamma$ |
|---|---|---|---|---|---|---|---|
| Anisole | 5681 | 8362 | 10894 | 13330 | 3018.3 | -58.7 | -0.9994 |
| o-anisidine | 5688 | | 10886 | 13287 | 3030.5 | -62.0 | -0.9999 |
| p-anisidine | 5676 | 8314 | 10831 | | 3032.6 | -65.1 | -0.9999 |
| p-anisaldehyde | 5751 | 8422 | 10949 | | 3082.8 | -69.0 | -0.9999 |
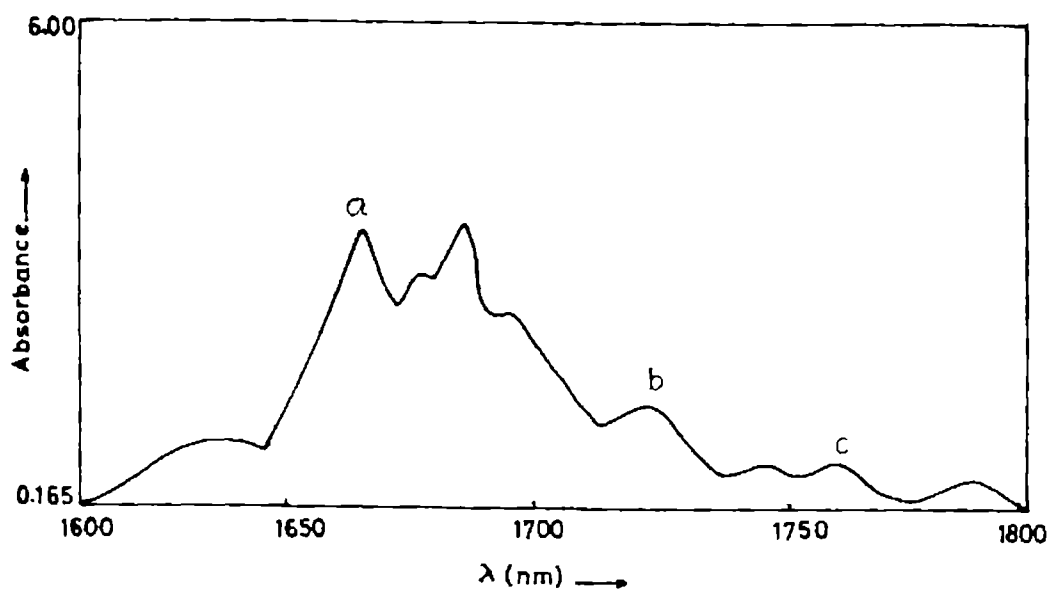
**Figure 2.23** Overtone spectrum of anisole in the ΔV=2 region (peak 'a' represents ring CH, 'b' in-plane methyl CH and 'c' out-of-plane methyl CH overtone bands)
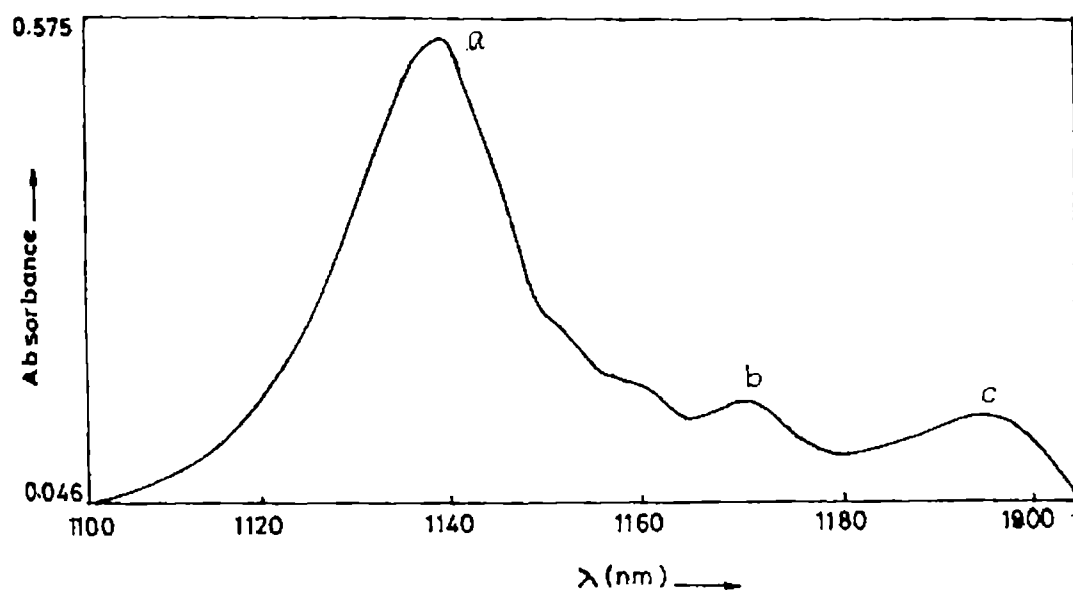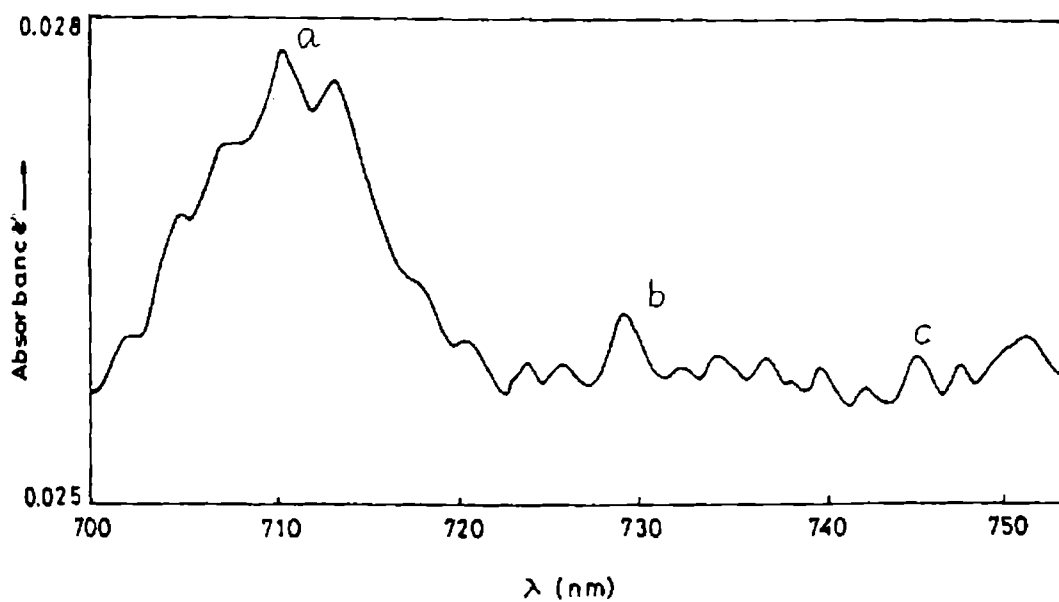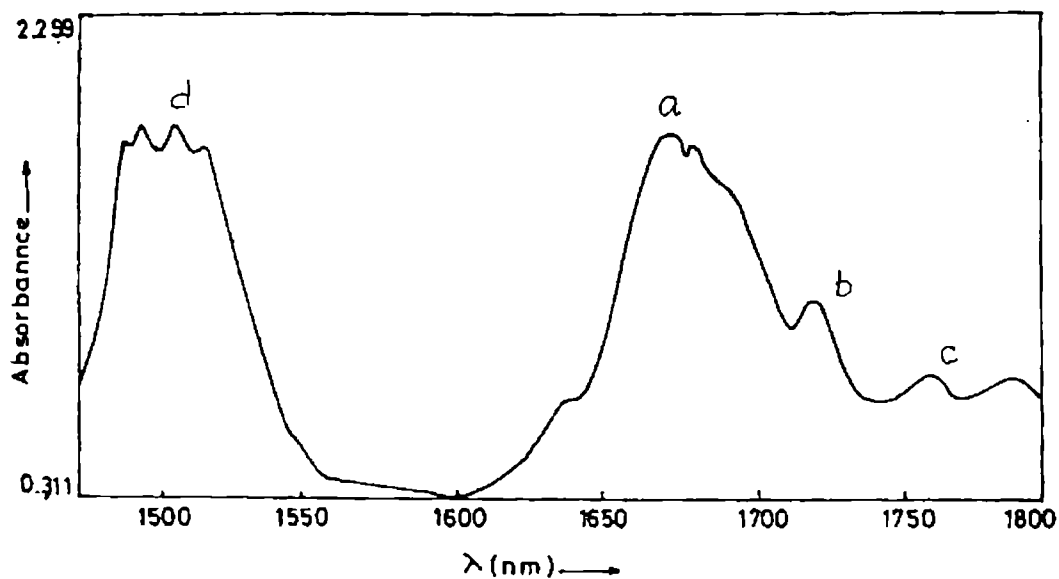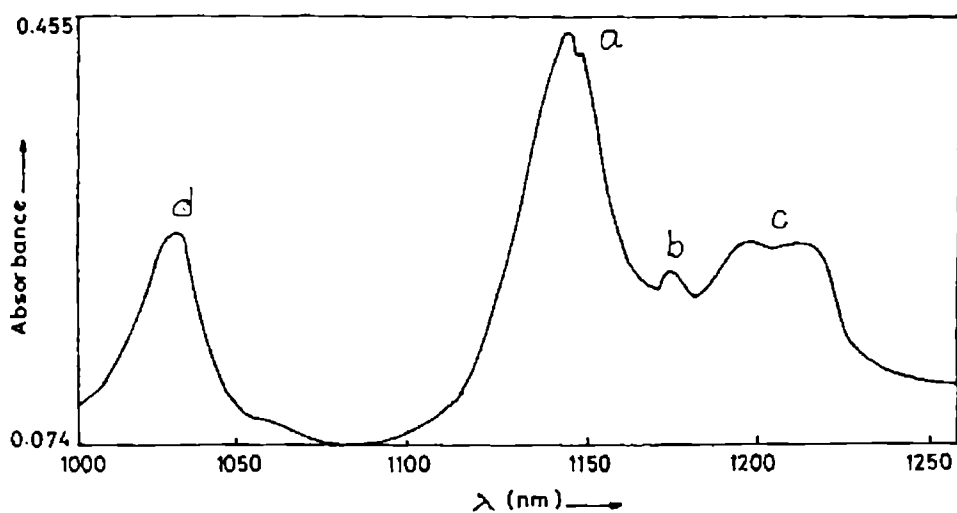


**Figure 2.24** Overtone spectrum of anisole in the ΔV=3 region (peak 'a' represents ring CH, 'b' in-plane methyl CH and 'c' out-of-plane methyl CH overtone bands)

66
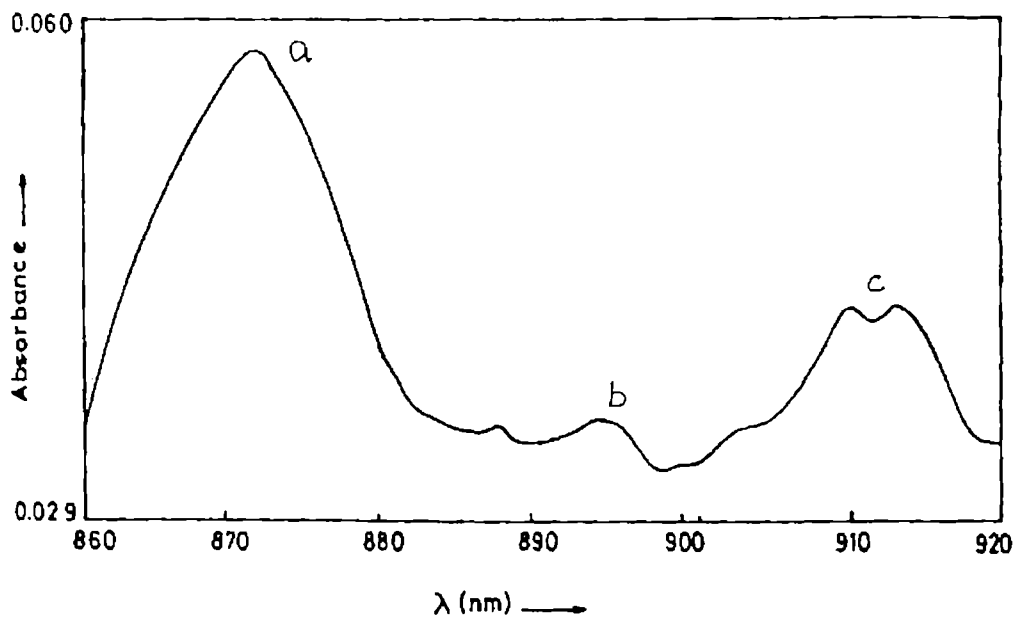
**Figure 2.25** Overtone spectrum of anisole in the $\Delta V=4$ region (peak 'a' represents ring CH, 'b' in-plane methyl CH and 'c' out-of-plane methyl CH overtone bands)



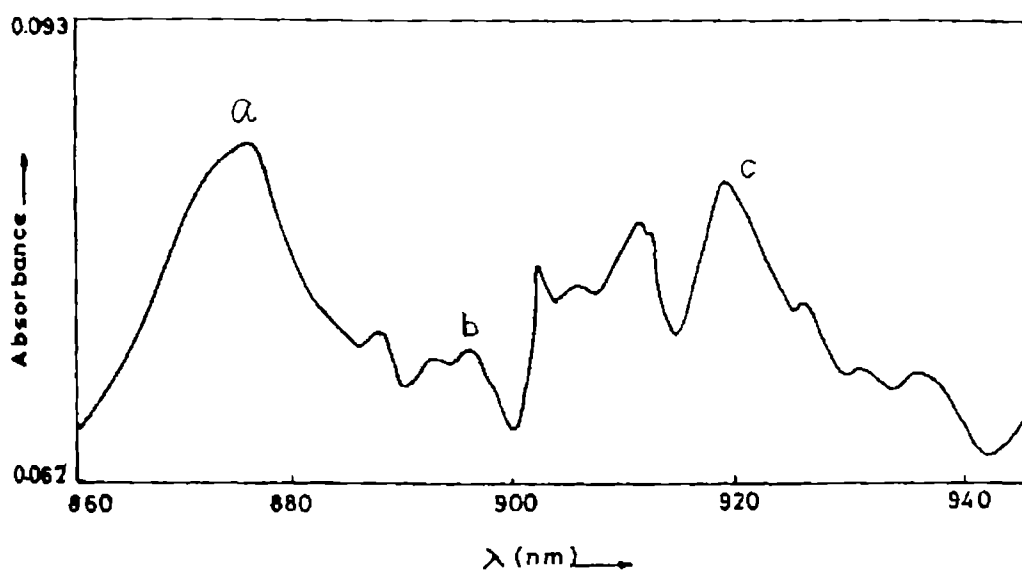**Figure 2.26** Overtone spectrum of anisole in the $\Delta V=5$ region (peak 'a' represents ring CH, 'b' in-plane methyl CH and 'c' out-of-plane methyl CH overtone bands)

**Figure 2.27** Overtone spectrum of o-anisidine in the ΔV=2 region (peak 'a' represents ring CH, 'b' in-plane methyl CH, 'c' out-of-plane methyl CH and 'd' represents NH overtone peak)



**Figure 2.28** Overtone spectrum of o-anisidine in the ΔV=3 region (peak 'a' represents ring CH, 'b' in-plane methyl CH and 'c' out-of-plane methyl CH and 'd' represents NH overtone bands)

**Figure 2.29** Overtone spectrum of o-anisidine in the $\Delta V=4$ region (peak 'a' represents ring CH, 'b' in-plane methyl CH and 'c' out-of-plane methyl CH overtone bands)
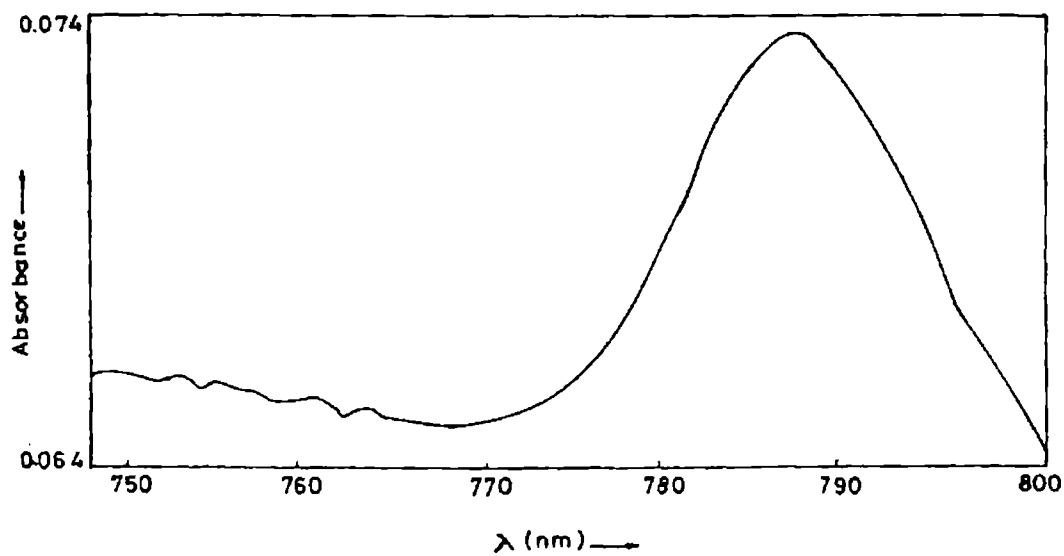


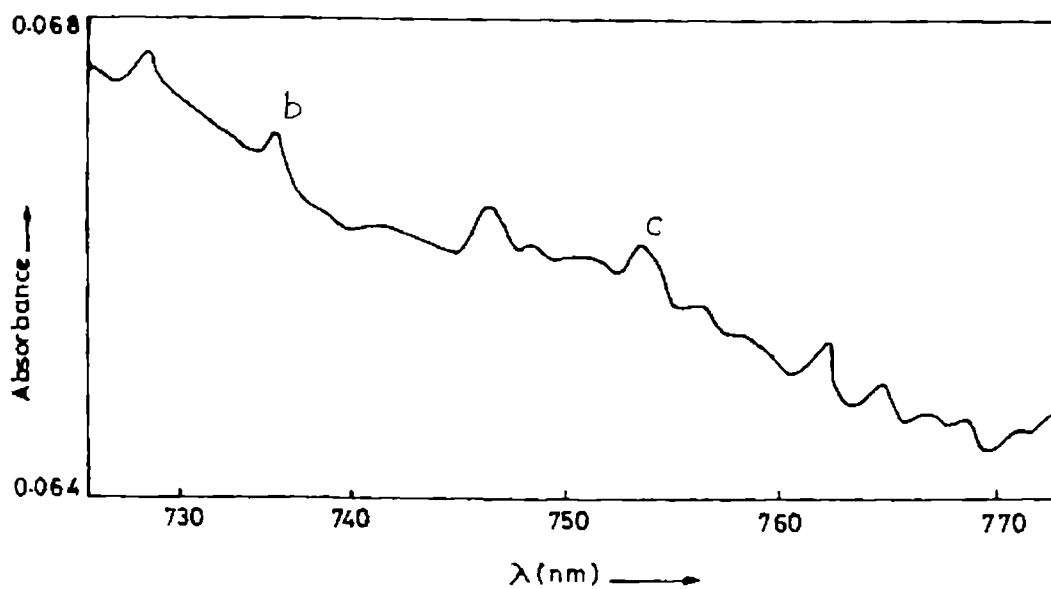**Figure 2.30** NH Overtone spectrum of o-anisidine in the $\Delta V=4$ region

69

**Figure 2.31** Overtone spectrum of o-anisidine in the ΔV=5 region (peak 'b' represents in-plane methyl CH and 'c' represents out-of-plane methyl CH)
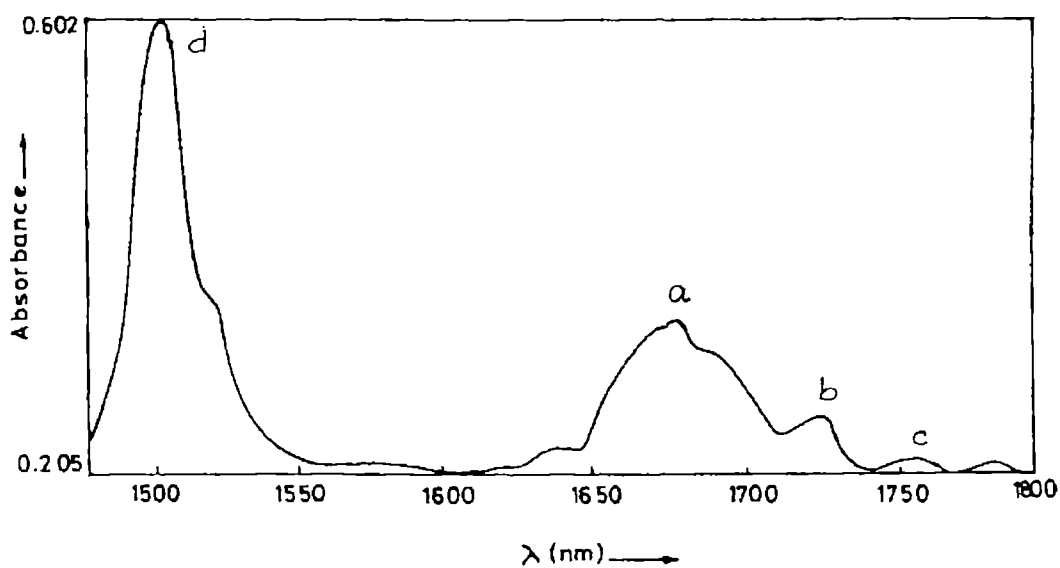


**Figure 2.32** Overtone spectrum of p-anisidine in the ΔV=2 region (peak 'a' represents ring CH, 'b' in-plane methyl CH, 'c' out-of-plane methyl CH and 'd' represents NH overtone band)

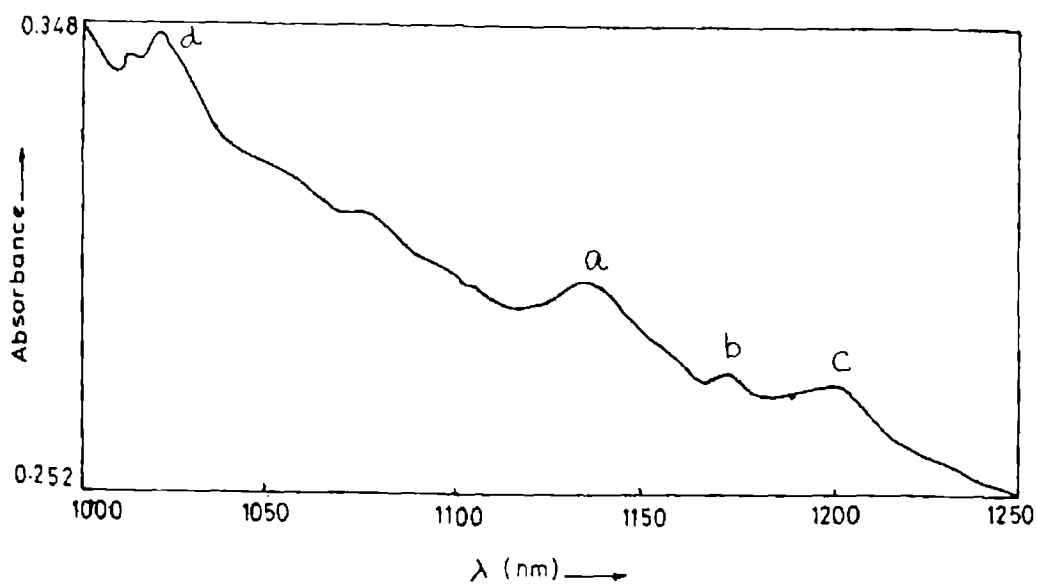Figure 2.33 Overtone spectrum of p-anisidine in the ΔV=3 region (peak 'a' representing CH, 'b' in-plane methyl CH, 'c' out-of-plane methyl CH and 'd' represents NH overtone band)
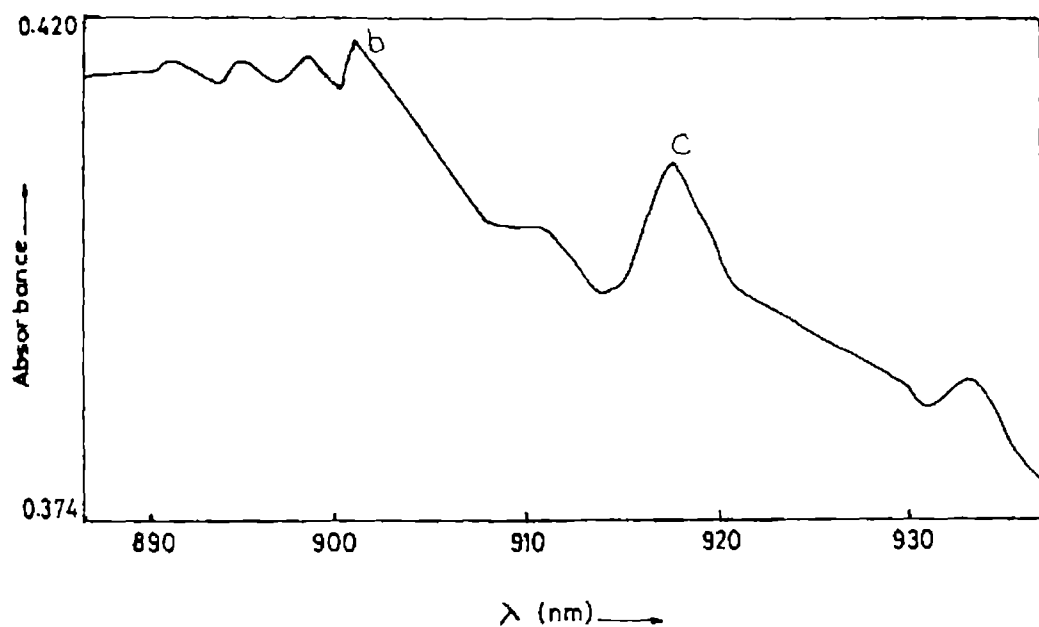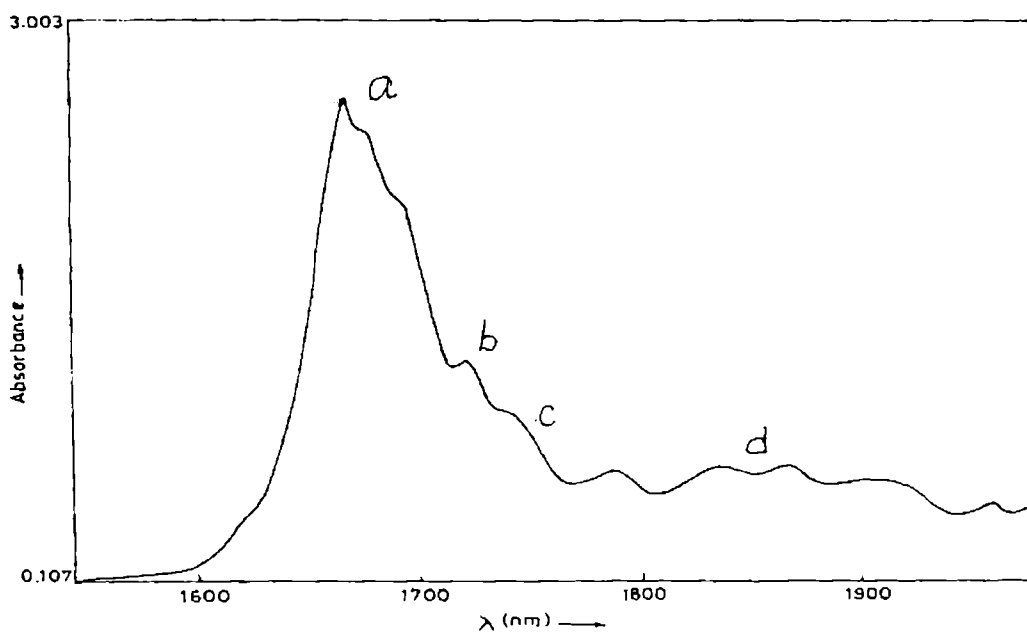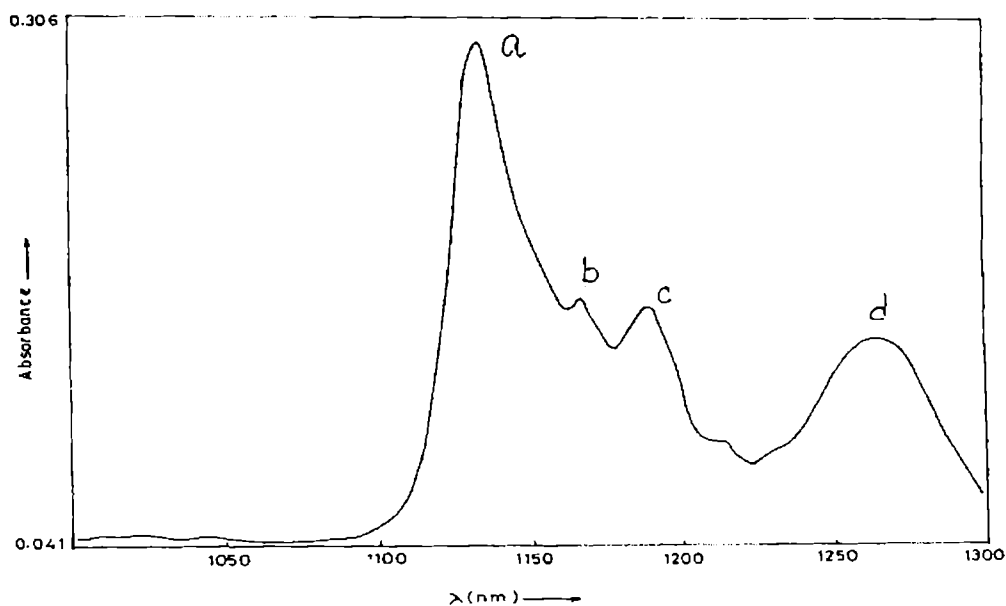


Figure 2.34 Overtone spectrum of p-anisidine in the ΔV=4 region ( in-plane methyl CH- b, 'c' out-of-plane methyl CH )

71

**Figure 2.35** Overtone spectrum of p-anisaldehyde in the $\Delta V=2$ region (peak 'a' represents ring CH, 'b' in-plane methyl CH, 'c' out-of-plane methyl CH and 'd' represents aldehydic CH overtone band)



**Figure 2.36** Overtone spectrum of p-anisaldehyde in the $\Delta V=3$ region (peak 'a' represents ring CH, 'b' in-plane methyl CH, 'c' out-of-plane methyl CH and 'd' represents aldehydic CH overtone bands )

**Figure 2.37** Overtone spectrum of p-anisaldehyde in the ΔV=4 region (peak 'a' represents ring CH, 'b' in-plane methyl CH, 'c' out-of-plane methyl CH and 'd' represents aldehydic CH overtone band)
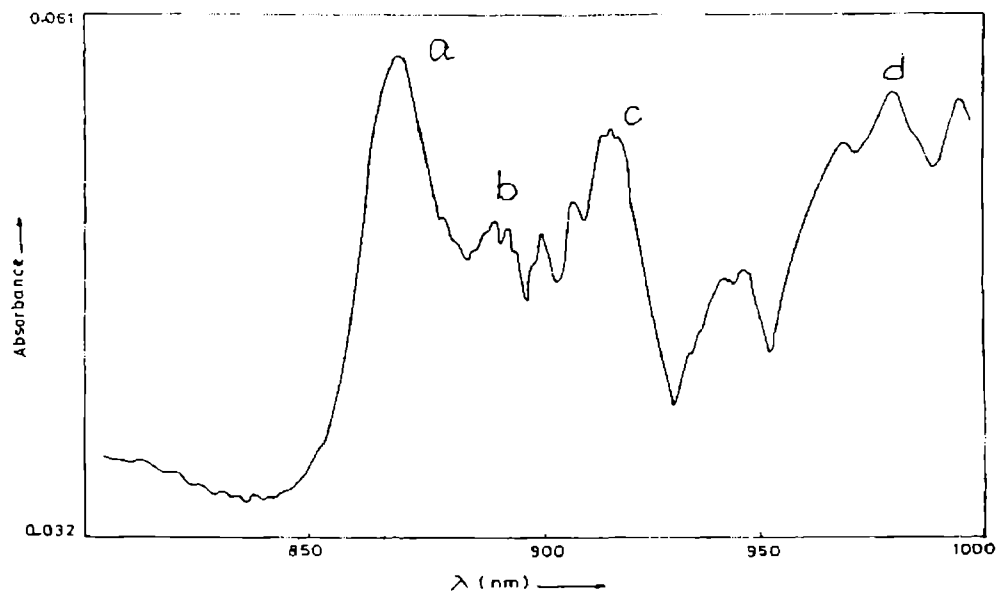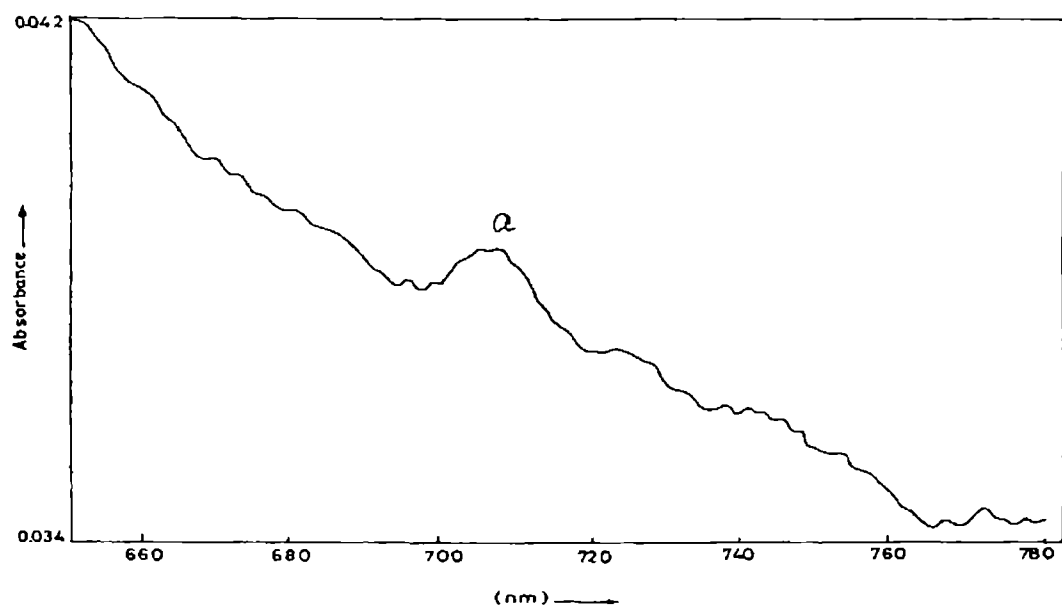


**Figure 2.38** Ring CH overtone spectrum of p-anisaldehyde in the ΔV=5region

73

## 2.7.1 Anisole

In the past, anisole the simplest alkyl aryl ether was investigated as a key molecule for the description of a number of molecular properties due to the possibility of torsion of the methoxy group with respect to the aromatic ring. Typically, in a molecule like anisole a planar configuration is expected to be energetically favored, because of the larger conjugation of the electronic system. But different spectroscopic methods led to contradicting results for the conformational arrangement of the methoxy group in anisole. Electron diffraction and microwave spectroscopy pointed to planarity of the molecule in the electronic ground state whereas photoelectron spectra predicted a mixture of planar and perpendicular conformers [44]. The analysis of the geometric and electronic structure of anisole is interpreted in terms of a mixture of planar and perpendicular conformations [45]. The study reveals that planar conformer is more stable. The planar conformer of anisole is stabilized by the interaction between the lone pair electron of the hetero atom oxygen and the mobile π electrons of the ring. Colle et al [45] explains that the lone pair perpendicular to the ring plane conjugate with antibonding π orbital. The planarity of anisole in both the ground state and the first excited state has been demonstrated by using high-resolution electronic excitation spectrum [46]. Anisole was taken as the parent molecule for reference in a systematic study on disubstituted aromatic molecules [47] More recently anisole has been considered as a model system for the study of intermolecular interactions due to the presence of the polar methoxy group. To improve understanding of the influence of the structure *ab initio* calculations have also been performed [42, 44]

The overtone spectra of anisole are shown in figures 2.25-2.28. The observed overtone peak positions and the calculated values of mechanical frequency and anharmonicity constants are listed in Table 2.5-2.7. At each overtone level three bands are clearly observable in the spectrum of anisole. The most intense band of the spectrum corresponds to the stretching overtone progression of the ring CH oscillators. The other two bands correspond to the nonequivalent methyl CH stretching overtones.

The fundamental vibrations in anisole are complicated due to the occurrence of Fermi resonance [44]. However no evidence of Fermi resonance is observed in the

overtone spectral regions. The coupling between the C-H oscillators is present in the first overtone region. The other overtone regions are free from these effects.

The aryl CH overtone spectra appear as a single band. The DFT calculation indicates $C_{methyl}$ -O rotational barrier in anisole as 3.05 kcal/mol, whereas the experimentally measured barrier height is 2.72kcal/mol [42]. Thus only a strongly hindered methyl rotation is possible in anisole. The steric repulsion between the methyl group and the ortho hydrogen atom would be the cause of the larger barrier height in anisole. The rotation of the- $OCH_3$ group around the bond with the aromatic ring is also a hindered one having a barrier energy 3.07kcal/mol. This high barrier points a strong conjugation of the oxygen atom with the $\pi$ electrons of the aromatic ring. This strong conjugation tends to keep the molecule in the planar form.

The ring C-H overtone peak positions in anisole are slightly blue shifted with respect to those of benzene. It can be seen from the Table 2.5 that this blue shift in overtone energy is due to an increased mechanical frequency of the ring C-H bonds compared to that in benzene. The methoxy group in anisole is an electron withdrawing type substituent $\sigma_1 = 0.31$ [15] and so it reduces the electron density at the ring carbon atoms. This results in a net positive charge on ring carbons thus increasing the force constant of the aryl C-H bonds.

The methyl local mode mechanical frequency and anharmonicity values are $3066cm^{-1}$ and $-54.5cm^{-1}$ for the in plane and $3018cm^{-1}$ and $-58.7cm^{-1}$ for the out of plane C-H bonds. The difference in mechanical frequency occurs due to the anisotropic environment created by the oxygen lone pair electrons, similar to the results in aliphatic ethers, methanol etc. The out-of-plane methyl C-H mechanical frequency decreases (or lengthening of C-H bonds occurs) due to the electron back donation from the lone pairs of the oxygen atom to the $\sigma^*$ orbital of the adjacent C-H bonds [40]. This effect is expected to be generally present in all methoxy-containing molecules and is relevant when the adjacent hydrogen atoms are in the trans position with respect to the lone pairs. In the case of anisole the situation seems to be favorable for the out-of-plane hydrogen atoms of the methyl group. The interpretation of the local mode results for anisole agrees with *ab initio* data, where the out of plane methyl $r_{CH}=1.096$ $A^0$ is reported to be greater than the in plane methyl $r_{CH}=1.089A^0$ [47]. The shorter in plane C-H bond is thus the

stronger than the longer out of pane C-H bonds. The mechanical frequency of both the in plane and out of plane methyl C-H bonds in a methoxy group is found to be increased compared with the methyl C-H bonds in alkanes due to the electron withdrawing nature of the oxygen atom. But the out of plane methyl C-H mechanical frequency is decreased from that of in plane methyl C-H due the lone pair trans effect.

## 2.7.2 O-anisidine and p-anisidine

The introduction of an additional substituent in anisole is expected to affect the interaction between the methoxy group and the ring in anisole, which influences the molecular geometry. Several studies were reported [42, 48] regarding the effects of substituents on the conformation of the methoxy group of anisole. Interaction between the substituents through benzene ring is of particular interest in disubstituted benzenes. Earlier studies revealed that halogen atoms and alkyl groups in the ortho position of anisole have a substantial effect on the torsional potential of the methoxy group indicating the conformation of the methoxy group can be controlled by the choice of the ortho substituent. Recently Tsuzuki et al [42] investigated the influence of the hydroxyl group at the ortho position of anisole on the torsional barrier of $O-CH_3$ group by high-level *ab initio* calculations. The study reveals o-hydroxy anisole prefers a planar configuration, in which the OH group forms an intra molecular hydrogen bond with the methoxy oxygen atom.

The amino group is often referred to as electron donating substituent in aromatic ring systems. $NH_2$ shares its lone pair electron with the p-electrons in a ring. When positioned appropriately on the aromatic ring (ortho or para position) the electron donating resonance property of the methoxy group release electron density into the ring and towards nitrogen in anisidines. At the same time inductive effect (which is considered to be more important in causing overtone shifts) of the methoxy group withdraws electrons from the ring. So for the methoxy group the net effect is the resultant of these two effects.

The anisole derivatives like p-cyano anisole prefer a planar conformation that allows the largest resonance interaction and is stabilized by the electron transfer from the lone pair electron to the antibonding $\pi$ orbital of the ring [45].

The ring CH local mode mechanical frequency in o-anisidine is close to that of anisole (less by ~5cm$^{-1}$) whereas the corresponding value in p-anisidine is much lesser (by ~22cm$^{-1}$) than in anisole (Table 2.5). A decrease in ring CH mechanical frequency in anisidines with respect to anisole is expected due to the electron-donating nature of the amino group. The important observation here is the appreciably smaller decrease in the ring C-H mechanical frequency for o-anisidine with respect to anisole, compared to the corresponding decrease for p-anisidine. The electron withdrawing effect of the methoxy group together with the electron donating nature of the $NH_2$ group is expected to cause a reduction in electron density at the nitrogen atom. This can exert a net attraction of the electron clouds associated with the hydrogen atom attached to the nitrogen and should results in an increase in NH mechanical frequency. However the observed NH mechanical frequency in o-anisidine is close to that of aniline. We propose that the comparable ring C-H mechanical frequency values for o-anisidine and anisole and the comparable NH mechanical frequency values for o-anisidine and aniline are due to the through space interaction that exists between the amino and methoxy groups. Such an interaction between the amino group and $OCH_3$ group is expected to exist in o-anisidine due to the proximity of the two substituent groups. This interaction reduces the electron withdrawing property of methoxy group as well as the electron donating property of the amino group. Thus in o-anisidine the ring CH mechanical value is close to that of anisole and the NH mechanical frequency value is close to that in aniline. A comparison with the N-H local mode parameters of p-anisidine could not be made since we could record only two N-H overtones of this compound.

**Table 2.8** Observed overtone transition energies (cm$^{-1}$), mechanical frequencies $X_1$ (cm$^{-1}$) and anharmonicities $X_2$ (cm$^{-1}$) of NH local modes of o-anisidine and aldehydic C-H local modes of p-anisaldehyde. The least square correlation coefficients ($\gamma$) are also given.

| Molecule | $\Delta V=2$ | $\Delta V=3$ | $\Delta V=4$ | $X_1$ | $X_2$ | $\gamma$ |
|---|---|---|---|---|---|---|
| Amino NH (o-anisidine) | 6652 | 9752 | 12690 | 3557.1 | -76.8 | -0.9999 |
| Aldehydic CH (p-anisaldehyde) | 5405 | 7929 | 10366 | 2867.2 | -55.4 | -0.9992 |

The methyl C-H absorption spectra of o-anisidine and p-anisidine show two distinct peaks at each overtone level. The observed values of methyl in-plane C-H mechanical frequency and anharmonicity are ~3079 cm$^{-1}$ and ~-59 cm$^{-1}$ whereas the corresponding values in p-anisidine are 3067 cm$^{-1}$ and 54.4 cm$^{-1}$. A comparison shows a higher value of the observed methyl in-plane C-H local mode parameters for o-anisidine w.r.t anisole and p-anisidine. This increase in methyl in-plane C-H values in o-anisidine occurs due to the interaction between the amino and methoxy groups. The local mode parameters of the in-plane methyl C-H in p-anisidine are very close to those of the in-plane methyl C-H in anisole, since the field effect in p-anisidine can be expected to be negligible in this case. The out-of-plane methyl C-H mechanical frequency in p-anisidine is close to that of o-anisidine. The increased values of the out of plane methyl C-H mechanical frequency, for either anisidines, with respect to anisole (Table 2.7) points to a decrease in the lone pair trans donation to the out-of-plane methyl C-H bonds. For both molecules the anharmonicity constant for out-of-plane methyl C-H is larger than that of in-plane methyl C-H.

In the ortho isomer the charge at the methoxy group does not change significantly with respect to the para derivative but the ring is less effective in transferring the charge from the $-NH_2$ group to the methoxy group. This is because of the through space interaction between the methoxy and amino groups. In the case of p-anisidine there is negligible direct interaction between the groups. Then the electron withdrawing effect of methoxy and the electron donating effect of amino groups on the ring mutually support.

## 2.7.3 p-anisaldehyde
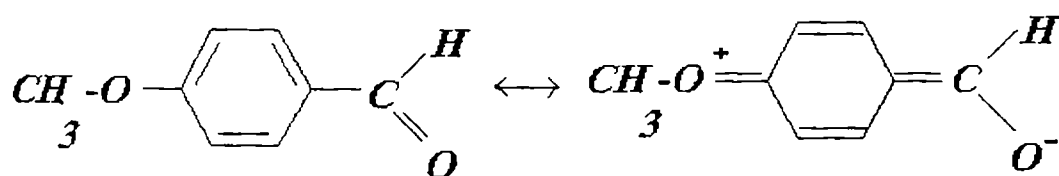


**Figure 2.39** The resonance structure of p-anisaldehyde in which the methoxy, the ring and the aldehyde groups are strongly conjugated. The occurrence of positive and negative charges at the O sites gives the bipolar structure for p-anisaldehyde.

The oxygen atom of the methoxy group can share its lone pair electrons with the mobile $\pi$ electrons of the ring (resonance effect) and can accommodate a positive charge. The ability of the oxygen to share more than a pair of electrons with the ring and to accommodate a positive charge is consistent with the basic character of the ether. Resonance can occur only when all the atoms involved lie in a plane. Any change in structure that prevents planarity will inhibit resonance. Thus the spectroscopic method provides valuable information regarding the degree of planarity of the molecule. Electron diffraction studies [48] pointed to planarity of the molecule p-anisaldehyde in the electronic ground state. The same conclusion was reached in a high-resolution study where only two planar conformational species were detected [49]. The planar conformation of a methoxy group allows the largest resonance interaction and is stabilized by lone pair of oxygen conjugated to the $\pi^*$ orbital of the ring [45]. In p-

anisaldehyde the lone pair effect of the methoxy group is found to be higher than the inductive effect. This results an electron donation from the methoxy to the aryl part. The aryl and the methyl C-H local mode parameters in the compound agree with the nature of the substituents.

The aryl C-H overtone peak positions of p-anisaldehyde are slightly blue shifted with respect to those of benzene. It can be seen from the Table 2.5 that this blue shift in overtone energy is due to an increased mechanical frequency of the ring C-H bonds compared to that in benzene. The -CHO group in p-anisaldehyde is an electron withdrawing type substituent and $OCH_3$ group is an electron donating type substituent which is in line with the above mentioned $\pi^*$ electron-lone pair interaction. The electron releasing group at one end and an electron withdrawing group at the other end tend to stabilize the charged structure (Figure 2.41). The two substitutions on benzene ring change the charge distribution at each carbon site and change the aryl C-H mechanical frequency. The increase in the ring C-H mechanical frequency with respect to benzene is assigned to the effect of bipolar resonance structure involving the three parts. In the bipolar structure of p-anisaldehyde involving methoxy, ring and aldehyde parts in which one double bond removed from the ring and the ring–substituent bonds are double bond gives a conjugated planar structure. Aryl-aldehyde bond length in p-anisaldehyde is shorter than that in benzaldehyde indicating increased double bond nature of this bond due to the polar structure. The removal of a double bond from the ring reduces the $\pi$ electron density at the ring carbon site similar to that produced by an electron withdrawing group attached to the benzene ring and consequent increase in the ring CH mechanical frequency [50].

In p-anisaldehyde, the oxygen atom in the aldehydic part attract mobile $\pi$ electrons towards it making the carbonyl carbon an electron deficient and this causes carbonyl carbon to withdraw electrons from the ring. Then the most preferred conformation of the aldehydic group is the conjugation stabilized planar form. The height of the barrier to rotation of the aldehyde group in p-substituted benzaldehyde is influenced by the nature of the substituent. In benzaldehyde the barrier to rotation of the aldehyde is 28kJ/mol whereas in p-anisaldehyde the corresponding value is 36kJ/mol, which is a reflection of the contribution of the bipolar boundary structure [38]. It is now

established that the aldehydic CH mechanical frequency is strongly influenced by the lone pair trans effect. This effect arise from the donation of electron density to the antibonding $\sigma$ orbital of the aldehydic C-H bond from the carbonyl oxygen lone pair situated trans to it. The observed values of aldehydic C-H mechanical frequency and anharmonicity in p-anisaldehyde are $2867cm^{-1}$ and $-55.4$ $cm^{-1}$. The aldehydic C-H mechanical frequency in p-anisaldehyde is slightly larger ($\sim10cm^{-1}$) and the anharmonicity value is closer to that in benzaldehyde [30]. The extent of donation of lone pair electron density from the trans lone pair to the aldehydic C-H antibonding orbital can be assumed to depend on the C=O bond length [6]. The experimental C=O bond length values in p-anisaldehyde and benzaldehyde [51] are $1.204$ $A^{0}$ and $1.212A^{0}$ respectively. One can expect that the small value of C=O distance in p-anisaldehyde causes an increase in the lone pair trans effect. In addition, aryl-aldehyde bond length in p-anisaldehyde is shorter than that in benzaldehyde indicating a strong interaction between the ring and the aldehydic group. This in turn can be expected to result in a decreased value of aldehydic C-H mechanical frequency in p-anisaldehyde compared to benzaldehyde. However, it is shown that the frequency increases if the lone pair electrons were delocalized via resonance structures [39]. It is then clear that aldehydic CH mechanical frequency increases due to the formation of resonance structure in p-anisaldehyde. The observed increase in mechanical frequency is thus the resultant of the above effects.

In p-anisaldehyde the in-plane methyl CH mechanical frequency and anharmonicity values are $3097cm^{-1}$ and $-60cm^{-1}$ whereas the corresponding values of the out-of-plane stretching vibrations are $3083cm^{-1}$ and $-69cm^{-1}$. It is observed that the mechanical frequencies of both types of methyl CH oscillators are shifted to higher values compared to both o-anisidine and p-anisidine. The increased value of methyl CH mechanical frequencies in this molecule arises due to the increased electron donation from the methoxy group to the ring. The smaller splitting between the two methyl CH in this molecule is seen as the indication of decreased availability of the electron lone pairs, apparently due to the formation of the resonance structures as explained above. The analysis of the p-anisaldehyde spectrum thus confirms that compared to anisole, the electron density increases at the ring and CHO sites with a corresponding decrease at the methoxy group.

## 2.7.4 Conclusions

The local mode model has been successfully applied to interpret the overtone spectra of stretching vibrations of molecules containing methoxy group. In all the molecules studied, two distinct peaks are observed at each overtone in the methyl region. The effect is explained as due to the donation electron density from an electron lone pair associated with the hetero atom to the $\sigma^*$antibonding orbital of the out of plane methyl C-H bonds which are situated trans to the lone pair thus weakening them, and causing the splitting the methyl C-H overtone bands. The study also reveals that the nature of the substituent and the relative position of the ring influence the local mode parameters of the different X-H oscillators in disubstituted benzenes. The observations made in the different methoxy compounds are successfully interpreted in terms of the interactions resulting from inductive and resonance effects.

## References

[1]     B.R.Henry, *Vibrational spectra and structure*, Ed. J. R. Durig (Elsevier, Amsterdam, 1981) Vol.10, p.269.

[2]     M.S.Child and L.Halonen, *Adv.Chem.Phys.*,57(1984)1.

[3]     B.R.Henry *Acc.Chem.Res*,20( 1987)429.

[4]     K.M.Gough and B.R.Henry, *J.Phys.Chem*, 88(1984) 1298.

[5]     A.W .Tarr and B.R.Henry, *Chem.Phys,Lett*,112(1984)295.

[6]     H.L.Fang, D.M. Meister and R.L Swofford, *J.Phys.Chem.*, 88(1984) 410.

[7]     H.L.Fang, R.L.Swofford, M.McDevitt and A.R.Anderson, *J.Phys.Chem.*, 89(1985)225.

[8]     M.K.Ahmed and B.R.Henry, *J.Phys.Chem.*90 (1986) 1993.

[9]     M.K.Ahmed,D.J.Swanton and B.R.Henry, *J.Phys.Chem.*,91(1987)293.

[10]    M.K.Ahmed and B.R.Henry, *J.Phys.Chem.*91 (1987) 3741.

[11]    M.G.Sowa, B.R.Henry, and Y.Mizugai, *J.Phys.Chem.*97 (1993) 809.

[12]    H.G.Kjaergaard and B.R.Henry, *J.Phys.Chem.*,99(1995)899.

[13]    D..M.Turnbull,M.G.Sowa, and B.R.Henry, *J.Phys.Chem.*,100(1996)13433.

[14]    H.G.Kjaergaard, D.M.Turnbull and B.R.Henry, *J.Phys.Chem.*,101(1997)2589.

[15]    Y.Mizugai, and M.Katayama, *J.Am.Chem.Soc.*, 102(1980)6424.

[16]    Y.Mizugai, M.Katayama,and N.Nakagawa, *J.Am.Chem.Soc.*, 103(1981)5061.

[17]    K.M.Gough and B.R.Henry *J.Phys.Chem*,87(1983)3433

[18]    R.Nakagaki and I.Hanazaki,Spectrochim.Acta A,40(1984)57.

[19]    T.M.A.Rasheed and V.P.N.Nampoori, *Pramana –J.Phys.*,42,(1994)245.

[20]    K. K. Vijayan, Sunny Kuriakose, S.Shaji, and T. M. A. Rasheed, *Asian J.Phys.*,11(2002)66.

[21]    C.K.N.Patel, A.C.Tam and R.J.Kerl, *J.Phys.Chem.*,71(1979)1470

[22]    Y.Mizugai and M. Katayama, *Chem.Phys.Lett.*,73(1980)240.

[23]    M.G.Sowa, B.R.Henry and Y.Mizugai, *J.Phys.Chem.*,97(1993)809.

[24]    R.K.Bansal, *Heterocyclic Chemistry*, (Wiley Eastern Ltd., New Delhi),1990,p.127.

[25]    D.L.Snavely, F.R.Blackburn,Y. Ranasinghe, V.A. Walter and M.G.del Riego, *J.Phys.Chem.*,96(1992)3599.

[26]    M.Katayama,K. Itaya, T.Nasu and J. Sakal, *J.Phys.Chem.*,95(1991)10592.

[27]    D.L.Snavely,J.A.Overly and V.A.Walters, *Chem.Phys.*,201(1995)567.

[28]    K.Hagen and L.Postmyr, *J.Phys.Chem.*A,103(1999)11460.

[29]    S.Shaji and T.M.A.Rasheed, *Spectrochim.Acta A*,57(2001)337.

[30]    Sunny Kuriakose , K.K.Vijayan and T.M.A. Rasheed, *Asian J.Spectrosc*, 1 (2001)17.

[31]    A.R.Katritzky, C.R.Palmer, F.J. Suinbourne, T.T. Tidwell and R.D. Topson *J.Am.Che.Soc.* ,91(1969)636.

[32]    P.Tomasik , C.D.Johnson,,*Advances in Heterocyclic Chemistry*,Ed.A.R.Katrizky, A.J.Boulton ,Academic Press ,NY,20(1976)38.

[33]    D.E.Reisner, R.W.Field, J.L. Kinsey and H.L. Dui, *J. Che.Phy.* , 80(1984) 5968.

[34]    J.S.Wong and C.B. Moore, *J.Che.Phys*, 77(1982) 603.

[35]    J.M.Jasinski, *Chem.Phys.Lett.*,123(1986)121.

[36]    R.Nakagaki and I. Hanazakl, *Chem. Phys. Lett*, 83(1981) 512.

[37]    R.T.Morrison and R.N.Boyd, *Organic Chemistry*, Prentice-Hall, India, 1971,p.399.

[38]    V.M.Potapov, *Stereochemistry*, Mir Publishers, Moscow, 1979,p.480.

[39]    L.J.Bellamy and D.W.Mayo, *J.Phys.Chem.*, 80(1976)1217.

[40]    D.C.McKean, *Chem.Soc.Rev.*, 7(1978)399.

[41]    Chemical Applications of Spectoscopy, Ed. W. West, InterScience Publishing Inc., New York , 1956

[42]    S.Tsuzuki, H.Houjou, Y.Nagawa and K.Hiratani, *J.Phys.Chem.*, 104,(2000)1332.

[43]    H.L.Fang, D.M. Meister and R.L Swofford, *J.Phys.Chem.*, 88(1984) 405.

[44]    C.Gellini, L.Moroni and M.Muniz-Miranda, *J.Phys.Chem.A,*, 106(2002) 10999.

[45]    M.D.Colle,G.Distefano, D.Jones and A.Modelli,J.Phys.Chem.A,104(2000)8227.

[46]    C.G.Eisenhardt, G.Pietraperzia and M.Becucci,
        *Phys.Chem.Chem.Phys.*,3(2001)1407.

[47]    C.G.Eisenhardt, A.S.Gemechu, H.baumgartel, R.Chelli, G.Cardini and
        S.Califano, *Phys.Chem.Chem.Phys.*, 3(2001)5358.

[48]    J.Brunvoll, R.K.Bohn and I.Hargittai, *J.Mol.Struct.*,129(1985)81.

[49]    S.Melandri, A.Maris, P.G.Favero, L.B.Favero, W.Caminati and R.Mayer,
        *J.Mol.Spectrosc.*, 185(1997)374.

[50]    T.M.A.Rasheed, *Spectrochim.Acta A*,52(1996)1493.

[51]    K.B.Borisenko, C.W.Bock and I.Hargittai, *J.Phys.Chem.*, 100(1996)7426.

# CHAPTER 3

# OVERTONE SPECTROSCOPIC STUDY OF SOME
# ALIPHATIC MOLECULES

# CHAPTER 3

# OVERTONE SPECTROSCOPIC STUDY OF SOME
# ALIPHATIC MOLECULES

## 3.1 Introduction

As already outlined in chapter1, the local mode model, in which X-H (X=C, N, O...) bonds are considered to be loosely coupled anharmonic oscillators, has been widely used to interpret the stretching vibrational overtone spectra of polyatomic molecules [1-3]. Vibrational overtone spectroscopy is now established as an important tool for elucidating molecular structural details [4-20]. To a first approximation, the peak positions of pure overtone transitions are represented by the one dimensional Birge-Sponer equation

$$\Delta E_{v,0} = AV + BV^2$$

where V is the quantum level of excitation. The C-H stretching mechanical frequency $X_1$ = A-B and the anharmonicity constant $X_2$ = B are calculated using the above equation from a least mean square fit of $\Delta E/V$ vs. V. The bond dissociation energy of the local oscillator is given by

$$D = -A^2/4B.$$

The properties of simple hydrocarbons have always been of interest since their molecular structure and nature of bonding serve as prototypes for much of carbon based chemistry. In this chapter the results of an experimental study of two aliphatic amines are described. The analysis of the NIR vibrational overtone spectrum of liquid phase t-butyl amine is carried out using the harmonically coupled anharmonic oscillator model. The overtone spectrum of n-butyl amine is analyzed using the simple local mode model. A comparison of the spectral results for the two compounds reveals the relative effects of substitution with $-NH_2$ group on the two parent compounds n-butane and neopentane.

## 3.2 Experimental

High purity (>99%) t-butyl amine and n-butyl amine supplied by M/s Central Drug House (P) Ltd., New Delhi, India is used for the present studies. The near infrared absorption spectra in the region 2000-700nm are recorded from pure liquid on a Hitachi Model 3410 UV-VIS-NIR spectrophotometer, which uses a tungsten lamp as the near infrared source. The spectra are recorded using a path length of 1cm with air as reference at room temperature $(26\pm2)^0C$. The liquid phase Raman spectrum of t-butyl amine is recorded at room temperature using a Q-switched Nd: YAG laser at operating at 532 nm as the excitation source. The experimental arrangement of the Raman spectrometer system is described in Chapter 4.

## 3.3 Analysis of the C-H overtone spectrum of t-butyl amine using $C_{3v}$ coupled oscillator Hamiltonian

A refined local mode model treats stretching vibrations in a molecule as a set of bond oscillators coupled by kinetic and potential energy terms. The strength of this coupling versus anharmonicity of the bond determines stretching energy levels. Large anharmonicity compared with coupling results in near local mode behavior of the molecule [21]. An understanding of the coupling of the pure local mode overtone state to other molecular vibrational states is obtained from the bandwidths of the overtone spectra [22].

If interactions among the molecular oscillators are significant, then combination bands also appear in the overtone spectrum. Two types of combinations are to be expected (1) a state in which two identical C-H stretching vibrations are simultaneously excited called local-local combination (2) a C-H stretching vibration and some lower frequency normal mode motion of the molecule are simultaneously excited called local-normal combination. The local mode picture also take into account the local symmetry of the molecule for the interpretation of overtone – combination spectra observed in

87

molecules containing $XH_2$, $XH_3$ and $XH_4$ groups and which maintains the relevant local symmetry [23-27]. The energies of the C-H oscillator are obtained from the Hamiltonian of the relevant group. An examination of the first overtone region ($\Delta V_{CH}=2$) is usually sufficient for observation of local symmetry effects. In higher overtone regions, the strengths of the combination bands relative to the LM overtones decreases, nearly all the vibrational energy is localized in one of a set of equivalent C-H oscillators [28-31]. Therefore, energy splitting due to symmetry effects is not generally observed at higher overtone levels. The molecular structure of t-butyl amine is shown in the Figure 3.1.

$$CH_3 - \overset{\displaystyle \overset{CH_3}{|}}{\underset{\displaystyle \underset{NH_2}{|}}{C}} - CH_3$$
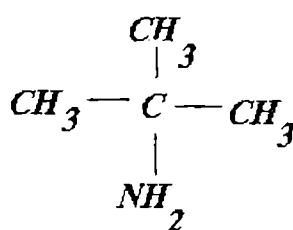
Figure 3.1 Molecular structure of t-butyl amine

The t-butyl amine molecule contains a central carbon atom surrounded by three $CH_3$ groups and an $NH_2$ group. If we consider that these units are independent as far as overtone excitations are concerned, then the C-H local mode states of the methyl groups in t-butyl amine can be described under $C_{3v}$ local symmetry arising from three identical coupled anharmonic oscillators similar to the three C-H bonds in a methyl radical. The spectra could then be assigned through the diagonalization of the local mode Hamiltonian matrices of the $C_{3v}$ symmetry group. The results obtained in the present work shows that the observed C-H pure local mode overtones and local-local combination states are well predicted by the $C_{3v}$ coupled oscillator Hamiltonian.

### 3.3.1 Theory

Sage and Williams III [32] presented a systematic quantum mechanical study of the nature of energies, wave functions and expected absorption spectra of the two

identical coupled anharmonic oscillators as a function of anharmonicity and coupling between the oscillators. The study reveals that the main factor that determines the nature of the energy level structure and wave function is the sum of the kinetic and potential coupling constants.

The vibrational Hamiltonian [26] for the ground electronic state of the three identical coupled oscillator systems is given by

$$(H-E_0)= \omega(V_1+V_2+V_3)- \omega(V_1^2+V_2^2+V_3^2+V_1+V_2+V_3) \, x + \omega\gamma \, (p_1p_2+p_2p_3+p_3p_1)$$
$$+ \omega\phi \, (q_1q_2+q_2q_3+q_3q_1) \qquad\qquad (1)$$

Here $\omega$, $\omega x$ and $E_0$ are the harmonic frequency, anharmonicity and ground state energy, respectively, of the local C-H oscillator. $V_1$, $V_2$ and $V_3$ are the quantum numbers of the three C-H oscillators. The parameter $\gamma$ and $\phi$ characterizes the kinetic energy coupling and potential energy coupling, respectively, between different C-H oscillators in a manifold.

They are defined by [26]

$$\gamma = -(1/2) \, G_{ij} / G_{ii} \qquad\qquad (2a)$$

and

$$\phi = (1/2) \, F_{ij} / F_{ii} \qquad i, j =1, 2, 3. \qquad\qquad (2b)$$

where $G_{ij}$ ($G_{ii}$) and $F_{ij}$ ($F_{ii}$) are the off-diagonal (diagonal) kinetic energy and potential energy constants, respectively.

$a^\dagger$ and $a$ are creation and annihilation operators related to normalized momentum($p_i$)and coordinate ($q_i$) variables by

$$p = a^\dagger - a \qquad\qquad (3a)$$

$$q = a^\dagger + a \qquad\qquad (3b)$$

For C-H oscillators x, $\gamma$ and $\phi$ are small. Also manifolds which corresponds to different values of $\Delta V= V_1+V_2+V_3$ will be well separated and hence coupling between different manifolds may be neglected. The Hamiltonian is diagonalyzed within a symmetrized local mode basis. The details of this model have been described in Chapter 1. The Hamiltonian matrix for the $CH_3$ unit is given in Table 1.2 for the manifolds $\Delta V_{CH}= V_1$, $V_2$ and $V_3$.

For constructing the $C_{3v}$ local mode Hamiltonian we require harmonic frequency $\omega$, anharmonicity $\omega x$ and effective coupling parameter $\omega\gamma'$ $=\omega$ $(\gamma$ -$\varphi)$. The values of $\omega$ and $\omega x$ for C-H bonds (and N-H bonds) are obtained by using the observed pure local mode transition energies in the Birge-Sponer relation

$$\Delta E_{V \leftarrow 0} = \omega \, (1\text{-}x) \, V - \omega x \, V^2 \qquad (4)$$

The effective coupling parameter $\omega\gamma'$ is related to the energy difference between $A_1$ and E states of the fundamental C-H stretching transition through the relation

$$3\omega\gamma' = E \, (|100>_E) - E \, (|100>_{A_1}) \qquad (5)$$

Substitution of $\omega$, $\omega x$ and $\omega\gamma'$ into the coupling matrices of the Hamiltonian (1) followed by diagonalization of these matrices give the calculated energies corresponding to the pure overtone and local-local combination peaks.

### 3.3.2 Results and discussion

The observed Raman spectrum of t-butyl amine in the spectral range 2400 - 4000 cm$^{-1}$ is shown in Figure 3.2. (The complete assignment of the pulsed laser Raman spectra of t-butyl amine is given in the Chapter 4.) The fundamental C-H stretching frequencies of t-butyl amine obtained from Raman spectrum are $v_{A1}$ = 2916 cm$^{-1}$ and $v_{E1}$ = 2964 cm$^{-1}$. The near infrared C-H and N-H vibrational overtone transitions of t-butyl amine in the region 2000-700nm are shown in Figure 3.3-3.6. Two absorption bands are seen for each overtone transition. One prominent band corresponds to the $CH_3$ overtone and the other band corresponds to $NH_2$ overtone excitation.
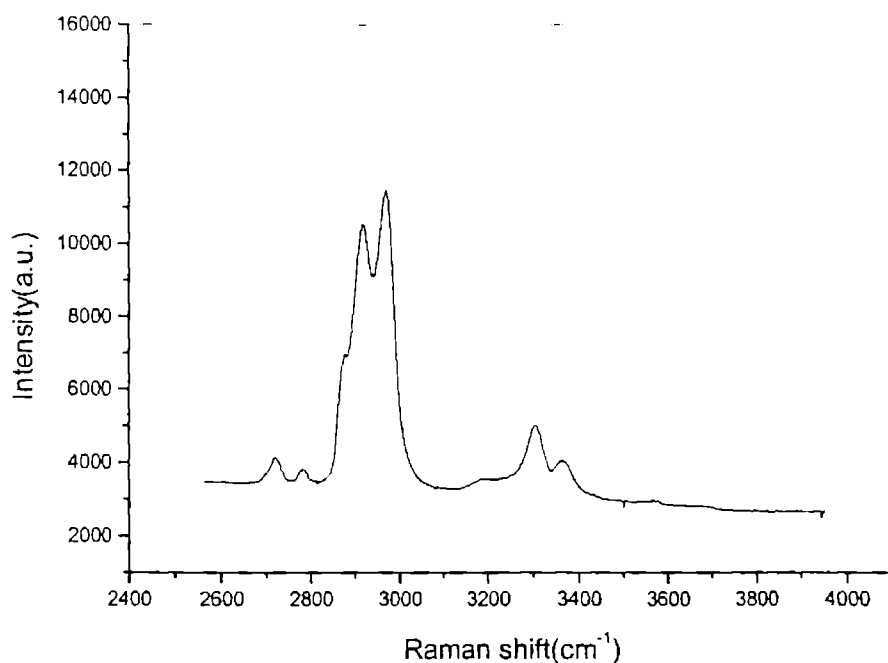
**Figure3.2** Pulsed laser Raman spectrum of t-butyl amine in the region 2400 - 4000 cm$^{-1}$

The pure overtone peak positions and their assignments are given in the Table3.1. For the assignment of the complete C-H stretching peaks, we make use of harmonically coupled local mode model for a XH$_3$ system [23, 24, 27, 33]. Only the pure overtone bands of N-H oscillators of this molecule are considered in the present analysis.

91

Table 3.1 Observed overtone transition energies (cm$^{-1}$), mechanical frequencies $\omega$ (cm$^{-1}$), anharmonicities $\omega x$ (cm$^{-1}$) and the effective coupling parameter $\omega \gamma'$ (cm$^{-1}$) of C-H in t-butyl amine. The least square correlation coefficient (R) is also given. The $\omega$, $\omega x$ and $\omega \gamma'$ values of neopentane [23] are given for a comparison.

| Molecule | $\Delta v=1$ | $\Delta v=2$ | $\Delta v=3$ | $\Delta v=4$ | $\Delta v=5$ | $\omega$ | $\omega x$ | $\omega \gamma'$ | R |
|----------|------|------|------|------|------|------|------|------|------|
| **t-Butyl amine** | | | | | | | | | |
| Methyl (CH) | 2948 | 5761 | 8438.8 | 10981.8 | 13397.6 | 3082.2 | -67.2 | 16.0 | -0.99999 |
| Amine (NH) | 6493.5 | 9510.2 | 12368.6 | | | 3478.9 | -77.3 | --- | -0.99999 |
| **Neopentane** | | | | | | | | | |
| Methyl (CH) | | | | | | 3076 | -68.1 | 14.7 | |

Table3.2 Calculated and observed transition energies (cm$^{-1}$) of C-H local mode overtone and local–local combination in t-butyl amine. All figures are rounded to nearest integers.

| State | Calculated | Observed |
|---|---|---|
| $|100>_{A1}$ | 2916 | 2916 |
| $|100>_{E}$ | 2964 | 2964 |
| $|200>_{A1}$ | 5744 | 5761 |
| $|200>_{E}$ | 5758 | 5761 |
| $|110>_{A1}$ | 5881 | 5881 |
| $|110>_{E}$ | 5915 | 5913 |
| $|300>_{A1}$ | 8435 | 8439 |
| $|300>_{E}$ | 8435 | 8439 |
| $|210>_{A1}$ | 8653 | |
| $|210>_{E}$ | 8685 | 8691 |
| $|210>_{E}$ | 8740 | |
| $|210>_{A2}$ | 8757 | |
| $|111>_{A1}$ | 8860 | |
| $|400>_{A1}$ | 10980 | 10982 |
| $|400>_{E}$ | 10980 | 10982 |
| $|310>_{A1}$ | 11364 | |
| $|310>_{E}$ | 11369 | |
| $|310>_{E}$ | 11391 | |
| $|310>_{A2}$ | 11404 | |
| $|220>_{A1}$ | 11508 | |
| $|220>_{E}$ | 11542 | |
| $|211>_{A1}$ | 11617 | |
| $|211>_{A1}$ | 11696 | |
| $|500>_{A1,E}$ | 13398 | 13398 |

The weighed average of pair of states $A_1$ and E predicts the local mode frequency of the fundamental C-H stretching transition as 2948cm$^{-1}$. The values of $\omega$ and $\omega x$ obtained from a fit of B-S plot using the pure local mode overtones in the $\Delta V_{CH}$ =1–5 regions and $\Delta V_{NH}$ =2–4 are given in Table3.1. The parameter $\omega \gamma'$ calculated using Eq (5) is also given in Table3.1.
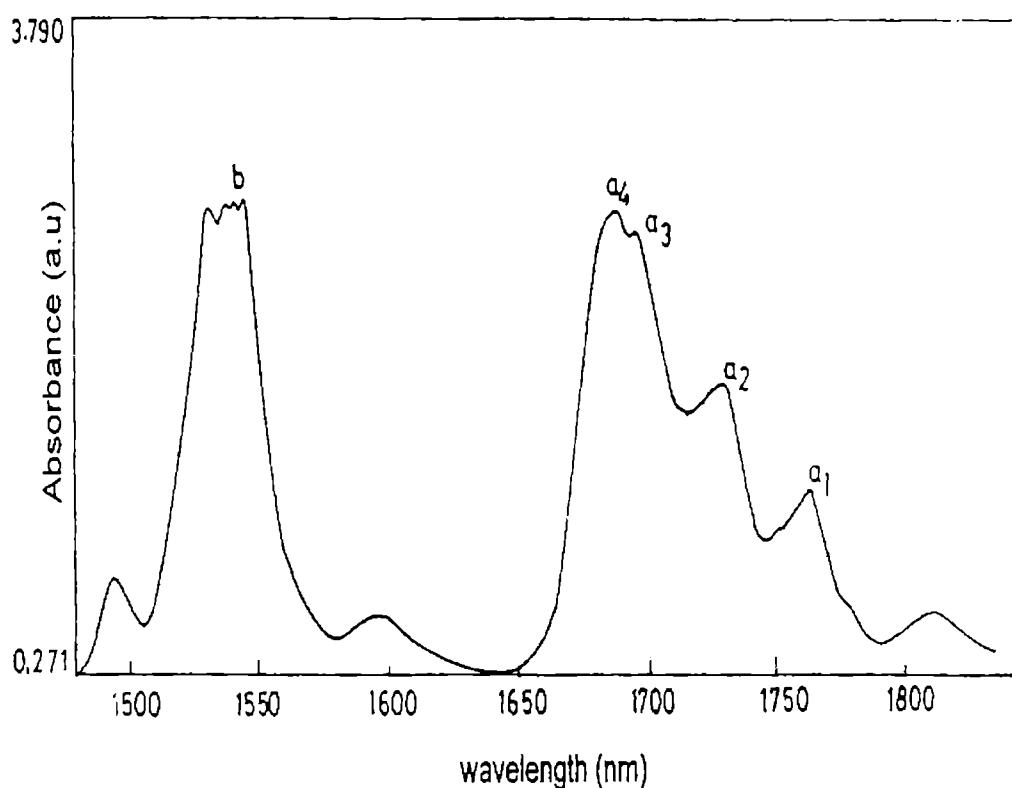


Figure 3.3 The C-H and N-H overtone band structure of t-butyl amine in the $\Delta V=2$ region. The positions marked are ($a_1$) local-normal combination state ($a_2$) pure local mode state $|200>_{A1,E}$ ($a_3$) $A_1$ component of local-local combination state $|110>$ ($a_4$) E component of local-local combination state $|110>$. The overtone peak of N-H is marked as 'b'
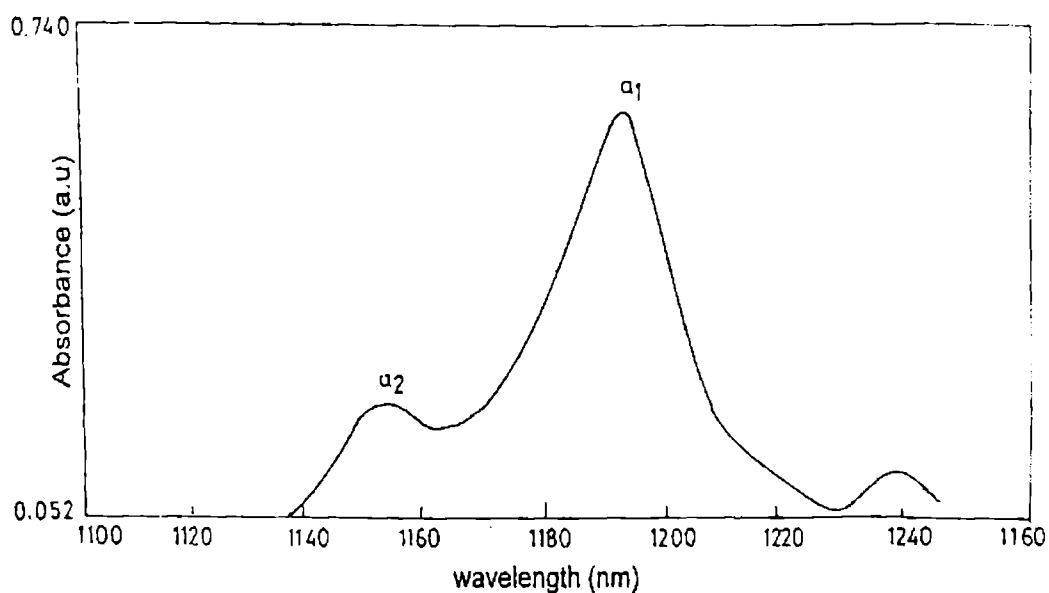
**Figure 3.4** The C-H overtone peaks of t-butyl amine in the $\Delta V=3$ region. The pure local mode state $|300>_{A_1,E}$ is marked as $a_1$ and the peak $a_2$ corresponds to $|210>_E$ transition.
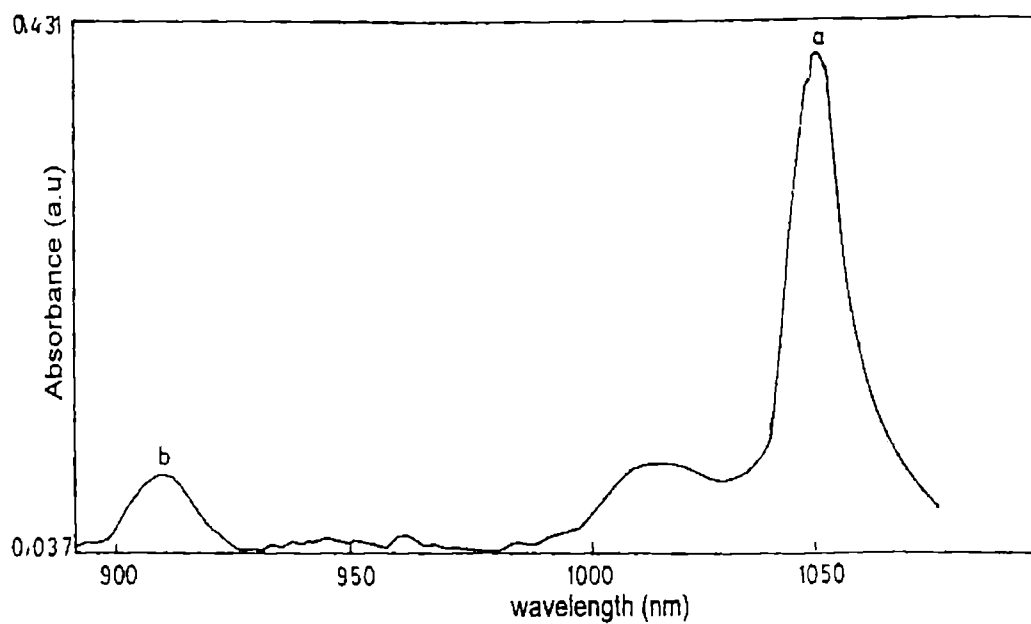


**Figure 3.5** The C-H overtone peak in the $\Delta V=4$ region (marked as 'a') and the N-H overtone peak in the $\Delta V=3$ region (marked as 'b') of t-butyl amine
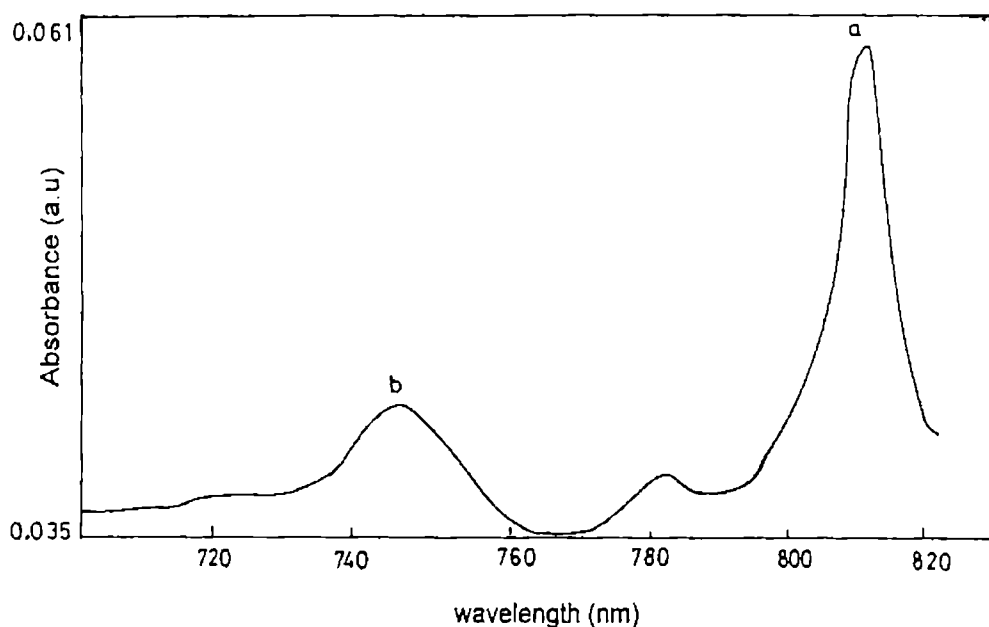
**Figure 3.6** The C-H overtone peak in the $\Delta V=5$ region (marked as 'a') and the N-H overtone peak in the $\Delta V=4$ region (marked as 'b') of t-butyl amine

Thus the entire local mode terms $\omega$, $\omega x$ and $\omega y'$ governing the coupling matrices of the Hamiltonian (1) are now available, the diagonalization of which give the values of calculated energies corresponding to the pure overtone and local-local combination peaks. Table3.2 gives the energy calculated by this method along with observed peak positions of these transitions for a manifold up to fourth overtone. The calculations exactly reproduce frequencies of $A_1$ ($2916\text{cm}^{-1}$) and E ($2964\text{cm}^{-1}$) components of the fundamental stretching transitions in the molecule. The energy of the fourth overtone state is calculated by the Birge-Sponer relation, since the values obtained by matrix diagonalization show only very small difference.

The C-H overtone spectrum shows the following features in various overtone regions. In addition to pure local mode overtone peaks, transitions to local mode combination states are also observed in first and second overtone regions. The first overtone region shows an intense band with doublet structure and two less intense peaks. In this region the doublet structure corresponds to local -local combination bands $|110>$

are more intense compared to the pure local mode overtone peak |200>. Similar effect is reported in liquid phase neopentane [23]. Henry et al stated one of the reasons for this feature is intramolecular vibrational energy redistribution between pure local mode state and local – local combination state consequent on nearly resonant condition existed in these states. Another reason they stated for this feature is opposing intensity contributions from mechanical and electrical anharmonicities. In the absence of mechanical and electrical anharmonicities only pure local mode state would show any intensity. But in the present case the combination band is more intense than the pure local mode band. The intensity pattern indicates state mixing may be dominant in the first overtone region. By simultaneously analyzing the absorption and Raman spectra of neopentane Henry et al [23] concluded that electrical anharmonicity is also a contributing factor for the intensity of the combination band. These explanations are likely to be true for the molecule t-butyl amine also. The second overtone region shows a strong pure overtone peak and a less intense local-local combination peak. In other overtone regions, only the pure overtone peaks are intense. These results are in accordance with the general trend in the overtone spectra of similar compounds.

The $A_1$ and E components in the $\Delta V=2$ overtone region are unresolved even though symmetry effects are observed in this region. In other overtone regions also these local mode pairs, whose energy levels are degenerate, give a common value as these states move closer at higher vibrational quantum levels. Results also show that local-local combination states are not observed in higher overtone regions. The strength of the effective inter-oscillator coupling between C-H bonds in a given manifold decreases when V increases and this influences the energy level structure in higher vibrational excitations. Hence in t-butyl amine symmetry effects are not observed for $\Delta V_{CH} \geq 3$ region and single peaks dominate the spectra in these regions as in neopentane. The C-H stretching vibrations at these levels are thus well described by uncoupled anharmonic oscillations localized into one of the equivalent C-H oscillators. This is consistent with earlier studies, which observed that as V increases the transition is concentrated to a pure local mode state [4].

The calculations show that the C-H harmonic frequency in t-butyl amine is increased by ~6.3cm$^{-1}$, the anharmonicity is almost unchanged and that the inter oscillator

coupling parameter is slightly increased with respect to the more symmetric molecule neopentane. Studies based on substituted compounds have shown that an electron withdrawing substituent causes an increase while an electron donating substituent causes a decrease in C-H mechanical frequency of the parent molecule [34-37]. Correlation between change in mechanical frequency and $\sigma_I$, the inductive part of Hammet $\sigma$, are also established from these earlier studies. One can therefore expect that the small increase of C-H mechanical frequency in t-butyl amine with respect to neopentane in line with the small electron withdrawing power ($\sigma_I$ =0.11) of the $-NH_2$ group [36,37] attached to the t-butyl part. Consistency of our analysis is also obtained by a comparison of the harmonic frequency observed in liquid t-butyl chloride. Among the two well resolved C-H overtone peaks observed in t-butyl chloride one corresponds to harmonic frequency $3081 cm^{-1}$ and the other corresponds to $\sim3050 cm^{-1}$. The splitting of overtone frequency in this molecule is stated as an indication of the non-equivalence of C-H oscillators and the lower component arising due to electron contribution from one of the lone pairs of the chlorine atom to the C-H bond trans to it [4]. The $-NH_2$ group attached to many molecules also shows similar lone pair effect. But pure local mode C-H overtone bands in t-butyl amine do not show a resolved structure, which points to the absence of this phenomenon in t-butyl amine. Thus the unresolved overtone spectra of t-butyl amine indicate the near equivalence of the C-H bonds. The assumption that the methyl groups are independent with regard to overtone excitation is justified; as the $C_{3v}$ coupled Hamiltonian model could satisfactorily predict the observed C-H stretching excitations.

### 3.3.3 Conclusions

The liquid phase C-H vibrational overtone spectrum of t-butyl amine in the near infrared region is successfully analyzed using coupled local mode model. The local mode parameters such as mechanical frequency, anharmonicity and the effective inter-oscillator coupling parameter are determined. Very good agreement is obtained between the observed transition energies of pure local mode overtone and local-local combination states and those calculated by diagonalization of the $C_{3v}$ Hamiltonian matrices. The

results also reveal that in t-butyl amine vibrational state mixing is pronounced only at the first overtone level.

## 3.4 A comparative study of the overtone spectra of n-butyl amine and t-butyl amine

This section contains a presentation of the results of an experimental study of the near infrared overtone spectrum of liquid phase n-butyl amine and a comparison of these results with the corresponding results obtained for liquid phase t-butyl amine. In contrast to the studies in the fundamental region, the localized nature of the X-H stretching overtones ensures that, changes relative to a parent molecule reflect primarily the electric nature of the substituent. It has long been known that the positions of the overtone band maxima for substituted benzenes are shifted relative to benzene. Mizugai and Katayama studied the frequency shifts of more than 30 kinds of liquid phase monosubstituted benzenes [36] and a number of disubstituted benzenes [38] at the fifth overtone level the by thermal lens technique. They observed that a frequency shift of the overtones from that of benzene are proportional to $\sigma_I$ values, the inductive part of the Hammet $\sigma$. Overtone frequencies are quite sensitive to inductive effects of adjacent substituents [36, 39]. The influence of lone pair electrons on overtone spectra is also well documented [40]. In nitrogen atom the electronic configuration leads trivalency and to the presence of a lone pair electron occupying hybridized orbitals in nitrogen containing compounds. These orbitals' spatial orientation allows interaction between the electron pair and suitably oriented bonds on neighboring atoms. In the present study we have examined he substituent effect in the selected aliphatic molecules with $-NH_2$ as substituent group, n terms of the change in the local mode parameters of X-H oscillators in these nolecules. This has led us to draw specific conclusions on the differing effects of the $-NH_2$ group in the two compounds.

99

## 3.4.1 Results and discussion

The molecular structure of n-butyl amine is shown in Figure 3.6.

$$CH_3\text{-}CH_2\text{-}CH_2\text{-}CH_2\text{-}NH_2$$

**Figure3.7** Molecular structure of n-butyl amine

The observed overtone absorption spectrum of t-butyl amine in the spectral regions of quantum levels V=2 to V=4 are already shown in Figures 3.3-3.6. The overtone spectra of n-butyl amine in the same region is shown in Figures3.8-3.11.The multiple peaks in some regions arise from combination bands; we could assign the pure overtone peaks from such structures as those giving good least square fit for the Birge-Sponer plot with the pure overtone peaks in the other regions.

Greenlay and Henry [41] reported the absorption spectra of the normal alkanes, propane through n-heptane, and several branched alkanes in the range 6500-16500cm^{-1}. Clearly resolved peaks are assigned as the absorption of nonequivalent C-H oscillators in the molecule. The spectra of the n-alkanes reveal two absorption peaks. It is observed that the relative intensity of the lower energy peak increases with increasing chain length. It is straightforward to assign this peak to the secondary C-H oscillator in the molecule. The higher energy peak whose intensity is relatively constant for the alkanes is assigned to the primary C-H. The transition energies found from liquid phase spectra of n-alkane occur in the order of methyl > methylene [41, 42]. The bond dissociation energies and mechanical frequencies are also in the same order [42]. Based on the earlier work of Greenlay and Henry [41] and that of Fang and Swofford [43] one can identify the prominent absorption peaks due to the distinct type of C-H oscillators in n-butyl amine. Henry et al [23, 44] reported the absorption spectra of liquid phase neopentane. The assignment of the present C-H overtone spectra in t-butyl amine is done based on the above results.

The assignment of peak positions, corresponding transition energies, the local mode parameters and the dissociation energies of the C-H and amine N-H oscillators are given in Table3.3. The C-H local mode parameters of liquid phase n-alkanes (average

100

value) [45] and liquid phase neopentane [23] are given in Table 3.3 for a comparison. As explained below, a comparison of local mode parameters of n-butyl amine and t-butyl amine respectively with those in n-butane and neopentane provides important results regarding the influence of $-NH_2$ group in the two compounds.

The molecule n-butyl amine is obtained by replacing one of the hydrogen atoms of a methyl group of n-butane by an $-NH_2$ group. Similarly t-butyl amine molecule is obtained by replacing one of the $CH_3$ groups of neopentane by an $-NH_2$ group. C-H stretching peaks involving methyl and methylene groups and N-H stretching peaks involving amine groups dominate the overtone spectra of n-butyl amine. The C-H overtone absorption bands of n-butyl amine in each region appear as doublet. N-H overtone band appear at the higher frequency side of the C-H band. The doublet structure in the C-H overtone regions is due to the presence of methyl and methylene C-H bonds in n-butyl amine. As already described in the previous section, the C-H overtone spectrum of t-butyl amine does not show a resolved structure. Hence all the C-H bonds in this molecule could be considered as equivalent. As in t-butyl amine, the N-H overtone bands in n-butyl amine also appear on the higher energy side of the C-H overtone bands.

The main interest in this study is to examine the way in which an amine group influences the strength of C-H bonds in the two molecules selected. This problem requires a careful study of local mode parameters. Several trends are seen both in the spectra and the local mode parameters given in the Table 3.3. A striking manifestation of the local mode description in the spectra is the resolution and relative intensities of the pure C-H overtone peaks corresponding to methyl and methylene C-H oscillators throughout the n-butyl amine, with the $CH_3$ peak appearing at higher energy. The overtone bands at the lower regions are more complex due to local mode CH-CH combination bands. In n-butyl amine the mechanical frequency of the methyl C-H is higher (about $\sim 65 cm^{-1}$) than that for the methylene C-H values whereas the anharmonicity values of methylene C-H is lower (about $\sim 7 cm^{-1}$) than that in methyl C-H.

**Table3.3** Observed overtone transition energies ($cm^{-1}$), mechanical frequencies $X_1$ ($cm^{-1}$), anharmonicities $X_2$ ($cm^{-1}$) and the least square correlation coefficient R of CH and NH oscillators in t-butyl amine and n-butyl amine.

| Molecule | $\Delta v=1$ | $\Delta v=2$ | $\Delta v=3$ | $\Delta v=4$ | $\Delta v=5$ | $X_1$ | $X_2$ | R |
|---|---|---|---|---|---|---|---|---|
| **t-butyl amine** | | | | | | | | |
| methyl(CH) | 2948 | 5761 | 8438.8 | 10981.8 | 13397.6 | 3082.2 | -67.2 | -0.99999 |
| amine(NH) | | 6493.5 | 9510.2 | 12368.6 | | 3478.9 | -77.3 | -0.99999 |
| | | | | | | | | |
| **n-butylamine** | | | | | | | | |
| methyl(CH) | | 5710.4 | 8383.6 | 10931.4 | 13374.3 | 3035.6 | -60.3 | -0.99992 |
| methylene(CH) | | 5621.5 | 8271.3 | 10813.1 | 13250.3 | 2971.4 | -53.6 | -1 |
| amine (NH) | | 6542.8 | 9573 | 12445.6 | | 3511.3 | -80 | -1 |
| | | | | | | | | |
| **neopentane** | | | | | | | | |
| methyl CH | | | | | | 3076 | -68.1 | |
| | | | | | | | | |
| **n-alkanes** | | | | | | | | |
| methyl CH | | | | | | 3036 | -60 | |
| methylene CH | | | | | | 3002 | -62 | |
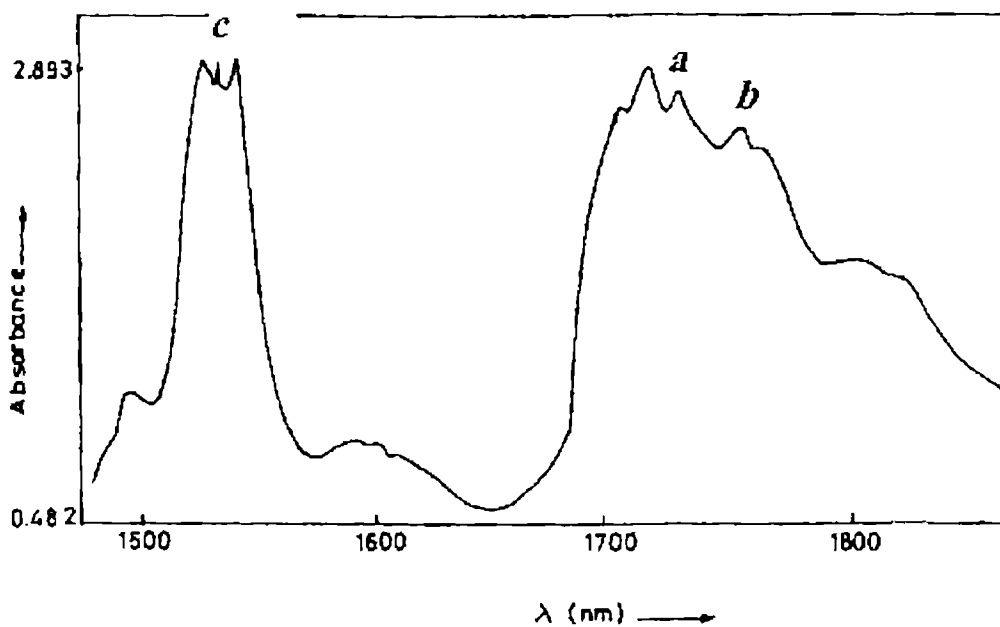
**Figure3.8** The methyl C-H (marked as 'a'), methylene C-H (marked as 'b') and

N-H (marked as 'c') overtone bands of n-butyl amine in the ΔV=2 region
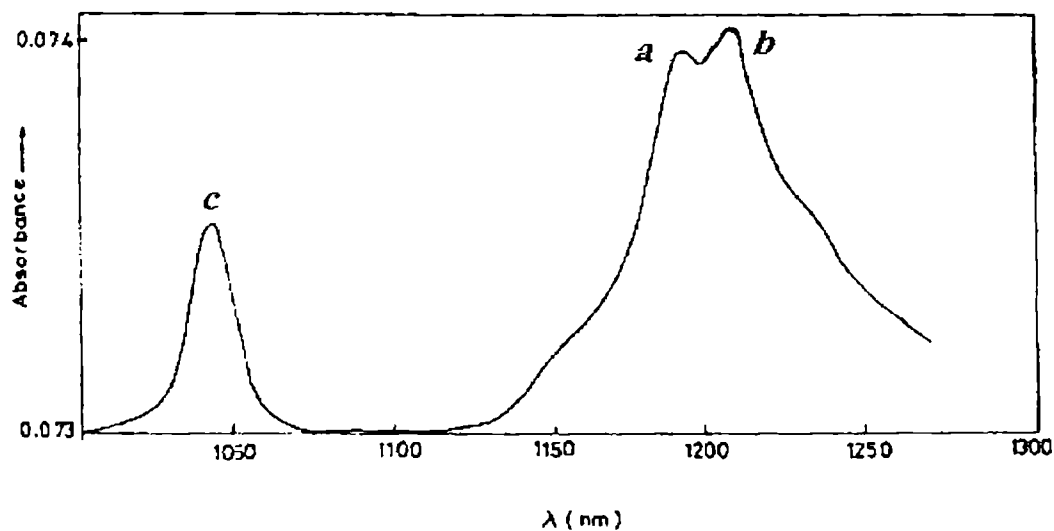


**Figure 3.9** The methyl C-H (marked as 'a'), methylene C-H (marked as 'b') and N-H

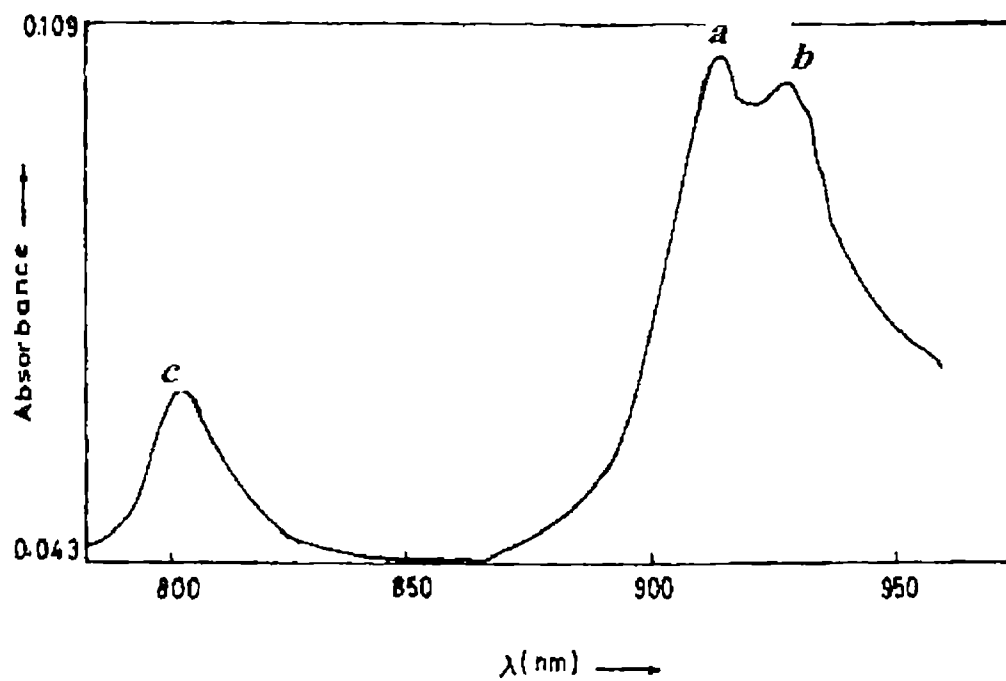(marked as 'c') overtone bands of n-butyl amine in the ΔV=3 region

103

Figure 3.10 The C-H (methyl marked as 'a' and methylene marked as 'b') and

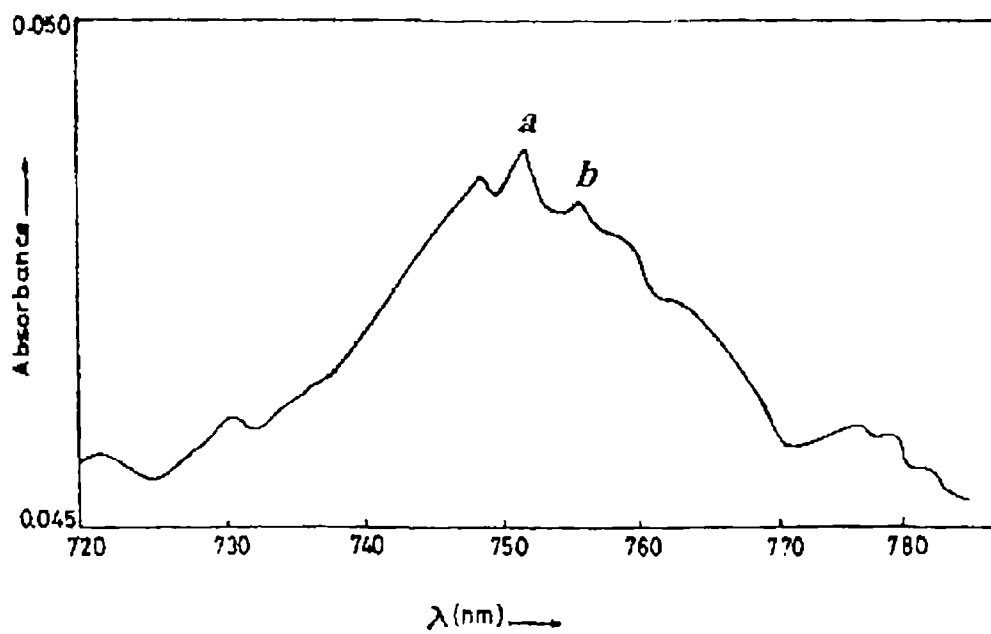N-H (marked as 'c') overtone bands of n-butyl amine in the ΔV=4 region



Figure 3.11 The methyl (marked as 'a') and methylene (marked as 'b')

C-H overtone  bands of n-butyl amine in the $\Delta V=5$ region

The observed values of N-H mechanical frequency and anharmonicity constant in n-butyl amine are 3511cm$^{-1}$ and -80cm$^{-1}$ respectively, whereas the corresponding values in t-butyl amine are ~3479cm$^{-1}$ and ~ -77cm$^{-1}$. The increase of mechanical frequency (~32cm$^{-1}$) and anharmonicity (~ 2.5cm$^{-1}$) in n-butyl amine over t-butyl amine can be explained as follows. It is well established in overtone spectroscopy that an electron-donating group increases mechanical frequency and an electron-withdrawing group decreases mechanical frequency [35, 36, 38, 46]. IR studies by McKean [47] reported that a nitrogen atom donate its unshared lone pair electrons into an anti bonding orbital of the adjacent trans-group. It is likely that a similar effect operates in n-butyl amine in which the non-bonding electron pair of nitrogen is donated into the adjacent -CH$_2$ group. One can therefore expect that the electron donating effect reduce the electron density at the nitrogen atom. This can cause a net attraction of the electron clouds associated with the amine hydrogen atoms towards the nitrogen atom. This causes an increase in N-H force constant resulting in an increase in N-H mechanical frequency value. But in t-butyl amine the –NH$_2$ group is attached to the central carbon atom and hence chances of lone pair trans effect is absent in this molecule. It can be seen from the Table 3.3 that the mechanical frequency of t-butyl amine is slightly increased when compared that in neopentane. This increase in mechanical frequency is consistent with the small electron withdrawing inductive effect of amino group $\sigma_I$ = +0.11 and the electron donating effect of the t- butyl group $\sigma_I$ = -0.08 [Ref. 36]. The inductive effect draws electrons from the t-butyl part and this effect increases the electron density of the N-H oscillator. This results in the decrease of the N-H mechanical frequency of t-butyl amine. The local mode parameters indicate that in t-butyl amine -NH$_2$ group act as an electron-withdrawing group whereas in n-butyl amine the -NH$_2$ group acts as an electron-donating group. In n-butyl amine the lone pair effect is more active compared to $\sigma_I$ effect. Consequently the electron density of N-H oscillators decreases and the mechanical frequency increases.

The observed values of methyl C-H mechanical frequency and anharmonicity in t-butyl amine are 3082cm$^{-1}$ and –67.2cm$^{-1}$ wheras the corresponding values in n-butyl amine are 3035.6cm$^{-1}$ and -60.3cm$^{-1}$. The primary C-H mechanical frequencies and anharmonicities of most of the branched alkanes are identical to those of primary C-H in n-

alkanes. The methyl CH mechanical frequency of    n-butyl amine is less than the mechanical frequency of n-butane [41]. However at room temperature n-butane is gas and the values given are for the vapor state. Hence we used the average value of liquid n-alkanes for a comparison [45]. This is possible because in liquid phase n-alkanes the observed local mode parameters corresponding to either $CH_3$ or $CH_2$ form a consistent set [41]. As in the n-alkanes, we see in n-butyl amine higher oscillator strength for methyl C-H as compared to methylene C-H. Comparison of the local mode parameters of methyl C-H in liquid phase n-butyl amine with that of n-alkanes demonstrates that there are no remarkable differences between them. It can be seen from the Table 3.3 that the methylene C-H is at significantly lower mechanical frequency than in n-alkanes. (There is a decrease of $\sim31 cm^{-1}$ for the methylene C-H mechanical frequency in n-butyl amine with respect to n-alkanes.) In n-butyl amine the $-NH_2$ group is attached to a methylene group and this decreases the mechanical frequency of methylene C-H oscillator. It is likely that an inductive effect of $NH_2$ group operates increases the mechanical frequency of the methylene C-H oscillator but the frequency increases is overwhelmed by the lone pair effect resulting in a net decrease in methylene frequency. The methylene C-H anharmonicity is also strongly affected in n-butyl amine.

The C-H stretching mechanical frequency of t-butyl group [23, 33] in liquid phase is reported as $\sim3080 cm^{-1}$ where as the value is found to be less than $3040 cm^{-1}$ in most of normal and branched alkanes [46]. This high value of mechanical frequency in t-butyl group may be due to the coupling of stretching overtone to other modes of vibration or due to coupling between methyl groups. In the fundamental region coupling probably occurs between C-H stretching and other lower frequency modes such as bending. In a recently published work Henry et al [48] have presented an extensive analysis of the vibrational properties to neopentane in the highly excited state. It is interesting that the analysis of higher overtones $\Delta V_{CH}$ = 5-8 gives evidence for a through space interaction between the methyl groups that has the effect of raising the C-H stretching frequency.

### 3.4.2 Conclusions

The near infrared vibrational overtone spectra of liquid phase n-butyl amine and t-butyl amine are spectrophotometrically recorded and analyzed using the local mode model. It is demonstrated how the influence of the environment on the C-H oscillator can be observed in the energies of the overtone peaks of the molecules studied. The observation is that the lone pair trans effect of $-NH_2$ group plays dominant role in n-butyl amine and the inductive effect of $-NH_2$ group plays dominant role in t-butyl amine in determining the C-H bond strength. The difference in the value of mechanical frequency in t-butyl amine and n-butyl amine is the manifestation of the substituent effect in these molecules. The well-known fact that secondary C-H bonds are more reactive than primary C-H is reflected in the significantly lower dissociation energy values for the secondary C-H.

## References

[1]     B.R.Henry, *Vibrational spectra and structure*, Ed. J. R. Durig (Elsevier, Amsterdam, 1981) Vol.10, p.269.

[2]     M.S.Child and L.Halonen, *Adv.Chem.Phys.* 57(1984)1.

[3]     B.R.Henry *Acc.Chem.Res*,20( 1987)429.

[4]     K.M.Gough and B.R.Henry, *J.Phys.Chem*,88(1984)1298.

[5]     R.Nakagaki and I.Hanazaki, *J.Phys.Chem*,86(1982)1501.

[6]     B.R.Henry,      K.M.Gough      and      M.G.Sowa,      *International Rev.Phys.Chem.*,5(1986)133.

[7]     H.L.Fang, R.L.Swofford, M.McDevitt and A.R.Anderson, *J.Phys.Chem.* 89(1985)225.

[8]     M.K.Ahmed and B.R.Henry, *J.Phys.Chem.*,90(1986)1993.

[9]     M.K.Ahmed,D.J.Swanton and B.R.Henry, *J.Phys.Chem.*,91(1987)293.

[10]    K.M.Gough, B.R.Henry, B.J.Schattka and T.A.Wildman, *J.Phys.Chem.*,95(1991)1579.

[11]    M.G.Sowa, B.R.Henry, and Y.Mizugai, *J.Phys.Chem.*,97(1993)809.

[12]    H.G.Kjaergaard and B.R.Henry, *J.Phys.Chem.*,99(1995)899.

[13]   D..M.Turnbull,M.G.Sowa, and B.R.Henry, *J.Phys.Chem.*,100(1996)13433.

[14]   H.G.Kjaergaard, D.M.Turnbull and B.R.Henry, *J.Phys.Chem.*,101(1997)2589.

[15]   M.S.Child, *Acc.Chem.Res*,18( 1985)45.

[16]   K.M.Gough and B.R.Henry *J.Phys.Chem*,87(1983)3433.

[17]   D.L.Howard and B.R.Henry, *J.Phys.Chem.A*,102(1998)561.

[18]   R.J.Proos and B.R.Henry, *J.Phys.Chem.A*,103(1999)8762.

[19]   C.Gellini, L.Moroni and M..M..Miranda, *J.Phys.Chem.A*,106(2002)10999.

[20]   K. K. Vijayan, Sunny Kuriakose, S.Shaji, and T. M. A. Rasheed, *Asian J.Phys.*,11(2002)66.

[21]   T.Lukka, E.Kauppi and L.J.Halone, *J.Chem.Phys.*, 102(1995)5200.

[22]   B.R.Henry and M.A.Mohammadi, *Chem.Phys.Lett.*,75(1980)99.

[23]   B.R.Henry, A.W.Tarr, O.S.Mortensen, W.F.Murphy and D.A.C.Compton, *J.Chem.Phys.*, 79(1983)2583

[24]   L.Halonen and M.S.Child, *J.Chem.Phys.*, 79(1983)4355.

[25]   L.Halonen and M.S.Child, *Mol.Phys.*, 46(1982)239.

[26]   O.S.Mortenson, B.R.Henry and M.A.Mohammadi, *J.Chem.Phys*, 79(1981)4800.

[27]   M.W.P.Petryk and B.R. Henry, *Can J.Chem.*, 79(2001)279.

[28]   A.W.Tarr and B.R.Henry, *J. Chem.Phys.*, 84(1986)1355.

[29]   M..K.Ahmed and B.R.Henry, *Can. J.Chem*, 66(1988)628

[30]   A.W.Tarr and B.R.Henry, *Chem. Phys. Letts,* 112(1984)295.

[31]   M.L.Sage and J.A.Williams III, *J.Chem.Phys.*,78(1983)1348.

[32]   T.M.A. Rasheed and S Shaji , *Asian J. Phys.*, 8(1999)199.

[33]   M.K.Ahmed and B.R.Henry, *J. Phys.Chem*, 91(1987)3741.

[34]   T.M.A.Rasheed, K.P.B.Moosad, V.P.N.Nampoori and K.Satyanandan, *J. Phys.Chem.*,91(1987)4228.

[35]   R Nakagaki and J Hanazaki, *Spectrochim. Acta*, A40(1984)57.

[36]   Y. Mizugai and M. Katayama, *J.Am.Chem.Soc*, 102(1980)6424.

[37]   L.N.Fergusan, *The Modern Structural Theory of Organic Chemistry*, Prentice-Hall of India, New Delhi,1969, p.420

[38]   Y Mizugai, M. Katayama and N.Nakagawa, *J.Am.Chem.Soc*, 103(1981)5061.

[39]   K.M.Gough and B.R.Henry, *J.Am.ChemSoc.*,106(1984) 2781.

[40]   L.J.Bellamy and D.W.Mayo, *J.Phys.Chem.*, 80(1976)1217.

[41]   W.R.A.Greenlay and B.R.Henry, *J.Chem.Phys.*,69(1978)82.

[42]   J.S.Wong and C.B.Moore, *J.Chem.Phys.*,77(1982)603.

[43]   H.L.Fang and R.L.Swofford, *J.Chem.Phys.*,73(1980)2607.

[44]   B.R.Henry and W.R.A.Greenlay, *J.Chem.Phys.*,72(1980)5516.

[45]   H.L.Fang, D.M..Meister and R.L.Swofford, *J.Phys.Chem.*,88(1984)410.

[46]   T.M.A.Rasheed and V.P.N.Nampoori, *Pramana-J. Phys.*, 42(1994) 245.

[47]   D.C.McKean, *Chem.Soc.Rev.*, 7(1978)399.

[48]   M.W.P.Petryk and B.R. Henry, *J.Phys.Chem.A*, 106(2002) 8599.

CHAPTER 4

# APPLICATION OF PULSED Nd: YAG LASER TO THE STUDY OF FLUORESCENCE AND RAMAN SPECTRUM OF SOME ORGANIC MOLECULES

CHAPTER 4

# APPLICATION OF PULSED Nd:YAG LASER TO THE STUDY OF FLUORESCENCE AND RAMAN SPECTRUM OF SOME ORGANIC MOLECULES

## 4.1 Introduction

Investigations on the molecular structure in both the ground and excited electronic states provide a better understanding about their molecular properties and related chemical reactions. Various spectroscopic techniques have been widely used for the precise determination of the different aspects of molecular structure. The principle underlying any such method is the interaction between the incident electromagnetic radiation and the molecules of the substance. Fluorescence and Raman spectroscopy are two important spectroscopic methods used for molecular structural studies. Fluorescence spectroscopy has been widely utilized to study electronic transitions in atoms and molecules whereas Raman spectroscopy provides information about the vibrational energy levels. The technological advances in lasers occurred for the past fifty years have provided scientists with most suitable spectroscopic light sources. The high degree of monochromaticity, coherence, directionality, and irradiance possessed by laser radiation make it ideal for recording fluorescence and Raman spectra under high emission intensity and /or spectral resolution. Laser induced fluorescence (LIF) is the technique in which the laser frequency is tuned to match a transition energy in an atom or a molecule and the resultant fluorescence is observed. When a beam of monochromatic light is scattered by a sample that does not absorb at the wavelength of the beam, the spectrum of the scattered light contains a number of blue and red shifted lines, with respect to the excitation, these constitute the Raman spectrum of the sample. Excellent reviews and textbooks are

111

available in both the above areas of spectroscopy [1-8]. Brief outlines of some reported works in the two areas are given in sections 4.2.2 and 4.3.2 below.

The use of pulsed lasers provide additional advantages for the fluorescence and Raman studies because of the following characteristics (1) the delivery of photons to the system can be achieved within a short well-defined time interval (2) high peak power. The evolution of the subsequent physical and chemical events can be followed by appropriate optical techniques. The development of high sensitive and fast response solid-state detectors called charge coupled devices (CCD) made it convenient for the detection and analysis of single shot fluorescence and Raman spectral emission induced by pulsed lasers. In the present study, the experimental capabilities of the combination of a pulsed laser and a CCD detector are used for investigating the LIF and /or Raman spectral details of some polyatomic molecules. The following sections give the details of the experimental arrangement, the presentation of the recorded LIF spectra of benzyl amine, poly benzyl amine, n-butyl amine, poly n-butyl amine and p-anisidine and Raman spectra of m-fluoroaniline, anisole, t-butyl amine and p-anisidine. The observed LIF and Raman lines, including some newly observed ones corresponding to low-lying vibrational levels, are assigned successfully.

## 4.2 LIF and Raman Spectroscopy

### 4.2.1 Laser induced fluorescence

Laser Induced Fluorescence is one of the most common forms of laser spectroscopy used today. LIF is a technique that relies on measurement of the excited state fluorescence that follows photo excitation. Among the very large number of known organic compounds only a small number exhibits fluorescence. Hence a molecule fluoresces itself provide valuable information regarding the molecular structure. The fluorescence of a molecule depends on the structure of the molecule and the environment in which the spectrum is measured. Fluorescence is exhibited both by free atoms and by molecules; it can occur in the gaseous, liquid and solid state, although not necessarily in all three phases of the same substance. Due to interactions of solute with solvent molecules the fluorescent spectrum is usually blurred out and a smooth curve is observed.

112

In vapour phase and in non-polar solvents the vibrational fine structure is sometimes appeared [9].

The principal limitation of LIF technique is the requirement that the excited state must have a significant fluorescent quantum yield. Different molecules emit many different fluorescent lines. The amount of fluorescence is related to a number of different factors - temperature, concentration, symmetry, etc. Since the intensity of fluorescence emission is related to concentration, it can be used as an analytical method. When the laser beam hits the sample only the species that has a transition of the same wavelength will be excited. Because of this selective excitation of molecules, all the fluorescence observed would be from these species. The other chemicals essentially become 'inactive' [10].

Heteroaromatic molecules containing $\pi$ electrons can be promoted to $\pi^*$ orbitals as these electrons are less tightly bound compared to $\sigma$ -electrons. Like heterocycles, most aromatic carbonyl compounds posses lowest excited singlet state of $(\pi,\pi*)$ or (n, $\pi*$) character. When a carbonyl group is conjugated with an aromatic system $(\pi,\pi*)$ florescence is appreciably lower in energy than the (n, $\pi*$). For many aliphatic aldehydes and ketones weak $(n,\pi*)$ fluorescence is observed [11].

## 4.2.2 LIF – An application overview

One of the important applications of LIF is in trace elemental analysis. The sample to be analyzed is atomized in plasma, in a furnace or in a laser flame, where it is excited using a tunable laser and the resulting fluorescence spectrum is recorded. The fluorescence frequencies provide an unambiguous fingerprint of the elements present [2]. LIF finds widespread use in the determination of spatial and / or temporal concentration profiles of atomic species in plasmas flames and discharges. Muraoka and Maeda [8] reviewed the application of LIF to measurements in plasma with particular emphasis on the understanding of plasma-surface interactions in high-temperature plasmas. The necessary hardware for the diagnostic including various tunable lasers, which are used for the purpose are described in this article. LIF is one of the most versatile diagnostic

methods used to probe combustion environments, both for species concentrations and for multi-dimensional imaging applications. Numerous atoms and diatomic molecules have been detected in flames with a variety of single photon and multi-photon approaches. Harrington and Smyth [12] conducted LIF measurement of formaldehyde in a methane/air diffusion flame at atmospheric pressure. This is an important optical measurement in flames of naturally occurring formaldehyde, an important intermediate in the oxidation of hydrocarbons.

Another important application of LIF is in high resolution molecular spectroscopy, leading to accurate determination of vibrational, rotational, spin-orbit constants etc and transition probabilities like Franck-Condon factors, radiative lifetimes etc. Santos et al [13] studied the fluorescence excitation spectrum of jet-cooled molecular beam of m-methyl aniline, corresponding to the $S_1 \leftarrow S_0$ electronic transition in the region 33700-34900cm$^{-1}$. Jungner and Halonen [14] reported dispersed fluorescence spectra from the rotation states of the excited CH stretching vibrational state in acetylene in the ground electronic state using an FTIR spectrometer. LIF method was used to investigate collision-induced processes in the hydrogen-stretching vibrational overtone region of the ground electronic state of acetylene, where the spectrum shows collision induced rovibrational symmetry changes [15]. Lee et al [16] recorded LIF excitation spectrum of jet cooled 4-(9-anthryl) aniline where the workers observed two kinds of vibrational progressions corresponding to the transitions of two weakly coupled electronic states. LIF spectroscopy was used to examine the vibrational dependence of three body forces in Ar$_2$HF at $V_{HF}$ =3 region [17]. LIF was also used to investigate overtone states of the ground electronic state of water [18]. LIF techniques using excitation in the A-X and D-X electronic systems have proven a reliable technique for two-dimensional imaging of nitric oxide (NO) concentrations in practical combustion systems. Lee et al [19] reported LIF detection of NO in high-pressure flames with A-X (0,0), (0,1) and (0,2) excitations.

Different types of absorption experiments have been used to study weak overtone transitions in molecular systems. However, there may exist states that cannot be accessed from the ground vibrational state by one-photon absorption, due to the symmetry of the molecule. Halonen and co-workers [20] developed a method called dispersed vibration-rotation fluorescence spectroscopy. They applied this technique to two small molecules

114

acetylene and water and illustrated the method to be suitable for studying molecular systems where some states are inaccessible with standard absorption experiments due to symmetry selection rules.

Kirby and Hanson [21] reported a new fluorescence imaging diagnostic technique called infrared planar laser induced fluorescence (IR PLIF), which is suitable for measurements of IR active molecules whose electronic transition lie in the vacuum ultra violet region. They employed a nanosecond pulsed laser system to generate high energy pulses at 2.35$\mu$m for excitation of CO, with ensuing fluorescence collected at 4.7 $\mu$m. In a subsequent paper these authors presented IR PLIF technique for $CO_2$ imaging also [22].

Two-photon induced fluorescence is now established to be a useful spectroscopic tool for elucidating the molecular electronic structure of excited states. This is because the selection rules for a two-photon transition are complementary to those for one photon transition [23]. It was shown that fluorescence induced by two-photon excitation using a picosecond light continuum generated in $D_2O$ is a useful and sensitive technique for studying of excited electronic states of large organic molecules in solution [24]. Two-photon induced fluorescence is recently used for bio-molecular imaging with three-dimensional resolution [25]. The temporal, spectral and intensity dependent properties of the two-photon induced fluorescence emission from the photodynamic phycoerythrin protein excited by a 1.06$\mu$m laser beam are reported by Chen et al [26]. Reeves et al [27] described a two-photon LIF scheme for the detection of the nitric oxide in an atmospheric pressure flow and hydrocarbon-air flame.

Takayanagi and Hanazaki [28] applied stimulated–emission-pumping LIF technique to investigate the dynamics of vibrationally excited states of van der Waals complexes, anisole-$d_0$.Ar and anisole-$d_3$.Ar produced in a supersonic expansion. Pepper et al [29] designed a new multi-channel laser induced fluorescence probe with novel optical fiber probe geometry, which was integrated into a cone penetrometer testing system for *in situ* contamination detection.

Kim et al [30] reported the fluorescence emission spectra and assignments of $NO_3$ radical excited at five different frequencies. On the basis of the analysis of the fluorescence bands and using the earlier literature, they suggested a molecular model for

the $NO_3$ radical. Misra et al [31] reported LIF of methyl thio radical in a supersonic jet environment, which enabled recording and identification of 21 vibronic bands for excitation in the 360-387nm regions with $0.2cm^{-1}$ resolution. Heintxe and Bauer [32] demonstrated the feasibility of detecting the silylene radical ($SiH_2$) in hydrogenated amorphous silicon plasma directly by LIF. Herti and Jolly [33] used LIF spectroscopy to measure $SiH_2$ radical densities in pure $SiH_4$, $H_2/SiH_4$ and $Ar/SiH_4$ radio frequency glow discharges used for amorphous silicon thin film deposition. Hayashi et al [34] introduced LIF spectroscopy as an *in situ* diagnostic for phenol and intermediate products in an aqueous solution degraded by pulsed corona discharges above water. Martinez et al [35] have presented collision-free lifetime data for various rovibrational levels of bromine B state using LIF technique. With its excellent space and time resolution, LIF spectroscopy is established to be a powerful *in situ* method for the detection of molecules.

## 4.2.3 Raman spectroscopy

Raman scattering is the inelastic scattering of light by a material that involves an exchange of energy between the incident light quanta and the molecules of the material. The scattered contains spectral lines on both the low energy (Stokes) and high energy (anti-Stokes) sides of the excitation line. This spectrum of the scattered light is called Raman spectrum and is of great scientific interest as it provides information about the structure, composition, and the vibrational, rotational and sometimes electronic states of the scattering material. The frequency shifts of the Raman lines from the excitation frequency equals the frequencies of the normal modes of molecular vibrations. A mode of vibration of a molecule is Raman active if a change in polarizability occurs during that mode of vibration. The classical and quantum theory of Raman effect are discussed in detail in many treatises [2,36]. The advantages of using laser as a Raman excitation source gave birth to the era of laser Raman spectroscopy [7]. When the laser frequency is tuned near or on the absorption band in the upper electronic state, the phenomenon of Resonance Raman Scattering (RRS) occurs, causing large increase in the scattering intensity and selective enhancement of some vibrational modes [2,37].

116

Raman spectroscopy is widely used to obtain information about the vibrational spectra of different polyatomic molecules. The molecular structure and composition of a material under study is encoded as a set of frequency shifts in the Raman scattered spectrum. This can lead to a better understanding of the chemical composition, especially in many organic compounds where different chemical groups have very characteristic vibrational frequencies. The presence of different chemical species leads to small modifications of the usual vibrational frequencies so that longer-range structure may be investigated. In crystalline solids the selection rule for scattering from the lattice vibrations indicate the symmetry of the crystal unit cell and can reveal phase changes. In Resonance Raman spectra one can sometime correlate a particular vibrational mode with particular electronic transition energy and learn more about the electronic structure of the material [2]. Raman spectral data are useful in detecting interaction between molecules. Thus if hydrogen bonding is present the Raman shift corresponding to the C-H and C=O vibrations appear at values distinctively lower than their normal values. The set of vibrational energy levels is unique for each kind of molecule. Thus a qualitative analysis of a mixture can be carried out by comparing the Raman spectrum of the mixture with the spectra of pure compounds that might be present in the mixture. Some of the recent works giving important applications of Raman spectroscopy are outlined below.

## 4.2.4 Raman spectroscopy- application overview

In addition to its wide range of applications in chemistry, physics, biology and material science [38], Raman spectroscopy is recently established to be is a potentially important clinical tool for real-time diagnosis of diseases. A review of the application of Raman spectroscopy in biology and medicine using visible laser excitation to present day technology based on NIR laser excitation and CCD detection is given by Hanlon et al [4].

Raman scattering has proven to be invaluable for a wide variety of laser based remote sensing applications. Raman lidar is used for profiling of atmospheric water vapour, aerosols and clouds. Inaba and Kobayasi [39] used Raman effect for atmospheric studies with a Raman lidar for pollution monitoring. Yamaguchi et al [40] used Raman spectroscopy for the measurement of temperature in minute regions of semiconductors.

High-pressure behavior of optical phonons in wurtzite zinc oxide is studied using Raman spectroscopy at room temperature [41]. Raman spectroscopy has been applied to the study of hard wood and soft wood. Good quality Raman spectra of most wood species can now be obtained by using NIR Fourier Transform (FT) Raman spectroscopy [42]. Another major advantage of the FT method compared conventional Raman is that the time required to obtain a spectrum has been significantly reduced. Raman spectroscopy is applied for identification and detection of the proportion of methanol in methanol-gasoline mixture. Raman spectroscopy can be applied to detect the edible oil's purity, relative freshness and usage levels [43]. Raman spectroscopy was used to get direct structural information about the lubricant organic films with a thickness greater than 10nm confined between two solid surfaces under conditions of pressure and sheer [44] Raman spectroscopy was used for characterization of organic-inorganic hybrid materials between the crystalline antimonic acid and two conductive polymers polypyrrole and polyaniline [45]. Kolev et.al [46] studied the Raman spectrum of benzophenone, benzophenone-$d_{10}$ and benzophenone-$^{18}$O in the 100 - 4000 cm$^{-1}$ region at room temperature. Nair and Eappen [47] reported the Raman spectrum of the low-lying vibrational states of o-chlorotoluene. Tocon et.al [48] reported the Raman spectrum and assignment of the vibrational levels of 4-fluoroaniline. A comparison of the spectrum with that of aniline was made and the substitution effect of fluorine was also evaluated. Studied. Arenas et al [49] reported the Raman spectrum of 2-methylpyridine. Henry et al [50] measured Raman spectrum of CH stretching vibration in neopentane and compared it with overtone absorption spectrum.

Fontaine and Furtak [51] developed a versatile technique called variable angle internal reflection Raman spectroscopy for controlling and modeling the optical field distribution in polymer or other transparent thin film systems. UV Raman spectroscopy broadens the application of Raman spectroscopy for the characterization of variety of catalysts owing to avoiding the fluorescence and increasing the sensitivity. Resonance Raman spectroscopy techniques opens up the broad prospects for Raman studies [52, 53]. Formation of cross-linked structures in polymer films on heating was investigated by *in-situ* Resonance Raman spectroscopy. Resonance Raman Spectroscopy (RRS) is used to study the excited state structure and dynamics of various photochemical and photo

physical process. Biswas and Umapathy [37] discussed various applications of RRS including excited state structure studies.

## 4.3 Experimental Details

### 4.3.1 Experimental setup for recording LIF and Raman spectra

We used the most common geometry of the perpendicular configuration for recording the LIF and Raman spectra. In this configuration, the sample is illuminated with an intense monochromatic beam of light and the emitted light is collected using a monochromator – detector assembly at a 90° angle from the laser beam path, so that the direct beam of light is not detected. The second harmonic emission from a Q-switched Nd: YAG laser (Spectra Physics, DCR 150) is used as the excitation line. Output pulses of 6ns duration at 532 nm and a repetition rates of 10 pulses per second are produced by the laser. An output power of 500 mW is found suitable for the LIF emission of many of the organic compounds in the region 550 - 700 nm that we studied. The laser beam is focused on the liquid samples taken in a quartz cuvette. The spectra are recorded at room temperature from high purity samples (Extra pure AR grade, 99.9 % from Sisco Research Laboratories, India). A sample compartment is used for isolation of the sample cuvette from ambient light. The compartment can be attached to the entrance slit of the monochromator – detector assembly. The emitted radiations are allowed to fall on a grating monochromator (TRIAX 320) through an entrance slit. A cutoff filter at 532 nm is used to prevent the scattered laser beam from the sample cell from entering the monochromator. The wavelength dispersed emission fall on CCD (Spectrum-One from ISA Jobin Yuon Spex Instruments Inc.) through an exit slit. The data are digitally recorded by interfacing the monochromator – CCD system to a PC using GPIB DAQ from NI and the program used is Spectra Max for Windows version 3.0. Emission intensities were collected as unit-less channel counts. The experimental layout and the photographs are shown in Figure 4.1

119
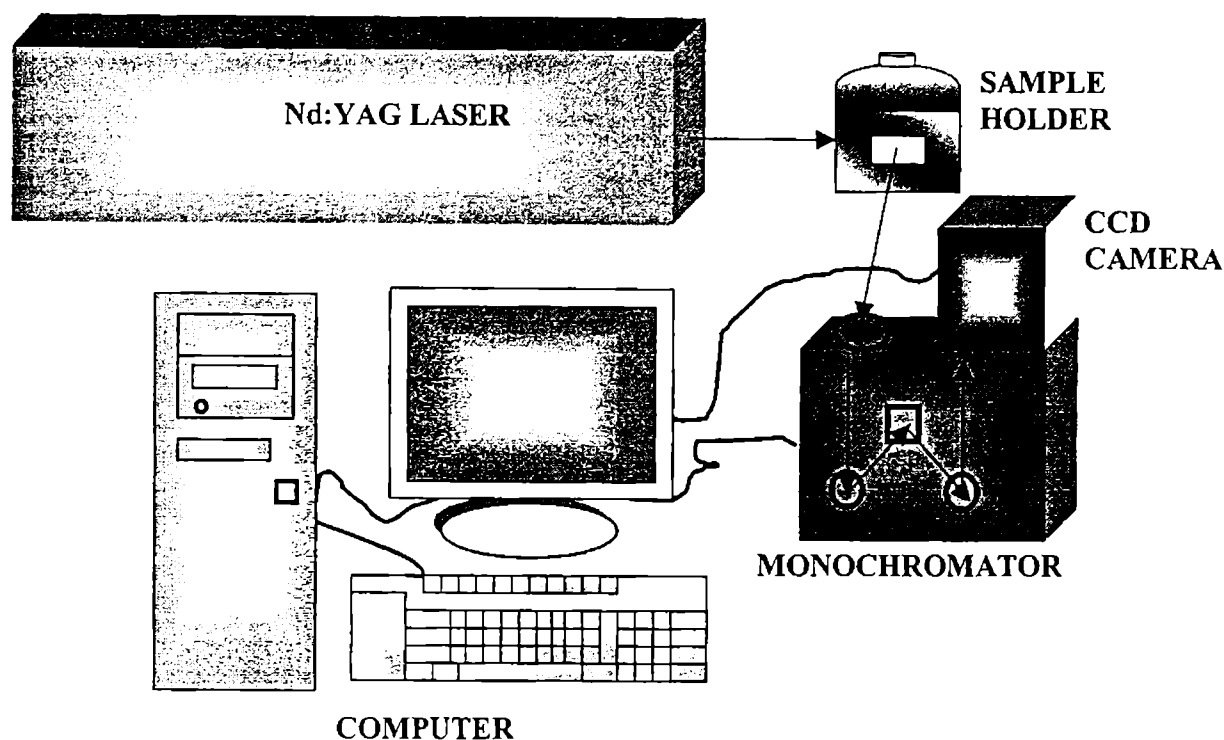
**Figure 4.1** The block diagram of the experimental setup used for LIF and laser Raman studies

## 4.3.2 Experimental considerations

The LIF spectra are obtained by exciting the sample by second harmonic out of the Q-switched Nd: YAG laser at 532 nm and the emissions from the samples are recorded using the monochromator – detector assembly. There are several experimental factors to be taken care of before recording the spectra. The output of the laser is to be made stable first. For this, firstly the flash lamp alone is switched on and the lasing rod is pumped for 15–20 minutes for thermal stability and then the laser is allowed to operate in the microsecond pulse mode for another 15 minutes. After making the flashing rate at minimum energy, the laser is switched over to the Q-switched mode which we get nanosecond pulses with very high peak power. The laser beam is allowed to fall directly into the sample kept in the sample compartment by taking special care to avoid back

(a)
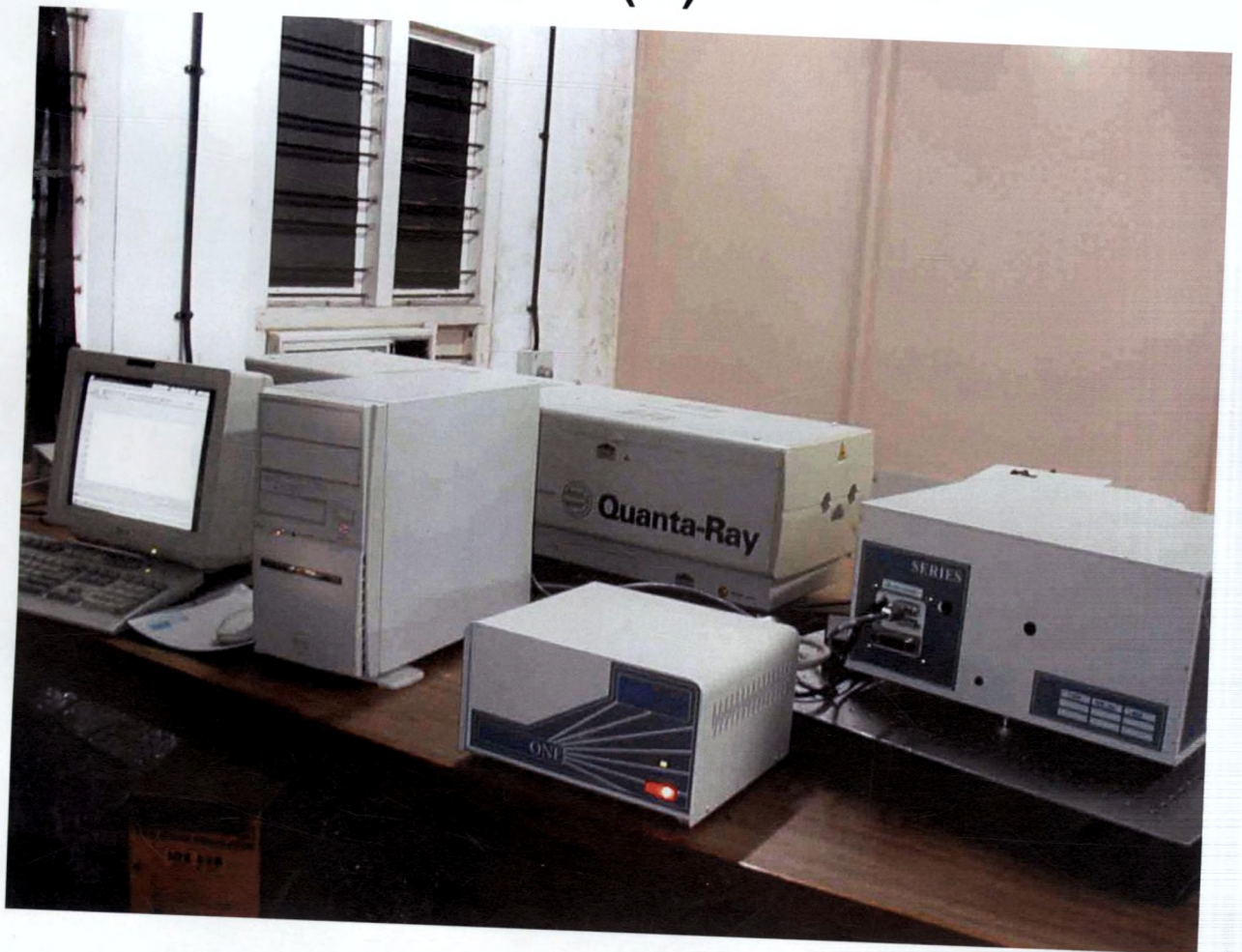


(b)

reflection of the laser beam. The position of the cuvette is slightly adjusted so that the reflected or scattered beams from the cell are not allowed to fall on the entrance slit of the monochromator. A cut off filter at 532 nm is used to prevent the laser beam falling into the monochromator. A reference spectrum is recorded to check the presence of any stray emissions or flash lamp lines. The calibration is done by recording the laser line and from the known emission lines of the neon lamp or mercury lamp. Once the calibrations are done and the setup is aligned properly, it is ready to start the measurements.

The sample is excited using the laser beam. The power of the laser beam is kept at 450 mW and the emission spectra are recorded at a longer wavelength region than the excitation wavelength. The region including the excitation line is excluded because it is very high in energy so that it can reach a saturation value and the weak emission peaks cannot be detected. Then the higher wavelength region is scanned for a wavelength range of 60 nm with a central wavelength by keeping entrance slit width of the order of 0.05 mm and the exit slit width the minimum of 0.001mm. Once the emission peak is obtained, the laser power is varied to check how the peak emission strength varies with the exciting power. Then the integration time is adjusted to a moderate value and the width of the exit slit is adjusted to a minimum value possible such that the fluorescence peak is very prominent with maximum spectral resolution. The laser power, entrance slit width, exit slit width and integration time is kept constant then and the emission spectrum is recorded in other regions of higher wavelength also. The software used allows to set the central wavelength, number of accumulations, integration time, cosmic removal, integration time, entrance and exit slit width, data file name etc. The data file can be exported as Microsoft excel data and the spectra can be plotted using the software Microcal Origin 5.

### 4.3.3 Preparation of polymer thin films

The thin films of polymer for the present study are obtained by high frequency discharge technique. An ac power supply operating at 4.5 MHz is utilized through capacitive coupling for high frequency plasma polymerization [54]. Aluminium foil rings are used to couple RF power to the reaction chamber. A glass tube of about 40cm in

length and 6cm in diameter is used as the polymerization chamber. The samples are prepared on clean optically flat glass substrates that are cleaned by chemical and ultrasonic methods prior to placing in the plasma polymerization chamber. The polymerization chamber is initially pumped to ~0.01torr and then the monomer (benzyl amine) is allowed to enter the chamber. After a steady monomer pressure of ~0.5torr is maintained, the RF is applied to obtain a glow discharge between the electrodes. The distance between the aluminium rings is adjusted to get uniform glow. Polymerization takes place and the polymer is deposited on the substrate placed between the electrodes. A uniform film of sufficient thickness (~3μm) for spectral measurements is obtained for a deposition time of about 20 minutes. Polymer films of n-butyl amine are also prepared in the same manner. The details of our polymerization setup are given in a recent thesis [55]

## 4.4   LIF Spectra of Polymer and Monomer Samples

The LIF emission spectrum of polymerized benzyl amine is shown in Figure 4.2. Most organic molecules absorb radiation in the visible and UV region. The visible spectra of organic molecules are associated with transition between electronic energy levels. The fluorescence wavelength is then a measure of the separation of the energy levels of the orbitals concerned. The transitions are generally between a bonding, lone pair orbital and an unfilled non-bonding or antibonding orbital. The radiative process is governed by the Frank-Condon principle, resulting in emission occurring from the lowest vibrational level in the excited state to a range of levels in the singlet ground state. According to Frank-Condon principle during an electronic transition the atoms in the molecule do not move. However electrons may reorganize.

The fluorescence in the visible radiation from majority of compounds is due to the deactivation of either $(n,\pi^*)$ or $(\pi,\pi^*)$ electronic excited state, depending on which of these is less energetic. In most of the electronic transitions the excited state more polar than the ground state. Then the dipole-dipole interaction with solvent molecules therefore lowers the energy of the excited state more than that in the ground state.

122

Even simple molecules have large number of electronic energy levels. In addition, each electronic level has a group of closely spaced vibrational levels associated with it. The excitation of electrons is accompanied by changes in the vibrational and rotational quantum numbers so that the line became a broad peak containing vibrational and rotational fine structure. The vibrational levels overlap to such an extent that the measured spectrum appears as a broad bell-shaped peak. This is similar to the fluorescence spectra of majority of organic compounds where the so many overlapping bands merge into one or two broad maxima when their spectra are measured in solution [10]. The benzyl amine molecule undergoes a $\pi^* \leftarrow \pi$ electronic transition. This excitation is strongly allowed and as a result the fluorescence is emitted. The fluorescent emission in this compound contains two equally intense peaks centered at 627nm and 650nm. Figure 4.3 shows the fluorescent spectrum of benzyl amine monomer when excited by 417nm using a spectrofluorometer. The fluorescent emission in benzyl amine monomer is centered at 485nm. When the length of the conjugated system increases, the wavelength of the fluorescence emission also increases correspondingly [9,10]. A change of shape of the molecule on electronic excitation is proved to be the reason for the appearance of doublet or triplet nature of the spectrum [56].
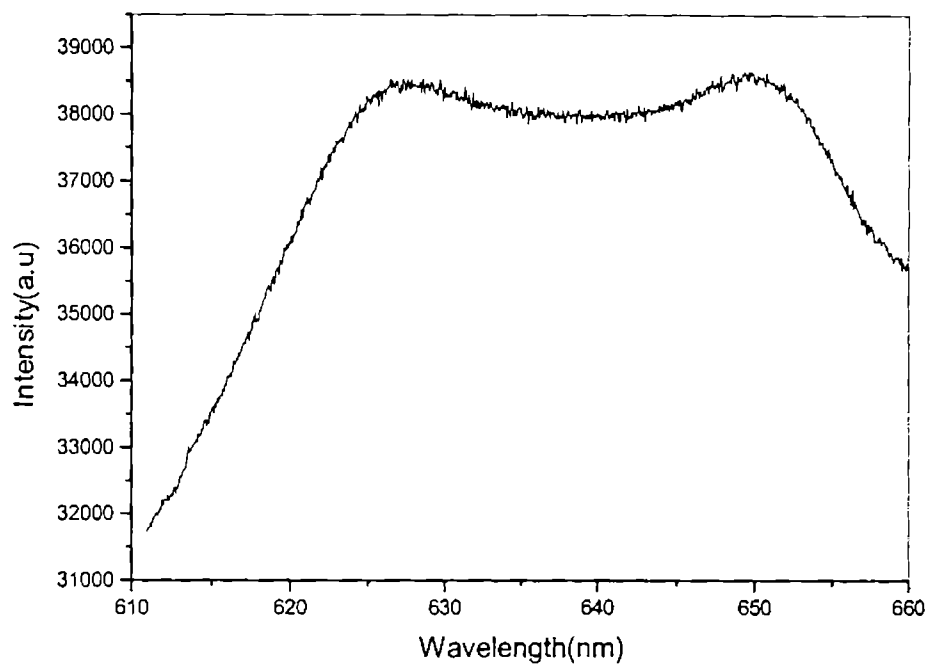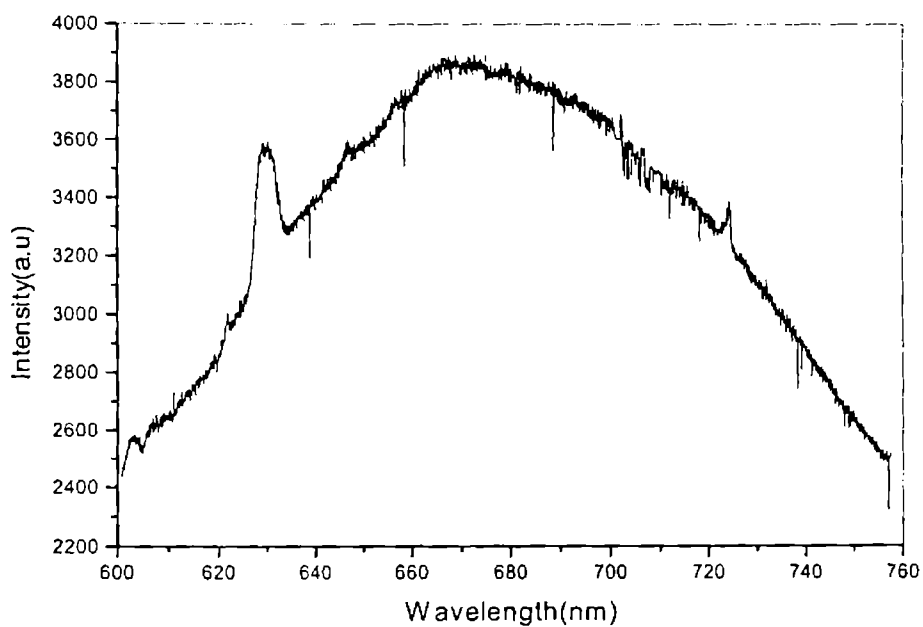
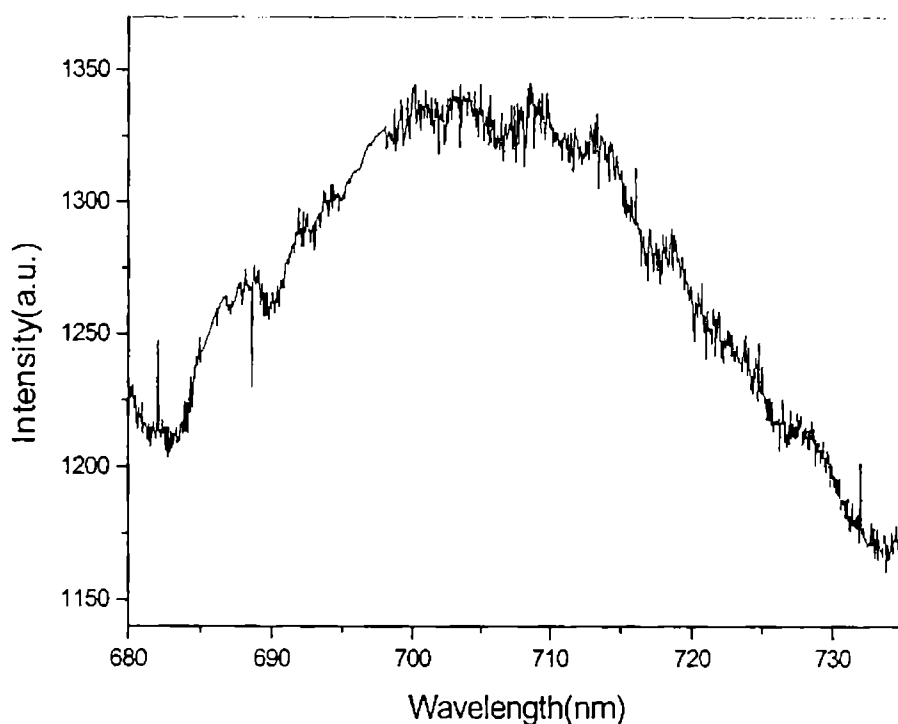**Figure4.2** LIF emission spectrum of benzyl amine polymer when excited by 532nm
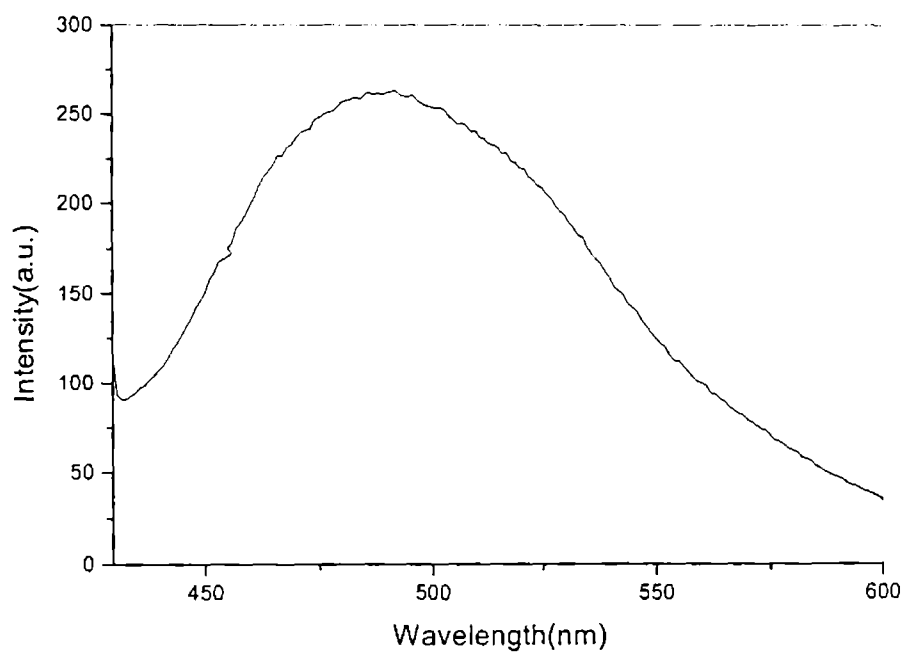


**Figure 4.3** Fluorescence spectrum of benzyl amine monomer under excitation by 417nm

124
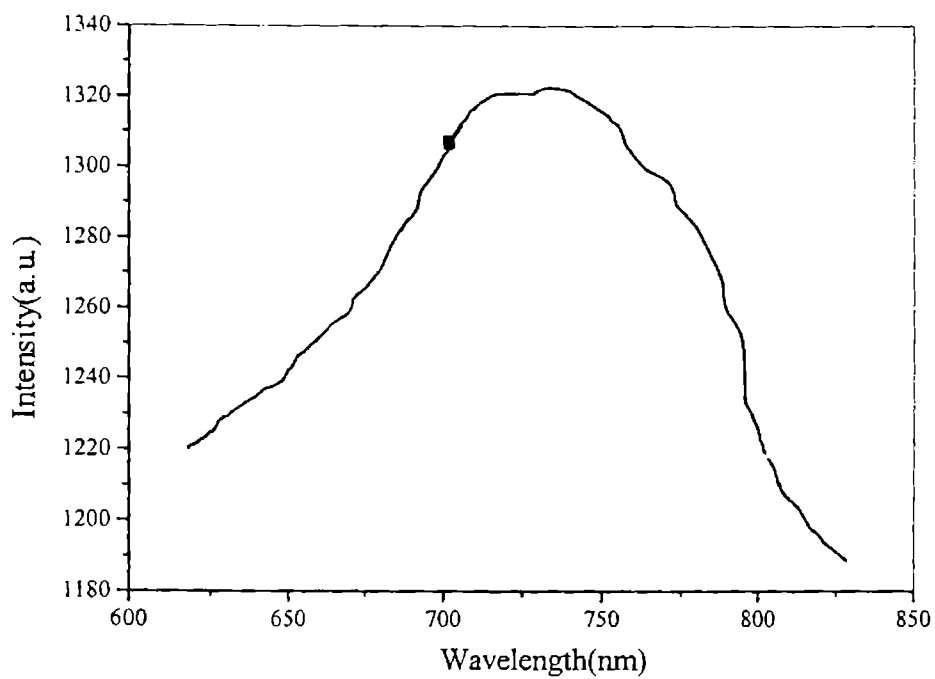
**Figure4.4** LIF emission spectrum of n-butylamine polymer under excitation by 532nm



**Figure 4.5** LIF emission spectrum of n-butyl amine monomer under excitation by 532nm

125

**Figure 4.6** LIF emission spectrum of p-anisidine under excitation by 532nm

LIF emission spectrum of n-butyl amine polymer is shown in the Figure 4.4. Very few aliphatic organic molecules exhibit fluorescence. All electrons in aliphatic compounds are either tightly bound or are involved in $\sigma$ bonding. As a result the fluorescence quantum yields of such molecules are usually very low [11]. N-butyl amine exhibits fluorescence emission and observed that it is centered at 725nm. Normally nonbonding electrons are the most easily removed in a molecule. The transition of a non-bonding electron on a heteroatom to an empty antibonding molecular orbital gives fluorescence. The non-bonding electrons on nitrogen atom in amines are loosely bound. The electronic absorption spectrum of methylamine ($CH_3NH_2$) is very similar in character to the absorption of ammonia ($NH_3$) except that the spectrum is shifted to the longer wavelength. The absorption corresponds to the removal of an electron from the lone pair orbital of the nitrogen atom into one of the Rydberg orbital [57]. We can expect

126

a similar type transition in n-butyl amine $(CH_3-CH_2-CH_2-CH_2-NH_2)$ shifted to longer wavelength. The fluorescent band in the polymerized butyl amine is further shifted to the longer wavelength region as the length of the chain increases. Since $n \rightarrow \sigma^*$ transition is more probable in amines than alcohols, the amines absorb at higher wavelength as compared to alcohols. LIF emission spectrum of n-butyl amine in the monomer form is shown in the Figure 4.5. The fluorescence is centered at 670nm.

LIF emission spectrum of p-anisidine is centered at 705nm (Figure 4.6). In analogy with the fluorescent spectrum of aniline the spectrum is due to $\pi^* \leftarrow \pi$ excitation transition. Molecules containing $\pi$ electrons can be promoted to $\pi^*$ orbitals as these electrons are less tightly bound compared to $\sigma$ -electrons.

## 4.5 Pulsed Laser Raman Spectra of Some Organic Compounds

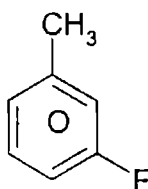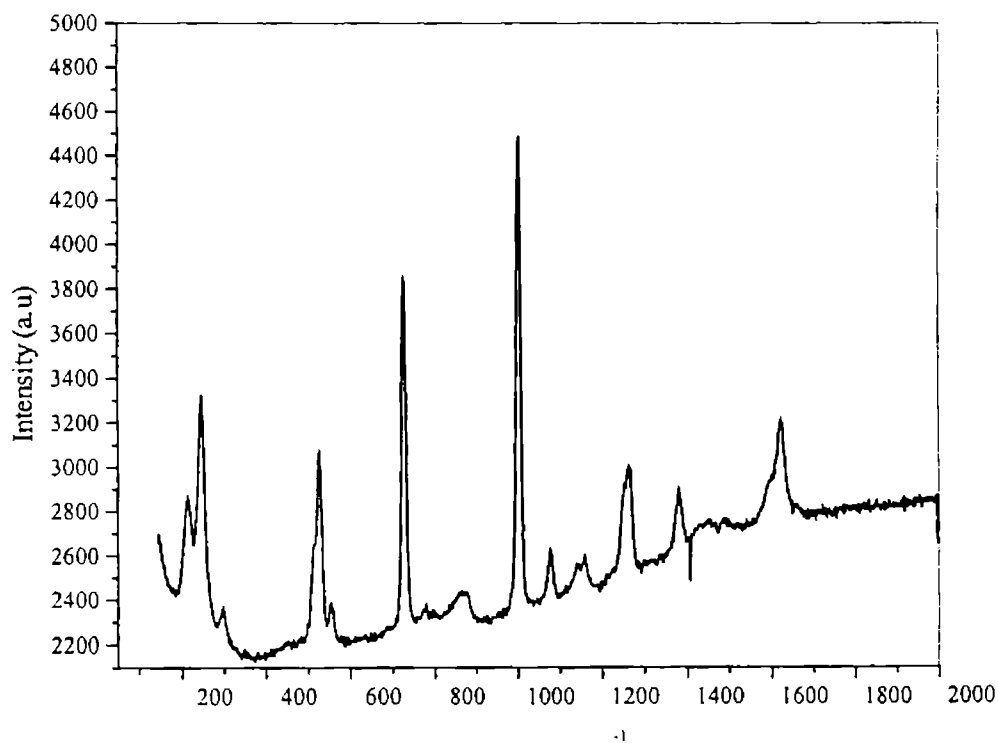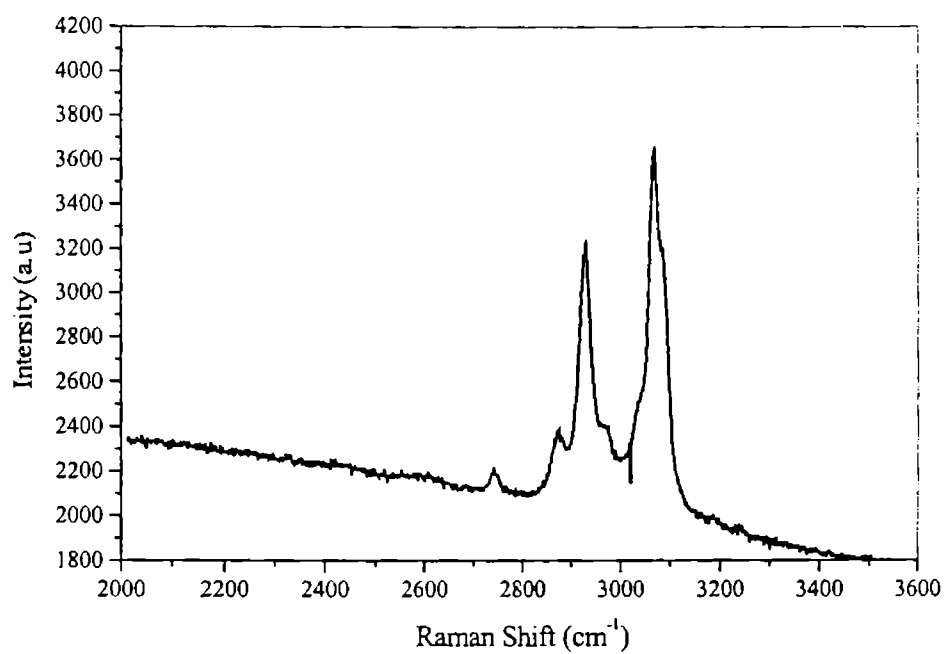### 4.5.1 Spectrum of m-fluorotoluene



Figure 4.7 molecular structure of 3-flurotoluene

The identification of the fundamental modes of vibration of hydrocarbon groupings in different molecules is of considerable importance for the systematic interpretation of IR and Raman spectra. It is known that most of the normal mode vibrations in monosubstituted and disubstituted benzenes are quite similar to those of benzene [58]. Santos et al [13] proved that this behavior works well in the case of m-methyl aniline. In the present studies the assignment of Raman lines have been made by comparison with those of other relevant substituted benzene molecules based on the general rule of Varsanyi [58].

The molecular structure of 3-flurotoluene is given in Figure 4.7. Pulsed laser Raman spectra of 3-fluorotoluene are shown in Figures 4.8 and 4.9. The assignment of the fundamental Raman modes of the sample is given in the Table 4.1. The transition at 527cm$^{-1}$ is assigned to the totally symmetric in-plane ring deformation mode by analogy with 538cm$^{-1}$ of benzene. The Raman spectra of benzene shows ~3062cm$^{-1}$ (aromatic C-H symmetric stretching) and ~992cm$^{-1}$ (C-C stretching) are the characteristic bands [36]. In 3-flurotoluene the corresponding values are 3069cm$^{-1}$ and 1004cm$^{-1}$. The Raman band at ~866cm$^{-1}$ is due to the ring breathing vibration. For molecules with one or two CH$_3$ groups attached directly to a benzene ring, two bands are regularly observed in the Raman spectra at positions ~2925cm$^{-1}$ and ~2865cm$^{-1}$. These two bands are assigned as the overtone of the CH$_3$ bending vibration at ~1450cm$^{-1}$ in Fermi resonance with the CH$_3$ symmetric vibration [59]. This phenomenon is clearly seen in the FT Raman spectra of toluene and xylene. Because of the Fermi resonance the overtone bands appear with a relatively high intensity and the CH$_3$ symmetric stretching bands with relatively low intensities.



Figure 4.8 Pulsed Laser Raman spectrum of 3-fluorotoluene in the range 50-2000cm$^{-1}$

**Figure 4.9** Pulsed Laser Raman spectrum of 3-fluorotoluene in the range 2000-3600cm$^{-1}$

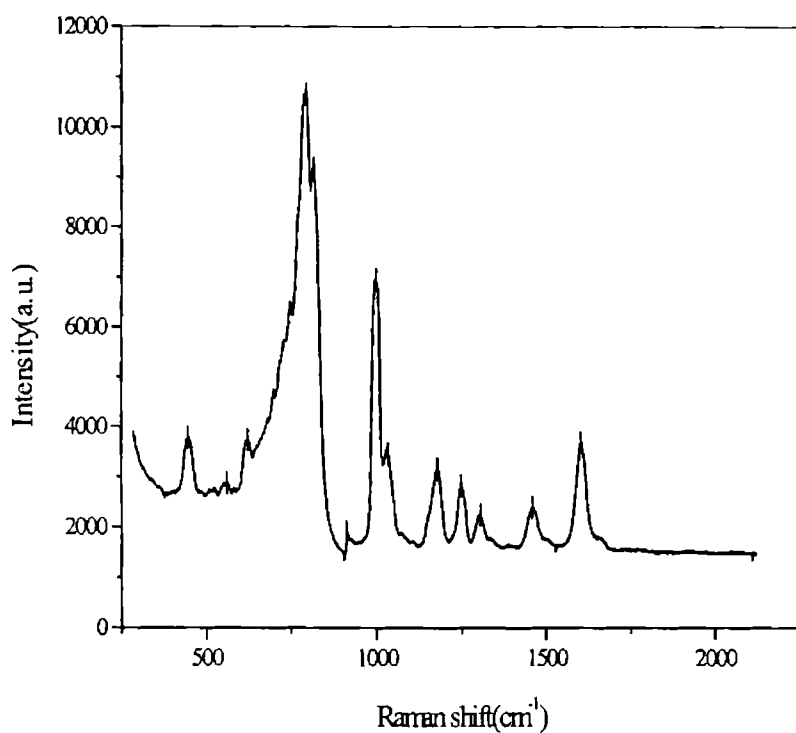**Table 4.1**   Assignments of the observed Raman peaks of 3-fluorotoluene

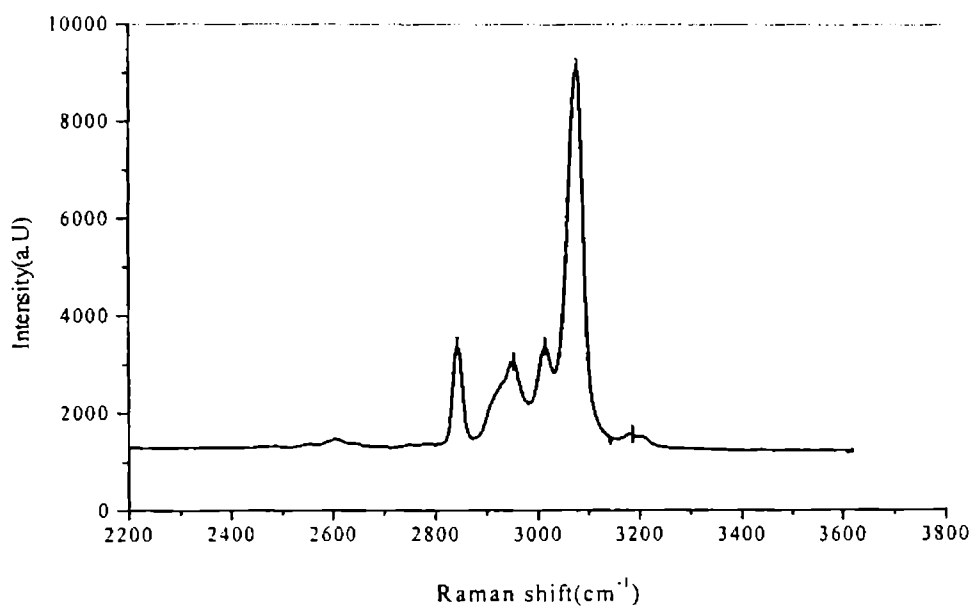| Raman shift (cm$^{-1}$) | Assignment |
| --- | --- |
| 214 | CH$_3$ torsion |
| 246 | C-C out of plane bending |
| 298 | overtone of ring torsion |
| 527 | in plane ring deformation |
| 726 | C-F stretching overtone of out- of- plane deformation (CF) mode |
| 866 | ring breathing vibration |
| 1004 | triagonal ring breathing |
| 1077 | in plane $\delta_{CH}$ (characteristic of meta  substitution) |
| 1159 | in plane CH bending |
| 1264 | C-F stretching |
| 1381 | CH$_3$ symmetric bending |
| 1449 | CH$_3$ bending |
| 1622 | aromatic ring $\nu_{CC}$ |
| 2742 | overtone of CH$_3$ symmetric deformation |
| 2877 | CH$_3$ symmetric stretching |
| 2930 | overtone of CH$_3$ asymmetric bending |
| 2967 | CH$_3$ asymmetric stretching |
| 3069 | aromatic CH symmetric stretching |

## 4.5.2 Spectrum of anisole

The molecular structure of anisole is given in the Figure 2.24. The pulsed laser Raman spectrum of anisole is shown in Figures 4.10 and 4.11. Balfour [60] has reported the assignment of the normal modes of anisole. Recently Eisenhardt et al [61] calculated normal mode frequencies by *ab initio* method and found that their values agree well with Balfour's assignment, but for the band at $2834cm^{-1}$. Balfour assigned this band as corresponding to the frequency of $CH_3$ symmetric stretching mode. In our experiment we observed this band at $2838cm^{-1}$. This value is exceptionally low compared with alkane values [62]. The occurrence of the C-H symmetric stretching mode for the methyl group of anisole at a low frequency still represents a problem under investigation. This could be related to evidence for the donation of electrons from the oxygen lone pair into an antibonding $\sigma$ orbital of trans CH bonds. However Rumi and Zerbi [63] recently presented strong evidence against the assignment of the band at $2834cm^{-1}$ to a fundamental vibration. These workers suggested the existence of a strong Fermi resonance between $CH_3$ symmetric stretching mode and the overtone of the $CH_3$ symmetric bending mode around $1500cm^{-1}$. A detailed investigation on the C-H stretching overtones by Gellini et al [64] confirmed this suggestion. Based on the assignment by Eisenhardt et al [61] the band at $\sim2953cm^{-1}$ is assigned as the fundamental asymmetric $CH_3$ stretching mode. The band at $3062cm^{-1}$ in benzene appeared at $3076cm^{-1}$ in anisole. The band at $999cm^{-1}$ observed in anisole is the trigonal ring breathing, which is highly diagnostic of the benzene ring ($\sim992cm^{-1}$). The $1600cm^{-1}$ band is frequently seen in substituted aromatics. The band at $1034cm^{-1}$ corresponds to a typical substituent sensitive monosubstituted aromatic property. The Raman band at $620cm^{-1}$ is also a quite indicative of monosubstituted benzene. It is observed that these substituent sensitive bands are slightly shifted to the higher frequency side with respect to benzene indicating the electron withdrawing nature of the methoxy group. The observed Raman bands and their assignments are given in the Table. 4.2

**Figure 4.10** Pulsed laser Raman spectrum of anisole in the region 250- 2250cm⁻¹



**Figure 4. 11** Pulsed laser Raman spectrum of anisole in the range 2200-3800 cm⁻¹

**Table4.2** Assignments of the observed Raman peaks of Anisole

| Raman shift (cm$^{-1}$) | Assignment |
| --- | --- |
| 447 | C-C-C in plane ring deformation |
| 558 | overtone of O-CH$_3$ torsion |
| 620 | C-C-C out of plane bending |
| 792 | C-C out of plane bending |
| 999 | Trigonal ring breathing |
| 1034 | O- CH$_3$ stretching |
| 1178 | CH$_3$rocking |
| 1247 | asymmetric stretching of C-OCH$_3$ |
| 1304 | stretching C-C |
| 1457 | symmetric bending CH$_3$ |
| 1599 | ring C=C stretching |
| 2838 | Methyl C-H symmetric stretching (lowered due to Fermi resonance) |
| 2953 | methyl C-H asymmetric stretching |
| 3014 | aromatic CH stretch |
| 3076 | aromatic CH symmetric stretch |
| 3186 | combination |

## 4.5.3 Spectrum of t-butylamine

The Raman spectrum of the pure liquid sample of t-butyl amine was taken by visible light excitation (532nm) using pulsed laser is presented in Figures 4.12-4.14. The molecular structure of t-butyl amine is shown in Figure 3.1

The infrared active symmetric deformation of $CH_3$ observed in alkanes at $\sim1375cm^{-1}$ splits up in two bands in t-butylamine – one at $1364cm^{-1}$ and the other at 1391 $cm^{-1}$ and one with the lower frequency is more intense [65]. The splitting is clearly seen in the IR spectrum of t-butylamine shown below. These bands are found absent in the Raman spectrum. However, first overtones of these bands are Raman active and these bands appeared at $2720cm^{-1}$ and $2782\ cm^{-1}$ respectively. These bands are relatively weak. The band at $745cm^{-1}$ is due to the C-C symmetric stretching involving the tertiary carbon in the t-butyl group is very intense [66]. The two overtone bands ($2720cm^{-1}$ and $2782\ cm^{-1}$) and the band at $745cm^{-1}$ in the Raman spectra are good candidates to characterize t-butyl amine. The $CH_3$ symmetric stretching vibration band occurs at $2879cm^{-1}$ and the asymmetrical $2971cm^{-1}$. It also gives bands near $1256cm^{-1}$ that is a prominent line both in the Raman and IR.



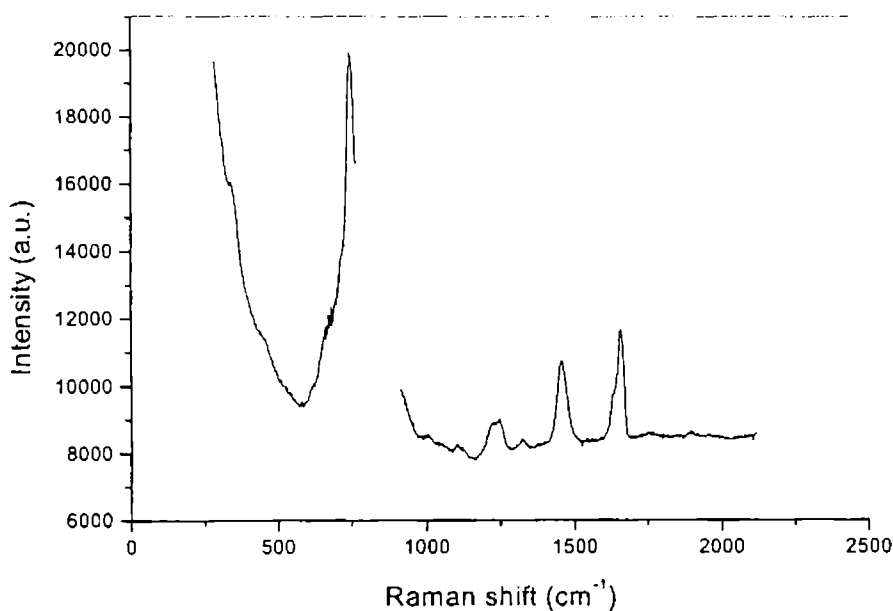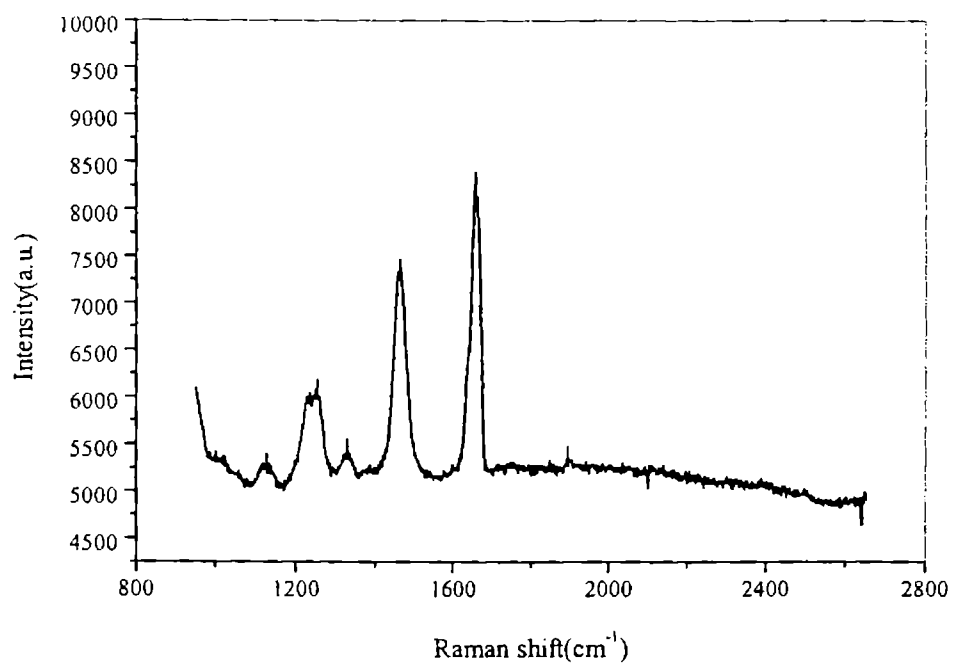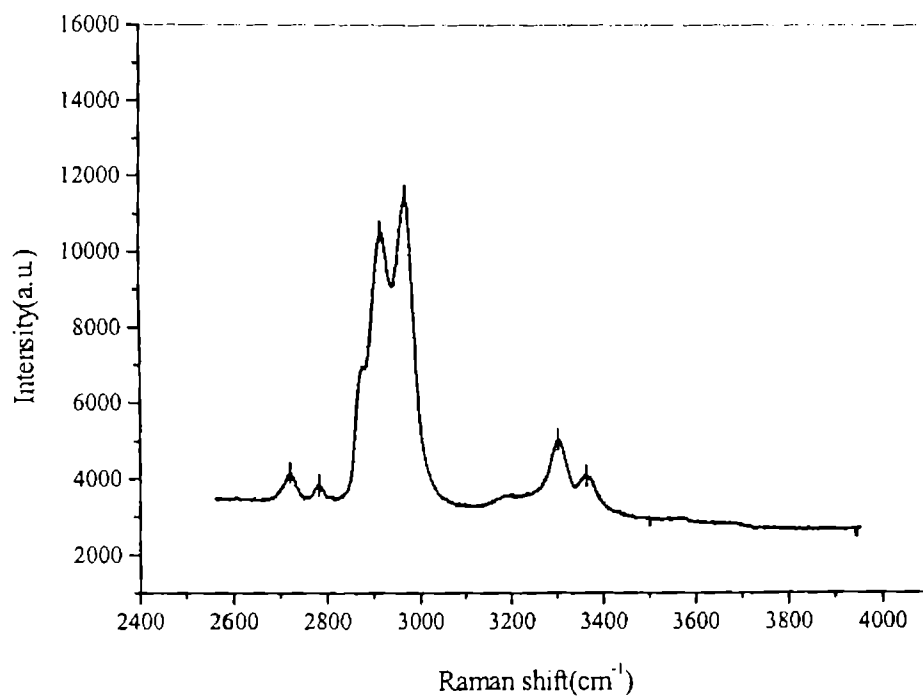Figure 4.12 Pulsed Raman spectrum of t-butylamine in the range $250\text{-}2250cm^{-1}$

**Figure 4.13**   Pulsed Laser Raman spectrum of t-butylamine



**Figure 4.14** Pulsed laser Raman spectrum of t-butylamine

135

**Table 4. 3**  Assignments of the observed Raman peaks of t-butyl amine

---

| Raman shift ($cm^{-1}$) | Assignment |
|---|---|
| 355 | skeletal deformation |
| 745 | C-C symmetric stretching |
| 1024 | $CH_3$ wagging |
| 1128 | C-C stretching |
| 1255 | C-C stretching |
| 1332 | $CH_3$ symmetric deformation |
| 1333 | $CH_3$ asymmetric deformation |
| 1661 | $NH_2$ bending |
| 2720 | overtone band |
| 2782 | overtone band |
| 2879 | $CH_3$ symmetric stretching |
| 2916 | $CH_3$ asymmetric stretching |
| 2964 | $CH_3$ asymmetric stretching |
| 3303 | $NH_2$ symmetric stretching |
| 3364 | $NH_2$ asymmetric stretching |

---
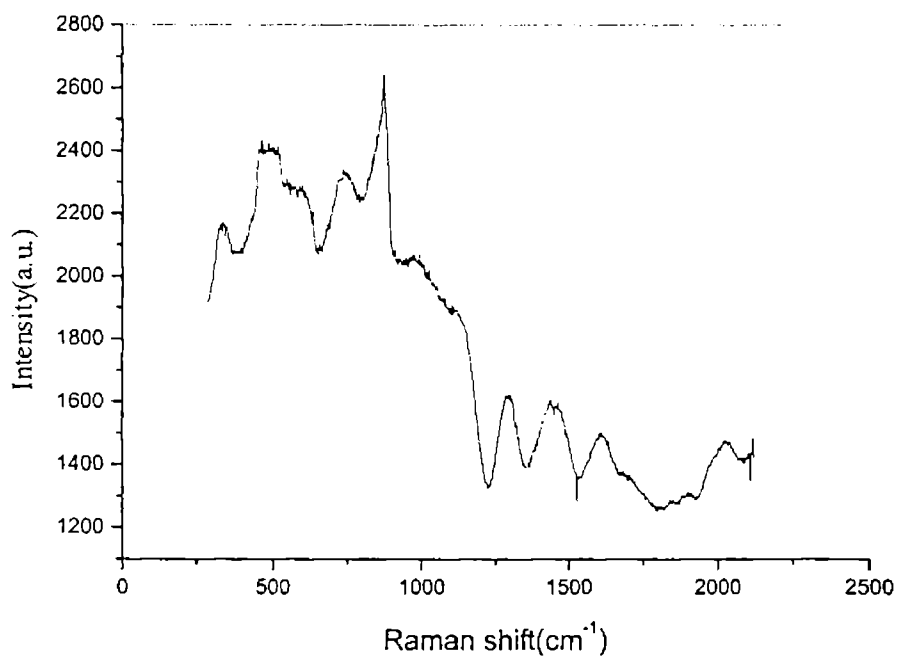
## 4.5.4 Spectrum of p-anisidine



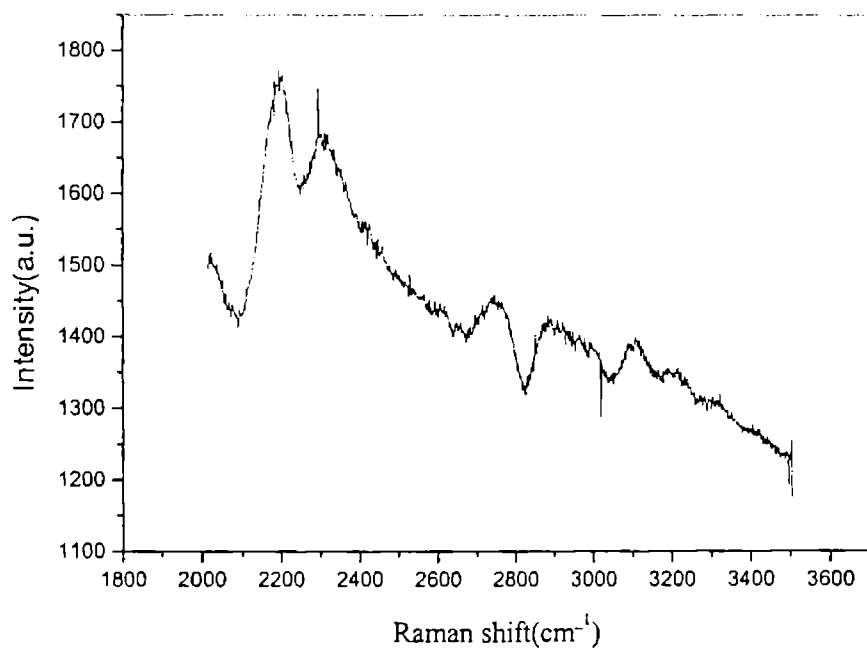**Figure 4.15** Pulsed laser Raman spectrum of p-anisidine



**Figure 4.16** Pulsed laser Raman spectrum of p-anisidine

**Table 4. 4**  Assignments of the observed Raman peaks of p-anisidine

| Raman shift (cm$^{-1}$) | Assignment |
| --- | --- |
| 332 | C-N bending |
| 462 | ring bending |
| 737 | out of plane CCH bending + ring torsion |
| 871 | out of plane CCH bending |
| 981 | CH$_3$ bending |
| 1295 | ring CH bending |
| 1429 | CH$_3$ symmetric bending |
| 1472 | CH$_3$ asymmetric bending |
| 1601 | ring C-C stretching |
| 1675 | NH$_2$ bending |
| 2020 | combination |
| 2880 | CH$_3$ symmetric stretching |
| 2970 | CH$_3$ antisymmetric stretching |
| 3405 | NH$_2$ symmetric stretching |
| 3498 | NH$_2$ asymmetric stretching |

Pulsed laser Raman spectrum of p-anisidine is shown in Figures 4.15 and 4.1 Table 4.4 lists the observed vibrational Raman frequencies, which are assigned t comparison with the frequencies reported for anisole and aniline. Due to the lo symmetry of the molecule several internal coordinates contribute to each normal mod The frequencies of the amino group found in the literature [57] as the NH$_2$ stretchir around 3300-3500cm$^{-1}$. The frequencies of the amino group in this molecule also lie this range. The other Raman peaks correspond to the aromatic ring and the substituents.

## 4.6 Conclusions

LIF spectra of benzyl amine monomer, benzyl amine polymer, n-butyl amine monomer, n-butyl amine polymer and p-anisidine, and Raman spectra of 3-fluorotoluene, anisole and t-butyl amine are recorded using Nd: YAG pulsed laser as an excitation source and CCD as detector. It is observed that the fluorescent peak positions of the polymerized samples are shifted towards the longer wavelength with respect to the corresponding monomer spectrum. The Raman active fundamental vibrational bands of all the samples are assigned and are compared with the reported frequencies. Assignments are given for some new low-lying vibrational modes observed in the present study. The experiment demonstrates the versatility and elegance of the pulsed laser–CCD geometry for studying molecular fluorescence and Raman spectra.

## References

[1]    *Advances in Laser Spectroscopy,* Ed. By B.A.Garetz and J.R.Lombardi , Heyden, London, 1982, Vol.1

[2]    *An introduction to Laser Spectroscopy,* Ed. by D.L.Andrews and A.A.Demidov, 1995,Plenum Press, New York.

[3]    *Fluorescence Spectroscopy, An introduction for biology and medicine,* Ed. By A.J.Pesce, C.Rosen and T.L.Pasby, Marcel Dekker Inc., New York,1971.

[4]    E.B.Hanlon, R.Manoharan, T.W.Koo, K.E.Shafer, J.T.Motz, M.Fitzmaurice, J,R,Kramer, I.Itzkan, R.R.Dasari and M.S.Feld, *Phys.Med.Biol.,*45(2000)1.

[5]    A.Jayaraman and S.K.Sharma, *Current Science,* 74(1998)308.

[6]    T.G.Spiro, *Current Science,* 74(1998)304.

[7]    E.R.Menzel, *Laser Spectroscopy, Techniques and Applications,* Marcel Dekker Inc.,New York,1995.

[8]    K.Muraoka and M. Maeda, *Plasma Phys.Control.Fusion,* 35(1993)633.

[9]    D.H.Williams and I.Fleming, *Spectroscopic Methods in Organic Chemistry,* Tata Mc-Graw Hill, New Delhi, 1990.

[10]   *Techniques in visible and ultraviolet spectroscopy*, Ed. A.Knowles and C.Burgess, Chapman and Hall, London, Vol.3, 1984.

[11]   *Fluorescence – Theory, Instrumentation and Practice*, Ed. G.G.Guilbault, Marcel Dekker Inc., New York, 1967.

[12]   J.E.Harrington and K.C.Smith,*Chem.Phys.Lett.*,202(1993)196.

[13]   L.Santos, E.Martinez, B.Ballesteros and J.Sanchez, *Spectrochim.Acta A*, 56(2000)1905.

[14]   P. Jungner and L. Halonen, *J.Chem.Phys.*,107(1997)1680.

[15]   S.Saarinen, D.Permogorov and L.Halonen, *J.Chem.Phys.*,110(1999)1424.

[16]   S.Lee, K.Arita and O.Kajimoto, *Chem. Phys. Lett.*,265(1997)579.

[17]   C.Chuang, S.N.Tsang, J.G.Hanson and W.Klemperer, *J.Chem.Phys.*,107(1997)7041.

[18]   M.Nela, D.Permogorov and A.Miani, *J.Chem.Phys.*,113(2000)1795.

[19]   T.Lee, D.Shin, J.B.Jeffries, R.K.Hanson, W.G.Bessier and C.Schulz, *American institute of Aeronautics and Astronautics*, 2002-0399.

[20]   M.Metsala, M..Nela, S.Yang, O.Vaittinen and L.Halonen, *Vibrational Sectrosc.*,29(2002)155.

[21]   B.J.Kirby and R.K. Hanson, *Appl.Phys.B*, 69(1999)505.

[22]   B.J.Kirby and R.K. Hanson, *Appl.Optics*,40(2001)6136.

[23]   G.Aruldhas, *Molecular structure and spectroscopy*, Prentice-Hall India, New Delhi, 2001,p.385.

[24]   C.Rulliere and P.Kottis, *Chem.Phys.Lett.*,75(1980)478.

[25]   W.Denk, J.H.Strickler and W.W. Webb, *Science*, 248(1990)73.

[26]   Z.Chen, D.L..Kaplan, K.Yang, J.Kumar, K.A.Marx and S.K.Tripathy, *Appl.Optics*,36(1997)1655.

[27]   M.Reeves, P.V.Farrell and M.P.Musculus, *Meas.Sci.Technol.*,10(1999)285.

[28]   M. Takayanagi and I.Hanazaki, *J.Chem.Phys.*,98(1993)6958.

[29]   J.W.Pepper, A.O.Wright and J.E.Kenny, *Spectrochim. Acta A*, 58(2002)317.

[30]   B.Kim, P.L.Hunter and H.S.Johnston, *J.Chem..Phys.*, 96(1992)4057.

[31]   P.Misra, X.Zhu and H.L.Bryant Jr., *Pure Appl.Opt.*,4(1995)587.

[32]   M. Heintxe and G,H.Bauer, *J.Phys.D:Appl.Phys.*,28 (1995)2470.

[33]    M. Herti and J. Jolly, *J.Phys.D:Appl.Phys.*,33 (2000)381.

[34]    D.Hayashi, W.Hoeben, G.Dooms, E.van Veldhuizen, W.Rutgers and G.Kroesen, *Appl.Optics*,,40(2001)986.

[35]    E.Martinez, F.J.Basterrechea, J.Albaladejo, F.Castano and P.Puyuelo,*J.Phys.B: At.Mol.Opt.Phys.*,24(1991)2765.

[36]    *Molecular spectra and molecular structure - Part II.*, G.Herzberg, D.Van Nostrand Co.Inc.,NewYork, 1962.

[37]    N. Biswas and U. Umapathy, *Current cience*, 74(1998)328.

[38]    L.A.Lyon, C.D.Keating, A.P.Fox, B.E.Baker, L.He, S.R.Nicewarner, S.P.Mulvaney and M.J.Natan, *Anal.Chem.*,70(1998)341.

[39]    H.Inaba and T.Kobayasi, *Opto-electronics*, 4(1972)101.

[40]    T.Yamaguchi,O.Ohkubo, N.Ikeda and T.Nomura, *Furukawa Review*,18(1999)73.

[41]    F.Decremps, J.P-Pores, A.M.Saitta, J-C.Chervin and A.Polin, *Physical Review*,65(2002)92101.

[42]    U.P.Agarwal and S.A.Ralph, *Applied Spectrosc.* ,51(1997)1648.

[43]    K.Anand,V.Asundi and R.Vasudeva,SAE World Congress, Detriot, USA,2000.

[44]    P.M.Cann and H.A.Spikes, *Lubrication Engg.*,48(1992)335.

[45]    F.A.Beleze and A.J.G.Zarbin, *J.Braz.Chem.Soc.,*12(2001)542.

[46]    T.M.Kolev and B.A.Stamboliyska, *Spectrochim.Acta A*, 56(1999)119.

[47]    K.P.R.Nair and S.M.Eappen, *Indian J.Pure and Appl.Phys.*,39(2001)750.

[48]    I.L-Tocon,M.Becucci, G.Pietraperzia, E.Castellucci and J.C.Otero, *J.Mol.Structure.*,565(2001)421.

[49]    J.F.Arenas, I.L.Tocon, J.C.Otero and J.I.Marcos, *J.Mol.Struct.*,410(1997)443.

[50]    B.R.Henry, A.W.Tarr, O.S.Mortensen, W.F.Murphy and D.A.C.Compton, J.Chem.Phys., 79(1983)2583.

[51]    N.H. Fontaine and T.E.Furtak, *Physical Review B*,57(1993)3807.

[52]    S.A.Asher, *Anal.Chem.*,65(1993)59.

[53]    J.E.P.da Silva, S.I.C. de Torresi and M.L.A.Temperini, *J.Braz.Chem.Soc.,*11(2000)91.

[54]    *Techniques and applications of plasma chemistry*, Ed. J.R.Hollahan and A.T.Bell,Wiley, New York, 1974.

[55]   Jyotsna Ravi, *Phtothermal and photoacoustic investigations on certain polymers and semiconducting materials*, Ph.D Thesis, April 2003,CUSAT, Kochi.

[56]   *Molecular spectroscopy: Modern research*, Ed. K.N.Rao and C.W.Mathews, Academic Press,NewYork,1972,p.181.

[57]   *Molecular spectra and molecular structure-Part III.*, G.Herzberg, Van Nostrand Reinhold Co.,NewYork, 1966.

[58]   G.Varsanyi, Assignments of Vibrational Spectra of Seven Hundred Benzene Derivatives, Wiley, New York, 1974.

[59]   A.B.Dempster,D.B.Powell and N.Sheppard, *Spectrochim Acta A*, 28(1972)373.

[60]   W.J.Balfour, *Spectrochim Acta A*, 39(1983)795.

[61]   C.G.Eisenhardt, A.S.Gemechu, H.baumgartel, R.Chelli, G.Cardini and S.Califano, *Phys.Chem.Chem.Phys.*, 3(2001)5358.

[62]   L.J.Bellamy and D,W.Mayo, J.Phys.Chem.,80(1976)1217.

[63]   M.Rumi and G. Zerbi, *J.Mol.Struct.(THEOCHEM)*,509(1999)11.

[64]   C.Gellini, L.Moroni and M.Muniz-Miranda, *J.Phys.Chem.A,,* 106(2002) 10999.

[65]   D.Lien-Vien, N.B.Cholthup, W.G.Fately and J.G.Grasselli,*The Handbook of Infrared and Raman Frequencies of Organic molecules*, Academic Press, Boston, 1991,Chapter 2.

[66]   J.B.Cooper,   K.L.Wise,   W.T.Welch,   R.R.Bledsoe   and   M.B.Sumner, *Appl.Spectrosc.*,50(1996)917.

# CHAPTER 5

# VIBRATIONAL OVERTONES OF ISOBUTANOL AND HIGH RESOLUTION SPECTROSCOPIC STUDY OF ITS HYDROXYL GROUP IN THE ΔV=3 REGION

# CHAPTER 5

# VIBRATIONAL OVERTONES OF ISOBUTANOL AND HIGH-RESOLUTION SPECTROSCOPIC STUDY OF ITS HYDROXYL GROUP IN THE ΔV=3 REGION

## 5.1 Introduction

Almost all lasers in one or another form have been applied in spectroscopic experiments since its development in the early 1960's. However many of the laser sources developed in the initial stage provide only a single lasing wavelength. Thus the true beginning of the era of modern laser spectroscopy is considered being aroused with the development of tunable coherent radiation source based on lasers. High-resolution spectroscopy has undergone a transformation during the last several years as a result of the considerable strides made over the experimental side and it has now become possible to do a line-by-line analysis of the spectra of polyatomic molecules. High resolution facilitates the determination of precise values of spectral line position and intensities, which makes the identification of molecular species more accurately. Tunable Diode Laser Absorption Spectroscopy (TDLAS) is one such technique that finds widespread use in obtaining high resolution spectra of gas species. As the name implies this technique utilizes a Tunable Diode Laser (TDL) source to access specific IR regions of the molecules. The use of TDL in conjunction with a long path length cell provides high sensitivity local measurements. This technique is commonly referred to as TDLAS.

The molecular rotational motion in solids and liquids are normally completely suppressed due to intermolecular interactions. At low pressures ($\leq 20$ torr) the molecules become essentially independent in gas phase with little or no effect due to the intermolecular interactions. Under these conditions, the interaction of the incident photon with the sample not only excites molecular vibrations but also molecular rotations. Then

each of the vibrational bands split into many fine lines. This means that vibrational bands in condensed phases are often sharper than they are in gas. It is often possible to distinguish possible structures or isomers by examining the patterns of vibrational spectrum or by counting the number of bands present.

The major application of TDL is high-resolution recording of vibrational-rotational spectra of molecules in the gas phase. Diode lasers have high spectral brightness and are coherent devices. These features allow the use of TDL for long path length measurements, with high degree of spatial resolution. The most important property of TDL is the probability of considerable emission frequency tuning with operating conditions changed. Since the gain curve position $v_s$ is determined by band gap energy $E_g$, all methods of changing $E_g$ can be used for coarse frequency tuning. $E_g$ can be tuned by varying the temperature T of the semiconductor crystal by applying pressure or a magnetic field [1]. The Fine frequency tuning, which is used for high-resolution spectroscopy is performed by shifting the frequency of effective cavity optical length mainly through change of index of refraction [1].

In measurements of trace gases by laser absorption spectroscopy, the absorption signal strength is proportional to the product of oscillator strength of the absorption transition and the number of molecules in the path of the laser beam. Hence at very low concentrations long path length is required for generating detectable absorption signals [2]. Use of multipass cell can increase the effective path length. The multipass optical system limits the beam divergence and provides large path length and facilitates operation at low pressure and thus broadening of spectral lines can be avoided.

The tunable diode laser based spectrometer used in the present work has a tunability range of 930-970nm. This range is ideal for the study the spectrum of the –OH group absorption frequencies of all OH containing molecules in the transition region $\Delta V=3$ by using a detector with a log output and hence use of chopper and lock-in amplifier can be avoided. In the present study, a near infrared tunable diode laser based high resolution spectrometer is used to investigate the highly resolved vibrational overtone band of the OH group in gas phase isobutanol in the $\Delta V=3$ region. A local mode analysis of the liquid phase overtone spectra of isobutanol is also carried out.

## 5.2 TDLAS- a brief review

The major application of TDLAS is high-resolution recording of vibrational-rotational spectra of molecules in the vapour phase [1]. Because of the versatility, selectivity and sensitivity of TDLAS numerous laboratory, ground based, aircraft and balloon-borne studies employ this technique.

Trace gas detection is of great interest in industrial process control and pollution monitoring. Nowadays the requirements for accurate and precise monitoring of trace gas constituents in the atmosphere has become increasingly important as a direct result of concerns over the cause and effects of atmospheric pollution. TDLAS has now established itself as one of the highly selective and versatile techniques for atmospheric analysis of trace gas constituents. The aim of diode laser trace gas monitoring is to establish absolute concentrations. TDLAS has been used for atmospheric concentration measurement of $CH_4$ [3], CO [4], HCl [5], $H_2O$ [6], $HNO_3$ [7], NO [6,7], $NO_2$ [7], $N_2O$ [8], $SO_2$ [7] etc. The applications of lead-salt and GaAs based tunable diode lasers for atmospheric trace gas monitoring are reviewed recently [9]. The necessity for reliable tools for trace gas monitoring is obvious but the type of technique depends very much on the particular application being addressed and the specific trace gas species of interest. High sensitivity laser spectroscopic techniques are needed to detect the very low mixing ratios or concentrations of trace species ranging from several parts per million to sub parts per trillion levels for carbon monoxide, hydroxyl radical etc. Operating at infrared wavelengths, most trace gases except nitrogen and oxygen to be monitored via their characteristic vibrational spectra and the high spectral resolution reduces the possibility of interferences from other species.

Sandstrom and Malmberg [10] demonstrated the potential of the TDLS technique for simultaneous contact free monitoring and measurement of the oxygen concentration as well as gas temperature in a reheating furnace during production. Werle et al [11] discussed the currently available semiconductors for spectroscopy in the near- and mid-infrared region based on direct band to-band transitions as gallium-arsenide, indium-phosphide, antimonides and lead-salt containing compounds together with the main features of different tunable diode laser absorption spectrometers for trace gas analysis.

In a recent paper Vicet et al [12] presented antimonide quantum well diode lasers emitting near 2.0-2.4 µm at room temperature and experimental TDLAS setup for open path gas detection using these devices.

Kormann et al [13] described the application of a three-laser tunable diode laser absorption spectrometer for atmospheric trace gas measurements. Gas monitors for industrial applications must have high reliability and require little maintenance. Monitors for *in-situ* measurements using TDLAS in the near infrared can meet these requirements.

Linnerud et al [14] demonstrated that *in-situ* open path measurements in the near infrared using TDLAS can be done with the accuracy and reliability required for industry in a number of different applications. Nelson et al [15] developed a tunable diode laser system to measure air-pollutant emission from on-road motor vehicles. The high resolution TDL spectroscopy of the van der Waals complex Ar-CH$_4$ in the 7µm region was analyzed and compared with a spectrum predicted from ab initio calculations [16].

## 5.3 High Resolution Overtone Spectroscopy – some reported works

High-resolution laser spectroscopy has been a powerful tool for investigating the structure of molecules, ions and free radicals. The potential importance of high-resolution spectroscopy in air pollution and other meteorological studies is evident from the number of publications in this field. High-resolution spectra of C-H, O-H, and N-H stretching vibrational overtone transitions that occur at higher frequencies have been studied earlier. It is difficult to record the high-resolution spectrum of higher vibrational states due to the very small value of transition dipole moment connecting the two states. Moreover, the spectrum must be recorded at low pressure to avoid the pressure broadening [17].

Recently, intensive experimental work has been focused to study the high-resolution spectra of stretching overtones, using various highly sensitive techniques like Fourier transform spectroscopy, intracavity laser absorption spectroscopy, laser photo acoustic spectroscopy, tunable diode laser spectroscopy etc. Taking advantage of high resolution Fourier transform spectroscopy, Zhu and co-workers recorded high-resolution spectra of GeH$_4$ [18] in the $\Delta V$ =2-5 and SiH$_4$ [19] in the $\Delta V$ =3-5 stretching overtone

regions. The above group also recorded the high-resolution spectra of the same molecules in the $\Delta V$ = 6-7 overtone regions using intracavity laser absorption spectroscopic technique. The high resolution Fourier transform spectrum of arsine ($AsH_3$) was recorded in the region 3989-4274$cm^{-1}$ at a resolution of 0.008$cm^{-1}$ by the same group [20].

Chou and coworkers [21] recorded the high resolution absorption line shapes of the R (7) and P (2) transitions in the first overtone band of HBr at room temperature using a pair of distributed feedback diode lasers operating near 2$\mu$m. Lummila et al [22] recorded the first and second CH overtone vibration–rotation absorption spectra of monoiodoacetylene (HCCI) using FTIR spectrometer with a resolution of about 0.005$cm^{-1}$ and third overtone spectrum using a ring laser spectrometer with a spectral resolution of about 0.02$cm^{-1}$.

Douketis et al [23] used photoacoustic technique to record the high-resolution vibrational overtone spectrum of $H_2O_2$ vapour. Held et al [24] studied the high resolution FTIR spectroscopy the first overtone of N-H stretch and the fundamental of C-H stretch in gas phase pyrrole. The first overtone N-H stretch is rotationally analyzed using an asymmetric top model and was found to exhibit two separate perturbations. Luckhaus [25] reported the rovibrational spectrum of hydroxylamine ($NH_2OH$) recorded by interferometric Fourier Transform Spectroscopy with a resolution up to 0.004$cm^{-1}$ close to the Doppler limit at room temperature, in the spectral range of 800$cm^{-1}$ up to the visible region. They also carried out detailed rotational analyses of all the fundamentals and overtones up to 10500$cm^{-1}$.

The measured intensities of several OH vibrational overtone bands of vapor phase methanol, ethanol and isopropanol were used to model the trends in the intensities as a function of excitation level [26]. Two empirical approaches were used for yielding intensity predictions for the higher overtone transitions up to sixth OH overtone level. These methods are applied to recent $HNO_3$ overtone measurements resulting in new intensity predictions for higher photochemically active overtone bands [25].

Murtz et al [27] demonstrated the use an offset-locked CO overtone laser sideband spectrometer as suitable for very high-resolution molecular spectroscopy in the 2.6–4.1$\mu$m spectral region. Hu et al [28] utilized high resolution Fourier–transform intra-

cavity laser absorption spectroscopy to record the $\Delta V_{OD} = 5$ stretching overtone of HOD at a resolution of 0.05cm$^{-1}$ in the region 12550-12900cm$^{-1}$.

High-resolution infrared emission spectrum of sodium monofluoride was recorded by Muntianu and coworkers [29] using a Fourier transform spectrometer and assigned a total of 1131 vibration-rotation transitions from the V=1$\rightarrow$ 0 to V=9$\rightarrow$ 8 vibrational bands. Vaittinen et al [30] reported local mode effects on the high-resolution overtone spectra of $H_2S$ recorded by intracavity laser absorption spectroscopy in the region 12270-12670cm$^{-1}$. The rovibrational analysis provided upper state rotational parameters for the three interacting vibrational states.

## 5.4.1 The TDLAS Experimental setup

The basic experimental arrangement used for the present work consists of a tunable diode laser, a sample cell, beam splitter, detection system and vacuum system. The block diagram of the experimental set up used is shown in the Figure 5.1. A brief description of the arrangement is given below.

**Source:** A tunable diode laser (Model No.6321, New Focus Inc.) having tuning range 935-975nm is a stable, narrow line-width laser source. Its tunability, temperature stability, single mode operation etc makes it an ideal source for high-resolution spectrometer. The maximum output of the source is 15mW. The laser is operated at a temperature of 20$^0$C. Out put power can be varied by changing the current. The grating spectral filter used in the laser head is narrow enough to force the laser to operate in a single longitudinal mode. The laser can be operated manually from the front panel of the controller or remotely using computer control.

**Beam splitter:** A beam splitter with variable split ratio splits the laser beam into two - reference beam and signal beam. The reference beam falls directly on the reference photodiode of the photodetector. The signal beam is fed into the multipass cell that contains the sample, and the output from the multipass cell falls on the signal photodiode of the detector.

149

**Sample cell:** For enhancing sensitivity of weak absorptions the contributions of several factors are to be considered. One simple way of achieving this by increasing the effective absorption path length as the radiation propagates back and forth within the cavity. Multipass advantage can be utilized for the purpose. A multipass cell (Model 5611, New Focus Inc.) is the absorption cell used in the present study and can be operated up to 760torr. Light enters and exits the cell through the front window assembly and makes 182 passes between the mirrors and provides an optical path length of 36m in the 0.3litre cell. The input and output beam height is 2.5 inches. Both input and output beams are in horizontal plane and cross at the center of the coupling mirror. The input and output beams enter and exit the cell at an angle from the centerline of the cell.

**The detector system:** Nirvana auto-balanced photoreceiver (Model 2017, New Focus Inc.) consists of two photodiodes labeled as signal and reference. There are three outputs- linear, log and signal monitor. This detector enables traditional balanced detection. In the balance mode the linear output provides a voltage proportional to the difference between the photocurrents of the signal and reference diodes. It also provides auto balance detection with zero D C voltage and noise suppressed A C signal proportional to received signal optical power. In this state the detection automatically balances the photocurrent from signal and reference diodes. The signal monitor output enables constant monitoring of the signal. The log output at auto-balanced state provides a convenient measurement of absorption present in the signal path. The output voltage is given as

**Log (output) $\sim -\ln [\{P_{ref}/ P_{sig}\} -1]$**

The log output is bandwidth limited up to the selected gain compensation cut-off frequency. Common mode noise within this bandwidth is cancelled in the log output. The split ratio of the detector is fixed to 2:1 by using the log output the chopper and lock-in-amplifier can be avoided.

The log output from the photodetector is directly interfaced with a PC using lab VIEW 6.0 software. The software is programmed to obtain the spectrum as wavelength against absorption, as the absorption in the cell is proportional to the output voltage.

**Sample container:** A sample container with fine needle valve is used for the regulated flow of the sample to the multipass cell. High purity spectroscopic grade liquid sample is taken in the sample container connected to the inlet of the multipass cell and when the pressure in the multipass cell reached the required value the sample is allowed to flow into the multipass cell using the needle valve that regulates the flow.

**Vacuum system:** A rotary pump is used to evacuate the multipass cell and for the sample gas feeding. The multipass cell is evacuated continuously while recording the spectra.

The calibration of the spectrophotometer is done using Hitran Database 1996.The setup provides a resolution of 0.01nm.

## 5.4.2 High-resolution overtone spectrum of isobutanol – Experimental

High purity isobutanol (extra pure AR, 99.5%) obtained from M/s SISCO Research Laboratories Pvt. Ltd., Mumbai, India is used for recording the spectrum. The sample was used without further purification. The overtone absorption spectrum of isobutanol in the gas phase was measured with a high-resolution tunable diode laser. The details of the arrangement are discussed and the experimental parameters are given below. The sample in the liquid phase is taken in the sample reservoir. When the required pressure is reached the valve connecting multipass cell and sample reservoir is opened.

## 5.4.3 Experimental parameters

The experimental conditions used for recording the spectrum of isobutanol vapour is given below.
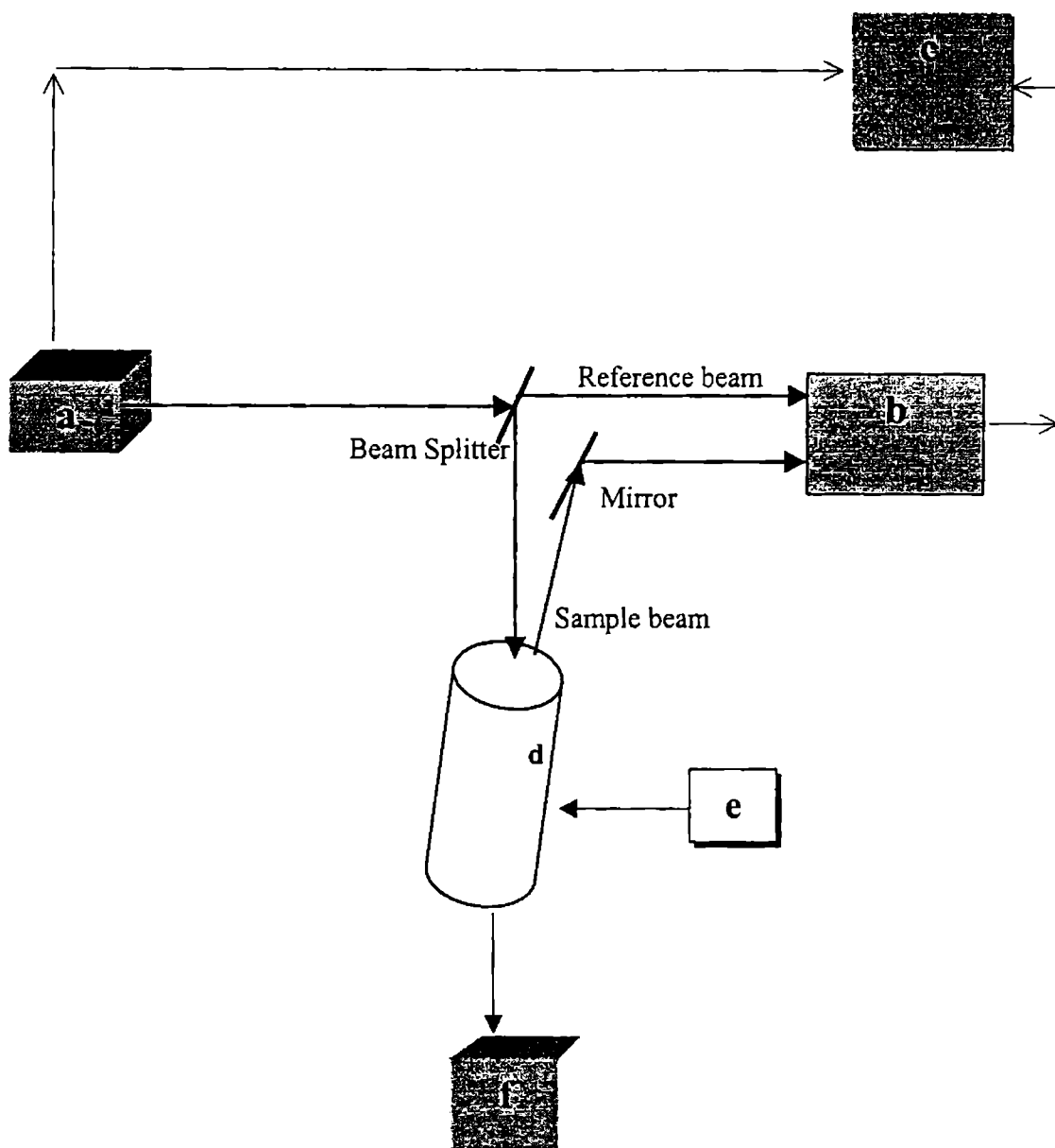
Laser power  = 2.8mW
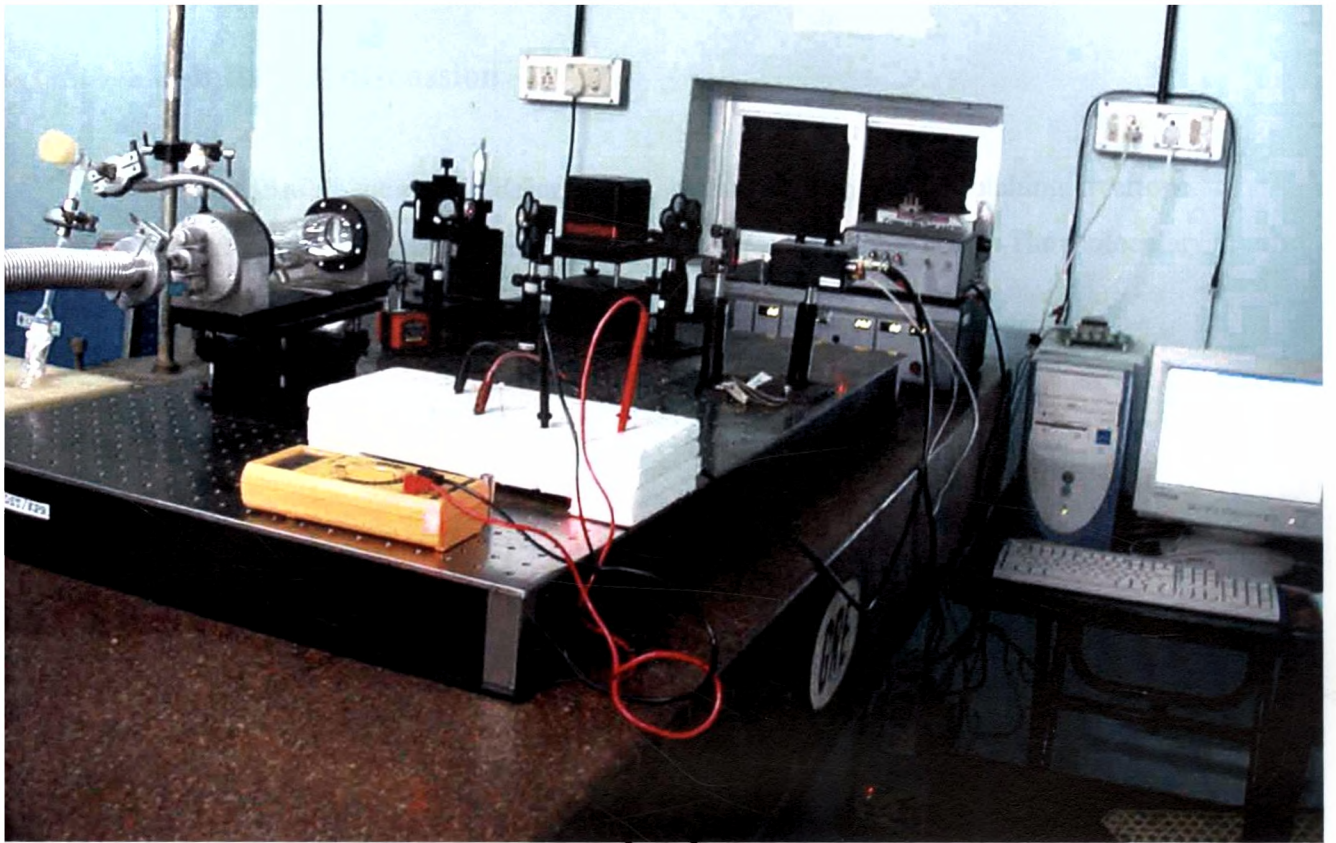
Scan speed   = 0.02nm

Temperature  = 20°C

Pressure     = 1.2mbar

Path length   = 36m
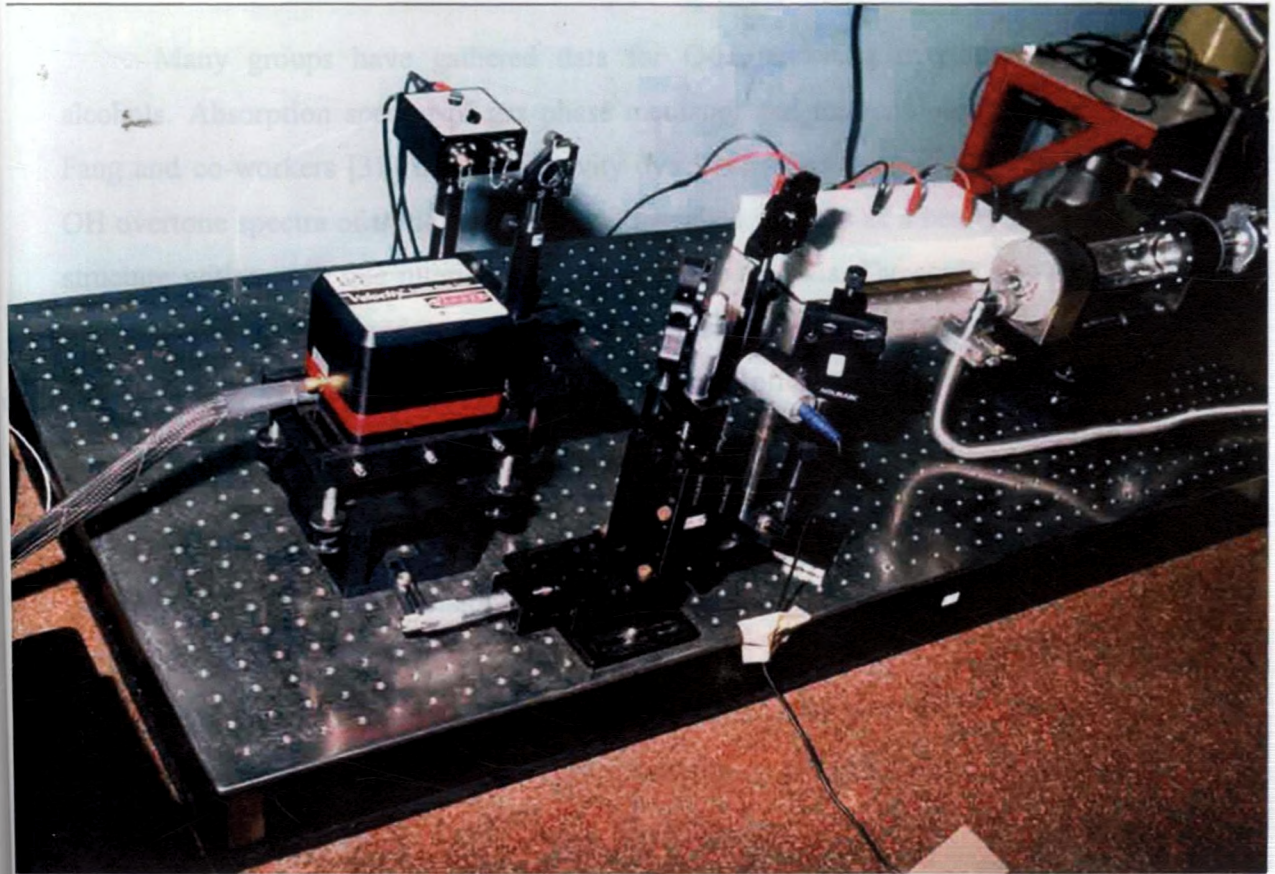
Tuning range  = 949-959nm

**Figure 5.1** Schematic representation of the high-resolution experimental setup: a-
Tunable diode laser, b-photodetector, c-computer, d-multipass cell (sample holder), e-
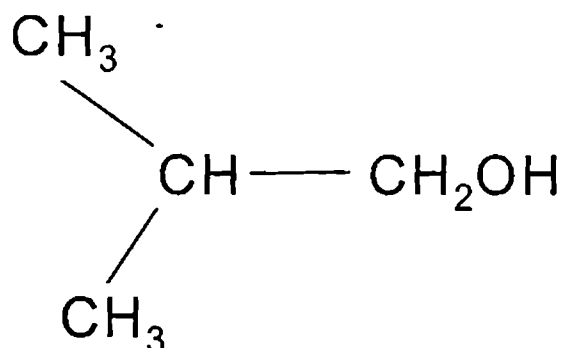sample container, f-vacuum system

(a)



(b)

## 5.4.4 Results and discussion

In the present work we describe the high-resolution O-H stretching overtone spectra of gas phase isobutanol in the $\Delta V=3$ region measured using TDLS. The molecular structure of isobutanol is given in Figure 5.2.

$$CH_3 \cdot$$
$$\diagdown$$
$$CH \text{——} CH_2OH$$
$$\diagup$$
$$CH_3$$

**Figure 5.2** Molecular structure of Isobutanol

Many groups have gathered data for O-H stretching overtones in different alcohols. Absorption spectra of gas phase methanol and methanol-d were reported by Fang and co-workers [31] using intracavity dye laser photo acoustic spectroscopy. The OH overtone spectra of these samples were described in terms of a nearly symmetric top structure with nearly free internal rotation about the top axis. The study also reveals the presence two types of conformationally non-equivalent C-H bands due to the presence of lone pair electrons on the oxygen atom. The solvent effects in O-H and O-D stretching overtone spectra of methanol have been measured in different solvents and found that the anharmonicity constants are almost identical but the mechanical frequencies change as a function of the solvent used [32]. An internal coordinate Hamiltonian model has been constructed to model the torsional motion in the O-H stretching vibrational overtone region of methanol [33].

Overtone absorption spectra of gas phase ethanol in $\Delta v=3\text{-}6$ region of O-H were studied by Fang and Swofford [34] by intracavity photo acoustic spectroscopy. Each O-H

153

overtone levels shows two side bands, which are assigned as the transitions of two conformers of the O-H bond in the *trans* and *gauche* position with respect to the methyl group. The torsional of the O-H group about the C-O axis give rise to two distinct conformers- one *trans* conformer and two equivalent *gauche* conformers.

Fang and Compton [35] reported overtone absorption spectra of gas phase 1-propanol, 2-propanol and tert-butyl alcohol measured with intracavity photoacoustic and FT-IR spectroscopy. The OH overtones in these molecules are considerably narrow and show both rotational and conformational structure. This implies a more isolated nature of O-H stretching vibration. The relatively broad C-H overtones also show evidence of conformational non-equivalent sites for methyl groups in an anisotropic environment.

Weibel et al [36] reported the OH fourth overtone absorption spectra of ethanol, ethanol ($1,1$-$d_2$) and ethanol ($2,2,2$-$d_3$), recorded using intracavity dye laser photoacoustic technique. The distinct absorption bands are assigned as due to the *trans* and *gauche* conformational isomers. Comparison of the spectra revealed a coupling between the O-H and methylene C-H vibrations in only the *gauche* conformer of ethanol, an effect that had not been observed in the fundamental spectrum. *Ab initio* electronic structure and vibrational frequency calculations are used to clarify and support the analysis of the ethanol O-H vibrational spectrum and to evaluate the relative energies of the conformers.

Since the energy differences between different conformers are very small, it is usually difficult to resolve this difference by standard procedures like nuclear magnetic technique, fundamental IR and Raman spectroscopy. But the vibrational overtones are very sensitive to the local environment; a difference of only $10cm^{-1}$ in fundamental frequencies can be resolved in the high vibrational overtone level, since the separation is amplified n times in the V=n overtone level. Overtone spectra are thus used to deduce the conformational details of several molecules, as demonstrated by Fang and Swofford [34] who studied the molecular conformation of gas phase ethanol using overtone spectroscopy. Wong and Moore [37] also studied the molecular conformation of alkanes and alkenes using vibrational overtone spectroscopy.

Several recent studies combine *ab initio* calculations and OH overtone spectra in order to correlate structural and spectral features. Fedorov and Snavely [38] measured the O-H overtone spectrum of gas phase isobutanol in the $\Delta V=4$ region using an

154

intracavity laser photoacoustic spectrometer. The geometry optimizations and total energies of five different conformations were calculated by both the ab initio 3-21G* and 6-31G** levels and demonstrate that a linear correlation exist between calculated OH bond lengths and the observed OH overtone transition energies. Xu et al [39] measured the O-H stretching vibrational overtone spectra in the $\Delta V$= 3, 4,and 5 regions of gaseous 2-butanol by using cavity ring-down spectroscopy (CRDS) and calculated electronic energies using density functional theory (DFT) at the B3LYP/6-31+G(d,p) and B3LYP/6-311+G(d,p) levels. Because of the complexity of 2-butanol nine stable conformers are found and no clear pattern of assignments emerged. Two bands are observed for each overtone level corresponding to these conformers. In a subsequent study Xu et al [40] reported the OH overtone spectra of isobutanol in the $\Delta V$=3- 5 regions using CRDS. They observed three bands corresponding to each overtone level. These three bands are assigned to the O-H stretching vibrational absorption of the five stable conformations of the molecule. This was further confirmed by DFT calculations using highly accurate B3LYP/6-31+G(d,p) and B3LYP/ 6-311+G(d,p) levels. The band intensities of each band are also obtained. The molecular vibrational abundance and O-H stretching frequencies of different vibrations of the calculated molecular conformations are in agreement with the experimental results. The range of calculated electronic energies among conformers is less than 0.7 kcal/mol.

The overtone spectrum of gas phase isobutanol obtained using the high-resolution spectrophotometer setup is shown in Figure 5.3. The experimental results obtained using high-resolution spectrophotometer and the reported values are given in Table 5.2. The reported values of O-H mechanical frequency and anharmonicity for different alcohols obtained from their overtones are given in the Table 5.1

155

**Table5.1** The O-H stretching mechanical frequencies and anharmonicities in different alcohols

| Molecule | mechanical frequency (cm$^{-1}$) | - anharmonicity (cm$^{-1}$) |
|---|---|---|
| Methanol [31] | 3855 | 86 |
| Ethanol [35] | 3832-3846 | 85-86 |
| 1-propanol [35] | 3831-3852 | 86 |
| 2-propanol [39] | 3791-3831 | 83-86 |
| 2-butanol [39] | 3798-3826 | 85 |
| t-butyl alcohol [35] | 3814 | 86 |
| Isobutanol [40] | 3826-3850 | 85-86 |

The mechanical frequency and anharmonicity of isobutanol are close to that of ethanol and 1-propanol. Isobutanol posses a stereo structure similar to those of ethanol and propanol [41]. However, it is noticed that the band profiles of the overtones of this molecule are different from other alcohols [40].

Isobutanol molecule exhibits different conformations because the hydroxyl group staggers between two CH bonds and -H(CH$_3$ )$_2$ groups rotate around C-C single bond. The conformations of isobutanol is named according to different dihedral angles of $H_6O_1C_2C_3$ and $O_1C_2C_3H_9$, where trans (t) is nearly 180$^0$, gauche (g) is near 60$^0$ and gauge' (g') is near –60$^0$. All the possible conformations are: Tt, Tg, Tg', Gg, G'g', Gt, G't, Gg' and G'g. It is confirmed by density function theory (DFT) calculations that all these conformations are stable. However among the total nine conformers possible, four of them viz, Tg, Gg, Gt, and Gg' are the mirror images of Tg', G'g', G't and G'g respectively. The distributions of these conformers and its mirror images are equal. Therefore there are only five different stable conformers for isobutanol. All the possible conformations of isobutanol are given in the Figure 5.4

The O-H trans conformations of form **a** and **b** are close to each other, O-H gauche conformations of form **c** and **d**, whose hydroxyl axis parallel to the methyl axis, are close

to each other. In gauche form **e** the hydroxyl axis is parallel to the carbonyl axis. Thus, in general, there are three kinds of conformations in isobutanol and corresponding to it three bands are observed in each overtone region. Therefore one band is due to the OH stretching overtone absorption of forms **a** and **b**, the second band is due to the OH stretching overtone absorption of forms **c** and **d**, and the third band is due to the OH stretching overtone absorption of form **e**. The assignments of this molecule is done in agreement with the previous experimental assignment for ethanol where the higher energy band is assigned to the conformation with the O-H bond trans to the alkyl group and the lower energy band is assigned to the two equivalent conformations with the O-H group gauche to the alkyl group. But in isobutanol the gauche conformations are not equivalent. The assignments of gauche conformations were done by ab initio calculations together with thermodynamical considerations [40]. The lowest energy peak of the observed triplet belongs to the most energetically favourable conformer that has the longest O-H bond. The relative percentage of the abundance of the molecular conformation follows the Boltzmann formula

$$\frac{N_i}{N_j} = \text{Exp} \left[ -(E_i - E_j)/kT \right]$$

Here $N_i/N_j$ is the population ratio of the two conformers, $E_i$ and $E_j$ are the total energies of the two conformers, and T is the temperature. From the calculated results the percentage for form **a**, **b**, **c**, **d**, and **e** isobutanol is 6%, 33%, 22%, 9% and 27% respectively [40].
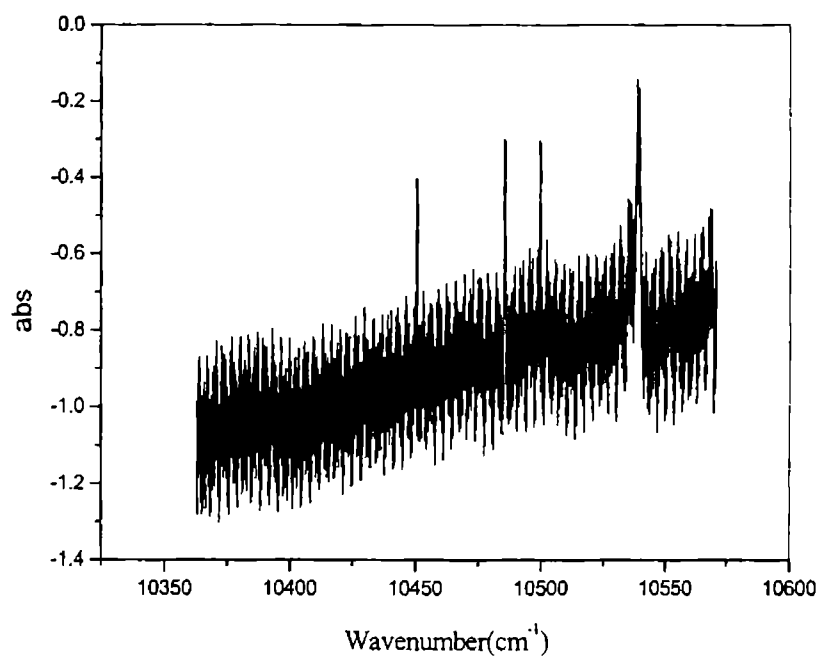
**Figure 5.** $\Xi$ High-resolution TDLS spectrum of OH stretching in the

$\Delta V = 3$ overtone region of isobutanol

**Table5.2** Comparison of TDLS results of isobutanol with the reported theoretical and experimental (cavity ring-down spectroscopy) values

| Conformation | TDLS | ab initio [40] | CRDS [40] |
|---|---|---|---|
| Form a | 10539 | 10542 | |
| Form b | | 10527 | 10525 |
| Form c | 10499 | 10490 | |
| Form d | 10485 | 10485 | 10486 |
| Form e | 10451 | 10449 | 10448 |

158

Form (a), TT

Form (b), Tg (Tg')

Form (c), Gg (G'g')

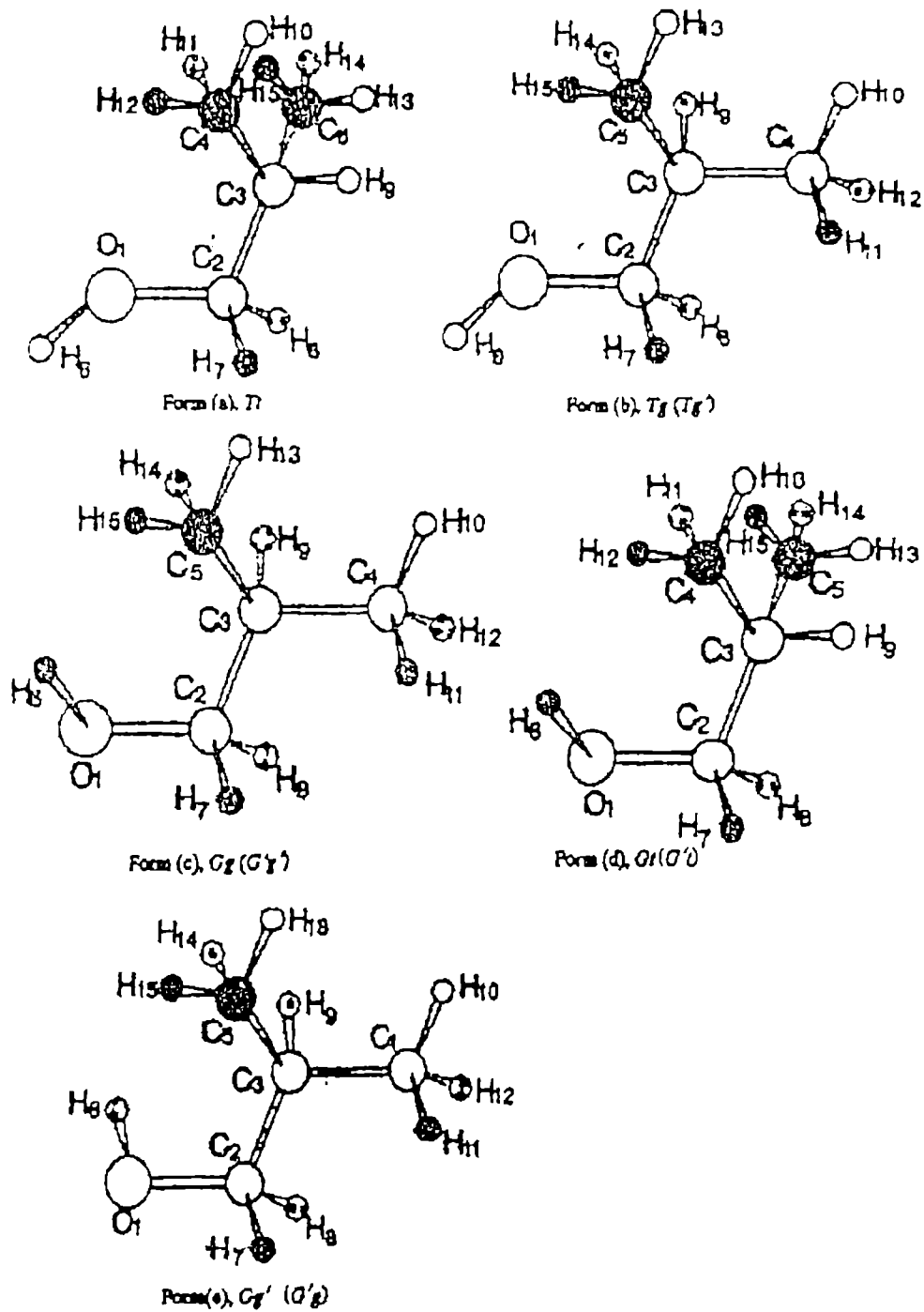Form (d), Gt (G't')

Form (e), Gg' (G'g)

Figure 5.4 Stable conformations of isobutyl alcohol

159

At a higher vibrational energy, the overtone spectrum is relatively simple for small molecules. The interpretation and assignment become more complex as the number of oscillators increases. This is especially true for molecules having several conformers where the vibrational overtone transitions have contributions from all the conformers. The rotational structures of the OH overtone in isobutanol are not yet analyzed, as they are so complicated owing to the above reason, and also due to the strong interaction with adjacent states causing loss of regularity in the spectral pattern.

## 5.4.5 Conclusions

The highly resolved overtone spectrum of the –OH group in isobutanol for the $\Delta V=3$ transition is recorded in a linear high-resolution spectrometer using tunable diode laser and a long path length cell. The resolved bands are assigned as the O-H stretching absorption of the three kinds of conformations of the hydroxyl group. The observed OH overtone peak positions corresponding to the different conformers agree with ab initio theoretical predictions and the reported CRDS results.

# 5.4 Overtone Spectroscopic Analysis of Liquid Phase Isobutanol

## 5.5.1 Introduction

The local mode model of molecular vibrations has been used extensively for the description of CH and OH stretching overtone spectra of polyatomic molecules [39,40,42]. The NIR spectra of CH stretching up to sixth overtone region and OH stretching up to fifth overtone region in normal, secondary, and tertiary butanol were studied by Rai and Srivastava [42] using thermal lens technique. Earlier works on these samples in the third and fourth harmonic regions were reported by Mizugai et al [43] and by Swofford et al [44]. Rai and Srivastava [42] also reported the IR spectra of the three

butyl alcohols and observed that the fundamental vibrational frequency for both the C-H and O-H bonds increases as one go from normal to tertiary butanol. Rai and coworkers [45] observed a considerable blue shift for OH stretching fundamental absorption peak of n-butanol on dilution with carbon tetrachloride. The magnitude of blue shift decreases for the $2 \leftarrow 0$ transition and there is no shift for the $3 \leftarrow 0$ transition. This observation is interpreted on the basis of formation of O-H...Cl hydrogen bond.

## 5.5.2 Experimental

High purity (>99%) isobutanol supplied by M/s SISCO Research Laboratories Pvt. Ltd., Mumbai, India is used for the present studies. The near infrared absorption spectra in the region 2000-700nm are recorded from pure liquid on a Hitachi Model 3410 UV-VIS-NIR spectrophotometer. The spectra are recorded using a path length of 1cm with air as reference at room temperature $(26 \pm 1)^0$C.

## 5.5.3 Results and discussion

The overtone spectra of liquid phase isobutanol recorded by using a conventional spectrophotometer in the spectral region $\Delta V_{CH}$= 2-6 and $\Delta v_{OH}$ =2-5 are given in Figures 5.3- 5.9. The peak assignments of the spectra is given in the Table 5.3 .The transition energies of the OH and CH stretching overtones are fitted to the one dimensional Birge – Sponer equation for an anharmonic oscillator. Calculated mechanical frequencies, anharmonicities and dissociation energies of the O-H and C-H stretching vibrations evaluated from the above spectra are given in the Table 5.3

The C-H overtone The transition frequencies of CH oscillators in alkanes and alkenes have been found from gas phase spectra and found that the progression occur in the order $v_{CH_4} > v_{-CH_3} > v_{-CH_2-} > v_{-CH-}$ [37,46]. Based on the work of Greenlay and Henry [46] and that of Rai and Srivastava [42] it is easy to identify the absorption peaks due to the distinctive types of C-H oscillators and O-H oscillator in the molecule of the present study.

The mechanical frequency and anharmonicity of O-H oscillator in isobutanol are 3834cm$^{-1}$ and - 91 cm$^{-1}$ respectively. The mechanical frequency value is found to be close to that of isobutanol in the gas phase (Table5.1). The observed values of methyl C-H mechanical frequency and anharmonicity in isobutanol are ~3043cm$^{-1}$ and ~ – 60cm$^{-1}$ respectively. These values are remarkably closer to the corresponding values in most of the normal and branched alkanes [47].

**Table 5.3** Observed overtone transition energies (cm$^{-1}$), mechanical frequencies $X_1$(cm$^{-1}$) and anharmonicities $X_2$ (cm$^{-1}$) of OH and CH of isobutanol. The least square correlation coefficients ($\gamma$) are also given.

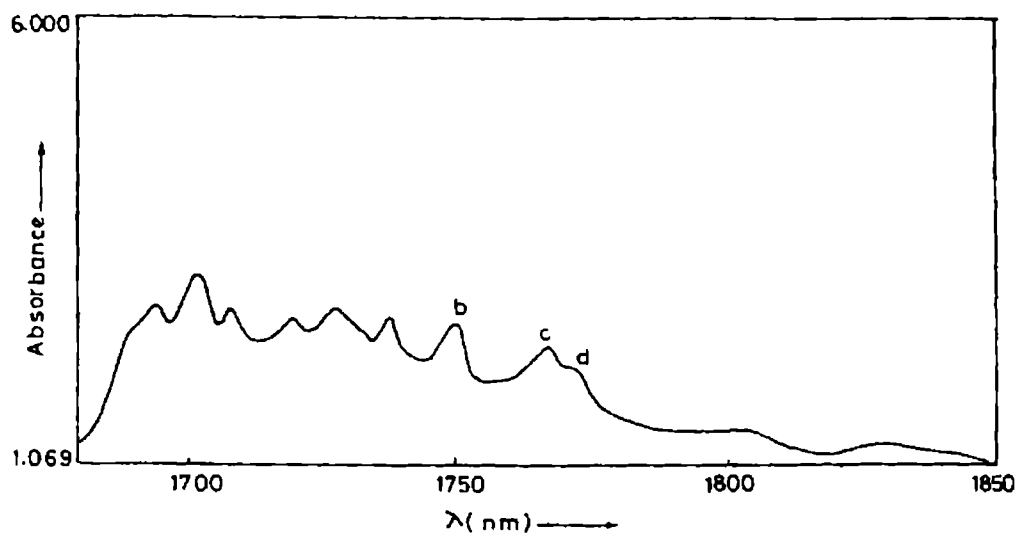| Oscillator | $\Delta V=2$ | $\Delta V=3$ | $\Delta V=4$ | $\Delta V=5$ | $\Delta V=6$ | $X_1$ | $X_2$ | $\gamma$ |
|---|---|---|---|---|---|---|---|---|
| **OH** | 7117 | 10423 | 13514 | 16437 | | 3834.3 | -91 | -0.9997 |
| **Methyl CH** | 5727 | 8412 | 10977 | 13426 | 15748 | 3042.8 | -59.7 | -0.9999 |
| **Methylene CH** | 5666 | 8319 | 10894 | 13340 | 15649 | 2998.3 | -55.4 | -0.9995 |
| **Methynic CH** | 5646 | 8293 | 10818 | 13261 | 15542 | 2995.5 | -57.7 | -0.9999 |

**Figure 5.5** Methyl ('b'), methylene ('c') and methyne ('d') CH overtone peaks of isobutanol in the $\Delta V= 2$ region
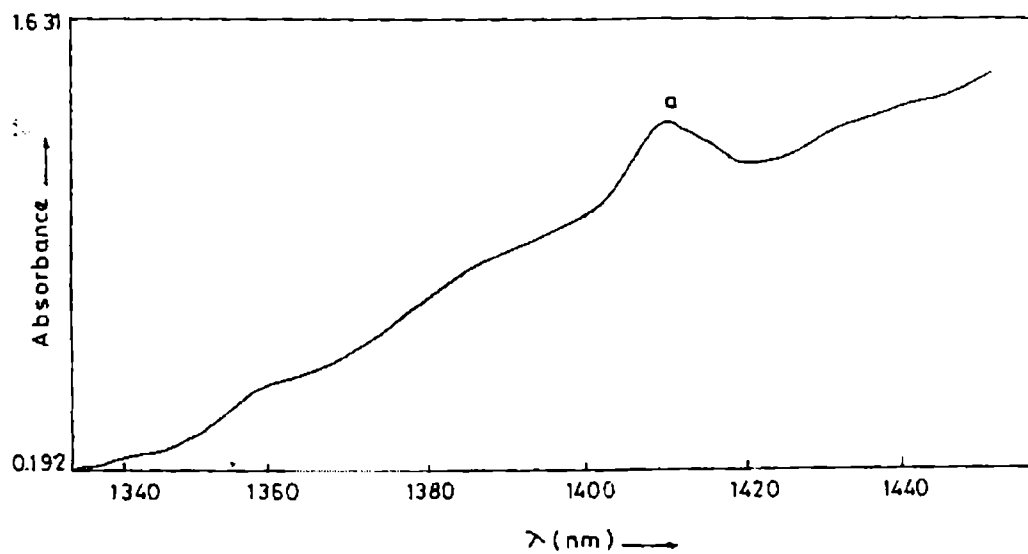


**Figure 5.6** The OH overtone peak of isobutanol in the $\Delta V= 2$ region
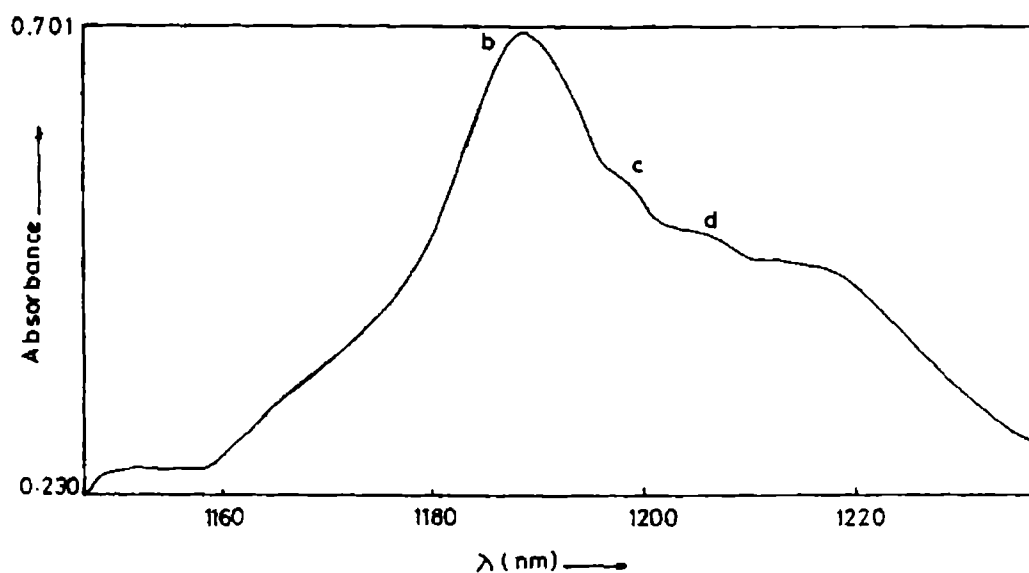
163

**Figure 5.7** Methyl ('b'), methylene ('c') and methyne ('d') CH overtone peaks of isobutanol in the $\Delta V$= 3 region
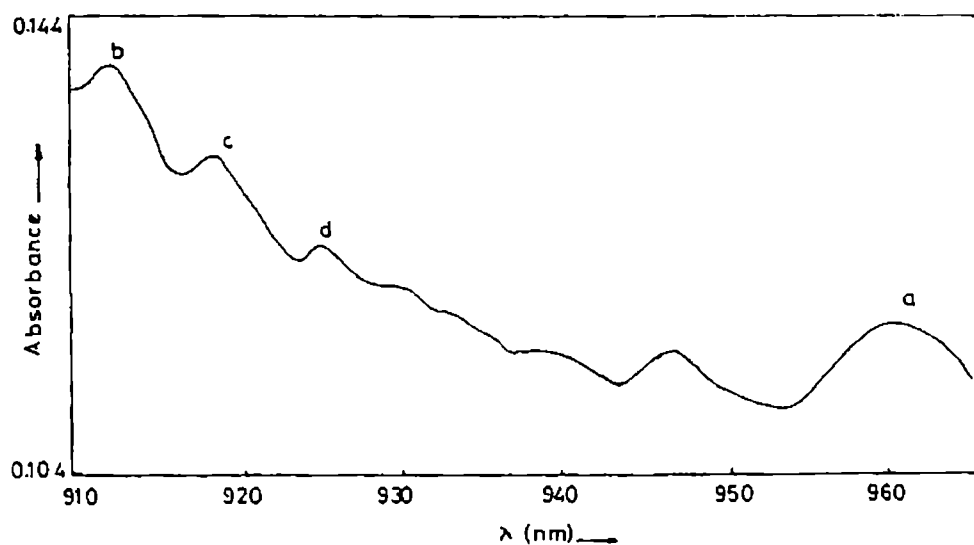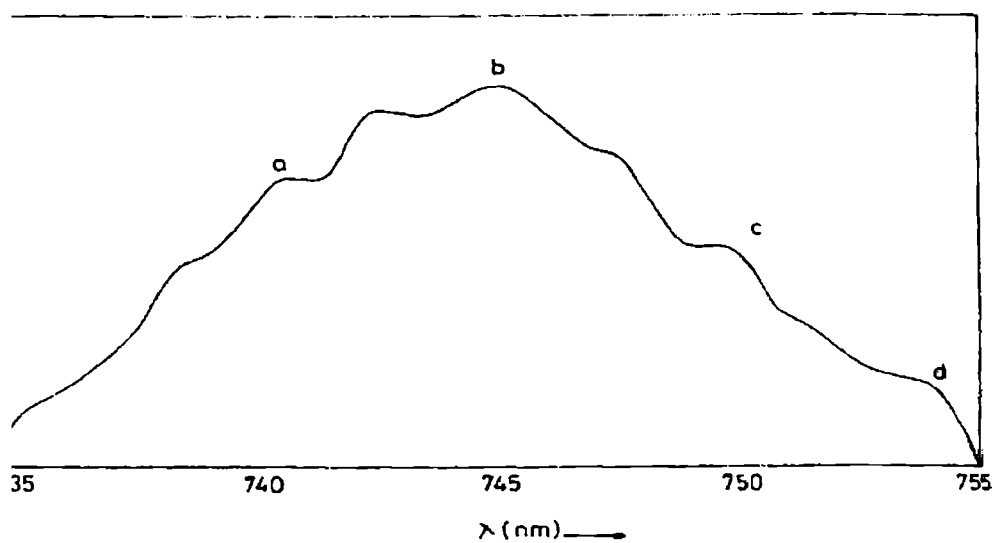


**Figure 5.8** The OH overtone peak ('a') in the $\Delta V$= 3 region and the CH overtor in the $\Delta V$= 4 region of isobutanol. Peaks marked as b, c and d represent methylene and methyne CH overtone peaks, respectively.

**5.9** The OH overtone peak ('a') in the $\Delta V = 4$ region and the CH overtone peaks $\Delta V = 5$ region of isobutanol. Peaks marked as b, c and d represent methyl, ᵢne and methyne CH overtone peaks, respectively



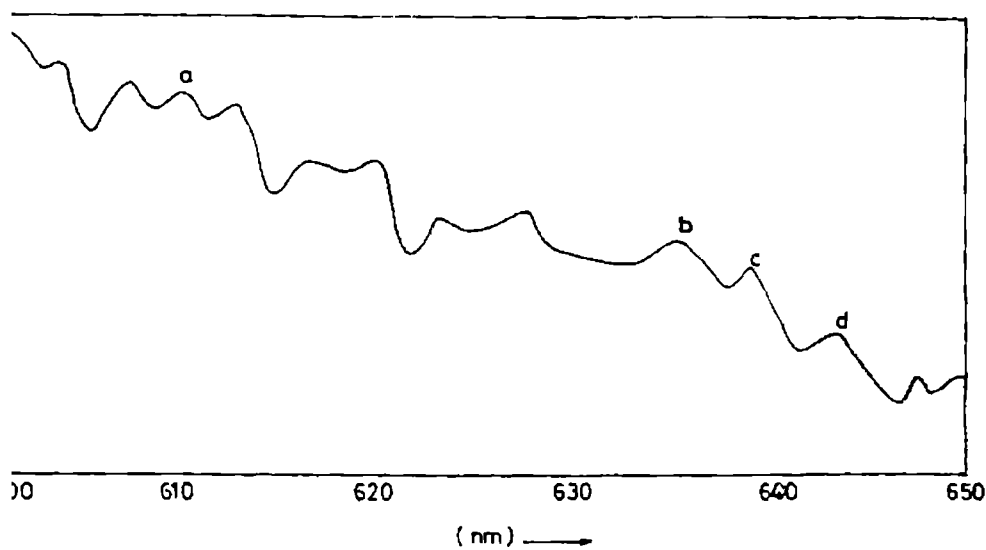**5.10** The OH overtone peak ('a') in the $\Delta V = 5$ region and the CH overtone peaks $\Delta V = 6$ region of isobutanol. Peaks marked as b, c and d represent methyl, ᵢne and methyne CH overtone peaks, respectively.

165

## 5.5.4 Conclusion

The overtone spectra of the C-H and O-H stretching vibrations of liquid phase isobutyl alcohol are measured using conventional absorption spectrophotometer. Resolvable peaks are observed for methyl, methylenic and methynic C-H bonds and O-H bonds. The peaks are assigned using the local mode model. The O-H overtone band in the $\Delta V=5$ region shows three distinct peaks as observed in the gas phase spectrum, indicating the presence of different conformers.

## References

[1]   V.S.Letokhov, *Laser Analytical Spectrochemistry*, Adam Hilger, Boston, 1985.

[2]   N.Subhash, M.K.Satheesh Kumar, T.M.A.Rasheed, K.P.Moosad, and K.Sathianandan, *J.Optics*, 16(1987) 51.

[3]   G.I.Mackay,D.R.Karecki and H.I.Schiff, Proc.SPIE 1433 Measurement of Atmospheric gases, 104-119 (1991).

[4]   A.Fried, B.Henry, D.D.Parrish, J.R.Carpenter and M.P.Buhr, *Atmos.Env.A*,25(1991)2277.

[5]   A.Fried, R.Sams and W.W.Berg, *Appl.Opt.*,23(1984)1867.

[6]   A.Fried, B.Henry and J.R.Drummond, *Appl.Opt.*,32(1993)821.

[7]   G.Schmidke, W.Kohn, U.Klocke, M.Knothe, W.J.Riedel and H.Wolf, *Appl.Opt.*,28(1989)3665.

[8]   J.Podolske and M.Loewenstein, *Appl.Opt.*,32(1993)5324.

[9]   M. Feher and P A Martin, *Spectrochim Acta A*, 51 (1995) 1579.

[10]  L.Sandstrom and D.Malmberg, *Spectrochim Acta A*, 58 (2002) 2449.

[11]  P.Werle, K.Maurer, R.Kormann, R.mucke, F.D'Amato, T.Lancia and A.Popov, *Spectrochim Acta A*, 58 (2002) 2361.

[12]  A.Vicet, D.A.Yarekha, A.Perona, Y.Rouillard, S.Gaillard and A.N.Baranov, *Spectrochim. Acta A*, 58 (2002) 2405.

[13]  R.Korman, H.Fischer, C.Gurk, F.Helleis, Th.Klupfel, K.Kowalski, R.Konigstedt, U.Parchatka and V.Wagner, *Spectrochim. Acta A*, 58 (2002) 2489.

[14]  I.Linnerud, P.Kaspersen and T. Jaeger, *Appl.Phys.B*,67(1998)297.

[15] D.D.Nelson, M.S.Zahniser, J.B.McManus, C.E.Kolb and J.L.Jimenez, *Appl.Phys.B*,67(1998)433.

[16] M.Wangler, D.A.Roth, V.M.Krivtsun, I.Pak, G.Winnewisser, M.Geleijns, P.E.S.Wormer, A.van der Avoird, *Spectrochim. Acta A*, 58 (2002) 2499.

[17] *Spectroscopy- Perspectives and Frontiers*, Ed. A.P.Roy, Narosa Publishing House, New Delhi, 1997,p.191.

[18] Q.S.Zhu and B.A.Thrush, *J.Chem.Phys.*,92(1990)2619.

[19] Q. S.Zhu, B.S.Zhang, Y.R..Ma and H.B.Qian,*Spectrochim.Acta A.*,46(1990)1217.

[20] S.F.Yang, X.Wang and Q.S.Zhu, *Spectrochim.Acta A.*,53(1997)157.

[21] S.Chou, D.S.Baer,and R.K.Hanson, *J. Mol.Spectrosc*, 200,138-142,2000.

[22] J.Lummila, O.Vaittinen, P.Jungner, L.Hlonen and A.Tolonen, *J. Mol.Spectrosc.*, 185,296,1997.

[23] C. Douketis and J.P.Reilly, *J.Chem.Phys.*91(1989)5239.

[24] A.Held and M.Herman *Chem.Phys.*,190(1995)407.

[25] D. Luckhaus, *J.Chem.Phys.*,106(1997)8409.

[26] J.A.Phillips, J.J.Orlando, G.S.Tyndall and V.Vaida, *Chem.PhysLett.*.,296(1998)377.

[27] M.Murtz, B.Frech, P.Palm, R.Lotze and W.Urban, *Optics Lett.*,23(1998)58.

[28] S.Hu, H.Lin, S.He, J.Cheng, and Q.Zbu, *Phys.Chem.Chem.Phys.*,1 (1999)3727.

[29] A.Muntianu, B.Guo and P.F.Bernath, *J.Mol.Spectrosc.*,176(1996)274.

[30] O.Vaittinen, L.Biennier, A.Camparge, J.M.Flaud and L.Halonen, *J..Mol.Spectrosc.*,184(1997)288.

[31] H.L.Fang, D.M.Meister and R.L.Swofford, *J. Phys.Chem.*,88(1984)405.

[32] I.Oref, *J.Chem.Soc.,Faraday Trans.*,82(1986)1289.

[33] H.Hannien, M.Horn and L.Halonen, *J.Chem..Phys.*, 111(1999) 3018.

[34] H.L.Fang and R.L.Swofford, *Chem.Phys. Lett.*,105(1984) 5.

[35] H.L.Fang and D.A.C.Compton, *J.Phys.Chem.*,92(1988)6518.

[36] J.D.Weibel, C.F.Jackels, and R.L.Swofford, *J.Chem.Phys.*,117(2002)4245.

[37] J.S.Wong and C.B.Moore,*J.Chem.Phys.*77(1982)603.

[38] A.V.Fedorov and D.L. Snavely, *Chem.Phys.*,254(2000)169.

[39] S.Xu, Y.Liu, G.Sha, C.Zhang and J.Xie, *J.Phys.Chem. A*,104(2000) 8671.

[40]    S.Xu, Y.Liu, J.Xie G.Sha, C.Zhang, *J.Phys.Chem.*A,105(2001) 6048.

[41]    D.R.Truax and H. Wicser, *Chem.Soc. Rev.*,5(1976)411.

[42]    S.B.Rai and P.K.Srivastava, *Spectrochimica Acta Part A*, 55 (1999) 2793.

[43]    Y.Mizugai, F.Takimoto, and M.Katayama, *Chem.Phys. Lett.*,76(1980)615.

[44]    R.L.Swofford, M.E.Long, M.S.Burberry and A.C.Albrecht,
         *J.Chem.Phys.*,66(1977)  664.

[45]    P.K.Srivastava, D.K.Rai and S.B.Rai, *Spectrochim.Acta A*,56(2000)1283.

[46]    W.R.A.Greenlay and B.R.Henry, *J.Chem.Phys.*,69(1978)82.

[47]    H.L.Fang, D.M.Meister and R.L.Swofford, *J.Phys.Chem.*,88(1984)410.

# SUMMARY AND CONCLUSIONS

The present work is mainly focused on the application of near infrared (NIR) vibrational overtone spectroscopy for characterizing X-H (X=C, N, O) bonds in some selected organic molecules. The NIR spectra of the liquid phase compounds are measured using a UV-Vis-NIR spectrometer. The Local Mode model is used for the interpretation of the observed vibrational overtone spectra of these molecules. This model treats a molecule as a set of loosely coupled anharmonic oscillators in which the vibrational energy is localized within one of the equivalent X-H oscillators. When more than one hydrogen atom is attached to a common heavy atom, a coupled local mode model (known as the local mode picture) is used for the analysis of the spectra. The local mode parameters such as mechanical frequency, anharmonicity, and kinetic and potential energy coupling coefficients are determined and the variations of these parameters in different series of molecules are studied. These analyses have yielded important information regarding molecular structure, conformation, intra- and inter-molecular interactions, anisotropic environments created by lone pair and / or $\pi$ electron interactions and the effect of substitution on the strength of individual X-H bonds on the parent molecules.

A comparison of the values of the local mode parameters of the ring C-H and N-H oscillators in benzyl amine and furfuryl amine indicate that the electron donation from the $-CH_2NH_2$ group to the aromatic ring is similar in either molecule. The hetero oxygen atom in furfuryl amine is thus not involved in any interaction to the $-CH_2NH_2$ group attached to the ring. The hetero oxygen atom in furfuryl amine plays the same role as in furan, namely, electron withdrawal from the ring carbon sites causing increase in ring C-H mechanical frequency with respect to that in benzyl amine.

The analysis of the vibrational overtone spectra of 2-furaldehyde yields the result that the effect of substitution of the electron-withdrawing group at 2- position of furan is much influenced by the presence of the heteroatom oxygen in the ring part. The substituent exerts their effect predominantly through inductive effect revealing the strong influence of short-range induction by the heteroatom.

The analysis of the vibrational overtone spectra of cinnamaldehyde shows that an electron withdrawing group substitution on the olefinic part of the molecule much influences the ring C-H mechanical frequency and anharmonicity values. This observation is explained as due to the presence of extended conjugation in the side chain. The large value observed for aldehydic C-H mechanical frequency is attributed as mainly due to the presence of indirect lone pair trans effect. The ring C-H bonds in benzoyl chloride are found to have slightly larger force constant than that in benzene.

The methoxy group exhibits some interesting phenomena due the anisotropic environment created by the oxygen atom attached to the methyl group. The local mode model is successfully applied to interpret the overtone spectra of the methoxy containing molecules anisole, o-anisidine, p-anisidine and p-anisaldehyde . In all these molecules the methyl group is found to be subjected to a conformationally anisotropic environment created by lone pair effect of the heteroatom oxygen. Consequently two distinct peaks are observed at each overtone in the methyl region. The effect is explained as the interaction of an electron lone pair with the methyl C-H bond situated trans to the lone pair. Lone pair electron population of the antibonding orbital weakens the out-of-plane C-H bonds and this has an effect of splitting the methyl CH overtone bands. The study also reveals that the nature of the substituent and the relative position of the ring influence the local mode parameters in substituted benzene.

The C-H vibrational overtone spectrum of t-butyl amine is successfully analyzed under the local mode picture, where the diagonalization of the $C_{3v}$ coupled oscillator Hamiltonian matrices predicted the transition energy values of the pure overtone and local-local combinations. The agreement between the observed peak energies and calculated values is found to be very good. The results also reveal that in t-butyl amine vibrational state mixing is pronounced only at the first overtone level. A comparative local mode study of the vibrational overtone spectra of n-butyl amine and t-butyl amine has demonstrated how the influence of the environment on the C-H oscillator can be observed in the energies of the overtone peaks of the molecules studied. It is concluded that the lone pair trans effect of -$NH_2$ group plays dominant role in n-butyl amine and inductive effect of -$NH_2$ group plays dominant role in t-butyl amine in determining the

C-H bond strength. The difference in the values of mechanical frequency in t-butyl amine and n-butyl amine is the manifestation of the substituent effect in these molecules.

A number of experiments in the area of laser spectroscopy are also carried out as a part of the present work. Chapter 4 contains a few examples of applications of laser induced fluorescence and laser Raman spectroscopy. The LIF spectra of benzyl amine monomer, benzyl amine polymer, n-butyl amine monomer, n-butyl amine polymer and p-anisidine, and laser Raman spectra of 3-fluorotoluene, anisole, t-butyl amine and p-anisidine are recorded using Nd: YAG pulsed laser as an excitation source and CCD as detector. It is observed that the fluorescent peak positions of the polymerized samples are shifted towards the longer wavelength with respect to the corresponding monomer spectrum. The Raman active fundamental vibrational bands of all the samples are assigned and are compared with the reported frequencies. Assignments are given for some new low-lying vibrational modes observed in the present study. This experiment demonstrates the versatility and elegance of the pulsed laser–monochromator-CCD setup for studying molecular fluorescence and Raman spectra.

Chapter 5 contains the details of the experimental work using a NIR tunable diode laser where the molecular spectral lines are examined under high spectral resolution. The highly rotationally resolved $\Delta V=3$ overtone spectrum of the –OH group in isobutanol is recorded in a high-resolution spectrometer using tunable diode laser and a long path length cell. The resolved bands are assigned as due to the O-H overtone absorption of the different kinds of molecular conformers. The observed O-H overtone peak positions corresponding to the different conformers agree well with ab initio theoretical predictions and the reported CRDS results. To our knowledge, this is the first TDLAS high resolution study of isobutanol molecule. The overtone spectra of the C-H and O-H stretching vibrations of liquid phase isobutyl alcohol are measured using conventional spectrophotometer. The distinct bands corresponding to methyl, methylene and methyne C-H bonds and O-H bonds are assigned and the local mode parameters determined. The O-H overtone absorption in the $\Delta V=5$ region shows three distinct peaks due to the different conformers as observed in the gas phase spectrum.

## List of papers published in journals

1. Overtone spectra of benzyl amine and furfuryl amine – a comparative study, **K. K. Vijayan**, Sunny Kuriakose and T. M. A. Rasheed, *Asian J. Phys.*, Vol.10, No.3, 2001.

2. Vibrational overtone spectrum of 2-furaldehyde in the NIR region, **K. K. Vijayan**, Sunny Kuriakose, S. Shaji and T. M. A. Rasheed, *Asian J. Phys.*, Vol.11, No.1, 2002, 66-69.

3. Overtone spectrum of cinnamaldehyde in the NIR region- Evidence for indirect lone pair trans effect, **K. K. Vijayan**, Sunny Kuriakose, S Shaji, Shibu M Eapen, K. P. R .Nair and T. M. A. Rasheed, Asian *J. Spectros.*, Vol.5, No.4, 2001,185-189.

4. CH overtone spectrum of t-butyl amine: a $C_{3v}$ coupled oscillator analysis using local mode parameters, **K. K. Vijayan**, Sunny Kuriakose, K.P.R.Nair and T. M. A. Rasheed, *Asian J. Spectros.*, Vol.6, No.3, 2002,125-131.

5. Overtone spectra of benzaldehyde and salicyladehyde: Evidence for the inhibition of indirect and direct lone pair trans effects, Sunny Kuriakose, **K. K .Vijayan**, and T. M. A. Rasheed, *Asian J. Spectros.*, Vol.1, No.1, 2001,17-23.

6. Overtone spectra of allyl chloride and allyl alcohol in the near infrared region, Sunny Kuriakose, **K. K.Vijayan**, S. Shaji, Shibu M Eapen, K. P. R. Nair and T. M.A. Rasheed, *Asian J.Phys.*, Vol.11, No.1, 2002,70-74.

7. Overtone spectrum of formamide in the near infrared region-Evidence for the inhibition of lone pair trans effect, Sunny Kuriakose, **K. K. Vijayan**, Shibu M Eapen, S. Shaji, K. P. R. Nair and T. M. A. Rasheed, *Asian J. Spectros.*, Vol.6, No., 2002,43-46.

8. Overtone spectrum of Phenyl hydrazine in the near infrared region. Sunny Kuriakose, **K. K. Vijayan**, K. P .R. Nair and T. M. A. Rasheed, *Asian J. Phys.*, (in press)

9. CH overtone spectrum of Nitromethane: a $C_{3v}$ coupled oscillator analysis using local mode parameters, Sunny Kuriakose, **K. K. Vijayan**, K.P.R.Nair and T. M. A. Rasheed (communicated)

## Seminar Presentations

1. Vibrational overtone spectrum of 2-furaldehyde in the NIR region , **K.K. Vijayan**, Sunny Kuriakose, Shibu M.Eappen, S. Shaji, K.P.R Nair and T.M.A Rasheed , National Symposium on Lasers, Spectroscopy and Laser Applications, 27- 30  December 2001, Meerut

2. Vibrational overtone spectrum of Cinnamaldehyde in the NIR region,
   **K.K. Vijayan**, Sunny Kuriakose, Shibu M.Eappen, S. Shaji, K.P.R Nair and
   T.M.A Rasheed, National symposium on Atomic Molecular Structure,Interactions
   and Laser Spectroscopy, 22-24 February 2002, Banaras Hindu University,
   Varanasi.

3. Overtone spectra of allyl chloride and allyl alcohol in the near infrared region,
   Sunny Kuriakose, **K.K. Vijayan**, Shibu M.Eappen, S. Shaji, K.P.R Nair and
   T.M.A Rasheed , National Symposium on Lasers, Spectroscopy and Laser
   Applications, 27-30 December 2001, Meerut.

4. Overtone spectrum of formamide in the NIR region,
   Sunny Kuriakose, **K.K. Vijayan**, Shibu M.Eappen, S. Shaji, K.P.R Nair and
   T.M.A Rasheed, National symposium on Atomic Molecular Structure,
   Interactions  and Laser Spectroscopy, 22-24 February 2002, Banaras Hindu
   University, Varanasi.

5. Aryl CH overtone Spectrum of liquid phase N, methyl aniline andN,Ndimethylaniline – A conformational structural analysis  using local mode model, Shibu M.Eappen, Venketeswara Pai. R, S. Shaji, Sunny Kuriakose, **K.K.Vijayan** K.P.R Nair and T.M.A Rasheed, National symposium on Atomic MolecularStructure, Interactions and Laser Spectroscopy, 22-24 February 2002, Banaras Hindu University, Varanasi.